INVESTIGATIONS ON THE EXTRACTION BEHAVIOR OF ACTINIDES IN IONIC LIQUID MEDIUM AND THE PHYSICOCHEMICAL AND AGGREGATION PROPERTIES OF THE IONIC LIQUID PHASE

By

CHEBROLU VENKATESWARA RAO

Enrolment No: CHEM02201604006

Indira Gandhi Centre for Atomic Research

Kalpakkam

A thesis submitted to the

Board of Studies in Chemical Sciences

In partial fulfillment of requirements

for the Degree of

DOCTOR OF PHILOSOPHY

of

HOMI BHABHA NATIONAL INSTITUTE

MAY 2021

Homi Bhabha National Institute

Recommendations of the Viva Voce Board

As members of the Viva Voce Committee, we certify that we have read the dissertation prepared by **Chebrolu Venkateswara Rao** entitled "**Investigations on the extraction behavior of actinides in ionic liquid medium and the physicochemical and aggregation properties of the ionic liquid phase**" and recommend that it may be accepted as fulfilling the thesis requirement for the award of Degree of Doctor of Philosophy.

Chairman - **Dr. A. Suresh** **Date:** 21/10/2021

Guide/Convener - **Dr. K.A.Venkatesan** **Date:**

K. A. Venkatesan **21/10/2021**

Examiner – **Prof. Tamal Banerjee** **Date:** 21.10.2021

Member 1- **Dr. K. Sundararajan** **Date:** 21.10.2021

Member 2 - **Dr. H.N. Jena** **Date:** 21.10.2021

Member 3 - **Dr. S. Ningshen** **Date:** 21/10/2021

Member 4 - **Dr. B. Anupkumar** **Date:** 21/10/21

Member 5 - **Dr. N. Sivaraman** N. Sivaraman **Date:** 21.10.2021

Final approval and acceptance of this thesis is contingent upon the candidate's submission of the final copies of the thesis to HBNI.

I hereby certify that I have read this thesis prepared under my direction and recommend that it may be accepted as fulfilling the thesis requirement.

K. A. Venkatesan
21/10/21

Date: 21/10/2021 **Dr. K. A. Venkatesan**

Place: IGCAR Kalpakkam **Guide**

STATEMENT BY AUTHOR

This dissertation has been submitted in partial fulfillment of requirements for an advanced degree at Homi Bhabha National Institute (HBNI) and is deposited in the Library to be made available to borrowers under rules of the HBNI.

Brief quotations from this dissertation are allowable without special permission, provided that accurate acknowledgement of source is made. Requests for permission for extended quotation from or reproduction of this manuscript in whole or in part may be granted by the Competent Authority of HBNI when in his or her judgment the proposed use of the material is in the interests of scholarship. In all other instances, however, permission must be obtained from the author.

Ch. Venkateswara Rao 21/10/21
Ch. Venkateswara Rao

DECLARATION

I, hereby declare that the investigation presented in the thesis has been carried out by me. The work is original and has not been submitted earlier as a whole or in part for a degree / diploma at this or any other Institution / University.

Ch. Venkateswara Rao
21/10/21

Ch.Venkateswara Rao

List of Publications arising from the thesis

Journal

a. Published

1. "Probing the absence of third phase formation during the extraction of trivalent metal ions in an ionic liquid medium", **Ch. Venkateswara Rao,** Alok Rout, K. A. Venkatesan, *New Journal of Chemistry,* **2019,** *43,* 5099-5108.
2. "Europium (III) complexation behaviour in an alkyl ammonium ionic liquid medium containing neutral extractants", **Ch. Venkateswara Rao,** Alok Rout, K. A. Venkatesan, *Separation and Purification Technology,* **2019,** *213,* 545-552.
3. "Thermophysical properties of neat and radiolytically degraded acidic extractants present in room temperature ionic liquid", **Ch. Venkateswara Rao,** Alok Rout, S. Mishra, K. A. Venkatesan, *Journal of Radioanalytical and Nuclear Chemistry,* **2019,** *321,* 907-916.
4. "Investigations on the radiation stability of incinerable CHON based ionic liquid containing diglycolamide", **Ch. Venkateswara Rao,** Alok Rout, K. A. Venkatesan, *Journal of Molecular Liquids,* 298, **2020,** *298,* 112020.
5. "Selective Separation of Zirconium (IV) from Uranium (VI) using Dioxoamide Ligand Present in Ammonium Based Ionic Liquid: An Application Towards Spent Metallic Fuel Reprocessing", **Ch. Venkateswara Rao,** Alok Rout, K. A. Venkatesan, *Separation and Purification Technology,* **2020,** *247,* 116963.
6. "Aggregation behavior of ionic liquid in molecular liquid medium: a dynamic light scattering study", **Ch. Venkateswara Rao,** Alok Rout, K. A. Venkatesan, *Separation Science and Technology,* **2021,** *56,* 757-765.

7. "Anion assisted extraction of U(VI) in alkylammonium ionic liquid: Experimental and DFT studies", **Ch. Venkateswara Rao,** Alok Rout, Anil Boda, Sk. Musharaf. Ali, K. A. Venkatesan, *Separation and Purification Technology,* **2021,** *261,* 118275.

b. Accepted: NIL

c. Communicated:

8. "Normalized polarity of tri-*n*-butyl phosphate metal complexes in ionic liquid using Reichardt's dye as polarity probe", **Ch. Venkateswara Rao,** Alok Rout, K. A. Venkatesan, *New Journal of Chemistry,* **2021.**

Other Publications: NIL

Conferences

1. "Investigation on the aggregation behavior of ionic liquid solvent", **Ch. Venkateswara Rao**, Alok Rout, K. A. Venkatesan, M. P. Antony, In Proceedings of Eighth DAE-BRNS symposium on emerging trends in separation science and technology **(SESTEC**). P-41, May 23-26, **2018, BITS Pilani, Goa**, **India.**
2. "Thermo physical properties of DGA-ionic liquid mixture", **Ch. Venkateswara Rao**, Alok Rout, S. Rajeswari, K. A. Venkatesan, M. P. Antony, In Proceedings of Eighth DAE-BRNS symposium on emerging trends in separation science and technology **(SESTEC)** P-42, May 23-26, **2018, BITS Pilani, Goa**, **India.**
3. Solvent extraction of americium(III) in a hydrophobic ammonium ionic liquid containing T2EHDGA and CMPO as extractant, **Ch. Venkateswara Rao**, Alok Rout, K. A. Venkatesan, In proceedings of fourteenth Biennial DAE BRNS Symposium Nuclear and Radiochemistry **(NUCAR).** P-77, January 15-19, **2019, BARC, Mumbai, India.**

4. "Complexation of Eu(III) in an alkylammonium ionic liquid medium containing some neutral extractants: extraction and aggregation behavior", **Ch. Venkateswara Rao**, Alok Rout, K. A. Venkatesan, In proceedings of fourteenth Biennial DAE BRNS Symposium Nuclear and Radiochemistry **(NUCAR),** P-78, January 15-19, **2019, BARC, Mumbai, India.**
5. "Physicochemical and radiolytic degradation properties of acidic extractants dissolved in ionic liquid medium", **Ch. Venkateswara Rao**, Alok Rout, K. A. Venkatesan, In proceedings of fourteenth Biennial DAE BRNS Symposium Nuclear and Radiochemistry **(NUCAR),** P-79, January 15-19, **2019, BARC, Mumbai, India.**
6. Selective separation of zirconium(IV) from uranium(VI) using dioxoamide ligand present in ammonium based ionic liquid medium", **Ch. Venkateswara Rao**, Alok Rout, K. A. Venkatesan, In Proceedings of 9th DAE – BRNS Biennial Symposium (Webinar) on emerging trends in separation science and technology, **e-SESTEC-2020,** p-26, March 22 – 26, **2021, BARC, Mumbai, India.**
7. "Radiation stability of quaternary Ammonium based ionic liquid based system", **Ch. Venkateswara Rao**, Alok Rout, K. A. Venkatesan, In Proceedings of 9th DAE – BRNS Biennial Symposium (Webinar) on emerging trends in separation science and technology. **e-SESTEC-2020,** p-65, March 22 – 26, **2021, BARC, Mumbai, India.**

Ch. Venkateswara Rao
21/10/21

Ch. Venkateswara Rao

DEDICATIONS

Dedicated to my family members

ACKNOWLEDGEMENTS

First of all, I would like to express my heartfelt thanks to my Ph.D supervisor **Dr. K.A. Venkatesan,** for his guidance, constant support, and valuable suggestions to improve the quality of the work throughout my PhD tenure. I take this opportunity to thank him for giving lot of liberty to me for planning the experiments and allow me to work. I owe my deepest gratefulness and respect to him.

I am pleased to express my deep sense of gratitude to former Dean, Chemical sciences & Director, Material chemistry and metal fuel cycle group, **Dr. N. Sivaraman** to have his constructive comments and providing the excellent research facilities.

I take immense pleasure in thanking to **Dr. C.V.S. Brahmananda Rao**, Dean, Chemical sciences for his valuble suggestions and continuous support during course of my PhD work.

I express my deep sense of gratitude to **Dr. Arun Kumar Bhaduri**, Director, IGCAR for the opportunity to pursue research in this premier institute.

I am extremely grateful to **Dr. K. Ananthasivan**, Director, Reprocessing Group, for his kind support and encouragement.

I extend of my sincere thanks to **Dr. Alok Rout** for his support, guidance, valuable suggestions, encouragement and motivation during the initial stage of learning the work and always helping me wherever I find in difficulty in perfoming the experiments.

I thank my doctoral committee chairman **Dr. A. Suresh** and members, **Dr. K. Sundararajan, Dr. H.N. Jena, Dr. S. Ningshen, Dr. B.Anupkumar and Dr. N. Sivaraman** for their time to time evaluation of the research work and valuable suggestions to improve my self.

I am very much delighted in thanking **Dr. M. Saibaba**, Former Director, Resource Management Group and **Dr. T. Lakshmi Narasimhan,** Former Associate director, Resource Management Group and **Dr. Vidya Sundararajan**, Head, Resource Management

Group for providing excellent ambience at JRF-enclave. I take this opportunity to thank them for his kind encouragement and moral support.

I would like to acknowledge my sincere gratitude to all my lab members, **Dr. A. S. Suneesh, Shri. B. Robert Selvan**, **Dr. T. Prathiba, Mr.Anjan Dawa** for their kind help and support throughout my doctoral research. I wish to put a special note of thanks to **Mrs. Amutha subha** for helping in handling radioactive materials, synthesis, and purification of organic compounds and her support throughout course of work.

I wish to extend my sincere thanks to my seniors **Dr. R. Rama, Dr. G. Murali Krishna, Dr. K. Rama swami, Mr. P. Amesh,** for their help and healthy atmosphere in the lab. I wish to sincere thanks to juniors**, Mrs. C.K. Mehjubin, Ms. Parvathy Narayan** for their valuable co-operation and support and timely help in the research work.

I wish to express my hearty thanks for all the members of Irradiated Fuel Studies Section, **Dr. M.P. Antony, Dr. P. Manoravi, Dr. G. Panner Selvam, Mrs. S. Rajeswari, Mr. G. Ganapathy, Mr. Ujwal Kumar Maithy, Mr. Kalayarasu, Mr. Amalraj, Mr.T. Bapuji and Mr. M. Kurananidhi** for their kind support.

The strong co-operation and kind support of all Solution Chemistry and Separation Science section members, **Dr. A. Suresh, Dr. C.V.S Brahmananda Rao, Dr. B.Srinivasulu, Dr. Pitchaiah, Dr. Gopa Kumar, Mrs. N. Navamani, Ms. Ganga, Mr P. Amaredrein, Mr. Hariharan** is deeply acknowledged.

I would like to express my sincere thanks to my friends from ICT Mumbai, **Dattatreya Hase** and **Akshay bhujbal**, for helping in recording the GC-MS and NMR experiments. I am extremely grateful to **Dr. SK. Musharf Ali** and **Dr. Anil Boda** Chemical Engineering Division, Bhabha atomic Research Institute, Mumbai for providing computational facilities.

I take immense pleasure in thanking to **Dr. B.S Panigrahi, Dr. K. C. Pitchaih, Dr. N. Ramanathan, Dr. B. Srinivasulu, Dr. B.P. Reddy, Dr. N. Desigan, Dr. Jammu**

Ravi, Mr. S. Rama Krishna Reddy, Mr. D. Siva Kumar, Dr. K. Yadagiri, Dr. K. Sambasiva Rao, Dr. G.Gopi, Dr. D. Sanjay Kumar, Mr. D. Bola Sankar, Mr. T. Suresh Kumar, Mr. V. Shiva, Mr. Ravindra Babu Mr. A. Anil Kumar and Mr. G. Jogeswarara Rao for their motivation and encouragement whenever I felt disappointed in the PhD work.

I profoundly thank the entire member in the Nuclear Radioanalytical Chemistry Section **Dr. R. Kumar, Dr. G.V.S. Ashok kumar, Dr. D. Saha, Mrs. Vithya, Mr. J. Brahmaji Rao, Dr. M. Bootha Rajan** for helping in the analysis of radioactive samples.

I would like express sincere thanks to my chemistry batchmates **Mr. Y.N.V. Samba Siva Rao, Mr. M. Mahima Kumar, Mr. P. Vinod Kumar, Mr. G. Jegan, Mr. V. Bharath Reddy, Mr. K. Raja, Mr. M. Harish, Mr. S.K. Barik, Ms. Lutin Swain, Ms. P.K Sruthi, Ms. Subramme Sarkar, Ms. Deepitha, Mrs. R. Rasitha, and JRF enclave friends** for making cheerful and healthy nature during the research work.

I also thank to **Dr. Ch. Jagadeeswara Rao, Dr. B.S. Panigrahi** and **Mr. H. Krishnan** of MMG and Safety group IGCAR for their kind co-operation in the Thermogravimetry, luminescence and irradiation studies. I am pleased to thank all the Chemistry Group, RRDD members of IGCAR for their moral support during this work.

I also express sincere graditude all my family members espscially **Mr. Ch. Rambabu, Mr. Ch. Rama Krishna,** childhood friends namely, **Mr. G. Kiran Kumar, Mr. D. Gopi Chand,** UG friends namely, **Mr. R.Likhith Kumar, Mr. N. Naga Babu,** & PG friends **Mr. M. Uma Maheshwara Rao, Mr. B. Surya Prasad, Mr. N.V. Chakradhar** and all my beloved teachers namely, **Mr. V. Nageshwara Rao, Mr. N. Prasad Rao, PG professors, Dr. A. Sathyanarayana, Dr. P. Shyamala,** etc for their support and encouragement to reach this position.

I express my hearty thanks to all the project students worked in my lab, **Ms. B. P. Subhashini, Ms. M. Tincy, Ms. M. Anu,** for their sincere help in doing some experiments.

I am very much thankful to **Homi Bhabha National Institue, Mumbai**, for providing me the opportunity to carry out my PhD work.

Finally, I would like to acknowledge the people who mean the world to me, my family. I would like to express my heartiest gratitude and honor to my parents, **Late. Shri. Ch. Sarma Rao** and **Late. Smt. Ch. Parvathy** for their unconditional love, support, faith, encouragement and confidence in me. They have been my driving force and inspiration in all pursuits of life. I am also grateful to my sisters **Smt. Ch. Varalakshmi and Smt. Ch. Bhanu** for being caring, loving, support and helpful to me. I would like to thank my brother **Shri. Ch. Veera Raghavaiah** for the support and unconditional love at home. They are literally being the pillars of my strength.

Last but not the least, I thank the Almighty for providing me good health, courage, enormous blessings and enabling me to complete the thesis.

Ch. Venkateswara Rao

Ch. Venkateswara Rao 21/10/21

CONTENTS

CHAPTER 2: Experimental

CHAPTER 3: Extraction behavior of uranium in CHON based ligand – ionic liquid system 95

Abstract

Reprocessing of spent nuclear fuel is essential for the sustained growth of nuclear power programme in India. Room temperature ionic liquids (RTILs) have been receiving increased attention for possible applications in the area of nuclear fuel reprocessing and waste management owing to their fascinating properties. The conventional ionic liquids containing 1-alkyl-3-methylimidazolium ($[C_n mim]^+$) cation in association with hexafluorophosphate ($[PF_6]^-$) or bis(trifluoromethylsulfonyl)imide ($[NTf_2]^-$) etc., have been extensively studied for the solvent extraction of actinides and lanthanides from aqueous solution. However, these ionic liquids have some limitations. For instance, they undergo the cation and anion exchange reaction with various ions present in the aqueous phase during the course of solvent extraction. Therefore, there is a need to develop or identify the appropriate cation-anion combination of the ionic liquid for solvent extraction application such that the resultant RTIL is devoid of these limitations, but retaining all the good properties of the ionic liquid. In addition, it is also desirable to select the ionic liquid, which is made up of CHON-atoms so that the ionic liquid is completely incinerable and the waste disposal of the spent ionic liquid becomes easy.

Therefore, the objective of the present work was to identify the ionic liquid which was devoid of above mentioned drawbacks and explore the possibility of using that ionic liquid for various applications in nuclear fuel cycle. In this context, some ammonium ionic liquids have been developed and explored for the solvent extraction of actinides and lanthanide fission products from nitric acid solutions. Since the results obtained from those studies were very peculiar and unique to an ionic liquid, the study was also focused on understanding the insights of solvent extraction by probing the co-ordination chemistry of metal-ligand complexes present in the extracted ionic liquid phase, determination of the polarity index of the extracted phase and radiolytic stability. For this purpose, the extracted ionic liquid phase was subjected to various spectroscopic studies and the results were reported in this thesis.

List of Figures

List of Tables

Chapter 1: Introduction

1.1. Nuclear Energy

Electricity is essential for the growth of economy and welfare of the nation. The electricity can be produced from the conventional resources such as coal, oil, natural gas, nuclear power and non-conventional resources such as solar, wind and bio-mass [1-3]. At present, the electrical energy is mainly produced from resources such as fossil fuels (70%), natural gas (21.4%), nuclear power (11%), and hydroelectric power (5%). The use of fossil fuels for the production of electricity releases considerable amount of greenhouse gases, which are responsible for global warming and climate changes happening all over the world [4]. Moreover, the consumption of these non-renewable fossil fuels for the production of electricity decreases the availability of valuable energy resources in the earth crust [5]. Therefore, there is a need to look into the alternative resources that produces electricity without emitting the greenhouse gases. In this context, the production of energy from renewable resources and nuclear reactors has evolved as promising alternatives to fossil fuels.

Among these resources, the nuclear option for the production of energy received much attention owing to the attractive features such as minimal emission of greenhouse gases, small space, less fuel requirement for the production of energy and breeding of fuel, high energy output etc,. Currently, there are 448 nuclear reactors operating worldwide, 58 reactors are under construction and 158 nuclear reactors are planned in the near future. In India, there are 22 nuclear reactors operating for the production of electricity contributing about 4 % of the total electricity generation and it is planned to increase its share to 30 % by the year 2050 [6-8]. The nuclear reactors employ uranium (natural or enriched) oxide and uranium-plutonium mixed oxide as a fuel for the generation of nuclear power. The fissile isotopes ^{235}U and ^{239}Pu present in the nuclear fuel undergoes nuclear fission reaction producing nearly 200 MeV of energy per fission. The heat energy liberated during fission reaction is converted into electrical energy and depending upon the type of fuel employed in a reactor, there are several types of nuclear reactors operating across the globe [7].

1.2. Indian nuclear power programme

In 1950s, Dr. Homi Jahangir Bhabha, the architect of Indian atomic energy programme, proposed a three-stage nuclear power programme aimed at the effective utilization of limited uranium resources and abundant reserves of thorium in India [8]. The first stage involves the operation of pressurised heavy water reactors (PHWR) for the production of energy, that use natural uranium as the fuel. The spent fuel obtained from PHWRs containing a small amount of the fissile isotope ^{239}Pu, is reprocessed for the recovery of the residual uranium and plutonium from fission products. Currently, there are 18 PHWRs, two BWRs, and one PWR operating in India with a total installed capacity of 6780 MWe [9]. The second stage involves the utilization of plutonium recovered from PHWRs, to fuel Fast breeder reactors (FBRs). In FBRs, the fertile thorium is used as a blanket in order to breed more fuel than that is consumed by converting the fertile ^{232}Th into fissile ^{233}U. A Fast Breeder Test Reactor (FBTR) with the capacity of 40 MWt in operation at Kalpakkam since 1985 is part of the second stage. India's first commercial fast breeder reactor, the Prototype Fast Breeder Reactor (PFBR) (500 MWe) is in the advanced stage of commissioning [10,11]. The third stage aims to utilize the ^{233}U, generated in the second stage, to fuel the thermal breeder reactors. The viability of the third stage has been demonstrated by the 30 kWt research reactor named Kalpakkam MINI (KAMINI) Reactor fuelled with ^{233}U is currently operational at Kalpakkam [12].

1.3. Nuclear Fuel cycle

Uranium is one of the major fissile elements found in the earth crust. The nuclear fuel cycle is a series of industrial processes that involves mining of uranium, production of electricity from nuclear fission reaction of U in a nuclear power reactor, reprocessing of spent nuclear fuel and the disposal of nuclear waste as shown in Fig. 1.1 [13-15]. The processes such as mining and milling, conversion, enrichment and preparation of the uranium bearing fuel in a suitable form are collectively called as 'front end' of the nuclear fuel cycle. After irradiation of the fuel in a nuclear reactor for the production of electricity, the used fuel known as the spent nuclear fuel is subjected to a series of processes including its temporary storage, reprocessing, recycling of uranium and plutonium and the disposal of radioactive waste. These processing steps are collectively called as the 'back end' of nuclear fuel cycle.

Fig. 1.1. Schematic representation of nuclear fuel cycle [14].

1.4. Reprocessing of spent nuclear fuel

The nuclear fuel discharged from the nuclear reactor is known as spent nuclear fuel. It is composed of fissile elements such as plutonium and depleted uranium and several other elements formed by the nuclear fission reaction, known as fission products [16,17]. The spent nuclear fuel is therefore reprocessed for the recovery of these fissile elements which is then used for refabrication of nuclear fuel. Two different technologically viable methods are available for reprocessing of spent nuclear fuels. They are based on (1) Aqueous reprocessing (PUREX) and (2) Non-aqueous reprocessing method.

1.4.1. Aqueous reprocessing

PUREX (Plutonium and Uranium Recovery by Extraction) process is an industrially well established solvent extraction process. The PUREX process involves the selective extraction of uranium and plutonium from spent nuclear fuel dissolver solution into organic phase, is composed of 1.1 M tri-*n*-butyl phosphate (TBP), as an extractant in *n*-dodecane (*n*-DD) as a diluent [18,19]. The PUREX process consists of three major steps namely the (i) head end step, which comprises of decladding, dissolution, and feed preparation, (ii) solvent extraction using TBP, which involves co-extraction of uranium and plutonium followed by partitioning of plutonium and stripping of uranium (iii) final purification and conversion of uranium and plutonium to their respective oxides. The heart of PUREX process is liquid-liquid extraction of uranium(VI) and plutonium(IV) from the dissolver solution (3 - 4 M nitric acid medium). The metal loaded organic phase is then contacted with the aqueous solution containing uranous nitrate stabilized with hydrazine or ferrous sulfamate, which selectively reduces Pu(IV) present in the organic phase to inextractable Pu(III) [19]. The stripping of Pu(III) into aqueous phase enables the mutual separation of uranium and plutonium from organic phase. The uranium present in the organic phase is then recovered using dilute nitric acid. The uranium is then concentrated and precipitated as ammonium diuranate and finally calcinated to obtain uranium oxide. The plutonium(III) obtained is once again purified by either solvent extraction or ion exchange method [19] and then it is precipitated as Pu(IV)oxalate. The oxalate product is calcinated to obtain plutonium oxide. However, there are few limitations in the PUREX process such as chemical and radiolytic degradation of the solvent system and the generation of large volume of secondary waste [19]. The flammability of hydrocarbon employed in the PUREX process is also another disadvantage [20]. The aqueous waste produced after the PUREX process is known as “high-level liquid waste” (HLLW) [21].

1.4.1.1. High level liquid waste management

The HLLW contains several elements such as trivalent actinides called as minor actinides (MA), lanthanide fission products, other fission products, corrosion products of structural materials present in 3 - 4 M nitric acid medium [20,21]. The long term radioactivity of HLLW is essentially due to the minor actinides such as ^{237}Np, ^{241}Am, ^{243}Am, ^{244}Cm, ^{245}Cm, ^{243}Cm and fission products such as ^{99}Tc, ^{107}Pd, ^{93}Zr, ^{129}I, ^{135}Cs, ^{137}Cs, and ^{90}Sr. Since the half-lives of these isotopes vary from few years to several hundred years, the HLLW poses a long-term risk to the public health and safety of environment [21]. Therefore, the success of nuclear energy depends on the safe management of HLLW. Currently, immobilization of HLLW in a suitable non-leachable ceramic or glass matrix, followed by the deposition in deep geological repositories is being practiced [20-23]. However, it demands long-term surveillance of the waste form over thousands of years due to the presence of these minor actinides as their half-lives are very high. Moreover, in case of accidental ground-water invasion into these repositories, the radiotoxic metal ions can be released into the environment due to their significant solubility and mobility in aqueous medium [20-24]. Since these repositories require long-term surveillance, the current method for the disposal of HLLW in deep geological repositeries is very expensive.

Alternatively, the partitioning and transmutation (P&T) [22-25] strategy for the disposal of HLLW involving the removal of long lived minor actinides from HLLW followed by their transmutation into short lived isotopes in accelerator driven systems (ADS) or fast-reactorsis being considered as a viable option for the safe management of HLLW. The success of P&T strategy depends on the efficient separation of minor actinides from HLLW and burning them in ADS. The concentration of transplutonium actinides (Am and Cm) in HLLW is ~20 ppm and the concentration of lanthanide fission products is ~3000 ppm. The transplutonium actinides exist in trivalent oxidation state and chemically behave similar to trivalent lanthanides (Ln(III)) [25,26]. Due to high neutron absorption cross-section of Ln(III), the transmutation of An(III) in ADS or fast reactors is not efficient. Moreover, Ln(III) do not form solid solutions in metal alloys or in mixed oxide transmutation targets, and they tend to segregate as separate phases with the tendency to grow further upon thermal treatment. In view of this, it is necessary to separate Ln(III) from An(III) prior to actinide transmutation [25].

Therefore, the current method for partitioning of minor actinides from HLLW involves the liquid-liquid extraction of Ln(III) and An(III) together from HLLW in the first extraction cycle, followed by lanthanide-actinide separation in the second cycle. For the co-extraction of Ln(III) and An(III) from HLLW, several processes based on ligands such as octylphenyl-*N,N*-diisocarbamoylmethylphosphine oxide (CMPO) [27], TriAlkyl Phosphine Oxides (TRPO) [28], Di-IsoDecyl-Phosphoric Acid (DIDPA) [29], DIAMide Extraction (DIAMEX) [30,31], diglycolamides (DGAs) [32,33] and *N,N,N',N'*-tetraalkyl-3,6-dioxaoctane diamides (DOODA) [34] are available. After co-extraction of Ln(III) and An(III) they are recovered back as a group with dilute nitric acid (0.01 M) or with dilute nitric acid solution containing complexing agents such as citric acid, lactic acid etc. From the product obtained, the mutual separation of Ln(III) and An(III) was carried out to separate An(III) from Ln(III). Several processes such as TALSPEAK, SETFICS and REVERSE TALSPEAK etc. have been proposed for mutual separations [35].

1.4.2. Non-aqueous reprocessing

The non-aqueous reprocessing of spent nuclear fuel is a high temperature (pyrochemical) method. In non-aqueous reprocessing, an inorganic molten salt ($\underset{\sim}{}$ at 773 K) medium composed of chlorides of alkali or alkaline earth metals is used as an electrolytic medium for reprocessing the spent nuclear fuel [36]. This method exploits the differences in the thermodynamic stabilities of the chlorides of various actinides and fission products for the dissolution of spent nuclear fuel in the inorganic molten salt medium. After dissolution the actinides are recovered by electrochemical methods such as electrowinning and electrorefining [36,37].

1.5. Solvent extraction for aqueous reprocessing and waste management

Liquid-liquid extraction commonly known as solvent extraction is an importantseparation technology employed in various industries such as nuclear, metallurgical, pharmaceutical, biochemical, food and beverage, chemical, petrochemical, catalysis and polymers etc., for separation of targets from other major components [26,38] . Solvent extraction is the preferential distribution of a solute (for example, desired metal ion, M) between two immiscible liquid phases such as aqueous and organic phases in contact with each other. The solute M, dissolved in one liquid distributes into another immiscible liquid phase until its chemical potential becomes equal in both the phases. This condition is referred as equilibrium. The distribution of a solute in organic phase depends upon the coordinating ability of the ligand (known as the extractant) present in organic phase. In most of the solvent extraction processes, extractant is usually dissolved in a non-reactive organic medium in which it is completely miscible, is called as a diluent. The distribution ratio (D_M) of a solute M is defined as the ratio of the concentration of a solute in organic phase ($[M]_{org}$) to that in aqueous phase ($[M]_{aq}$) at equilibrium, as shown in equation 1.

$$D_M = \frac{[M]_{org}}{[M]_{aq}} \tag{1}$$

D_M is constant for given pair of liquids at constant temperature. In metal recovery operations, the valuable component is a metal ion or metal complex present in aqueous feed solution. This solution is contacted with an immiscible organic phase containing the active extractant. The extractant coordinates with the metal ion present in aqueous phase and transfers into the organic phase by a series of chemical reactions. This process is refered as “extraction”. The metal ion present in the loaded organic phase is recovered by ‘back extraction” using suitable aqueous reagents. This process is refered as “stripping”. The organic phase after stripping is called lean organic phase and is recycled back for extraction. The metal ion present in the aqueous phase then goes for final purification. In nuclear fuel cycle, solvent extraction process is usually employed for the recovery of uranium and thorium from various primary and secondary resources. Solvent extraction plays an important role in reprocessing of spent nuclear fuel and waste management.

1.6. Room temperature ionic liquids

In the recent past, room temperature ionic liquids have been receiving increased attention for possible applications in the area of nuclear fuel reprocessing and waste management [39-59]. Room temperature ionic liquids (RTILs) are compounds composed fully of dissociated ions and melt at temperatures lower than or equal to 373 K [60-62]. Typical examples of cation-anion combinations for making RTILs are shown in Fig. 1.2. The RTILs have many attractive properties such as insignificant vapour pressure, ability to dissolve a wide range of organic and inorganic compounds, wide electrochemical window, and tunability of properties by suitable combination of cation and anion etc,. Consequently, there has been a significant increase in the studies related to the use of RTILs in aqueous and non-aqueous reprocessing applications. Essentially, RTILs are investigated as possible substitute to the molecular diluent in solvent extraction procedures and as an alternative to high temperature molten salt in non-aqueous reprocessing applications [63,64]. However, some RTILs have also been employed as liquid ion exchangers in various solvent extraction procedures with conventional diluents [65]. Some of the striking features of RTILs that make them promising for nuclear fuel cycle application are listed below.

- The selectivity of target metal ion can be easily manipulated by the change of cation anion combinations of RTIL diluent, rather than redesigning the structure of the extractant.
- Presence of ionic diluent in organic phase facilitates a new mode of recovery of metals by direct electrodeposition from the extracted phase.
- Ionic liquids can be functionalized with organic moieties for task specific applications.

- RTILs can be designed to be completely incinerable, which would simplify the management of spent organic waste.
- Due to negligible vapor pressure of RTILs, the fire hazard is almost insignificant.

In addition, unusual extraction of metal ions has been observed when traditional extractants are used in conjunction with RTIL diluents. Thus, RTILs provide excellent challenges and opportunities to researchers and also shows the potential for technological applications.

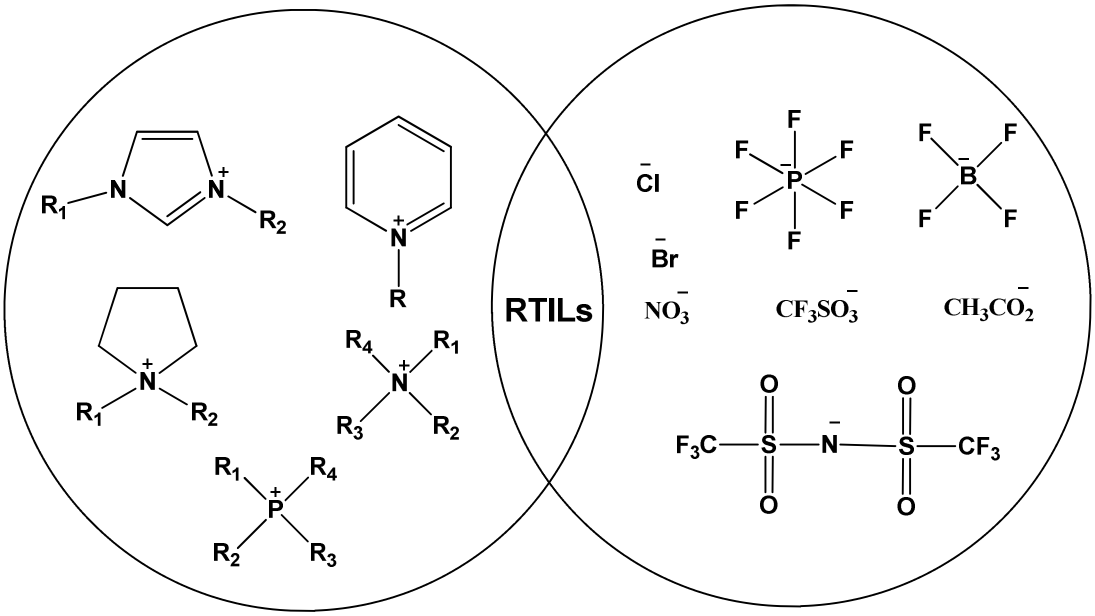

Fig.1.2. Structures various cations and anions used to form ionic liquids.

The history of RTIL has been reviewed in detail by Wilkes and Seddon [66,67]. The chemistry of salts with low melting points was on track in the second half of 19th century. The protic ionic liquid, ethanolammonium nitrate with the melting point of 52-55ºC was discovered by Gabriel [68]. Later in 1914, Paul Walden [69] reported the first stable and useful RTIL, namely, ethyl ammonium nitrate with a melting point of 12.5 ºC. Subsequently, the application of ionic liquids in various areas led to the synthesis of a variety of ionic liquids with desired physical and chemical properties. Based on the properties of RTILs, it can be classified into three main generations which are given below [70,71].

(i) First generation ionic liquids

The first generation ionic liquids are a mixture of organic species with $AlCl_3$. These ionic liquids are known as chloroaluminates [72]. The important property of these ionic liquids is their tunable viscosity, melting point and variable acidity of the melt. Major limitation of the first generation ionic liquid is the need of inert atmosphere for handling these type of ionic liquids due their hygroscopic property. However, these ionic liquids have been used as electrolytes in batteries.

(ii) Second generation ionic liquids

The air and water stable ionic liquids comprise the 2nd generation of ionic liquids. In 1992, Wilkis and Zoworoto [73] reported series of ionic liquids with imidazolium/pyridinum cation with anions such as tetrafluoroborate (BF_4^-) and hexafluorophosphate (PF_6^-) which have less reactivity towards water. However, the 2nd generation ILs with anions such as bis(trifluoromethanesulfonyl)imide (NTf_2^-), perfluoroalkylphosphate (FAP^-) are moisture stable and can easily handled without inert atmosphere due to the hydrophobic nature of anions.

(iii) *Third generation ionic liquids*

Third generation ionic liquids are task specific ionic liquids and chiral ionic liquids. In recent past, task specific ionic liquids (TSILs) have been received much attention and TSILs incorporate a functional group such that it can be applied to a specific task of interest.The cationic or anionic part of the room temperature ionic liquid tethered covalently with organic functionality is known as functionalized ionic liquid (FIL) or task specific ionic liquid (TSIL) [74,75]. These types of ionic liquids exhibit the properties of both ionic liquid and organic functionality, which makes them suitable for a wide range of applications in synthesis, catalysis and separation technology [76-85]. A sub class of functionalized ionic liquids known as ionic liquids with strongly coordinating anion wherein the anion of the ionic liquid itself is a functional moiety [85-89].

1.6.1. Synthesis of RTILs

Several reports are available for the synthesis of RTILs [90-92]. Most of the RTILs are synthesized by alkylation followed by an anion exchange reaction (metathesis). The alkylation of organic compounds such as 1-methyl imidazole, 1-methyl pyrrolidine or 1-methyl piperidine using alkyl halides results in the formation of organic halides. The anion exchange of these organic halides with some metal salts results in the formation of ILs. The ILs, after the synthesis is usually purified by solvent extraction followed by charcoal treatment. An illustration of the synthesis of RTIL is described in Fig. 1.3.

$$B + R\text{-}X \xrightarrow{\text{Reflux}} [B\text{-}R]^+ X^- \xrightarrow[M^+ A^-]{\text{Anion Exchange}} [B\text{-}R]^+ A^-$$

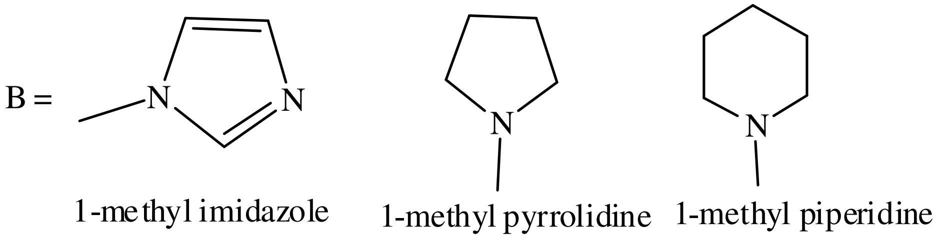

R = C_nH_{2n+1}, n = 2, 3 and so on.
X = Cl, Br, I etc.
M = H or Li or Na etc.
A = BF_4, PF_6, SCN, $N(CF_3SO_2)_2$

Fig. 1.3. Synthetic procedure for the preparation of RTILs.

Similarly the quarternary alkyl ammonium ionic liquids were synthesized by using the anion exchange of organic halides with some metal salts results in the formation of ionic liquids [92]. The Ionic liquids, after the syntheses are usually purified by solvent extraction followed by charcoal treatment. An illustration of the synthesis of quarternary alkyl ammonium ionic liquid is described in Fig. 1.4.

$$[H_3CNR_3]^+ [Cl]^- \xrightarrow[M^+ A^-]{\text{Anion Exchange}} [H_3CNR_3]^+ [A]^-$$

$R = C_4H_9$ or C_8H_{17}

M = Li or Na or K etc.

$A = NO_3, N(CF_3SO_2)_2$

Fig. 1.4. Synthetic procedure for the preparation of quaternary alkyl ammonium ionic liquid.

1.6.2. Properties of RTILs

RTILs have several fascinating properties, unique to the combination of a particular cation and anion. These include negligible vapor pressure at ambient temperatures, wide liquid range, high polarity, high thermal stability, appreciable electrical conductivity, wide electrochemical window (thermodynamic stability) and solubility of organic and inorganic species. Some properties of the RTILs relevant to the present study are described below.

1.6.2.1. Melting Point

Room temperature ionic liquids have melting points less than 100 °C. Melting point of RTILs depends on the crystal structure, size and symmetry of the ions, charge density of the ions, efficiency of hydrogen bonding and the Vander Waals interactions [93]. When melting points of ionic liquids are compared with that of inorganic salts (for example, 803 °C for NaCl and 70 °C for 1-butyl-3-methylimidazolium chloride) it is clear that the most of the reduction in melting temperature is caused by replacing the small inorganic cations by bulky asymmetric organic cations. The melting point of many ionic liquids is very uncertain due to their supercooling nature [93,94].

1.6.2.2. Density

The densities of most of the RTILs are more than that of water and these values are in the range of 1.12 to 2.4 g cm^{-3}. The densities of many ILs have been reported in the book 'Ionic liquids in Synthesis' by Wasserscheid and Welton [93]. In the case of imidazolium based ILs, the density of IL decreases with an increase in the chain length of the alkyl group attached to the imidazolium cation [94,97]. For quaternary ammonium based RTILs with different anions such as $[NO_3]^-$, Cl^- and $[CH_3COO]^-$, the density is in the range of 0.8-0.9. The presence of impurities and water has an influence on their densities to a large extent [95].

1.6.2.3. Viscosity

The viscosity of RTILs is two to ten times greater than the viscosity of the conventional organic solvents due to the strong electrostatic and other interaction forces between the oppositely charged ions. For example, the viscosity of $[C_4mim][PF_6]$ is ~430 cP [96], $[C_4mim][BF_4]$ is ~154 cP [95], and $[C_4mim][NTf_2]$ is ~52 cP at 25 ^{o}C [97]. Since the viscosity of the RTIL is dependent on electrostatic interaction, the delocalization of charge on the cation or anion results in lowering the viscosity [93-99]. Seddon *et al.* reported that the viscosity of 1-alkyl-3-methylimidazolium based ILs increases with increasing the alkyl chain length attached to imidazolium cation [95]. Moreover, it was reported that quaternary ammonium based ILs were more viscous than imidazolium based ILs containing the same anion [92].

1.6.2.4. Vapour pressure

The pressure exerted by a vapour in equilibrium with its liquid phase is known as vapour pressure. Generally, RTILs exhibit very low vapour pressure due to their ionic nature. Therefore, RTILs have been recognized as non-volatile liquids at normal pressures and even at high temperatures [100,101].

1.6.2.5. Polarity

The stability extraction of metal ion depends upon the stability of the metal-ligand complex in organic phase, which in turn depends upon the degree of interaction between medium and metal-ligand complex, or simply the polarity of the medium [102-104]. Since ionic liquids comprise entirely of ions, it is quite likely that the use of ionic liquid as diluent could dramatically increase the polarity of organic phase. However, determining the polarity of organic phase is a challenging job and so far only indirect methods have been suggested for measuring the polarity of the medium [105-106]. Among the various methods the most easiest method is to use solvatochromic probes such as pyridinium-N-phenolate betaine dye, known as Reichardt's dye N(30) or betaine dye, for the measurement of polarity of the medium [30,31]. The Reichardt's dye exhibits the maximum absorption (λ_{max}) in the visible region and depending upon the polarity of the medium, the position of λ_{max} is different. In the recent past, several reports are available dealing with the determination of the normalized polarity values of RTILs using Reichardt's dye as solvatochromic probe [107]. However, the polarity of the organic solution containing the nitric acid in ionic liquid, ligand in ionic liquid, and metal-ligand complexes in ionic liquid medium etc., have not been explored so far. Infact, the polarity of the organic phase obtained after liquid-liquid extraction is important for understanding the insights of solvent extraction as well as third phase formation behavior.

1.6.2.6. Thermal stability

Most of the RTILs are thermal stable due to their ionic nature [60,61,108]. For instance, Bonhote *et al.* reported that C_4mimNTf$_2$ was stable up to 400 ^oC and decomposes rapidly above 440 ^oC [109]. Ngo *et al.* reported that the thermal stabilities of imidazolium based RTILs increase with alkyl chain length attached to the imidazolium cation [110]. Jagadeeswara Rao *et al.* investigated and reported the thermochemical properties of ionic liquids such as [Hbet][NTf$_2$], [C_3mpip][NTf$_2$] and [C_4mpyr][NTf$_2$] [111].

1.6.3. Applications of RTILs

The applications of RTILs are on the increase in various fields such as organic synthesis, electrochemistry, catalysis, analytical chemistry, separation technology, cellulose processing and biochemistry etc, [112-119]. Initially, the RTILs were proposed as solvents in organic synthesis by Fry and Pienta [120]. The application of RTILs in organic synthesis was reported in detail by Sethi *et al.* [121] and also in the book 'Ionic Liquids in Organic Synthesis' edited by Malhotra [122]. The review articles on the applications of RTILs in various areas by Koel, catalytic applications of task specific ILs authored by Geirnoth, electrodeposition of metals using ILs by Simka *et al.* and applications of RTILs in electrochemical sensors by Wei *et al.* are reported in leiterature [123,75,124,125]. Similarly, Davis *et al.* and D. Han *et al*. reported the applications of RTILs in different areas of separation technology [74,126]. In addition to academic research, RTILs have also been used in several industrial applications. For instance, a review on the applications of RTILs in chemical industry has been reported by Plechkova and seddon [119] . The industrial application of RTILs as performance additives was reported by Weyershausen *et al.* BASF made the first attempt of using RTILs for various industrial processes [127]. Eastman operated an IL based plant for the synthesis of 2,5-dihdrofuran from 1996 to 2004 [119].

1.6.4. The role of RTILs in nuclear fuel industry

RTILs are receiving an upsurge for possible applications in the different stages of the nuclear fuel cycle, In aqueous reprocessing, the RTILs are being explored as diluent or extractant in solvent extraction applications. The replacement of a molecular diluent (*n*-dodecane) by RTIL in solvent extraction process was introduced by Huddleston and Dietz *et al* [91,128]. Initially, Dai *et al.* [129] and subsequently Visser *et al.* [130] reported to separate group I and II metal ions from aqueous medium using a solution of crown ether in imidazolium based ionic liquid and Visser *et al.* [131] extensively studied the extraction of cesium and strontium from nitric acid medium by using various crown ethers (18C6, DCH18C6, and DtB18C6) in $[C_nmim][PF_6]$ (n = 4, 6, 8) ionic liquid. The extraction of U(VI) from nitric acid medium by a solution of TBP in $[C_4mim][PF_6]$ or $[C_4mim][NTf_2]$ was reported by Giridhar *et al.* and this study indicates the possibility of varying the distribution ratio of uranium(VI) by changing the cation-anion combinations [132,133]. The mechanism of U(VI) extraction in TBP dissolved in ionic liquid was investigated in detail by Dietz [134]. Similarly, Billard *et al.* investigated the mechanism of U(VI) extraction in $TBP/[C_4mim][NTf_2]$ and the model proposed by the authors involves the extraction of U(VI) through the cation exchange of $[UO_2(TBP)_n]^{2+}$ species with $[C_4mim]^+$ ion and $H^+(TBP)_n$ in ionic liquid phase at low acidities [135]. Anion exchange of $[UO_2(NO_3)_3(TBP)_m]^-$ species with NTf_2 of ionic liquid was stated to be responsible for uranium extraction at high acidities [135,136]. Rama *et al.* investigated the extraction of U(VI) in trialkylphosphates in 1-alkyl-3-methyl imidazolium bis(trifluoromethylsulfonyl)imide $[C_nmim][NTf_2]$ (n = 4, 6, 8) [137]. Rout *et al.,* reported the mutual separation of europium(III) and americium(III) using RTIL as diluent with acidic extractants [138]. Nakashima *et al.* [139] studied, in detail, the extraction of trivalent lanthanides in $CMPO/[C_4mim][PF_6]$ and reported that the extraction efficiency of CMPO for metal ions was higher in ionic liquid medium as compared to the dodecane system. Panja *et al*. reported the extraction behavior of Am(III), Pu(IV) and U(VI) using *N*,*N*,*N′*,*N′*-tetra-octyl diglycolamide (TODGA) in imidazolium based ionic liquid and reported that the distribution ratio of Am(III), Pu(IV) and U(VI) were found to be higher in ionic liquid system than that obtained in *n*-DD diluents [140]. The organic functionalities that can perform specific applications are covalently tethered to the cationic or anionic part of the RTIL are known as functionalized ionic liquids (FILs) or task specific ionic liquids (TSILs). The presence of the functional group and ionic moieties in the resultant FIL is expected to show the properties of both organic functionality and ionic liquid property. In this context, various studies have been reported in the recent past for the separation of actinides and fission products from a wide variety of acid feed solutions using FILs [141-144].

1.6.5. Third phase formation behaviour in liquid-liquid extraction

One of main concerns in the extraction of trivalent actinides and lanthanides from HLLW using the conventional solvent system is the third phase formation. It is the splitting of organic phase into a couple of phases during the course of solvent extraction. The problem of third phase formation in a counter-current solvent extraction procedure is described elsewhere [145]. In a conventional liquid-liquid extraction systems, the solvent phase is composed of a polar ligand diluted in an inert molecular diluent medium, such as *n*-dodecane. Due to the polar nature of the ligand, it tends to undergo aggregation in organic phase, which eventually leads to third phase formation. Few options are available for preventing the third phase formation. The first option is to add phase modifiers to the organic phase for dispersing the third phase. However, there are problems associated with the addition of phase modifiers, as described elsewhere [146]. Alternatively, the best method for preventing the third phase formation is to employ strongly polar diluent in place of a molecular diluent (*n*-DD) for stabilizing the polar metal-ligand complex formed in organic phase. One such polar compound is the room temperature ionic liquid, which can be exploited for preventing the third phase formation

1.6.6. Radiolytic stability of ionic liquid

In the last two decade, room temperature ionic liquids (RTILs) have been extensively studied for the separation of metal ions, both radioactive and non-radioactive, from aqueous solution composed of nitric acid and hydrochloric acid medium [147-152]. When the solvent phase (ligand + diluent) is proposed for the treatment of radioactive solutions, it is necessary to evaluate the radiation stability of the solvent phase. In this context the radiation stability of the $[C_n mim][NTf_2]$ ionic liquid has been studied by several authors over the last two decades and published reviews on the radiation chemistry of ionic liquids [151-153]. The reports revealed that $[NTf_2]^-$ ionic liquids undergo radiolytic degradation yielding significant amount of the aqueous soluble products such as F^-, SO_4^{2-}, CF_3SO_3H, etc., [154]. It should be noted that all these degradation products are undesirable for employing $[NTf_2]^-$ ionic liquids for solvent extraction applications in nuclear fuel cycle. Nevertheless, several authors continued the studies with ionic liquids containing P, F and S atoms in the cation or anionic part of the ionic liquid, perhaps owing to the extraordinary extraction of radioactive metal ions, when ionic liquids are employed in conjunction with common ligands. Therefore, the limitations of these conventional ionic liquids have been disregarded, when compared to extraordinary extraction achieved in ionic liquid medium. However, it is realized that unless the issue of ion exchange, both cation and anion exchange, and the radiolytic stability of the ionic liquid are addressed, the ionic liquids would not find much application in nuclear fuel cycle (solvent extraction).

1.7. Motivation for the present study

Reprocessing of spent nuclear fuel (SNF) is essential for the sustained growth of nuclear power program in India. PUREX process has been adopted globally for the recovery of valuable materials such as uranium and plutonium from the spent nuclear fuel dissolver solution. The literature survey shows that there are several challenges in the extraction of metal ions using the traditional extractants present in molecular diluent medium (*n*-DD). These include low extraction efficiency, third phase formation and radiolytic degradation etc. To overcome these problems, RTILs have been used as diluent in the present study and explored for solvent extraction applications.

The ionic liquids employed for solvent extraction application usually contained 1-alkyl-3-methylimidazolium $[C_nmim]^+$ cation in association with an anion. To make the ionic liquid suitable for solvent extraction, the $[C_nmim]^+$ cation is combined with hydrophobic anions such as $[PF_6]^-$ or bis(trifluoromethanesulfonyl) imide ($[NTf_2]^-$) etc., and studied for the extraction of metal ions in conjunction with traditional extractants. However, the inherent property of the ionic liquid namely the cation and anion exchange with various ions present in the aqueous phase could not be avoided during solvent extraction. Such ion exchange behavior of ionic liquid is regarded as a “dirty” process, owing to the fact that the ionic liquid is irreversibly lost from the organic phase. In addition, the presence of organic ions in aqueous phase pollutes the aqueous phase and therefore further treatment of aqueous phase becomes difficult. In view of this, it is necessary to choose appropriate cation-anion combination of the ionic liquid such that the RTIL is devoid of undergoing any ion exchange, but retaining all the good properties of the ionic liquid. Moreover, for the separation of target metals from radioactive feed solution, it is also desirable to select the ionic liquid, which is made up of CHON-atoms so that the ionic liquid is completely incinerable and the waste disposal of the spent ionic liquid becomes easy.

In recent past, the ionic liquids containing quaternary alkyl ammonium cations for instance methyltrioctylammonium cation $[N_{1888}]^+$ are becoming popular for the extraction of radioactive metal ions in nuclear fuel cycle. The important features of these quaternary alkyl ammonium ionic liquids suitable for nuclear fuel cycle applications are (a) they are made up of C and N atoms, obeying the CHON-principle; (b) strongly hydrophobic and therefore they do not undergo cation exchange; (c) the viscosity of the aqueous equilibrated quaternary alkyl ammonium ionic liquid is less than 100 mP.s, which can be acceptable for solvent extraction application; (d) unlike *n*-dodecane, the use of ionic liquids in general, and quaternary ammonium ionic liquid in particular, do not result in third phase formation. It should be noted that the anion associated with $[N_{1888}]^+$ ion usually undergoes anion exchange with anions present in aqueous phase. However, when the $[N_{1888}]^+$ is combined with $[NO_3]^-$ anion, the resultant ionic liquid, $[N_{1888}][NO_3]$ can be regarded as acceptable for nuclear fuel cycle applications, since the feed solution for reprocessing applications is composed of nitric acid medium. Therefore the anion NO_3^- is “akin” to reprocessing feed solutions, while the anions containing F, S and P atoms are regarded as “alien” ions for reprocessing applications.

1.8. Objective of the present study

The objective of the present work was to identify the ionic liquid which was devoid of above mentioned drawbacks and that ionic liquid explore the possibility of using that ionic liquid for various applications in nuclear fuel cycle. In this context, some ammonium ionic liquids have been developed and explored for the solvent extraction of actinides, lanthanide fission products from nitric acid solutions. Since the results obtained from those studies were very peculiar and unique to an ionic liquid, the study was also focused on understanding the insights of solvent extraction by probing the co-ordination chemistry of metals present in the extracted ionic liquid phase, determination of the polarity index of the extracted phase and radiolytic stability. For this purpose, the extracted ionic liquid phase was subjected to dynamic light scattering and spectroscopic studies such as UV-Visible, ATR-FTIR, Raman spectroscopy and DFT calculations. The results obtained were compared with those obtained in a molecular diluent medium (*n*-dodecane) and with conventional imidazolium based ionic liquids and reported in this thesis.

References

1. J. Goldemberg, Energy: What everyone needs to know. Oxford University Press; 2012.
2. K. Menyah, Y. Wolde-Rufael, CO_2 emissions, nuclear energy, renewable energy and economic growth in the US, Energy policy. 38 (2010) 2911-2915.
3. S. Shafiee, E. Topal, When will fossil fuel reserves be diminished?, Energy Policy. 37 (2009) 181-189.
4. R.B. Grover, S. Chandra, Scenario for growth of electricity in India. Energy Policy 34 (2006) 2834-2847.
5. S. David, Future Scenarios of fission based reactors, Nucl. Phys. A. 751 (2005) 429–441.
6. S.A. Bhardwaj, Indian nuclear power programmed–Past, present and future. Sadhana 38 (2013) 775-794.
7. http://www.energy.gov/ne/articles/nuclear-101-how-does-nuclear-reactor-work
8. H.J. Bhabha, The role of atomic power in India and its immediate possibilities, Proc. of the international conference on the peaceful uses of atomic energy held in Geneva, 1 (1955) 103.
9. http://www.npcil.nic.in/main/AllProjectOperationDisplay.aspx
10. R.D. Kale, India's fast reactor programme–A review and critical assessment, Progress in Nuclear Energy. 122 (2020) 103265.
11. Baldev Raj, History and evolution of fast reactor design in India, IGC Newslett. (2006) 69.
12. S. Usha, R.R. Ramanarayanan, P. Mohanakrishnan, R.P. Kapoor, Research reactor KAMINI, Nucl. Eng. Des. 236 (2006) 872-880.

13. P.A. Baisden, G.R. Choppin, Nuclear waste management and the nuclear fuel cycle, Radiochemistry and nuclear chemistry. (2007) 1-63.
14. Nuclear Energy Agency, Advanced Nuclear Fuel Cycles and Radioactive Waste Management, Oecd. (2006) 244.
15. R.G. Cochran, E.E. Lewis, N. Tsoulfanidis, W.F. Miller, The nuclear fuel cycle: analysis and management. American Nuclear Society (1990).
16. D.D. Sood, S.K. Patil, Chemistry of nuclear fuel reprocessing: Current status, J. Radioanal. Nucl. Chem. 203 (1996) 547–573.
17. P.K. Dey, N.K. Bansal, Spent fuel reprocessing: A vital link in Indian nuclear power program. Nucl. Eng. Des. 236 (2006) 723.
18. H.A.C. Mckay, J.H. Miles, J.L. Swanson, The PUREX Process. In Science and Technology of tributyl phosphate (Applications of Tributyl Phosphate in Nuclear Fuel Reprocessing); W.W. Schulz, J.D. Navratil, K.P. Bender, Eds.; CRC Press, Inc: Boca Raton Florida, U.S.A., Vol. III (1990) 1.
19. J.L. Swanson, The PUREX process. Part 3. PUREX Process Flowsheets In Science and Technology of tributyl phosphate (Applications of Tributyl Phosphate in Nuclear Fuel Reprocessing); W.W. Schulz, J.D. Navratil, K.P. Bender, Eds.; CRC Press, Inc: Boca Raton Florida, U.S.A., Vol. III (1990) 55.
20. J. Veliscek-Carolan, Separation of actinides from spent nuclear fuel: A review, J. Hazard. Mater. 318 (2016) 266-281.
21. I.W. Donald, B.L. Metcalfe, R.J. Taylor, The immobilization of high level radioactive wastes using ceramics and glasses, J. Mater. Sci. 32 (1997) 5851-5887.

22. M. Salvatores, G. Palmiotti, Radioactive waste partitioning and transmutation within advanced fuel cycles: Achievements and challenges, Prog. Part. Nucl. Phy. 66 (2011) 144-166.

23. J.N. Mathur, M.S. Murali, K.L. Nash, Actinide partitioning-A review, Solvent Extr. Ion Exch. 19 (2001) 357–390.

24. C. Madic, N. Ouvrier, EUROPART: EUROpean research program for the PARTitioning of minor actinides from high active wastes arising from the reprocessing of spent nuclear fuels, Radiochim. Acta. 96 (2008) 183–185.

25. S.A. Ansari, P. Pathak, P.K. Mohapatra, V.K. Manchanda, Aqueous partitioning of minor actinides by different processes, Sep. Purif. Rev. 40 (2011) 43–76.

26. G.M. Ritcey, Solvent extraction in hydrometallurgy: Present and future, Tsinghua Sci. Technol. 11 (2006) 137–152.

27. E.P. Horwitz, D.G. Kalina, The extraction of Am (III) from nitric acid by octyl(phenyl)-N,N-diisobutylcarbomylmethylphosphine oxide- tri-n-butylphosphate mixtures, Solvent Extr. Ion Exch. 2 (1984) 179–200.

28. X. Liu, J. Liang, J. Xu, Simplified Chinese TRPO process to extract and recover transuranium elements from high-level liquid waste, Solvent Extr. Ion Exch. 22 (2004) 163–173.

29. Y. Morita, J.P. Glatz, M. Kubota, L. Koch, G. Pagliosa, K. Roemer, A. Nicholl, Actinide Partitioning from HLW in a continuous DIDPA extraction process by means of centrifugal extractors, Solvent Extr. Ion Exch. 14 (1996) 385–400.

30. O. Courson, M. Lebrun, R. Malmbeck, G. Pagliosa, K. Romer, B. Satmark, J.P. Glatz, Partitioning of minor actinides from HLLW using the DIAMEX process. Part 1 -

Demonstration of extraction performances and hydraulic behaviour of the solvent in a continuous process, Radiochim. Acta, 88 (2000) 857–863.

31. R. Malmbeck, O. Courson, G. Pagliosa, K. Römer, B. Sätmark, J.P. Glatz, P.R. Baron, Partitioning of minor actinides from HLLW using the DIAMEX process. Part 2-“Hot” continuous counter-current experiment, Radiochim. Acta, 88 (2000) 865–871.
32. Y. Sasaki, Y. Sugo, S. Suzuki, S. Tachimori, The novel extractants diglycolamides for extraction of lanthanides and actinides in HNO_3-n-dodecane system, Solvent Extr. Ion Exch. 19 (2001) 91-103.
33. S.A. Ansari, P. Pathak, P.K. Mohapatra, V.K. Manchanda, Chemistry of diglycolamides: Promising extractants for actinide partitioning, Chem. Rev. 112 (2012) 1751–1772.
34. H. Narita, T. Yaita, S. Tachimori, Extraction of lanthanides with N, N’-dimethyl-N, N’-diphenyl-malonamide and-3,6-dioxaoctanediamide, Solvent Extr. Ion Exch. 22 (2004) 135–145.
35. A.V. Gelis, G.F. Vandegrift, A. Bakel, D.L. Bowers, A.S. Hebden, C. Pereira, M.Regalbuto, Extraction behaviour of actinides and lanthanides in TALSPEAK, TRUEX and NPEX processes of UREX+, Radiochim. Acta. 97 (2008) 231-245.
36. A.V. Bychkov, O.V. Skiba, Review of non-aqueous nuclear fuel reprocessing and separation methods, Chemical Separation Technologies and Related Methods of Nuclear Waste Management, Springer, Dordrecht (1999) 71–98.
37. C.C. Mcpheeters, R.D. Pierce, T.P. Mulcahey, Application of the pyrochemical process to recycle of actinides from LWR spent fuel, Prog. Nucl. Energy. 31 (1997) 175.
38. Rydberg, Solvent extraction principles and practice, revised and expanded. CRC press; 2004.

39. J.D. Holbrey, K.R. Seddon, Ionic Liquids. Clean Products and Processes. 1 (1999) 223-236.

40. K. Binnemans, Lanthanides and actinides in ionic liquids, Chem. Rev. 107 (2007) 2592-2614.

41. N. K. Gupta, Ionic liquids for TRansUranic Extraction (TRUEX)—Recent developments in nuclear waste management: A review, J. Mol. Liq. 269 (2018) 72-91.

42. I. Billard, A. Ouadi, C. Gaillard, Liquid–liquid extraction of actinides, lanthanides, and fission products by use of ionic liquids: from discovery to understanding, Anal. Bioanal. Chem. 400 (2011) 1555-1566.

43. X. Sun, H. Luo, S. Dai, Ionic liquids-based extraction: a promising strategy for the advanced nuclear fuel cycle, Chem. Rev. 112 (2011) 2100-2128.

44. P.K. Mohapatra, Actinide ion extraction using room temperature ionic liquids: opportunities and challenges for nuclear fuel cycle applications, Dalton Trans. 46 (2017) 1730-1747.

45. P.R.Vasudeva Rao, K.A. Venkatesan, Alok Rout, T.G. Srinivasan, K. Nagarajan, Potential applications of room temperature ionic liquids for fission products and actinide separation, Sep. Sci. Technol. 47 (2012) 204-222.

46. M. Straka, Toward a Greenish Nuclear Fuel Cycle: Ionic Liquids as Solvents for Spent Nuclear Fuel Reprocessing and Other Decontamination Processes for Contaminated Metal Waste, Phys. Sci. Rev. 1 (2016) 74.

47. I. Billard, Ionic liquids: new hopes for efficient lanthanide/actinide extraction and separation?. Handbook on the physics and chemistry of rare earths, Elsevier. 43 (2013) 213-273.

48. Alok Rout, PhD Thesis: Room temperature ionic liquids for the separation of actinides and fission products. Homi Bhabha National Institute, 2012.

49. R. Rama, PhD Thesis: Solvent extraction and electrochemical studies of lanthanmides and actinides in room temperature ionic liquid medium containing various extractants. Homi Bhabha National Institute, 2017.

50. V.A. Cocalia, K.E. Gutowski, R.D. Rogers, The coordination chemistry of actinides in ionic liquids: A review of experiment and simulation, Coord. Chem. Rev. 250 (2006) 755-764.

51. A.V. Mudring, S. Tang, Ionic liquids for lanthanide and actinide chemistry, Eur. J. Inorg. Chem. 18 (2010) 2569-2581.

52. S. Stumpf, I. Billard, P.J. Panak, S. Mekki, Differences of Eu (III) and Cm (III) chemistry in ionic liquids: investigations by TRLFS, Dalton Trans. 2 (2007) 240-248.

53. A.E. Visser, R.D. Rogers, Room-temperature ionic liquids: new solvents for f-element separations and associated solution chemistry, J. Solid State Chem. 171 (2003) 109-113.

54. X. Sun, D. Wu, Ji. Chen, D. Li, Separation of scandium(III) from lanthanides(III) with room temperature ionic liquid based extraction containing Cyanex 925, J. Chem. Technol. Biotechnol. 82 (2007) 267–272.

55. Z.B. Xie, H.T. Kang, Z.S. Chen, S.H. Zhang, Z.G. Le, Liquid–liquid extraction of U (VI) using malonamide in room temperature ionic liquid, J. Radioanal. Nucl. Chem. 308 (2016) 573-578.

56. Alok Rout, K.A. Venkatesan, T.G. Srinivasan, P.R. Vasudeva Rao, Liquid–liquid extraction of Pu(IV), U(VI) and Am(III) using malonamide in room temperature ionic liquid as diluents, J. Hazard. Mater. 221(2012) 62-67.

57. A.N. Turanov, V.K. Karandashev, M. Boltoeva, C. Gaillard,V. Mazan, Synergistic extraction of uranium (VI) with TODGA and hydrophobic ionic liquid mixtures into molecular diluent, Sep. Purif. Technol. 164 (2016) 97-106.

58. Alok Rout, K.A. Venkatesan, T.G. Srinivasan, P.R. Vasudeva Rao, Ionic liquid extractants in molecular diluents: Extraction behavior of europium (III) in quarternary ammonium-based ionic liquids, Sep. Purif. Technol. 95 (2012) 26-31.

59. Alok Rout, K.A. Venkatesan, T.G. Srinivasan, P.R. Vasudeva Rao, Tuning the extractive properties of Purex solvent using room temperature ionic liquid, Sep. Sci. Technol. 8 (2013) 2576-2581.

60. T. Welton, Room-temperature ionic liquids. Solvents for synthesis and catalysis, Chem. Rev. 99 (1999) 2071–2084.

61. M. Freemantle, An Introduction to Ionic liquids, RSC Publishing. 2010.

62. M. J. Earle, K.R. Seddon, Ionic liquids. Green solvents for the future, Pure Appl. Chem. 72 (2000) 1391-1398.

63. K.A. Venkatesan, T.G. Srinivsan, P.R. Vasudeva Rao, A review on the electrochemical applications of room temperature ionic liquids in nuclear fuel cycle, Journal of nuclear and radiochemical sciences. 10 (2009) 1_R1-6.

64. K.A. Venkatesan, Ch. Jagadeswara Rao, K. Nagarajan, P.R. Vasudeva Rao, Electrochemical Behaviour of Actinides and Fission Products in Room-Temperature Ionic Liquids, Int. J. Electrochem. 2012 (2012).

65. M.L. Dietz, J.A. Dzielawa, Ion-exchange as a mode of cation transfer into room-temperature ionic liquids containing crown ethers: Implications for the ‘greenness’ of

ionic liquids as diluents in liquid–liquid extraction, Chem. Commun. 20 (2001) 2124–2125.

66. J.S. Wilkes, A short history of ionic liquids—from molten salts to neoteric solvents, Green Chem. 4 (2002) 73–80.

67. K.R. Seddon, Ionic liquids: A taste of the future, Nat. Mater. 2 (2003) 363–365.

68. S. Gabriel, J. Weiner. “Ueber einige Abkommlinge des Propulamins” Ber, Eur. J. Inorg. Chem, 21 (1888) 2669-2679.

69. P. Walden, Bull. Acad. Imper. Sci. (St. Petersberg), (1914) 1800.

70. M. Smiglak, A. Metlen, R.D. Rogers, The Second Evolution of Ionic Liquids: From Solvents and Separations to Advanced Materials—Energetic Examples from the Ionic Liquid, Cookbook. Acc. Chem. Res. 40 (2007) 1182 – 1192.

71. W.L. Hough, M. Smiglak, H. Rodríguez, R.P. Swatloski, S.K. Spear, D.T. Daly, J. Pernak, J.E. Grisel, R.D. Carliss, M.D. Soutullo, J.H. Davis, The third evolution of ionic liquids: active pharmaceutical ingredients. New J. Chem. 31 (2007) 1429-1436.

72. J. S. Wilkes, J. A. Levisky, R. A. Wilkes, C. L. Hussey, Dialkylimidazolium chloroaluminate melts: a new class of room temperature ionic liquids for electrochemistry, spectroscopy andsynthesis. Inorg. Chem. 21 (1982)1263-1264.

73. J. S. Wilkes, M. J. Zaworotko, Air and water stable 1-ethyl-3-methylimidazolium based ionic liquids, J. Chem. Soc. Chem. Comm. 1 (1992) 965 - 967.

74. J.H. Davis Jr, Task-specific ionic liquids, Chem. Lett. 33 (2004) 1072.

75. C. C. Brasse, U. Englert, A. Salzer, H. Waffenschmidt, P. Wasserscheid, Ionic Phosphine Ligands with Cobaltocenium Backbone: Novel Ligands for the Highly Selective,

Biphasic, Rhodium-Catalyzed Hydroformylation of 1-Octene in Ionic Liquids, Organometallics. 19 (19) (2000) 3818 - 3823.

76. P. Wasserscheid, H. Waffenschmidt, P. Machnitzki, K. Kottsieper, O. Selzer, Cationic phosphine ligands with phenylguanidinium modified xanthene moieties—a successful concept for highly regioselective, biphasic hydroformylation of oct-1-ene in hexafluorophosphate ionic liquids, Chem. Commun. (2001) 451 - 452.

77. R. Giernoth, Task-Specific Ionic Liquids. Angew. Chem. Int. Ed. 49 (16) (2010) 2834–2839.

78. A. E. Visser, R.P. Swatloski, W.M. Reichert, R. Mayton, S. Sheff, A. Wierzbicki, J.H. Davis, R. D. Rogers, Task specific ionic liquids incorporating novel cations for the coordination and extraction of Hg^{2+} and Cd^{2+}: Synthesis, characterization and extraction studies, Envir. Sci. Technol. 36 (2002) 2523-2529.

79. A. E. Visser, R.P. Swatloski, W.M. Reichert, R. Mayton, S. Sheff, A. Wierzbicki, J.H. Davis Jr, R.D. Rogers, Task specific ionic liquids for the extraction of metal ions from aqueous solutions, Chem. Commun. 1 (2001)135-136.

80. I. L. Odinets, E. V. Sharova, O. I. Artyshin, K. A. Lyssenko, Y. Nelyubina, V.Myasoedova, V. Galina, N. P. Molochnikova, E. A. Zakharchenro, Novel class of functionalized ionic liquids with grafted CMPO-moieties for actinides and rare earth elements recovery, Dalton Trans. 39 (2010) 4170-4178.

81. A. Ouadi, B. Gadenne, P. Hesemann, J. E. Moreau, I. Billard, C. Gaillard, S. Mekki, G. Moutiers, Task-Specific Ionic Liquids Bearing 2-Hydroxybenzylamine Units: Synthesis and Americium-Extraction Studies, Chem. Eur. J. 12 (2006) 3074–3081.

82. A. Ouadi, O. Klimchuk, C. Gaillard, I. Billard, Solvent extraction of U(VI) by task specific ionic liquids bearing phosphoryl groups, Green Chem. 9 (2007) 1160–1162.
83. H. Luo, S. Dai, P. V. Bonnesen, A.C. Buchanan, Separation of fission products based on ionic liquids: Task-specific ionic liquids containing an aza-crown ether fragment. J alloys and Compds. 418 (2006) 195–199.
84. P. Nockemann, B. Thijs, S. Pittois, J. Thoen, C. Glorieux, K.V. Hecke, L. Van Meervelt, B. Kirchner, K. Binemanns, Task specific ionic liquid for solubilizing metal oxides, J. Phys. Chem. B. 110 (2006) 20978-20992.
85. J. H. Olivier, F. Camerel, R. Ziessel, Lanthanide Ion Extraction by Trifluoromethyl-1,3-diketonate-Functionalised Ionic Liquids Adsorbed on Silica, Chem. Eur. J. 17 (2011) 9113- 9122.
86. X. Sun, Y. Ji, L. Zhang, J. Chen, D. Li, Separation of cobalt and nickel using inner synergistic extraction from bifunctional ionic liquid extractant (Bif-ILE), J. Hazard. Matter. 182 (2010) 447-452.
87. H. Mehdi, K. Binnemans, V. Hecke, L.V. Meervelt, P. Nockemann, Hydrophobic ionic liquids with strongly corodinating anions, Chem. Commun. 46 (2010) 234-236.
88. X. Sun, Y. Ji, F. Hu, Bo. He, Ji. Chen, D. Li, The inner synergistic effect of bifunctional ionic liquid extractant for solvent extraction, Talanta. 81 (2010) 1877–1883.
89. Y. Hua-Ling, W. Wei, C. Hong-Min, C. Ji, Extraction Mechanism of Rare Earths with Bifuncional Ionic Liquids (Bif-ILs) [A336][CA-12]/[A336][CA-100] in Nitrate Medium. Chin. J. Anal. Chem. 39 (2011) 1561–1566.
90. A. Stark, K.R. Seddon, Ionic liquids, In: Kirk-Othmer Encyclopedia of Chemical Technology, Vol. 26, John Wiley, New York, 2007.

91. J.G. Huddleston, A.E. Visser, W.M. Reichert, H.D. Willauer, G.A. Broker, R.D. Rogers, Characterization and comparison of hydrophilic and hydrophobic room temperature ionic liquids incorporating the imidazolium cation, Green Chem. 3 (2001)156–164.

92. J. P. Mikkola, P. Virtanen, R. Sjöholm, Aliquat 336 - A versatile and affordable cation source for an entirely new family of hydrophobic ionic liquids, Green Chem. 8 (2006) 250-255.

93. P. Wasserscheid, E. T. Welton, Ionic Liquids in Synthesis. Wiley-VCH verlag GmbH & Co. KGaA, 2008.

94. K.R. Seddon, A. Stark, M.J. Torres, Viscosity and Density of 1-Alkyl-3-ethylimidazolium Ionic Liquids, In Clean solvents, American Chemical Society. (2002) 34-49.

95. K.R. Seddon, A. Stark and M.J. Torres, Influence of chloride, water, and organic solvents on the physical properties of ionic liquids, Pure Appl. Chem. 72 (2001) 2275-2287.

96. K.N. Marsh, J.A. Boxall, R. Lichtenthaler, Room temperature ionic liquids and their mixtures—a review, Fluid Ph. Equilibria. 219 (2004) 93-98.

97. H. okuda, K. Hayamizu, K. Ishii, M.A.B.H. Susan, M. Watanabe, Physicochemical properties and structures of room temperature ionic liquids. 2. Variation of alkyl chain length in imidazolium cation, J. Phys. Chem. B 109 (2005) 6103-6110.

98. Y. Song, L. Liu, X. Zhu, X. Wang, H. Jia, X. Xiao, H. Yu, X. Yang, Physicochemical properties of ionic liquids based on imidazolium/pyrrolidinium cations and maleate/phthalate anions, Solid State Ionics. 179 (2008) 516-521.

99. Holbrey, John D., Robin D. Rogers, Rob A. Mantz, Paul C. Trulove, Violina A. Cocalia, Ann E. Visser, Jessica L. Anderson et al. "Physicochemical properties" Ionic liquids in synthesis 2 (2008).

100. Y.U. Paulechka, D.H. Zaitsau, G.J. Kabo, A.A. Strechan, Vapor pressure and thermal stability of ionic liquid 1-butyl-3-methylimidazolium Bis (trifluoromethylsulfonyl) amide, Thermochim. Acta, 439 (2005)158-160.

101. J.D. Holbrey, K.R. Seddon, The phase behaviour of 1-alkyl-3-methylimidazolium tetrafluoroborates: Ionic liquids and ionic liquid crystals, J. Chem. Soc., Dalton Trans. 13 (1999) 2133 - 2139.

102. M.A. Ab Rani, A. Brant, L. Crowhurst, A. Dolan, M. Lui, N.H. Hassan, R. Wilding, Understanding the polarity of ionic liquids, Phys. Chem. Chem. Phys. 13 (2011) 16831-16840.

103. R.M. Couto, C. Lourenço, P.C. Simões, L.C. Branco, Task specific ionic liquids as polarity shifting additives of common organic solvents, New J. Chem. 38 (2014) 5559-5565.

104. J.M. Lee, S. Ruckes, J.M. Prausnitz, Solvent polarities and Kamlet–Taft parameters for ionic liquids containing a pyridinium cation, J. Phys. Chem. B 112 (2008) 1473-1476.

105. N. Li, Y.A. Gao, L. Zheng, J. Zhang, L. Yu, X. Li, Studies on the micropolarities of bmimBF4/TX-100/toluene ionic liquid microemulsions and their behaviors characterized by UV– Visible spectroscopy, Langmuir. 23 (2007) 1091-1097.

106. J.N. Canongia Lopes, M.F. Costa Gomes, P. Husson, A.A. Pádua, L.P.N. Rebelo, S. Sarraute, M. Tariq, Polarity, viscosity, and ionic conductivity of liquid mixtures

containing [C4C1im][Ntf2] and a molecular component, J. Phys. Chem. B 115 (2011) 6088-6099.

107. C. Reichardt, Polarity of ionic liquids determined empirically by means of solvatochromic pyridinium N-phenolate betaine dyes, Green Chem. 7 (2005) 339-351.
108. M. Kosmulski, J. Gustafsson, J.B. Rosenholm, Thermal stability of low temperature ionic liquids revisited, Thermochim. Acta. 412 (2004) 47-53.
109. P. Bonhote, A.P. Duasm, B. Papageorgiou, K. Kalyanasundaram, M. Graetzel, Hydrophobic, highly conductive ambient-temperature molten salts, Inorg. Chem. 35 (1996) 1168-1178.
110. H. L. Ngo, K. LeCompte, L. Hargens, A. B. McEwen, Thermal properties of imidazolium ionic liquids, Thermochim. Acta. 357 (2000) 97–102.
111. Ch. Jagadeeswara Rao, R. Venkata Krishnan, K.A. Venkatesan, K. Nagarajan, T.G. Srinivasan, Thermochemical properties of some bis (trifluoromethyl-sulfonyl) imide based room temperature ionic liquids, J. Therm. Anal. Calorim. 97 (2009) 937-943.
112. R.L. Vekariya, A review of ionic liquids: Applications towards catalytic organic transformations, J. Mol. Liq. 227 (2017) 44-60
113. A.I. Siriwardana, Industrial applications of ionic liquids. Electrochemistry in Ionic Liquids, Springer, Cham. (2015) 563-603.
114. M. Volland, V. Seitz, M. Maase, M. Flores, R. Papp, K. Massonne, V. Stegmann, K. Halbritter, R. Noe, M. Bartsch, W. Siegel, Separation of acids from chemical reaction mixtures by means of ionic liquids, U.S. Patent Application 11/952,242 (2007).

115. A.A.C. Hijo Toledo, G.J. Maximo, M.C. Costa, E.A.C. Batista, A.J. Meirelles, Applications of Ionic Liquids in the Food and Bioproducts Industries, ACS Sustainable Chem. Eng. 4 (2016) 5347–5369

116. K. Nakashima, F. Kubota, T. Maruyama, M. Goto, Feasibility of ionic liquids as alternative separation media for industrial solvent extraction processes, Ind. Eng. Chem. Res. 44 (2005) 4368-4372.

117. K.E. Gutowski, Industrial uses and applications of ionic liquids, Phys. Sci. Rev. 3 (2018) 5.

118. H.Zhao, Innovative applications of ionic liquids as “green” engineering liquids, Chem. Eng. Commun. 193 (2006) 1660-1677.

119. N.V. Plechkova, K.R. Seddon, Applications of ionic liquids in the chemical industry, Chem. Soc. Rev. 37 (2008) 123–150.

120. S.E. Fry, N.J. Pienta, Effects of molten salts on reactions. Nucleophilic aromatic substitution by halide ions in molten dodecyltributylphosphonium salts, J. Am. Chem. Soc. 107 (1985) 6399-6400.

121. A.R. Sethi, P. Smith, N. Srinivasan, T. Welton, Ionic liquids as solvents for organic synthesis, In: Green industrial applications of ionic liquids, Eds. R.D. Rogers, K.R. Seddon, S. Volkov, NATO science series, Kluwer Academic publishers, Netherlands (2002).

122. S.V. Malhotra, ed., Ionic liquids in organic synthesis, American Chemical Society (2007).

123. M. Koel, Ionic liquids in chemical analysis, Crit. Rev. Anal. Chem. 35 (2005) 177-192.

124. W. Simka, D. Puszczyk, G. Nawrat, Electrodeposition of metals from non-aqueous solutions, Electrochim. Acta. 54 (2009) 5307-5319.

125. D. Wei, A. Ivaska, Applications of ionic liquids in electrochemical sensors, Anal. Chim. Acta. 607 (2008) 126-135.

126. D. Han, K.H. Row, Recent applications of ionic liquids in separation technology, Molecules. 15 (2010) 2405-2426.

127. Weyershausen B, Lehmann K. Industrial application of ionic liquids as performance additives, Green Chem. 7 (2005) 15-19.

128. M.L. Dietz, Ionic liquids as extraction solvents: where do we stand?, Sep. Sci. Technol. 41 (2006) 2047 -2063.

129. S. Dai, Y.H. Ju, C.E. Barnes, Solvent extraction of strontium nitrate by a crown ether using room-temperature ionic liquids, J. Chem. Soc., Dalton Trans. 1 (1999) 1201-1202.

130. A.E. Visser, R.P. Swatloski, W.M. Reichert, S.T. Griffin, R.D. Rogers, Traditional extractants in non-traditional solvents: Group 1 and 2 extractions by crown ethers in room temperature ionic liquids, Ind. Eng. Chem. Res. 39 (2000) 3596 - 3604.

131. A.E. Visser, Metal ion separations in aqueous biphasic systems and room-temperature ionic liquids, The University of Alabama. 2002.

132. P. Giridhar, K.A. Venkatesan, T.G. Srinivasan, P.R. Vasudeva Rao, Extraction of uranium (VI) from nitric acid medium by 1.1 M tri-n-butylphosphate in ionic liquid diluent, J. Radio anal. Nucl. Chem. 265 (2005) 31-38.

133. P. Giridhar, K.A. Venkatesan, T.G. Srinivasan, P.R. Vasudeva Rao, Effect of alkyl group in 1-alkyl-3-methylimidazolium hexafluorophosphate ionic liquids on the extraction of uranium by tri-n-butylphosphate diluted with ionic liquids, J. Nucl. Radiochem. Sci. 5 (2004) 21-26.

134. M.L. Dietz, D.C. Stepinski, Anion concentration-dependent partitioning mechanism in the extraction of uranium into room-temperature ionic liquids, Talanta. 75 (2008) 598-603.

135. I. Billard, A. Ouadi, E. Jobin, J. Champion, C. Gaillard, S. Georg, Understanding the Extraction Mechanism in Ionic Liquids: UO_2^{2+}/HNO_3/TBP/C_4-mimTf$_2$N as a Case Study, Sol. Extr. Ion. Exch. 29 (2011) 577-601.

136. C. Gaillard, M. Boltoeva, I. Billard, S. Georg, V. Mazan, A. Ouadi, D. Ternova, C. Hennig, Insights into the Mechanism of Extraction of Uranium (VI) from Nitric Acid solution into an Ionic Liquid by using Tri-n- butyl phosphate, Chem. Phys. Chem. 6 (2015) 2653-2662.

137. R. Rama, Alok Rout, K.A. Venkatesan, M.P. Antony, A. Suresh, Comparision in the solvent extraction behavior of uranium (VI) in some trialkyl phosphates in ionic liquid, Radiochim. Acta. 104 (2016) 865-872.

138. Alok Rout, S. Karmakar, K.A. Venkatesan, T.G. Srinivasan, P.R. Vasudeva Rao, Room temperature ionic liquid diluent for the mutual separation of europium (III) from americium (III), Sep. Purif. Technol. 81 (2011) 109-115.

139. K. Nakashima, F. Kubota, T. Maruyama, M. Goto, Ionic liquids as a novel solvent for lanthanide extraction, Ana. Sci. 19 (2003) 1097-1098.

140. S. Panja, P.K. Mohapatra, S.C. Tripathi, P.M. Gandhi, P. Janardan, A highly efficient solvent system containing TODGA in room temperature ionic liquids for actinide extraction, Sep. Purif. Technol. 96 (2012) 289-295.

141. A. Sengupta, P.K. Mohapatra. M. Iqbal, J. Huskens, W.A. Verboom, Diglycolamide-functionalized task specific ionic liquid (TSIL) for actinide extraction: solvent extraction, thermodynamics and radiolytic stability studies. Sep. Purif. Technol. 118 (2013) 264-270.

142. P.K. Mohapatra, P. Kandwal, M. Iqbal, J. Huskens, M.S. Murali, W.A. Verboom, novel CMPO-functionalized task specific ionic liquid: synthesis, extraction and spectroscopic investigations of actinide and lanthanide complexes. Dalton Trans. 42 (2013) 4343-4347.

143. Alok Rout, K.A. Venkatesan, T.G. Srinivasan, P.R. Vasudeva Rao, Extraction behavior of actinides and fission products in amide functionalized ionic liquid, Sep. Purif. Technol. 97 (2012)164-171.

144. Alok Rout, K.A. Venkatesan, T.G. Srinivasan, P.R. Vasudeva Rao, Unusual extraction of plutonium (IV) from uranium (VI) and americium (III) using phosphonate based task specific ionic liquid, Radiochim. Acta. 98 (2010) 459-466.

145. P.R. Vasudeva Rao, Z. Kolarik, A review of third phase formation in extraction of actinides by neutral organophosphorus extractants, Solvent Extr. Ion Exch. 14 (1996) 955-993.

146. D. Whittaker, A. Geist, G. Modolo, R. Taylor, M. Sarsfield, A. Wilden, Applications of diglycolamide based solvent extraction processes in spent nuclear fuel reprocessing, part 1: TODGA. Solvent Extr. Ion Exch. 36 (2018) 223-256.

147. B. J. Mincher, J. F. Wishart, The radiation chemistry of ionic liquids: a review, Solvent Extr. Ion Exch. 32 (2014) 563–583.

148. L.Yuan, J. Peng, L. Xu, M. Zhai, J. Li, G. Wei, Radiation-induced darkening of ionic liquid [C_4mim][NTf_2] and its decoloration, Rad. Phys. Chem. 78 (2009) 1133–1136.

149. P. K. Verma, R. B. Gujar, A. S. Kanekar, Y. K. Bhardwaj, P. K. Mohapatra, Effect of irradiation on the hydrodynamic parameters and extraction efficiency of several frequently used ionic liquids, Rad. Phys. Chem. 158 (2019)180-187.

150. Ch. Jagadeeswara Rao, K.A. Venkatesan, B. V. R. Tata, K. Nagarajan, T. G. Srinivasan, P.R Vasudeva Rao, Radiation stability of some room temperature ionic liquids. Radiat. Phys. Chem. 80 (2011) 643-649.

151. D. Allen, G. Baston, A. E. Bradley, T. Gorman, A. Haile, I. Hamblett, J. E. Hatter, M. J. F. Healey, B. Hodgson, R. Lewin, K. V. Lovell, B. Newton, W. R. Pitner, D. W. Rooney, D. Sanders, K. R. Seddon, H. E. Sims, R. C. Thied, An investigation of the radiochemical stability of ionic liquids. Green Chem. 4 (2002)152-158.

152. L. Berthon, S. I. Nikitenko, I. Bisel, C. Berthon, M. Faucon, B. Saucerotte, N. Zorza, Ph. Moisy, Influence of gamma irradiation on hydrophobic room-temperature ionic liquids [BuMeIm][PF_6] and [BuMeIm][$CF_3SO_2)_2N$], Dalton Trans. (2006) 2526–2534.

153. G. Le Rouzo, C. Lamouroux, V. Dauvois, A. Dannoux, S. Legand, D. Durand, P. Moisy, G. Moutiers, Anion effect on radiochemical stability of room-temperature ionic liquids under gamma irradiation, Dalton Trans. 31(2009) 6175-6184.

154. I.A. Shkrob, T.W. Marin, S.D. Chemerisov, J.F. Wishart, Radiation and radical chemistry of NO_3^-, HNO_3, and dialkylphosphoric acids in room-temperature ionic liquids, J. Phys. Chem. B 115 (2011)10927-10942.

Chapter 2: Experimental

This chapter deals with the description of materials, methods and experimental conditions employed in the present study. The experimental procedure involved in the synthesis of extractants, RTILs, preparation of stock solutions and indicator solutions for liquid-liquid extraction studies are discussed. The details of instrumental techniques employed for the experimental studies have been discussed briefly.

2.1. Chemicals and reagents

All the reagents and chemicals employed in the study were of analytical grade (AR, purity > 98 %) and they were used as received unless otherwise indicated.

2.1.1. Inorganic and organic salts

Calcium chloride

Calcium chloride (≥ 99.9 %) was obtained from Sigma Aldrich, Mumbai, India.

1,2-dihydroxy benzene

1,2-dihydroxy benzene (> 99 %) was procured from Sigma Aldrich, Mumbai, India.

Ethylenediaminetetraaceticacid

Ethylenediaminetetraacetic acid (EDTA) was received from Sigma Aldrich, Mumbai, India and it was used for complexometric titrations.

Europium nitrate

Europium(III) nitrate hexahydrate (≥ 99.0 %) was obtained from Sigma Aldrich, Mumbai, India.

Hexamethylenetetramine

Hexamethylenetetramine (HMTA) was procured from Sigma Aldrich, Mumbai, India. It was used for the determination of concentration of trivalent lanthanides in aqueous and ionic liquid phases respectively.

Lithium bis(trifluoromethylsulfonyl)imide

Lithium bis(trifluoromethylsulfonyl)imide ($LiNTf_2$) (> 98 %) was supplied by Alpha Aesar, Mumbai, India.

Methylthymol blue sodium salt

Methylthymol blue sodium salt (ACS grade) was received from Merck, Mumbai, India.

Neodymium nitrate

Neodymium (III) nitrate hexahydrate, was procured from Sigma Aldrich, Mumbai, India.

Oxalic acid

Oxalic acid was obtained from Sigma Aldrich, Mumbai, India.

Phenolphthalein

Phenolpthalein was procured from Merck, Mumbai, India.

Potassium hydrogen phthalate

Potassium hydrogen phthalate (KHP) was obtained from Glaxo Laboratories, India and it was used for standardization of sodium hydroxide solution.

Potassium nitrate

Potassium nitrate was received from SD Fine Chemicals, Mumbai, India.

Potassium oxalate

Potassium oxalate was purchased from Loba Chemie Private Limited, Mumbai, India and it was used for the estimation of free acidity (concentration of nitric acid) of aqueous and ionic liquid phases containing hydrolysable metal ions.

Thorium nitrate

Thorium nitrate was received from Indian Rare Earths Ltd., Mumbai, India.

Quaternaryalkylammonium chlorides

Quaternaryalkylammonium chlorides such as methyl-tri-*n*-octylammonium chloride (> 98 %) and tri-*n*-butyl-methyl ammonium chloride (> 98 %) were procured from Alpha Aesar and Sigma Aldrich, Mumbai, India.

Reichardt's dye

Reichardt's dye (2,6-diphenyl-4-(2,4,6-triphenylpyridinium-1-yl)phenolate) was procured from Sigma Aldrich, Mumbai, India.

Silicagel

Silicagel (60-120 and 100-200) for column chromatography was supplied by SD Fine chemicals Limited, Chennai, India and it was dried at 373 K for one hour prior to use.

Silver nitrate

Sodium nitrate was procured from Sigma Aldrich, Mumbai, India.

Sodium hydroxide

Sodium hydroxide was obtained from Sigma Aldrich, Mumbai, India.

Sodium nitrate and sodium nitrite

Sodium nitrate and sodium nitrite (> 99 %) were obtained from Alfa Aesar, Mumbai, India.

Sodium carbonate and sodium bicarbonate

Sodium carbonate and sodium bicarbonate were purchased from Alfa Aesar, Mumbai, India.

Uranyl nitrate and uranium oxide

Uranyl nitrate and uranium oxide (U_3O_8) were obtained from Nuclear Fuel Complex, Hyderabad, India, and the uranium content was estimated by Davies and Gray method [1].

Xylenol orange

Xylenol orange was received from Merck, Mumbai, India.

Zirconium

Anhydrous Zirconium (IV) chloride (99.9 %) was procured from Sigma Aldrich, Mumbai, India. Zirconium sponge (nuclear grade) was obtained from Nuclear Fuel Complex, Hyderabad, India

2.1.2. Organic chemicals and reagents

Acetoxyacetyl chloride

Acetoxyacetyl chloride (97 %) was purchased from Thermo Fischer Scientific, India and it was used without any purification.

Alkylhalides

1-Bromobutane (> 99 %) was procured from Merck, India and also from SD Fine Chemical, India Limited. Further it was purified by distillation before use.

1-Chlorobutane (> 99 %) was procured from Sigma Aldrich, India. Further it was purified by distillation before use.

Bis(2-ethylhexyl)phosphoric acid

Bis(2-ethylhexyl)phosphoric acid (D2EHPA) was procured from Sigma Aldrich, Mumbai, India. And it was further purified by copper (II) precipitation method as described elsewhere [2].

Chloroacetyl chloride

Chloroacetyl chloride (> 98 %) was procured from Sigma Aldrich, Mumbai, India.

Carbamoylmethylphosphinoxide

Octyl-phenyl-*N,N*-diisobutylcarbamoylmethylphosphinoxide (CMPO) (> 98 %) was supplied by National Chemical Laboratories, Pune, India and it was purified by column chromatography.

Dialkylamines

Dialkylamines such as dihexylamine, di-2-ethylhexylamine, dioctylamine and didecylamine were procured from Sigma Aldrich, Mumbai, India.

Diglycolicanhydride

Diglycolicanhydride (> 90 %) was obtained from Sigma Aldrich, Mumbai, India.

Diluents

n-Dodecane (> 98 %) was purchased from Alfa Aesar, Mumbai, India. The *n*-parafiins such as *n*-hexane, *n*-octane and *n*-decane were obtained from Ranbaxy Fine Chemicals Limited, New Delhi India.

Methylimidazole

1-Methylimidazole (> 99 %), was procured from Fluka, India and it was used after distillation.

Methylpyrrolidine

1-Methylpyrrolidine (> 97 %) was received from Fluka, India and it was used after distillation.

Methylpiperidine

1-Methylpiperidine (> 97 %) was supplied by Fluka, India and it was used after distillation.

***N,N,N,N',N'*-tetra(2-ethyl hexyl)diglycolamide**

N,N,N',N'-tetra(2-ethylhexyl)diglycolamide (T2EHDGA) was received from Orion Chemicals, Mumbai, India and it was purified by column chromatography.

Organic solvents

Acetone, Ethylacetate, Dichloromethane and Chloroform were procured from Fischer Inorganics and Aromatics Limited, Chennai, India. Acetonitrile, methanol and ethanol (HPLC grade ≥ 99.9 %) were received from Sigma Aldrich, Mumbai, India.

Triethylamine

Triethylamine was supplied by Merck, Mumbai, India and it was further purified by distillation before use.

Tri-*n*-butyl phosphate

Tri-*n*-butyl phosphate (TBP) (≥ 99 %) was procured from Sigma Aldrich, Mumbai, India. It was washed with dilute sodium carbonate solution or sodium hydroxide followed by distilled water and then dried in a rotary evaporator.

2.1.3. Acid solutions

The acid solutions such as HNO_3 H_2SO_4 and HCl (AR grade) were procured from Merck Private Limited, Mumbai, India. The stock solutions of desired concentrations were prepared by the dilution of concentrated acid with distilled water. The concentration of acid was estimated by standard NaOH solution with phenolphthalein as indicator.

2.1.4. Radioactive tracers

$^{(152+154)}$Eu(III)

The radio isotope $^{(152+154)}$Eu(III) in the form of $EuCl_3$ was purchased from Board of Radiation and Isotope Technology (BRIT), Mumbai, India. The HCl was evaporated off and the tracer solution was prepared by re-dissolving in dilute nitric acid. The purity of $^{(152+154)}$Eu(III) was ascertained by γ-counting technique.

^{241}Am(III)

The radio isotope ^{241}Am(III) in the form of Am_2O_3 was obtained from Bhabha Atomic Research Centre, Mumbai, India. The tracer solution was prepared by dissolving in dilute nitric acid and the purity of ^{241}Am(III) was ascertained by γ-counting technique.

2.2. Instrumentation

2.2.1. Gamma counter

The gamma radioactivity of ^{241}Am, $^{(152+154)}$Eu was estimated by NaI(Tl) detector coupled with single channel analyzer. The NaI(Tl)-photo multiplier tube (PMT) integral assembly was procured from Harshaw, USA and other electronic modules were obtained from Electronic Corporation of India Limited (ECIL), Hyderabad, India. The values obtained for the gamma counting analysis were within the error range of ± 5 %.

2.2.2. Gamma chamber for irradiation

An indigenous, compact, self-shielded (Gamma Chamber 5000, BRIT) gamma chamber was used for the irradiation studies. The radiation field was provided by a set of stationary cobalt-60 gamma sources placed in a cylindrical cage that offers a gamma dose of 2.7 kGy/hr. The samples were placed in an irradiation chamber located in the gamma irradiator and kept in a static condition during irradiation. The gamma chamber was calibrated using Fricke dosimeter before placing the samples for irradiation.

2.2.3. Rotary evaporator

A rotary evaporator (model: R-3000 from M/s. Buchi Laboratories Technique AG, Switzerland) was used for drying RTILs at 353 K and to distill off volatile solvents under vacuum.

2.2.4. pH meter

All pH measurements were made using Cyberscan 500 pH, Metrohm. The pH meter was calibrated at 298 K with standard buffers of pH 4, 7 and 10.

2.2.5. Karl Fischer titrator

The concentration of water present in the organic phase before and after the extraction was determined by Karl Fischer titration (Metrohm KF-831 Karl Fischer titrator). Double distilled water or Millipore water was used to calibrate the instrument. Known weights of the samples were taken for the determination of water content. The values obtained for the water analysis were within the error range of ± 5 %.

2.2.6. Dynamic light scattering

Size of aggregates in the IL phase was measured using Zetasizer-nano ZS 90 DLS spectrometer (Malvern Instrument Company, UK) provided with a 4 mW He-Ne laser beam (wavelength of 632.8 nm) [3-5]. The scattering angle for measurement was set at 90° path length was 4 mm. All these experiments were carried out at 298 K. The accuracy in the measurement of particle size was verified using NIST standard polystyrene Latex colloidal suspension (Duke cooperative private limited, USA) of size 60 nm before and after measurement of samples. The measurements were carried out for five times independent of each measurement to obtain the reproducibility of the data. The average standard deviation of measured data was ± 5 %.

Dynamic light scattering (DLS) technique is a well-recognized method for determining the size of aggregates and their distribution in the liquid phase. The schematic diagram of dynamic light scattering technique is shown in Fig. 2.1. The principle of DLS technique for the measurement of aggregate size and distribution of aggregates is described elsewhere [3-5]. The DLS technique determines average hydrodynamic diameter of the particle suspension by measuring the fluctuations in the intensity of scattered photons. It is well recognized that the aggregates suspended in a liquid are under constant Brownian motion due to the interactions and random collisions with neighboring molecules or aggregates. When a monochromatic and coherent beam of light falls on such a suspension, the light is scattered at various angles and the scattered photons carry information about the size and distribution of aggregates intensity. The DLS technique measures the time dependent fluctuations in the scattering intensity to determine the translational diffusion coefficient (D), and subsequently the hydrodynamic diameter (D_h). The apparent hydrodynamic diameter of the species can be calculated by using a Stokes–Einstein equation with the assumption that the scattering species as hard sphere, is given in equation 2.1.

The algorithm employed for the determination of average aggregate size, and distribution of aggregates was based on the cumulant analysis, which extracts the data from auto correlation function generated by the autocorrelator built-in the equipment. Poly dispersive Index (PDI) in dynamic light scattering studies describes that the width of peak is a Gaussian distribution. The PDI of 0.2 or less indicates that the sample is mono dispersive and the PDI of more than 0.7 is not suitable for the DLS analysis. In the present study the PDI was determined to be less than 0.1, and those with acid and Nd(III) or Eu(III) extracted samples ranged from 0.2 to 0.5.

$$d_h = \frac{k_B T}{3\pi\eta D} \tag{2.1}$$

Where d_h is hydrodynamic diameter of the aggregate, k_B is the Boltzmann constant, T is the temperature of the measurement and η is the viscosity of the dispersion medium.

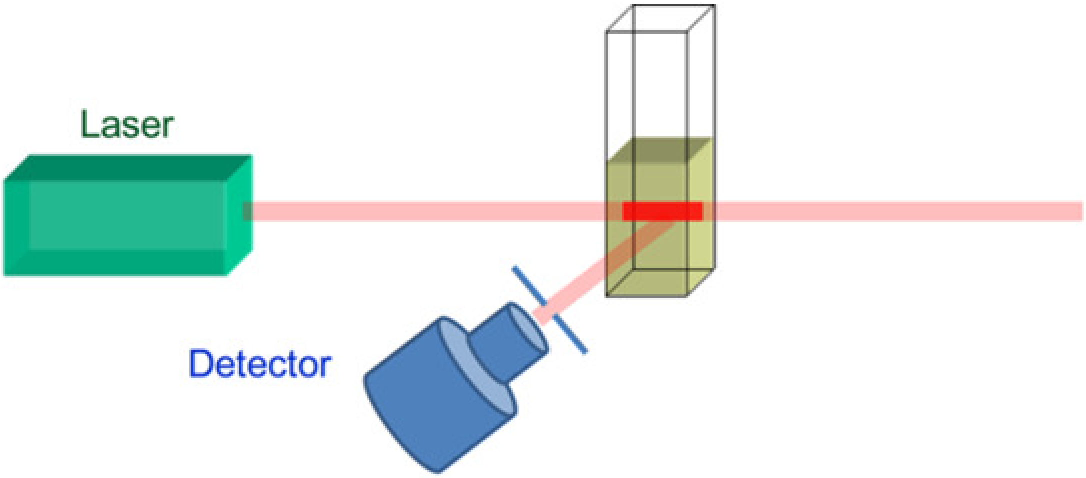

Fig. 2.1. Schematic diagram of dynamic light scattering.

2.2.7. NMR spectrometer

A Brucker Avance III 500 MHz (AV 500) multi nuclei solution NMR spectrometer was used for recording proton (^{1}H) and ^{13}C NMR of synthesized samples. $CDCl_3$ or DMSO-d6 containing 0.03 % of TMS was used as the solvent.

2.2.8. FT-IR spectrometer

The Fourier transformed infrared (FTIR) spectrum of the sample was recorded using BRUKER TENSOR II FT-IR spectrometer equipped with an ATR (attenuated total reflectance) diamond crystal. Few micro liter of sample was placed on the diamond disk and the spectrum was recorded from 4000 to 600 cm^{-1}. For each sample the data was acquired for about 16 scans with a resolution of 4 cm^{-1}. The acquired data was corrected to the background spectrum (without sample) and presented as ATR-FTIR spectrum of the sample.

2.2.9. Raman spectrometer

Raman spectrum of the sample was recorded using an Renishaw (Gloucestershire, UK) inVia Raman microscope system containing with a Leica microscope. It contained a 785 nm excitation laser with a power of 300 mW and charge couple device (CCD) detector. A 20X or 10 X objective lens was used and the laser exposure time was 10 s.

2.2.10. Luminescence spectrometer

All the luminescence spectra were recorded by using Edinburgh spectrofluorimeter FLS920 (Edinburgh instruments, UK) with a 450 W xenon lamp as the excitation source. Fused silica cuvette with a path length of 2 mm was used as the sample cell for recording these luminescence spectra. The band pass of 3 nm was set for both the excitation and emission monochromators. A long-wavelength pass filter (UV–39, Shimadzu) with a maximum and uniform transmittance (>85%) >400 nm was placed in front of the emission monochromator, to reduce the scatter of the incident beam into the emission monochromator. Spectra were recorded at room temperature with a 90° collection geometry.

2.2.11. Spectrophotometer

The UV-Visible-NIR spectra of all the samples were recorded by using Shimadzu UV-VIS-NIR spectrophotometer (UV-3600). Quartz cuvettes with 1 cm path length were used in all the spectrophotometric measurements. The measurements were carried out for three times independent of each measurement to obtain the reproducibility of the data. The average standard deviation of measured data was ± 5 %.

2.2.12. Densitometer

Densities (ρ) of ionic liquid phase sample were measured using DMA 4500 digital vibrating U-tube densitometer supplied by Anton paar, Austria (with automatic viscosity correction). The temperature of the cell was controlled at ± 273.01 K with a built in solid state thermostat. Temperature stability was better than ± 0.002 K. ASTM grade I water was used for density standard. Apparatus was calibrated using ambient air ($\rho = 0.00118$ $g.cm^{-3}$) and Millipore quality water ($\rho = 0.99704$ $g.cm^{-3}$) at 298 K. All the measurements were carried out at atmospheric pressure (1 bar) and the temperature range from 298 to 333 K. The uncertainty in the values of density is $\pm 1 \times 10^{-5}$ $g.cm^{-3}$.

2.2.13. Viscometer

The viscosity (η) of ionic liquid phase samples were measured using Lovis 2000 ME, a rolling ball viscometer supplied by Anton paar, Austria. ASTM grade I water was used for viscosity standard. Apparatus was calibrated using ambient air ($\eta = 0.0186$ mPa.s) and Millipore quality water ($\eta = 0.89$ mPa.s) at 298 K. This equipment measures the rolling time of a ball passing through liquids based on Hopplers principle. All the measurements were carried out at atmospheric pressure (1 bar) and the temperature range from 298 to 333 K. The uncertainty in the values of viscosity was about ± 2 x 10^{-3} mPa.s.

2.2.14. Refractometer

The refractive index (n) of the ionic liquid phase samples were measured using a Anton Parr refractometer (Model: Abbemat 3200). The 'n' values measured in the temperature range of 298 to 333 K with an accuracy of ± 0.0001 nD.

2.2.15. Thermogravimetric analyzer

A thermogravimetric analyzer (Setsys-12, M/s. SETRAM, France) was employed for the thermal analysis of ionic liquid phase samples. The temperature calibration was carried out by determining the melting temperatures of pure In, Sn and Au samples. In this experiment, about 10 mg of the sample was subjected to the heating ramp of 10 K/minute from ambient temperature and the weight loss of the sample was recorded as a function of temperature. Before heating, the sample was kept in the thermogravimetric analyser for about 30 minutes to equilibrate the sample with ambient condition. The sample was then heated in argon gas atmosphere from ambient temperature to 800 K.

2.2.16. Electronic single pan balance

A calibrated electronic single pan balance (AUW 220D SHIMADZU) with a sensitivity of ± 0.01 mg was used to for weighing various chemicals and solutions.

2.3. Analytical procedures

2.3.1. Arsenazo(III) reagent solution

Arsenazo (III) solution was prepared by dissolving 200 mg of sodium salt of Arsenazo (III) in 0.01 M NaOH solution.

2.3.2. Standard EDTA solution

The solution of EDTA was prepared by dissolving required quantity of EDTA salt by weight in distilled water to get the desired concentration solution. This solution was then standardized by using standard neodymium solution (5.135 mg/gm) at pH 6 (adjusted using saturated solution of HMTA) using methyl thymol blue as indicator.

2.3.3. Methylthymol blue indicator

It was prepared by dissolving 200 mg of methylthymol blue sodium salt in 100 mL standard flask using distilled water. It was used for the estimation of concentration of trivalent lanthanides in aqueous and ionic liquid phases.

2.3.4. Preparation of sodium hydroxide solution

A known weight of sodium hydroxide pellets was dissolved in distilled water and made up to the required volume to get the solutions on molar basis. The concentration of sodium hydroxide was standardized by acid-base titration with potassium hydrogen phthalate using phenolphthalein as indicator.

2.3.5. Preparation of aqueous complexing agents

A known weight of various aqueous complexing agents were dissolved in distilled water and made up to the required volume to get the solutions on molar basis. The acidity of the corresponding solutions was adjusted to the concentration by adding calculated amount of concentrated nitric acid.

2.3.6. Phenolphthalein indicator

Phenolphthalein indicator was prepared by dissolving 500 mg of phenophthalein in 100 mL of 1:1 mixture of distilled water and methanol. It was used as indicator in acid-base titrimetry.

2.3.7. Xylenol orange indicator

It was prepared by dissolving 200 mg of xylenol orange in 100 mL standard flask using distilled water. It was used for the estimation of concentration of zirconium in aqueous and ionic liquid phase respectively.

2.3.8. Preparation of Zr(IV) stock solution

The stock solution of zirconium (IV) in nitric acid was prepared by dissolving the nuclear grade zirconium sponge in nitric acid as per the procedure discussed elsewhere [6]. The amount of zirconium present in the stock solution was determined by standard EDTA titration and back titration with $Th(NO_3)_4$ solution by procedure described elsewhere [6].The zirconium stock solution was diluted with appropriate concentration of nitric acid to obtain aqueous feed solution for extraction studies. The concentration of Zr(IV) in aqueous phase obtained after extraction was determined by titrimetry as discussed elsewhere [6].

2.3.9. Preparation of U(VI) stock solution

The stock solution of uranium (100g/L and 200 g/L) was prepared by dissolving uranyl nitrate (supplied by Nuclear fuel complex, Hyderabad, India) in dilute nitric acid medium. The concentration of uranium present in stock solution was estimated by using Davis & Gravy method, described elsewhere [1]. The uranium stock solution was diluted with appropriate concentration of nitric acid to obtain aqueous feed solutions for extraction studies. The concentration of U(VI) in aqueous phase obtained after extraction was determined by a spectrophotometric method using Arsenazo(III) as the colouring agent, as discussed elsewhere [7].

2.3.10. Preparation of solutions with various concentrations of NO_3^- ion

The total nitrate ion concentration was varied from 0.1 to 0.8 M in nitric acid by taking appropriate amount of sodium nitrate salt and required quantity of nitric acid with higher concentration (10 M) in distilled water (up to the required volume) in order to make the desired solution with fixed acidity.

2.3.11. Preparation of solutions for solvatochromic measurements

The stock solution of Reichardt's dye served as a polarity probe and it was prepared by dissolving Reichardt's dye (10^{-2} M) in acetonitrile. The ionic liquid samples for solvatochromic measurements were prepared as follows.

Sample 1: A required amount of ionic liquid was weighed and mixed with 1 mL of polarity probe solution, and then diluted to 10 mL in a standard flask using acetonitrile. The concentration of ionic liquid in this solution was varied from 0.02 to 0.35 M.

Sample 2: A known weight of $LiNTf_2$ or $[C_4mim][Cl]$ was dissolved in ionic liquid such that the concentration of $LiNTf_2$ and $[C_4mim][Cl]$ was varied from 0.01 to 1.0 M. About 0.2 mL of this ionic liquid solution was mixed with 1 mL of polarity probe solution and diluted to 10 mL in a standard flask using acetonitrile.

Sample 3: The ionic liquid (5 mL) was equilibrated with an aqueous solution (5 mL) containing nitric acid of various concentrations (0.1 M to 5 M) at 298 K (± 0.1). The equilibration was carried out in a stoppered equilibration tube immersed in a constant temperature water bath. The equilibration tubes were rotated in an up-side-down manner for about one hour. After equilibration, the test tube was centrifuged and allowed the phases to settle. About 0.2 mL of ionic liquid phase was mixed with the probe solution (1mL) and then diluted to 10 mL in a standard flask using acetonitrile.

Sample 4: A required quantity of metal nitrate (metal = Th^{4+}, UO_2^{2+}, Nd^{3+}) was dissolved in ionic liquid. The amount of metal in ionic liquid was varied from 0.1 to 5 g/L. About 0.2 mL of this solution was mixed with 1 mL of polarity probe solution and the resultant solution was diluted to 10 mL in a standard flask using acetonitrile.

Sample 5: The solution of TBP (0.2 to 1.1 M) in ionic liquid was prepared. About 0.2 mL of this ionic liquid solution was mixed with 1 mL of polarity probe solution and then diluted to 10 mL in a standard flask using acetonitrile.

Sample 6: A solution of metal nitrate (metal=Th^{4+}, UO_2^{2+}, Nd^{3+}) in 1.1 M TBP/ionic liquid was prepared. The amount of metal in this solution was varied from 0.1 to 5 g/L. About 0.2 mL of this solution was mixed with 1 mL of polarity probe solution and diluted to 10 mL in a standard flask using acetonitrile.

All the sample solutions discussed above were then subjected to spectrophotometric measurements. A visible absorption spectrum was recorded from 400 to 800 nm and the wave length (λ_{max}) at absorbance maxiumum was measured. The sample preparation and the measurements were performed in triplicate to check the reproducibility of the data. It was found that reproducibility was excellent (> 98 % reproducible).

2.4. Liquid-Liquid extraction studies

All the liquid-liquid extraction experiments were conducted in duplicate at 298 K with 1:1 aqueous:ionic liquid phase ratio. The organic phase was the solution of molecular extractant in diluent (RTIL or *n*-dodecane) in the desired concentration. The aqueous phase was desired concentration of nitric acid spiked with a radioisotope or a metal ion dissolved in nitric acid. The ionic liquid phase was pre-equilibrated with desired concentration of nitric acid prior to metal ion extraction. The extraction experiments involved equilibration of equal volumes (1 mL) of ionic liquid phase and aqueous phase in a 10 mL capacity test tube immersed in a constant temperature water bath and rotated in up-side-down manner for about an hour unless otherwise mentioned. After equilibration the radioactivity present in both ionic liquid and aqueous phases was measured. The γ-radioactivity for ^{241}Am(III) and $^{(152+154)}$Eu(III) isotopes was measured using a well-type NaI(Tl) scintillation detector. The distribution ratio (D_M) and % of extraction of the metal ion were determined using the equation 2.2 and 2.3.

$$D_M = \frac{[M]_{IL}}{[M]_{aq}} \tag{2.2}$$

$$\%\ \text{Extraction} = \frac{D_M}{D_M + 1} \times 100 \tag{2.3}$$

where M_{IL} and M_{aq} (M = ^{241}Am (III) or $^{(152+154)}$Eu (III)) are the radioactivity of radionuclide in ionic liquid and aqueous phases respectively.

The concentration of zirconium and uranium present in aqueous phase was determined by titrimetry and spectrophotometry respectively, as discussed in section 2.3.3 and 2.3.4. From the initial concentrations of zirconium and uranium present in aqueous phase and their values determined at equilibrium after extraction, the distribution ratio and % of extraction of zirconium and uranium were determined using equation 2.4 and 2.5.

$$D_M = \frac{[M]_{ini} - [M]_{fin}}{[M]_{fin}} \tag{2.4}$$

$$\%\ \text{Extraction} = \frac{[M]_{ini} - [M]_{fin}}{[M]_{in}}\ \text{X}\,100 \tag{2.5}$$

where M is either Zr(IV) or U(VI). The subscripts “ini” and “fin” indicates the initial and final concentration of zirconium or uranium in aqueous phase.

The separation factor (SF) of zirconium over uranium was determined using equation 2.6.

$$\text{Separation Factor (SF)} = \frac{D_{Zr(IV)}}{D_{U(VI)}} \tag{2.6}$$

2.4.1. Enthalpy of extraction

The enthalpy change accompanied by the extraction of metal ion from the desired concentration of nitric acid in aqueous phase was determined by measuring the distribution ratio of metal ion as a function of temperature using Van't Hoff equation of the form shown in equation 2.7.

$$\frac{\partial \ln D}{\partial (1/T)} = \frac{-\Delta H_{tot}}{R} \tag{2.7}$$

where R is universal gas constant ($R = 8.314\ J.K^{-1}.mol^{-1}$), plot of ln D against 1/T was drawn and the enthalpy of extraction was calculated from the slope of straight line obtained by the linear regression of extraction data.

2.5. Experimental procedures

The experimental procedures adapted for obtaining the results discussed in each chapter are presented here.

2.5.1. Extraction behavior of uranium in CHON based ligand-ionic liquid system

2.5.1.1. Effect of HNO_3 concentration

The ionic liquid $[N_{1888}][NO_3]$ and 0.1 M DOHyA/$[N_{1888}]$[NO3] or *n*-DD were prepared and it was pre equilibrated with desired concentration of nitric acid in order to fix the equilibrium acidity. Extraction of uranium as a function of nitric acid concentration (0.5 to 7 M) was studied by equilibrating 1 mL of pre-equilibrated organic phase with 1 mL of desired concentration of nitric acid solution containing uranium. The concentration of uranium in respective nitric acid concentration is 4×10^{-4} M.

2.5.1.2. Kinetics of extraction

The ionic liquid [N_{1888}][NO_3] and 0.1 M DOHyA in [N_{1888}][NO_3] were pre-equilibrated with 3 M HNO_3. Extraction of uranium as a function of equilibration time was studied by equilibrating 1 mL of pre-equilibrated organic phase with 1 mL of aqueous phase containing uranium present in 3 M HNO_3.

2.5.1.3. Effect of DOHyA concentration

The extraction of U(VI) as a function of DOHyA concentration in the ionic liquid phase was studied by equilibrating 1 mL of nitric nitric acid solution (1,3,5 M) containing uranium with 1 mL of DOHyA/[N_{1888}][NO_3] (which was pre-equilibrated with respective nitric acid concentration) for one hour. The concentration of DOHyA in IL was varied from 0.05 to 0.25 M

2.5.1.4. Loading studies

The amount of U(VI) in the nitric acid phase was varied from 0.1 to 50 g/L. Then the resultant aqueous solution was contacted with equal volume (1 mL) of ionic liquid ([N_{1888}][NO_3]) and DOHyA/[N_{1888}][NO_3]) for equilibration. Using the distribution ratio measurement, the amount of uranium(VI) loaded in to ionic liquid phase was determined

2.5.1.5. Sample preparation for spectroscopic studies

The ionic liquid phase [N_{1888}][NO_3] and DOHyA/[N_{1888}][NO_3] were equilibrated with 3 M HNO_3 and 3 M HNO_3 containing various concentrations of uranium for one hour. The concentration of uranium in 3 M HNO_3 is varied from 10 to 50 g/L. After equilibration, the test tubes were centrifuged and phases inside the test tube were allowed to settle. About 0.1 mL of the sample was taken from the equilibrated ionic liquid phase and the FT-IR spectrum was recorded. Similarly the Raman spectrum of the ionic liquid phase was recorded.

2.5.1.6. Radiolytic degradation studies

The ionic liquid $[N_{1888}][NO_3]$ and 0.1 M DOHyA in $[N_{1888}]$[NO3] were irradiated into various dose rates upto 500 kGy. The irradiated ionic liquid phase was pre-equilibrated with 3 M HNO_3. Extraction of uranium as a function of absorbed dose was studied by equilibrating 1 mL of pre-equilibrated ionic liquid with 1 mL of aqueous phase containing uranium present in 3 M HNO_3.

2.5.1.7. Computational protocol

The geometries of DOHyA and the complexes of U(VI) with DOHyA ($[UO_2(NO_3)_m(DOHyA)_n]$) were optimized in gas phase using BP86 functional [8,9] with SVP (split valence plus polarization) basis set as available in Turbomole package [10]. All the geometry optimizations were carried out without symmetry. Scalar relativistic effects were incorporated for U atom by keeping 60 electrons in the core of U atom using relativistic effective core potential (ECP) [11]. The hessian calculations were carried at the BP/SVP level of theory. The energetics was calculated with B3LYP functional [12,13] using triple zeta valence plus polarization (TZVP) as basis set which is well in producing the energetic of metal complex systems [14-20]. The Gibbs energy of complexation was computed at T = 298.15 K and P = 1 atm. The solvent effects were included using Conductor like Screening Model (COSMO) solvation model [21,22]. The default atomic COSMO radii were used for all the elements. The dielectric constant of medium, ε of water, dodecane, ionic liquids $[N_{1888}][NO_3]$ and $[N_{1888}][NTF_2]$ were taken as 80, 2, 20 and 12. Further, the natural population analysis (NPA) was conducted at the B3LYP/TZVP level of theory. Atom in molecule (AIM) analysis was performed on the complexes using the Bader concepts at the B3LYP/TZP/ZORA (zero order regular approximation) level of theory using ADF package [23,24].

2.5.1.8. Stripping studies

The extracted uranium was recovered from the loaded ionic liquid phase using dilute nitric acid (0.01 M). Prior to stripping, the uranium was loaded into ionic liquid phase by equilibrating equal volumes of ionic liquid and aqueous phase containing 0.1 g/L uranium in 3 M nitric acid. The aqueous phase was removed and contacted the ionic liquid phase with equal volumes of 0.01 M nitric acid. The equilibration was carried out for 1 hr. The aqueous phase was separated from the ionic liquid phase. The ionic liquid phase was again equilibrated with equal volume of fresh 0.01 M nitric acid. This procedure was repeated until the recovery of uranium was near quantitative from the loaded ionic liquid phase.

2.5.2. Europium(III) complexation behaviour in ammonium ionic liquid medium containing neutral extractants

2.5.2.1. Effect of HNO_3 concentration

The ionic liquid $[N_{1444}][NTf_2]$ and 0.05 M T2EHDGA or CMPO in $[N_{1444}][NTf_2]$ were prepared and it was pre equilibrated with desired concentration of nitric acid in order to fix the equilibrium acidity. The concentration of nitric acid in aqueous phase was varied from 0.5 to 8 M. Extraction of europium as a function of nitric acid concentration was studied by equilibrating 1 mL of pre-equilibrated ionic liquid phase with 1 mL of desired concentration of nitric acid solution (0.5 to 8 M) spiked with $^{(152+154)}$Eu tracer (10^{-4} M).

2.5.2.2. Aggregation behavior

The ionic liquid $[N_{1444}][NTf_2]$ and 0.05 M T2EHDGA or CMPO in $[N_{1444}][NTf_2]$ were prepared and it's aggregate size was measured. Further the ionic liquid phase 0.05 M T2EHDGA or CMPO in $[N_{1444}][NTf_2]$ was equilibrated with desired concentration of nitric acid. The equilibrated ionic liquid phase was subjected to dynamic light scattering measurements.

Similarly aggregate size of ionic liquid phase studied in presence of Eu(III) ion concentration also.

2.5.2.3. Effect of concentration of T2EHDGA or CMPO

The extraction of Eu(III) as a function of extractant concentration in the ionic liquid phase was studied by equilibrating 1 mL of 3 M nitric acid solution with 1 mL of T2EHDGA or CMPO/[N_{1444}][NTf_2] (which was pre-equilibrated with 3 M HNO_3) spiked with Eu tracer for one hour. The concentration of extractants in IL was varied from 0.005 to 0.1 M

2.5.2.4. ATR-FTIR Studies

The ionic liquid phase 0.05 M T2EHDGA or CMPO in [N_{1444}][NTf_2] was equilibrated with desired nitric acid solution (1-5 M) for one hour. Similarly the ionic liquid phase was equilibrated with 3 M HNO_3 containing various concentrations of Eu(III). The concentration of Eu(III) in 3 M HNO_3 was varied from 1-10 g.L^{-1}. After equilibration, the test tubes were centrifuged and phases inside the test tube were allowed to settle. A bout 0.1 mL of the equilibrated ionic liquid phase containing nitric acid or Eu(III) ion was taken and the FT-IR spectrum was recorded.

2.5.2.5. Luminescence studies

The luminescence spectra of the aqueous phase and ionic liquid phase samples were recorded. The samples were taken in a fused silica cuvette of path length 2 mm. The spectra were corrected with blank, which was obtained by recording the luminescence spectra of the sample without Eu(III) ion in the solution. Time resolved spectra were recorded using the same instrument with a μs-Xe flash lamp as excitation source. Luminescence life times were determined by fitting the observed luminescence data into the first order exponential decay function described elsewhere [25]. Number of water molecules present in the inner sphere of the metal-solvate was determined using equation 2.7 [25, 26].

$$N_{\mathrm{H_2O}} = \frac{1.05}{\tau} - 0.7 \qquad (2.7)$$

where N_{H2O} is the number of water molecules present in the inner coordination sphere of the Eu(III) in the ionic liquid phase and τ stands for the observed life time in ms.

2.5.2.6. Radiolytic degradation studies

The radiolytic degradation of the ionic liquid phase, composed of 0.05 M T2EHDGA (or CMPO)/[N_{1444}][NTf2] was carried out by irradiating the organic phase in a ^{60}Co gamma chamber facility. The absorbed gamma dose by the sample was varied from 0 to 500 kGy. The distribution ratio of Eu(III) in the irradiated sample was measured as a function of absorbed dose.

2.5.3. Selective separation of zirconium(IV) from uranium(VI) using dioxoamide ligand present in ammonium ionic liquid medium

2.5.3.1. Effect of HNO_3 concentration

The ionic liquid [N_{1444}][NTf_2] and 0.05 M BD in [N_{1444}][NTf_2] or *n*-DD were prepared and it was pre equilibrated with desired concentration of nitric acid (0.5 to 5 M) in order to fix the equilibrium acidity. Extraction of zirconium as a function of nitric acid concentration was studied by equilibrating 1 mL of pre-equilibrated ionic liquid phase with 1 mL of desired concentration of nitric acid solution containing zirconium (1 g.L^{-1}).

2.5.3.2. Kinetics of extraction

The ionic liquid [N_{1444}][NTf_2] and 0.05 M BD in [N_{1444}][NTf_2] were pre-equilibrated with 3 M HNO_3. Extraction of zirconium as a function of equilibration time was studied by equilibrating 1 mL of pre-equilibrated ionic liquid phase with 1 mL of aqueous phase containing zirconium present in 3 M HNO_3.

2.5.3.3. Effect of concentration of BD

The extraction of Zr(IV) as a function of BD concentration in the ionic liquid phase was studied by equilibrating 1 mL of 3 M nitric acid solution with 1 mL of BD/[N_{1444}][NTf_2] (which was pre-equilibrated with 3 M HNO_3) containing zirconium for one hour. The concentration of BD in IL was varied from 0.01 to 0.2 M

2.5.3.4. Loading studies

The amount of Zr(IV) in the nitric acid phase was varied from 1 to 19 g/L. Then the resultant aqueous solution was contacted with equal volume (1 mL) of ionic liquid phase BD/[N_{1444}][NTf_2]) for equilibration. Using the distribution ratio measurement, the amount of zirconium(IV) loaded in to ionic liquid phase was determined

2.5.3.5. Effect of temperature

Enthalpy change accompanied by the extraction of Zr(IV) in 0.05 M BD/[N_{1444}][NTf_2] was determined by measuring the distribution ratio of Zr(IV) in 3 M HNO_3 containing zirconium at various temperatures ranging from 298 to 333 K.

2.5.4. Probing the absence of third phase formation during the trivalent metal ions in an ionic liquid medium

2.5.4.1. Effect of HNO_3 concentration

The ionic liquid [N_{1888}][NO_3] and 0.1 M T2EHDGA or CMPO in [N_{1888}][NO_3] were prepared and it was pre equilibrated with desired concentration of nitric acid (0.01 to 8 M) in order to fix the equilibrium acidity. Extraction of americium as a function of nitric acid concentration was studied by equilibrating 1 mL of pre-equilibrated ionic liquid phase with 1 mL of desired concentration of nitric acid solution spiked with ^{241}Am tracer (10^{-4} M).

2.5.4.2. Aggregation behavior of ionic liquid phase

The ionic liquid $[N_{1888}][NO_3]$ and 0.1 M T2EHDGA or CMPO in $[N_{1888}][NO_3]$ were prepared and they were equilibrated with desired concentration of nitric acid. The aggregate size of ionic liquid phase was measured as a function of nitric acid concentration. Further the ionic phase was equilibrated with 3 M HNO_3 containing varied Nd(III) concentration (0.5 to 5 g/L), then the aggregate size of ionic liquid phase was measured as function of Nd(III) concentration.

2.5.4.3. Effect of concentration of extractant

The extraction of Am(III) as a function of extractant concentration in the ionic liquid phase was studied by equilibrating 1 mL of respective nitric acid (1, 3, 5 M) solution with 1 mL of T2EHDGA or CMPO/$[N_{1888}][NO_3]$ (which was pre-equilibrated with corresponding HNO_3) spiked with Am tracer for one hour. The concentration of extractant in IL was varied from 0.01 to 0.3 M

2.5.4.4. Effect of NO_3^- concentration

The effect of NO_3^- concentration on the distribution ratio of Am(III) was studied by equilibrating 0.1 M T2EHDGA or CMPO/$[N_{1888}][NO_3]$ with 3 M HNO_3 solution containing various $NaNO_3$ concentration (0.1 to 0.8 M) spiked with ^{241}Am tracer. The concentration of NO_3^- ion was varied by adding the required quantity of $NaNO_3$ in aqueous phase.

2.5.4.5. Effect of radiation dose

The radiolytic degradation of the ionic liquid phase, composed of 0.1 M T2EHDGA (or CMPO)/$[N_{1888}][NO_3]$ was carried out by irradiating the ionic liquid phase in a ^{60}Co gamma chamber facility. The absorbed gamma dose by the sample was varied from 0 to 500 kGy. The distribution ratio of Am(III) in the irradiated sample was measured as a function of absorbed dose.

2.5.5. Aggregation behavior of ionic liquid in molecular liquid medium

2.5.5.1. Effect of concentration of [N_{1888}][D2EHP]

The ionic liquid [N_{1888}][D2EHPA] in *n*-DD was prepared in different concentrations as 0.01 to 0.1 M. The aggregate size of organic phase was measured as a function of ionic liquid concentration.

2.5.5.2. Effect of HNO_3 concentration

The organic phase composed of 0.05 M [N_{1888}][D2EHPA] in *n*-DD and 0.05 M [N_{1888}][NO_3]+ 0.05 M D2EHPA in *n*-DD were prepared and they were equilibrated with desired concentration of nitric acid. The aggregate size of ionic liquid phase was measured as a function of nitric acid concentration.

2.5.5.3. Aggregation behavior of Nd(III) extracted phase

The organic phase 0.05 M [N_{1888}][D2EHPA]/*n*-DD was prepared and pre-equilibrated with desired concentration of nitric acid. The pre-equilibrated organic phase was equilibrated with aqueous phase containing different metal ion concentration (1-5 g/L). The aggregate size of organic phase was measured as function of different metal ion concentration.

2.5.5.4. Effect of temperature

The organic phase 0.05 M [N_{1888}][D2EHPA]/*n*-DD was prepared. The aggregate size of organic phase was measured as a function of different temperature from 298 to 333K.

2.5.6. Normalized polarity indices of tri-*n*-butyl phosphate complexes in ionic liquid using Reichardt's dye as polarity probe

2.5.6.1. Determination of polarity

The polarity of ionic liquid phase was determined by using Reichardt's dye as polarity probe procedure discussed elsewhere [27-33]. The λmax of the visible absorption spectrum and the colour of the Reichardt's dye changes with polarity of the medium in which Reichardt's dye is present. Since the λmax of Reichardt's dye is dependent on the polarity of the medium, the energy of that transition ($E_T(30)$) can be regarded as a measure of polarity of the components present in the medium [34-41]. The $E_T(30)$ is defined as the molar transition energy of the Reichardt's dye no. 30 measured in solvents of different polarity measured under standard conditions (25 ^{0}C and 1 atm) and it can be calculated using equation 2.8 [34-41].

$$E_T(30) = \frac{h\,c\,N_A}{\lambda} = \frac{28591}{\lambda\,(nm)}\,\text{kcal.mol}^{-1} \tag{2.8}$$

where h is Plancks constant, C is velocity of light, N_A Avogadros number, $E_T(30)$ is molar transition energy of Reichardt's dye.

From equation 2.8, $E_T(30)$ values were determined to be 30.7 and 63.1 kcal.mol^{-1}for TMS and water respectively, reported in literature [28]. To avoid the units, the dimensionless normalized polarity scale (E_T^N) ranging from E_T^N = 0 for TMS and E_T^N =1 for water was introduced and the E_T^N values for the solvent phase can be determined using equation 2.9 [28,34,35]. Therefore the polarity values of the ionic liquid phases were determined based on equation 2.8, and reported in normalized polarity scale.

$$E_T^N = \frac{E_T(\text{solvent}) - E_T(\text{TMS})}{E_T(\text{water}) - E_T(\text{TMS})} = \frac{E_T(\text{solvent}) - 30.7}{32.4} \tag{2.9}$$

2.5.6.2. Polarity of ionic liquid

The ionic liquids [C_4mim][NTf_2], [C_4mpyr][NTf_2] and [C_4mpip][NTf_2] in acetonitrile was prepared. The concentration of ionic liquids varied from 0.02 to 0.35 M. The normalized polarity of ionic liquid phase was measured as a function of ionic liquid concentration.

2.5.6.3. Polarity of acid loaded ionic liquid phase

The ionic liquids [C_4mim][NTf_2], [C_4mpyr][NTf_2] and [C_4mpip][NTf_2] were prepared and equilibrated with desired nitric acid concentration. The concentration of nitric acid was varied from 0.1 to 5 M. The normalized polarity of ionic liquid phase was measured as a function of initial nitric acid concentration.

2.5.6.4. Effect of [C_4mim]$^+$ or NTf_2^- concentration

The ionic liquid [C_4mim][Cl] was added to [C_4mim][NTf_2] of different concentrations 0.01 to 0.1 M. Then the normalized polarity of ionic liquid phase was studied as a function of [C_4mim]$^+$ concentration. Similarly $LiNTf_2$ was added to [C_4mim][NTf_2] of different concentrations 0.01 to 0.1 M. Then the normalized polarity of ionic liquid phase was studied as a function of [NTf_2]$^-$ concentrations.

2.5.6.5. Polarity of ionic liquid phase containing extractant

The normalized polarity as a function of extractant concentration in the ionic liquid was studied by preparing different concentrations of TBP in [C_4mim][NTf_2]. The concentration of TBP in [C_4mim][NTf_2] was varied from 0.1 to 1.1 M.

2.5.6.6. Polarity of metal loaded ionic liquid phase

The ionic liquids [C_4mim][NTf_2], [C_4mpyr][NTf_2] and [C_4mpip][NTf_2] were prepared. The normalized polarity of ionic liquid phase as a function of concentration of metal ion in ionic liquid was studied by preparing different concentration of metal ion (UO_2^{2+}, Nd^{3+}) in ionic liquid phase. The concentration of metal ion in IL was varied from 0.1 to 5 g/L.

2.5.6.7. Polarity of ionic liquid phase containing metal-ligand complex

The ionic liquid phase 1.1 M TBP in [C_4mim][NTf_2], [C_4mpyr][NTf_2] and [C_4mpip][NTf_2] was prepared. The normalized polarity of ionic liquid phase as a function of concentration of metal ion in ionic liquid was studied by preparing different concentration of metal ion (UO_2^{2+}, Nd^{3+}, Th^{4+}) in ionic liquid phase. The concentration of metal ion in IL was varied from 0.1 to 5 g/L.

2.5.7. Investigations on the radiolytic stability of incinerable CHON-based ionic liquid containing diglycolamide

2.5.7.1. Effect of radiation dose

The ionic liquid $[N_{1888}][NO_3]$, T2EHDGA, 0.1 M T2EHDGA/$[N_{1888}][NO_3]$ and 0.1 M T2EHDGA/n-DD were prepared and irradiated as a function of absorbed dose from 0 to 500 kGy. Unirradiated and irradiated organic phase was pre-equilibrated with desired concentration of nitric acid in order to fix the equilibrium acidity. Extraction of americium as a function of nitric acid concentration was studied by equilibrating 1 mL of pre-equilibrated organic phase with 1 mL of desired concentration of nitric acid solution (0.5 to 5 M) spiked with ^{241}Am tracer. It should be noted that the amount of dose received by the organic phase during the treatement of nuclear waste is about 0.2 kGy in a single centrifugal contactor [42]. Depending upon the number of centrifugal contacts and duration of the cycle, it is quite likely to vary up to 50 kGy. Therefore, it is desirable to study the effect of gamma radiation with about one order more (i.e., up to 500 kGy) for understanding the radiolytic stability of organic phase.

2.5.7.2. ATR-FTIR studies

Few microlitres of unirradiated and irradiated ionic liquid phase as $[N_{1888}][NO_3]$ and 0.1 M T2EHDGA in $[N_{1888}][NO_3]$ was placed on a diamond crystal and the ATR-FTIR spectrum was recorded from 4000 to 600 cm^{-1} (16 scans). The spectrum obtained was then corrected to the background (without sample) and presented as ATR-FTIR spectrum of the sample.

2.5.7.3. Effect of T2EHDGA concentration

The extraction of Am(III) as a function of extractant concentration in the ionic liquid phase was studied by equilibrating 1 mL of 3 M nitric acid solution with 1 mL of unirradiated and irradiated T2EHDGA/[N_{1888}][NO_3] (which was pre-equilibrated with 3M HNO_3) spiked with Am tracer for one hour. The concentration of T2EHDGA in IL was varied from 0.01 to 0.3 M and the absorbed dose of T2EHDGA/[N_{1888}][NO_3] was upto 500 kGy.

2.5.7.4. Loading studies

The solutions of unirradiated and irradiated (500 kGy) ionic liquid [N_{1888}][NO_3], 0.1 M T2EHDGA/[N_{1888}][NO_3] and also 0.1 M T2EHDGA(irradiated)/[N_{1888}][NO_3] and T2EHDGA /[N_{1888}][NO_3] (irradiated) were prepared. The amount of Nd(III) in the nitric acid phase was varied from 1 to 70 g/L. Then the resultant aqueous solution was contacted with equal volume (1 mL) of unirradiated and irradiated ionic liquid phase [N_{1888}][NO_3] and 0.1 M T2EHDGA /[N_{1888}][NO_3] for equilibration. Using the distribution ratio measurement, the amount of neodymium (III) loaded into ionic liquid phase was determined.

2.5.7.5. Stripping studies

The extracted americium was recovered from the loaded ionic liquid phase using dilute nitric acid (0.01 M). Prior to stripping, the americium was loaded into ionic liquid phase by equilibrating equal volumes of ionic liquid and aqueous phase containing americium in 3 M nitric acid. Then the aqueous phase was removed and contacted the ionic liquid phase with equal volumes of 0.01 M nitric acid. The equilibration was carried out for 1 hr. The aqueous phase was separated from the ionic liquid phase. The ionic liquid phase was again equilibrated with equal volume of fresh 0.01 M nitric acid. This procedure was repeated until the recovery of americium was near quantitative from the loaded ionic liquid phase.

2.5.8. Thermophysical properties of ionic liquid solvent system.

2.5.8.1. Viscosity and density measurements

The viscosity and density of neat extractants (D2EHPA or HDEHDGA) and extractants in ionic liquid [C_4mim][NTf_2] medium was measured as a function of temperature. The concentration of extractants in ionic liquid phase was varied from 0.02 to 0.1 M and temperature range of measurements is from 298 to 333 K.

2.5.8.2. Effect of HNO_3 concentration

The solutions of 0.06 M D2EHPA or HDEHDGA in [C_4mim][NTf_2] were prepared and it was equilibrated with desired concentration of nitric acid. The concentration of nitric acid was varied from 0.01 to 1.0 M. The values of viscosity and density of equilibrated ionic liquid phase was measured as a function of temperature.

2.5.8.3. Effect of concentration of extractant

The solutions of varied concentration of D2EHPA or HDEHDGA in [C_4mim][NTf_2] were prepared. The concentration of extractants in [C_4mim][NTf_2] was varied from 0.02 to 0.1 M. The viscosity and density of ionic liquid phase as a function of extractant concentration in the ionic liquid phase at various temperatures was measured.

2.5.8.4. Effect of concentration of metal ion

The solution of 0.06 M D2EHPA or HDEHDGA/[C_4mim][NTf_2] was prepared and pre-equilibrated with 0.01 M nitric acid one hour. The amount of Nd(III) in the nitric acid (0.01 M) phase was varied from 1 to 5 g/L. Then the resultant aqueous solution was contacted with equal volume of ionic liquid phase 0.06 M D2EHPA or HDEHDGA/[C_4mim][NTf_2] for equilibration.

The values of viscosity and density were measured for the equilibrated ionic liquid phase as a function of Nd(III) concentration at various temperatures.

2.5.8.5. Effect of radiation dose

The solution of 0.06 M D2EHPA or HDEHDGA/[C_4mim][NTf_2] was prepared and irradiated up to 500 kGy by γ-dose. The values of viscosity and density were measured for the irradiated ionic liquid phase as a function of absorbed dose at various temperatures.

2.5.8.6. Phase separation time measurement

The phase separation time (PST) is the time taken for the disappearance of all primary droplets at the interface formed after equilibration of aqueous and ionic liquid phases. The solutions of 0.06 M D2EHPA or HDEHDGA in [C_4mim][NTf_2] was prepared and irradiated up to 500 kGy by γ-dose. Unirradiated ionic liquid phase was equilibrated with desired concentration of nitric acid. The concentration of nitric acid in aqueous phase was varied from 0.01 to 1 M. After equilibration the time taken for the separation of aqueous and ionic liquid phase was measured. In a separate experiment, the irradiated ionic liquid phase equilibrated with 3 M HNO_3 as a function of absorbed γ-dose. After equilibration the time taken for the separation of aqueous and ionic liquid phase was measured using stop watch with a resolution of 0.01 seconds. The measured PST values are average of three independent experiments and the uncertinity in the values is ± 5 %.

2.6. Synthesis and characterization of RTILs and extractants

2.6.1. 1-Butyl-3-methylimidazolium bis(trifluoromethylsulfonyl)imide ([C_4mim][NTf_2])

1-butyl-3-methylimidazolium bis(trifluoromethlsulfonyl)imide was prepared as described elsewhere [43] and the synthetic procedure is shown in Fig. 2.2. First step is preparation of 1-butyl-3-methylimidazolium chloride ([C_4mim][Cl]) and it involves refluxing a mixture of 1-

methylimidazole with 1-chlorobutane in the mole ratio of 1:1.2 at 343 K for 72 hours. The resulting product ($[C_4mim][Cl]$) was washed few times with ethyl acetate. Then excess ethyl acetate was removed and further final product was dried under vacuum at 353 K for more than 24 hours. A white crystalline solid was obtained after cooling.

The second step involves anion exchange reaction between $[C_4mim][Cl]$) and Lithium bis(trifluoromethylsulfonyl)imide ($Li^+ \, {}^-N(CF_3SO_2)_2$) in the mole ratio of 1:1. This reaction mixture was stirred for overnight at 298 K in water medium. After stirring, the bottom layer of ionic liquid was removed and washed four times with distilled water in order to remove unreacted precursors and LiCl. The final product was dried at 353 K under vacuum in order to remove the moisture. Around 85 % yield was obtained.

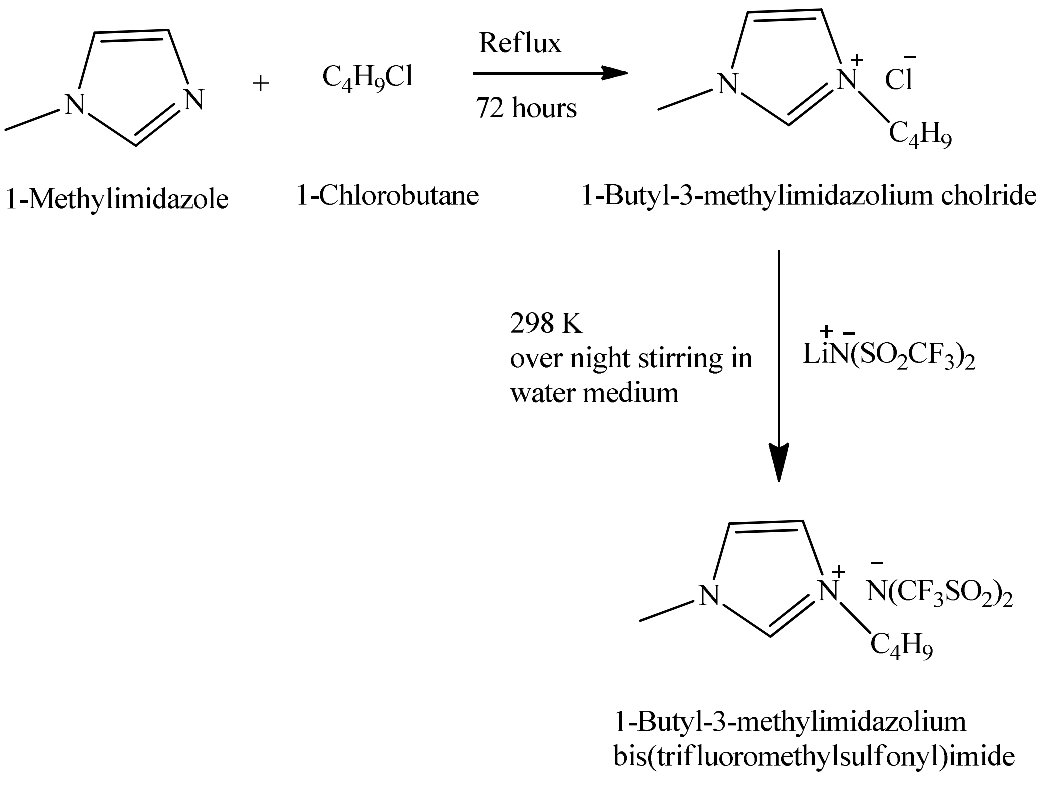

Fig. 2.2. Synthesis of 1-butyl-3-methylimidazolium bis(trifluoromethylsulfonyl)imide.

2.6.2. 1-Butyl-1-methylpyrrolidinium bis(trifluoromethylsulfonyl)imide ([C_4mpyr][NTf_2])

1-butyl-1-methyl pyrrolidinium bis(trifluoromethylsulfonyl)imide was prepared as described elsewhere [43] and the synthetic procedure is shown in Fig. 2.3. First step is preparation of 1-butyl-1-methylpyrrolidinium bromide ([C_4mpyr][Br]) and it involves refluxing a mixture of 1-methyl with 1-bromobutane in the mole ratio of 1:1.2 at 343 K for 72 hours. The resulting product ([C_4mpyr][Br]) was washed few times with ethyl acetate. The excess ethyl acetate was removed and further dried under vacuum at 353 K for more than 24 hours. A white crystalline solid was obtained after cooling.

The second step involves the anion echange reaction between [C_4mpyr][Br]) and Lithium bis(trifluoromethylsulfonyl)imide (Li^+ $^-N(CF_3SO_2)_2$) in the mole ratio of 1:1. This reaction mixture was stirred for overnight at 298 K in water medium. After stirring, the bottom layer of ionic liquid was removed and washed four times with distilled water in order to remove unreacted precursors and LiCl. The final product was dried at 353 K under vacuum in order to remove the moisture. Around 85 % yield was obtained.

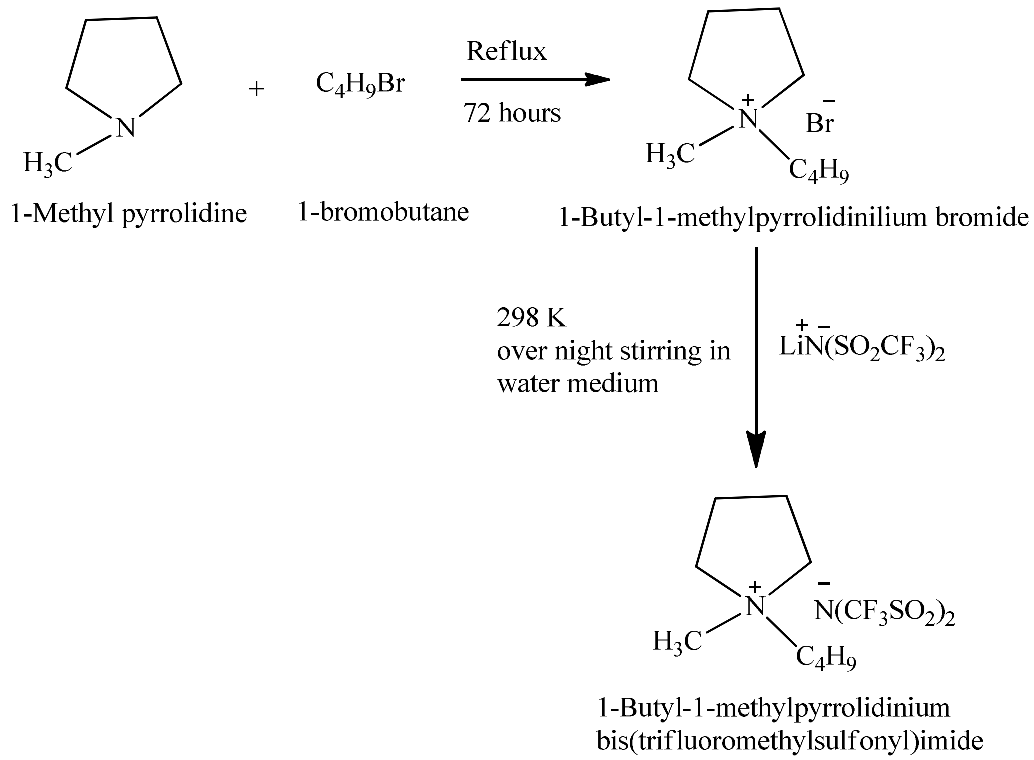

Fig. 2.3. Synthesis of 1-butyl-1-methylpyrrolidinium bis(trifluoromethylsulfonyl)imide.

2.6.3. 1-Butyl-1-methyl piperdinium bis(trifluoromethylsulfonyl)imide ([C$_4$mpip][NTf$_2$])

1-butyl-1-methyl pyrrolidinium bis(trifluoromethylsulfonyl)imide was prepared as described elsewhere [43,44] and the synthetic procedure is shown in Fig. 2.4. First step is preparation of 1-butyl-1-methylpyrrolidinium bromide ([C$_4$mpyr][Br]) and it involves refluxing a mixture of 1-methyl piperidine with 1-bromobutane in the mole ratio of 1:1.2 at 343 K for 72 hours. The resulting product ([C$_4$mpip][Br]) was washed few times with ethyl acetate. The excess ethyl acetate was removed and further final product was dried under vacuum at 353 K for more than 24 hours. A white crystalline solid was obtained after cooling.

The second step involves anion exchange reaction between [C$_4$mpip][Br]) and Lithium bis(trifluoromethylsulfonyl)imide (Li^+ $^-N(CF_3SO_2)_2$) in the mole ratio of 1:1. This reaction mixture was stirred for overnight at 298 K in water medium. After stirring, the bottom layer of ionic liquid was removed and washed four times with distilled water in order to remove unreacted precursors and LiCl. The final product was dried at 353 K under vacuum in order to remove the moisture. Around 85 % yield was obtained.

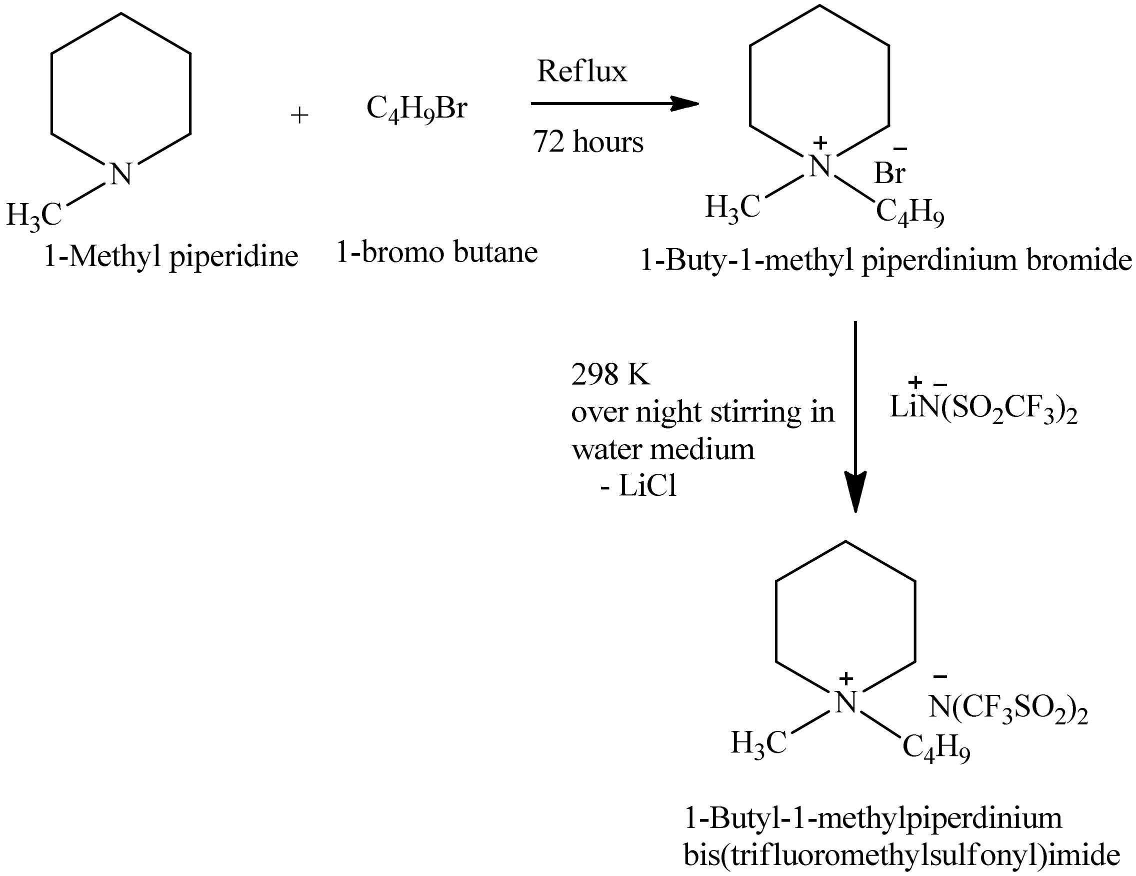

Fig. 2.4. Synthesis of 1-butyl-1-methylpipyridinium bis(trifluoromethylsulfonyl)imide.

2.6.4. Tri-*n*-butylmethyl ammonium bis(trifluoromethylsulfonyl)imide [N_{1444}][NTf_2])

The synthesis involves in the reaction between [N_{1444}][Cl] and and Lithium bis(trifluoromethylsulfonyl)imide ($LiN(CF_3SO_2)_2$) in the mole ratio of 1:1 and the synthesis scheme is shown in Fig. 2.5. [45]. This reaction mixture was stirred for 4 hours at 298 K in water medium. After stirring, the bottom layer of IL was washed several times with distilled water and the product was treated with charcoal. Then it was dried at 353 K under vacuum in order to remove the moisture. Absence of chloride ion in the final product was ascertained by testing with acidified $AgNO_3$ solution. Around 90% yield was obtained for $[N_{1444}][NTf_2]$.

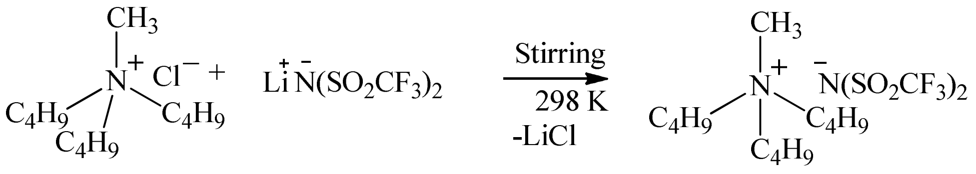

Tri-butyl-methyl ammonium chloride

Lithium (bistrifluoromethylsulfonyl)imide

Tri-butyl-methyl ammonium bis(trifluoromethylsulfonyl)imide

Fig. 2.5. Synthesis of tri-butylmethylammonium bis(trifluoromethylsulfonyl)imide.

2.6.5. Methyl-*n*-tri-octyl ammonium bis(trifluoromethylsulfonyl)imide ($[N_{1888}][NTf_2]$)

The synthesis involves in the reaction between $[N_{1888}][Cl]$ and and Lithium bis(trifluoromethanesulfonyl)imide ($LiN(CF_3SO_2)_2$) in the mole ratio of 1:1 and the synthesis scheme is shown in Fig. 2.6. [45,46]. This reaction mixture was stirred for 4 hours at 298 K in water medium. After stirring, the bottom layer of IL was washed several times with distilled water and the product was treated with charcoal. Then it was dried at 353 K under vacuum in order to remove the moisture. Around 90 % yield was obtained for $[N_{1888}][NTf_2]$.

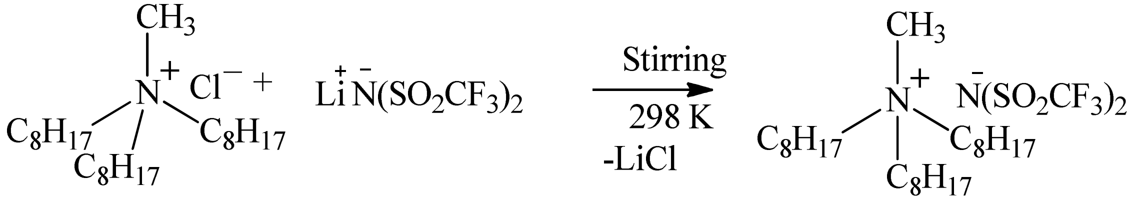

Methyl-tri-*n*-octyl ammonium chloride

Lithium bis(trifluoromethylsulfonyl)imide

Methyl-tri-*n*-octyl ammonium bis(trifluoromethylsulfonyl)imide

Fig. 2.6. Synthesis of methyl-tri-octylammonium bis(trifluoromethylsulfonyl)imide.

2.6.6. Methyl-tri-*n*-octyl ammonium nitrate ([N$_{1888}$][NO$_3$]

The synthesis involves the reaction between [N$_{1888}$][Cl] and and sodium nitrate and the synthesis scheme is shown in Fig. 2.7. [45]. A solution of 250 mL of 0.5 M methyl-tri-n-octyl ammonium chloride in benzene is equilibrated 4 to 5 times with 4 M sodium nitrate solution and then ionic liquid phase is separated and then washed extensively with water. The ionic liquid phase was tested for the absence of chloride ion (using acidified AgNO$_3$). Benzene was removed by evaporation under reduced pressure in rotary evaporator at 343 K. Then it was dried at 353 K under vacuum in order to remove the moisture. A thick viscous liquid, which turned to semi solid upon cooling, around 90 % yield was obtained.

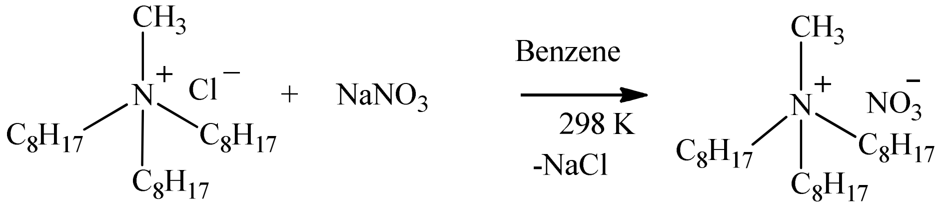

Methyl-tri-*n*-octyl ammonium chloride

Sodium nitrate

Methyl-tri-*n*-octyl ammonium nitrate

Fig. 2.7. Synthesis of methyl-tri-*n*-octylammonium nitrate.

2.6.7. Synthesis of *N,N*-dioctyl-2-hydroxyacetamide

The synthesis of *N,N*-di-octyl-2-hydroxyacetamides was carried out by the procedure described elsewhere [47,48]. The schematic procedure for the synthesis of DOHyA is shown in Fig. 2.8.

A 250 mL three neck round bottom flask taken and filled around 50-60 mL neat chloroform and acetoxy acetyl chloride (one eq) and the RB flask containing solution is immersed in an ice-bath maintained at 0-5^{0}C. A solution of tri-ethylamine (1.2 eq) and *N,N*-dioctylamine (one eq) in neat chloroform (50 mL) taken in dropping funnel and then added drop wise to acetoxy acetyl chloride solution under inert atmosphere. The reaction mixture was stirred for four to five hours at room temperature and then the chloroform was removed under high pressure vacuum. The crude was then extracted with *n*-hexane then two times washed with water to remove all the precipitated triethylamine hydrochloride and unreacted amine. The hexane extracted solution was then successively twice washed with 1 M HCl and with water then saturated sodium bi-carbonate solutions. Finally, the compound was dried over anhydrous sodium sulphate and removed the *n*-hexane from the compound by rotary evaporator.

The product obtain from the above step was taken into single neck flask and dissolved in methanol. The desired amount of potassium hydroxide was dissolved in 50 mL of ethanol at room temperature. The potassium hydroxide solution was added to the RB flask and stirred for the three hour at room temperature. After completion of the reaction, the methanol was removed from the reaction mixture by using rotatary evaporator. The mixture was dissolved in n-hexane and transferred to the separating funnel for the workup. The mixture was washed as mentioned in above in successive manner of water, 1 M HCl and sodium carbonate and finally dried over anhydrous sodium sulphate and the hexane removed under high vaccum. The crude product was then purified by column chromatography over silica gel using 10 % ethyl acetate-petroleum ether as eluent. The characterization data for the N,N-dioctyl hydroxyacetamide is given below. The yield obtained was 85-90 %.

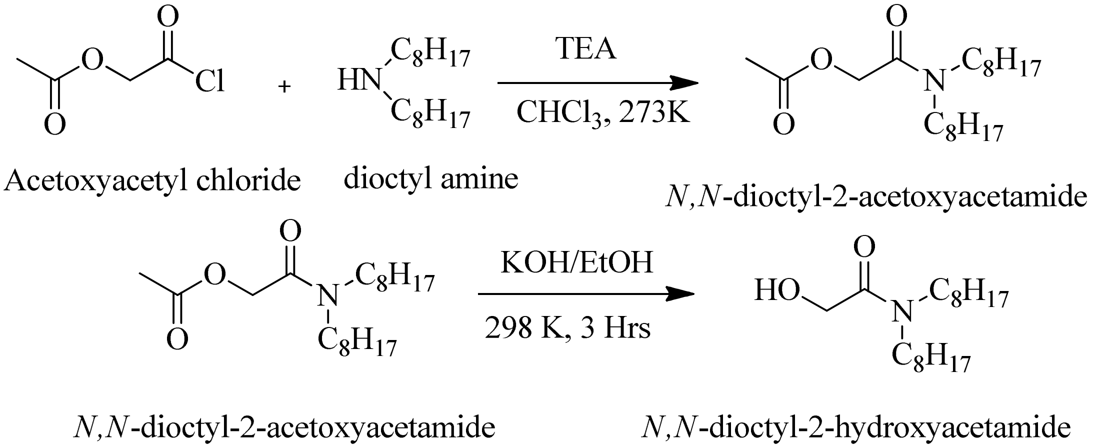

Fig. 2.8. Reaction scheme for the synthesis of DOHyA.

<u>Characterization:</u>

***N,N*-di-octyl-2-hydroxy acetamide (DOHyA):** (pale yellow liquid) ^{1}H NMR (500 MHz, $CDCl_3$, δ relative to TMS): 4.138 (d, 2H, J=4Hz), 3.706 (t, 1H, J=4Hz), 3.361 (t, 2H, J=8Hz), 3.047 (t, 2H, J=8Hz), 1.538 (m,4H), 1.286 (m,20H), 0.883 (m, 6H). ^{13}C NMR (500 MHz, $CDCl_3$, δ relative to TMS): 171.01, 59.71, 46.11, 45.82, 31.77(d), 29.31, 29.22(d), 29.12, 28.52, 27.54, 26.96, 26.81, 22.60(d), 14.03(d).

IR (neat, ν cm^{-1}): 3410 (medium, broad, O-H stretch), 2926, 2858 (strong, C-H stretch), 1652 (very strong, C=O stretch), 1462 (medium, -CH2-scissoring), 1402 (medium, C-N stretch), 1278 (medium, -CH2-wagging), 1090 (strong, C-O stretch of hydroxyl group).

2.6.8. Synthesis of Benzodioxodiamide derivatives

The synthesis of Benzodioxodiamide and their derivatives were prepared by the procedure described elsewhere [49]. The path way for the synthesis of Benzodioxodiamide is shown in Fig. 2.9.

A 250 mL three neck round bottom flask taken and filled around 50-60 mL neat chloroform and chloro acetyl chloride (one mol) and the RB flask containing solution is immersed in an ice-bath maintained at 0-5^{0}C. A solution of tri-ethylamine (1.2 eq) and *N,N*-di-2-ethylhexylamine (one eq) or *N,N*-di-decylamine in neat chloroform (50 mL) taken in dropping funnel and then added drop wise to chloro acetyl chloride solution under inert atmosphere. The reaction mixture was stirred for four to five hours at room temperature and then the chloroform was removed under high pressure vacuum. The crude was then extracted with *n*-hexane then two times washed with water to remove all the precipitated triethylamine hydrochloride and unreacted amine. The hexane extracted solution was then successively twice washed with 1 M HCl and with water then saturated sodium bi-carbonate solutions. Finally, the compound was dried over anhydrous sodium sulphate and removed the *n*-hexane from the compound by rotary evaporator.

The amide derivative (2 moles) obtained after the reaction was reacted with 1,2-dihydroxybenzene (1 mol) in ethanol medium. The desired amount of potassium hydroxide was dissolved in 50 mL of ethanol at room temperature. The potassium hydroxide solution was added to the RB flask and stirred for the three hour at room temperature. After completion of the reaction, the ethanol was removed from the reaction mixture by using rotatary evaporator. The mixture was dissolved in *n*-hexane and transferred to the separating funnel for the workup. The mixture was washed as mentioned in above in successive manner of water, 1 M HCl and sodium bi-carbonate and finally dried over anhydrous sodium sulphate and the hexane removed under high vaccum. The crude product was then purified by column chromatography over silica gel using 10 % ethyl acetate-petroleum ether as eluent. The characterization data for the 2-ethylhexyl derivative as BD and decyl derivative as BDD is given below. The yield obtained was 85-90 %.

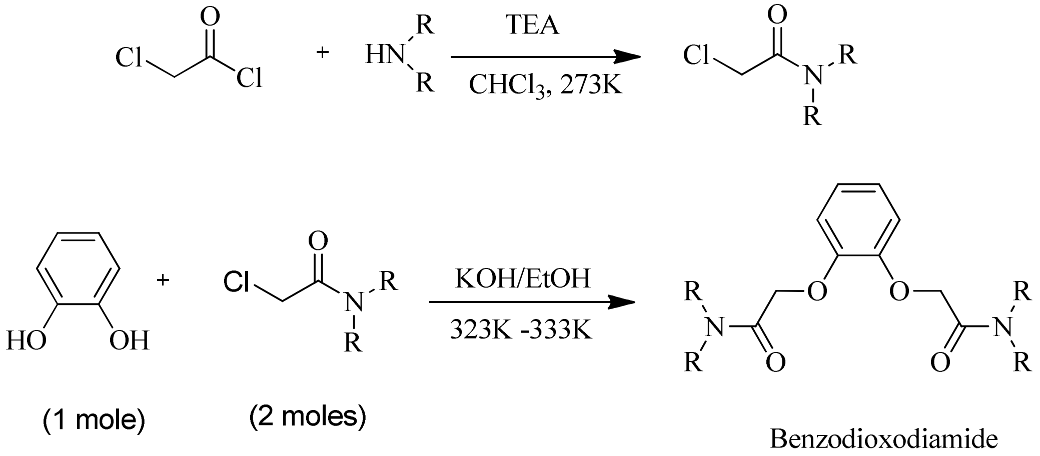

(R = 2-ethylhexyl (or) decyl, TEA = Triethylammine)

Fig. 2.9. Reaction scheme for the synthesis for BD and BDD.

Characterization

BD: ^{1}**H NMR** (500 MHz; $CDCl_3$; Me_4Si)**:** BD: 0.81-0.91 (m, 24H), 1.24-1.28 (m, 32H), 3.12-3.33 (m, 8H), 4.1 (s, 4H), 4.77 (m, 4H), 6.88-6.91 (m, 4H). BDD: 0.83-0.93 (m, 20H), 1.27-1.3 (m, 56H), 3.21-3.34 (m, 8H), 4.3 (s, 4H), 6.87-6.91 (m, 4H). **FTIR(ν/cm^{-1}):** BD: 2961-2859 cm^{-1}(CH stretch), 1645 cm^{-1} (CO stretch), 1496 cm^{-1} (CH aromatic ring), 1460 cm^{-1}(N-CH_2 stretch), 1377 cm^{-1} (CH bend), 1193 cm^{-1} (CH wagging), 1059 cm^{-1} (-OCH_2- stretch), 744 cm^{-1} (CH rock).

BDD: ^{1}**H NMR** (500 MHz; $CDCl_3$; Me_4Si)**:** BDD: 0.83-0.93 (m, 20H), 1.27-1.3 (m, 56H), 3.21-3.34 (m, 8H), 4.3 (s, 4H), 6.87-6.91 (m, 4H). **FTIR(ν/cm^{-1}):** BDD: 2971-2852 cm^{-1}(CH stretch), 1648 cm^{-1} (CO stretch), 1496 cm^{-1} (CH aromatic ring), 1463 cm^{-1}(N-CH_2 stretch), 1376 cm^{-1} (CH bend), 1189 cm^{-1} (CH wagging), 1057 cm^{-1} (-OCH_2- stretch), 747 cm^{-1} (CH rock).

2.6.9. Methyl-tri-*n*-octylammonium (2-ethylhexyl)phosphate [N_{1888}][D2EHP]

The Synthesis of [N_{1888}][D2EHP] was carried out as per the procedure described elsewhere [50]. The schematic procedure for the synthesis of [N_{1888}][D2EHP] is shown in Fig. 2.10.

A 100 mL of 0.5 M [N_{1888}][Cl]/$CHCl_3$ was prepared and taken in a RB flask. And this solution is equilibrated with 4 M NaOH solution for one hour. After phase separation aqueous phase was discarded and the ionic liquid phase was again equilibrated with fresh sodium hydroxide solution. This procedure was repeated 5-6 times until the Cl^- ion in organic phase was negligible (tested with acidified $AgNO_3$ solution).

The second step involves the refluxing of the above product [N_{1888}][OH] with bis-2-ethylhexyl phosphoric acid (D2EHPA) in 1: 1 mole ratio at 333 K for 10 hour. The resulting product ([N_{1888}][D2EHPA]) was washed with 3-4 times of and purified by dissolving in acetonitrile in solution with activated charcoal and stirring for more than 24 hours at room temperature. The charcoal was removed by vacuum filtration using Whattman 42 filter paper and then the product was dried at 353 K under vacuum in order to remove the moisture. A thick viscous liquid was obtained. The characterization data for [N_{1888}][D2EHPA] is given below. The yield obtained was 90 %.

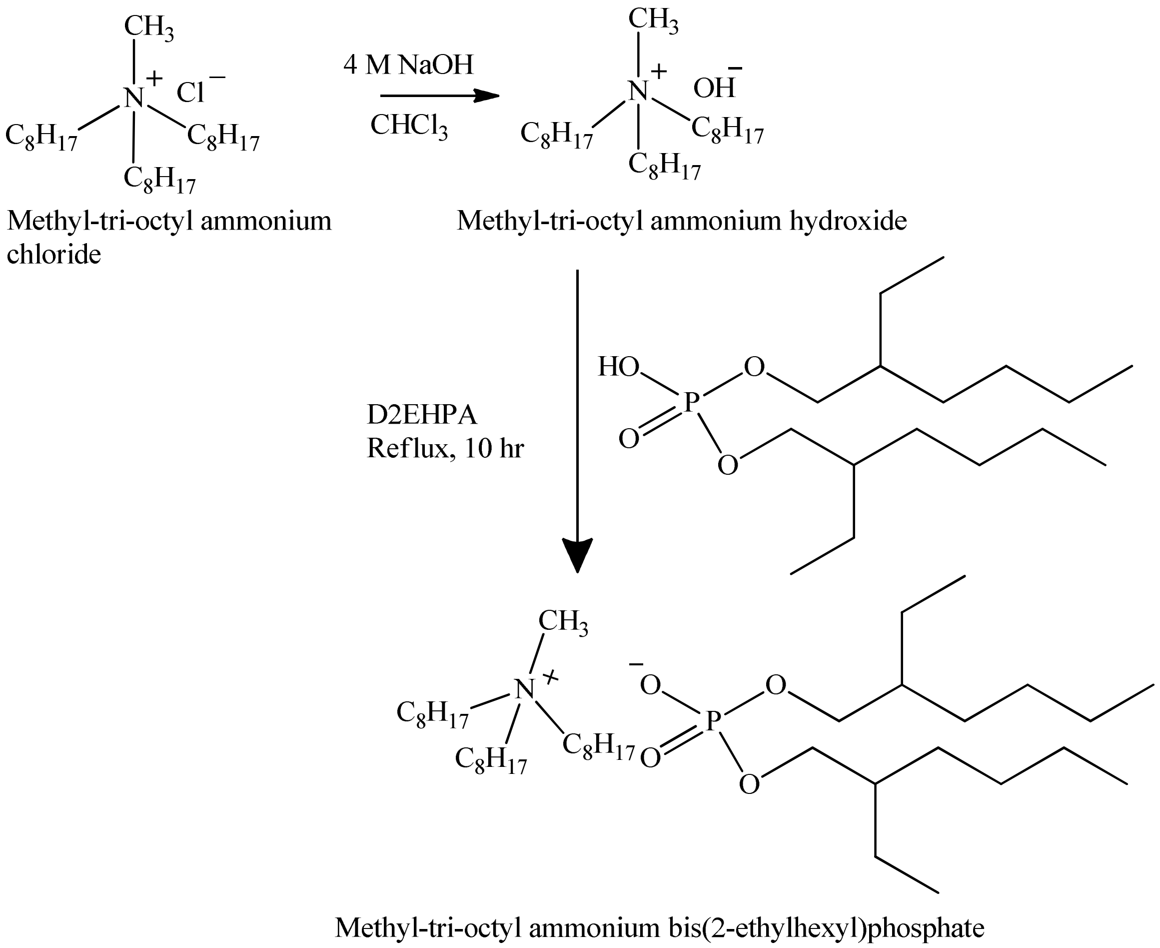

Fig. 2.10. Reaction scheme for the synthesis of $[N_{1888}]$[D2EHP].

Characterization

$[N_{1888}]$[D2EHP]: δ_H (500 MHz, CD3COCD3, Me4Si): 0.89 (9H, m), 1.3 (30H,m),1.8 (6H,m), 3.25 (3H,s), 3.5 (6H,m), 1.29 (m, 6H), 1.33 (m, 12H), 1.42 (m,4H), 1.45 (m, 4H), 1.45 (m, 1H), 1.51 (m, 1H). **δ_C(500 MHz, CD_3COCD_3, Me_4Si) :** 61.24 (3 x CH_2N), 47.5 (CH_3N), 31.6, 29.3, 28.9, 28, 26 (various CH_2), 22.3 (CH_2CH_3), 13.4 (3 x CH_3), 26.1 (CH_2), 28.8 (CH_2), 31.2 (CH_2), 32.5 (CH_2), 36.5 (CH), 49.1 (CH_2), 11.5 (CH_3). **FTIR (ν/cm^{-1}):** 1465 (CH_3-N^+), 1379(C-H symmetric deformation), 2800-3000 (C-H stretching), 1050-970 (P-O-C), 1248(P=O), 1680(P–OH).

2.6.10. Synthesis of bis(2-ethylhexyl) diglycolamic acid (HDEHDGA)

Synthesis of HDEHDGA was carried out as per the procedure described elsewhere [51]. The schematic procedure for the synthesis of HDEHDGA is shown in Fig. 2.11. Diglycolic anhydride (1eq.) was dissolved in chloroform (30 mL) and the solution was taken in a three neck round bottom flask. A solution of bis(2-ethyhexyl)amine (1eq.) and tri-ethylamine (1.2 eq) in chloroform solution was taken in a dropping funnel and added drop-wise to diglycolic anhydride solution about an hour. The reaction mixture was stirred at room temperature for six hours to obtain bis (2-ethyl hexyl) diglycolamic acid. After completion of reaction, the chloroform was removed from the reaction mixture and dissolved in *n*-hexane. The dissolved solution was transferred into the separating funnel then washed with distilled water followed by ~1 M HCl and again by distilled water in order to remove the unreacted reactants, if any. The diglycolic anyhydride is water soluble and can be washed out. The organic phase was dried with anhydrous sodium sulphate, and the solvent was removed under vacuum. The characterization detail of the HDEHDGA is given below.

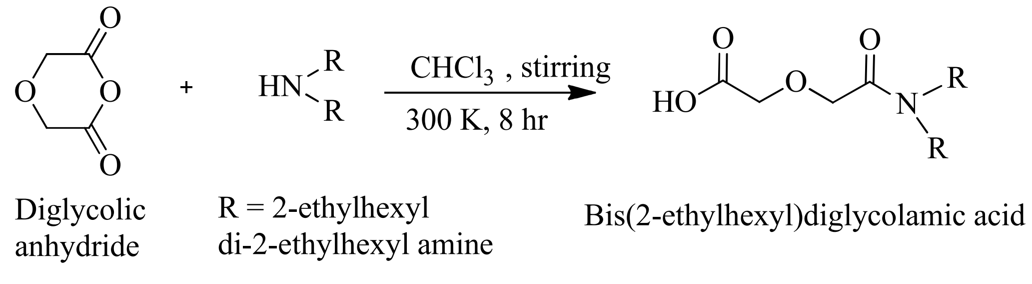

Fig. 2.11. Reaction scheme for the synthesis of bis(2-ethyhexyl)diglycolamic acid.

Characterization

HDEHDGA: (pale yellow viscous liquid, yield 95 %) **: ^{1}H-NMR (**500 MHz, DMSO-d_6, TMS, 298 K), δ 10.67 (s, 1H, $COO\underline{H}$), 4.32 (s, 2H, -OCH_2-), 4.11(s, 2H, -$C\underline{H}_2O$-), 3.17-3.31 (m, 4H, 2 $C\underline{H}_2$ - N), 2.96-2.98 (m, 2H, $C\underline{H}$), 1.15-1.24 (m, 16H, $C\underline{H}_2$-R), 0.77-0.84(m, 12H, $C\underline{H}_3$). **^{13}C NMR** (500MHz, $CDCl_3$, TMS , 298K): **δ_C:** 172.22 ($\underline{C}O$), 172.14 ($\underline{C}O$), 77.21(-$O\underline{C}H_2$), 71.1(-$\underline{C}H_2O$-), 49.34 (-$\underline{C}H_2$-N), 37.16 ($\underline{C}H$), 30.35, 28.47, 23.58, 22.86, 13.9 (various $\underline{C}H_2$ groups), 10.47 ($\underline{C}H_3$). MS (EI+, m/z): 356.5. **FTIR (ν/cm^{-1}):** 3454 (-OH in COOH), 1739 (-CO in COOH), 1622 (-CO in –CON), 1226 (-C-O-C-).

2.7. Some typical spectra of synthesized ionic liquid and extractants

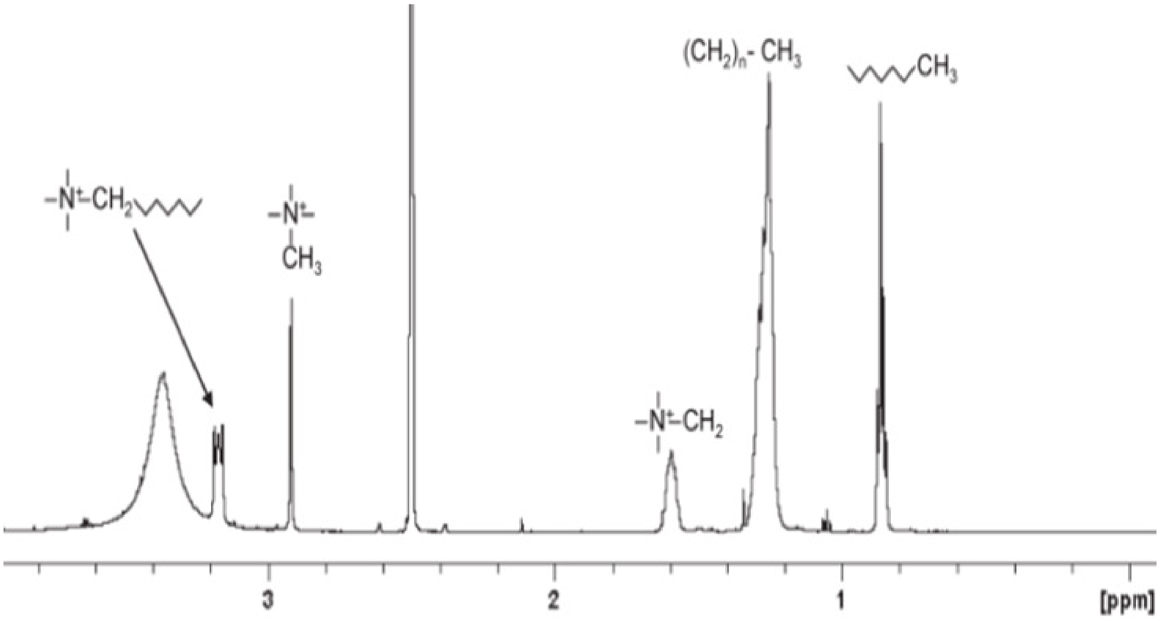

Fig. 2.12. ^{1}H NMR spectrum of $[N_{1888}][NO_3]$.

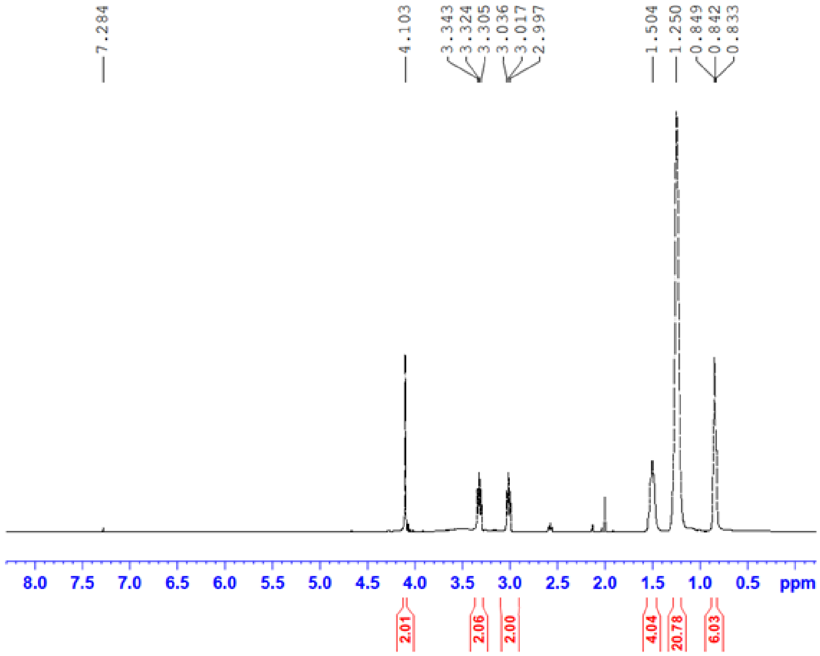

Fig. 2.13. ^{1}H NMR spectrum of DOHyA.

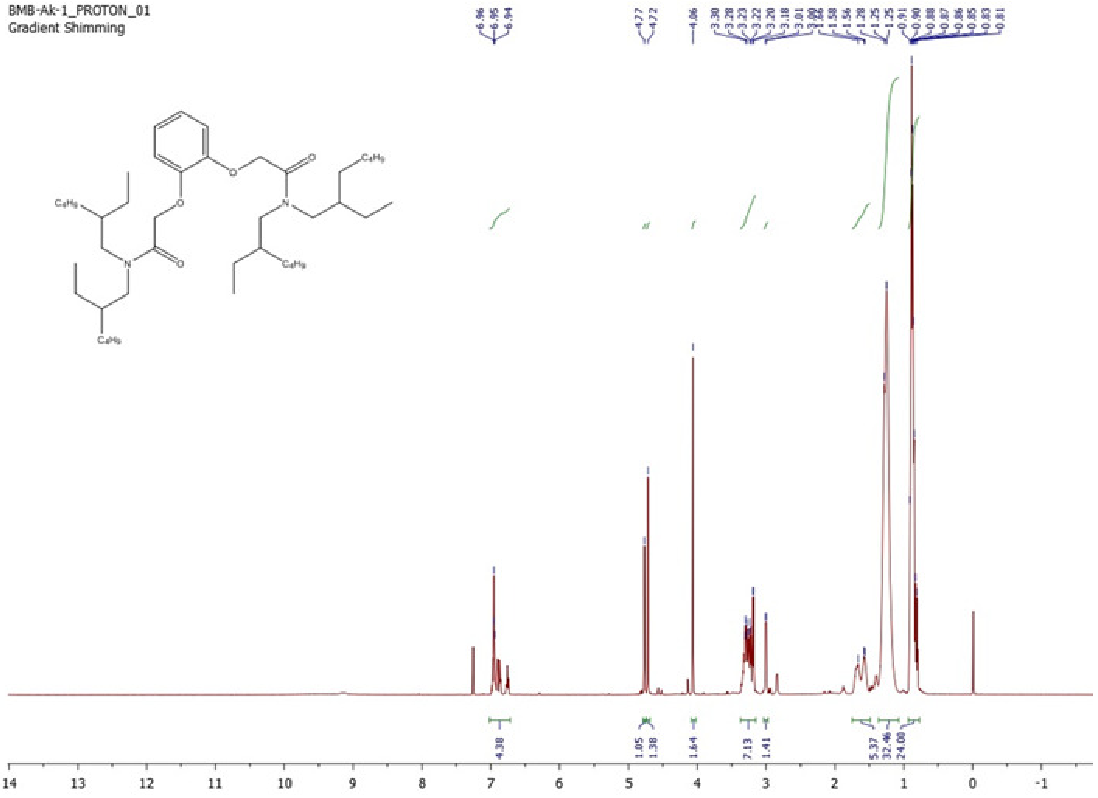

Fig. 2.14. ^{1}H NMR spectrum of BD.

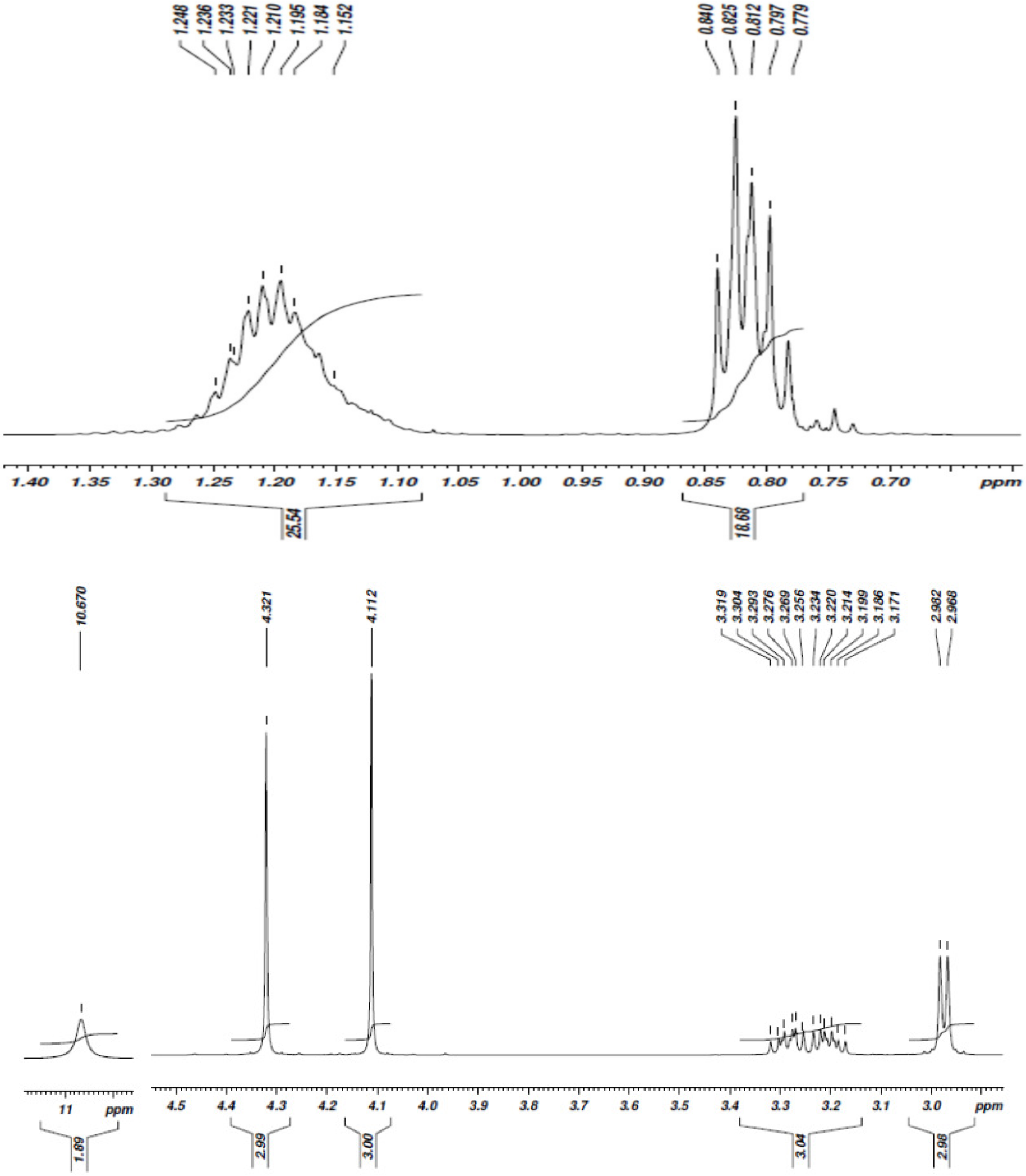

Fig. 2.15. ^{1}H NMR spectrum of HDEHDGA.

References

1. W. Davies, W. Gray, A rapid and specific titrimetric method for the precise determination of uranium using iron (II) sulphate as reductant, Talanta 11 (1964) 1203–1211.
2. J.A. Partridge, R.C. Jensen, Purification of Di-(2-Ethylhexyl)Phosphoric Acid by Precipitation of Copper(II) Di-(2-Ethylhexyl)Phosphate, J. Inorg. Nucl. Chem. 31 (1969) 2587–2589.
3. P.A. Hassan, S. Rana, G. Verma, Making sense of Brownian motion: colloid characterization by dynamic light scattering, Langmuir. 31 (2014) 3-12.
4. A. Cao, Light scattering. Recent applications, Anal. Lett. 36 (2003) 3185-3225.
5. R. Pecora, R. ed., Dynamic light scattering: applications of photon correlation spectroscopy. Springer Science & Business Media 2013.
6. R. Chiarizia, M.P. Jensen, P.G. Rickert, Z. Kolarik, M. Borkowski, P. Thiyagarajan, Extraction of Zirconium Nitrate by TBP in n-Octane: Influence of Cation Type on Third Phase Formation According to the “Sticky Spheres” Model, Langmuir. 20 (2004) 10798-10808.
7. A.H. Orabi, Determination of uranium after separation using solvent extraction from slightly nitric acid solution and spectrophotometric detection, J. Radiat. Res. Appl. Sci. 6 (2013) 1-10.
8. A.D. Becke, Density-functional exchange-energy approximation with correct asymptotic behavior, Phys. Rev. A 38 (1988) 3098.
9. J.P. Perdew, Density-functional approximation for the correlation energy of the inhomogeneous electron gas, Phys. Rev. B 33 (1986) 8822.

10. TurbomoleV6.3, A development of University of Karlsruhe and Forschungszentrum Karlsruhe GmbH (1989-2007) TURBOMOLE GmbH, since (2007), A development of University of Karlsruhe and Forschungszentrum Karlsruhe GmbH (1989-2007) TURBOMOLE GmbH, since (2007), (2009).
11. X. Cao, M. Dolg, Segmented contraction scheme for small-core actinide pseudopotential basis sets, J. Molec. Stru. THEOCHEM, 673 (2004) 203-209.
12. A.D. Becke, A new mixing of Hartree-Fock and local density-functional theories, J. Chem. Phys. 98 (1993) 1372-1377
13. C. Lee, W. Yang, R.G. Parr, Development of the Colle-Salvetti correlation-energy formula into a functional of the electron density, Phys. Rev. B 37 (1988) 785.
14. F. Neese, Prediction of molecular properties and molecular spectroscopy with density functional theory: from fundamental theory to exchange-coupling, Coord. Chem. Rev. 253 (2009) 526-563.
15. S.M. Ali, J.M. Joshi, A.K. Singha Deb, A. Boda, K.T. Shenoy, S.K. Ghosh, Dual mode of extraction for Cs+ and Na+ ions with dicyclohexano-18-crown-6 and bis(2-propyloxy)calix[4]crown-6 in ionic liquids: Density functional theoretical investigation, RSC Advances, 4 (2014) 22911-22925.
16. R.M.R. Dumpala, N. Rawat, A. Boda, S.M. Ali, B.S. Tomar, Complexation of thorium with pyridine monocarboxylate-N-oxides: Thermodynamic and computational studies, J. Chem. Thermodyn. 122 (2018) 13-22.
17. A. Leoncini, S.A. Ansari, P.K. Mohapatra, A. Boda, S. Musharaf Ali, A. Sengupta, J. Huskens, W. Verboom, Benzene-centered tripodal diglycolamides: Synthesis, metal ion

extraction, luminescence spectroscopy, and DFT studies, Dalton Trans. 46 (2017) 1431-1438.

18. A. Sengupta, S. Jayabun, A. Boda, S.M. Ali, An amide functionalized task specific carbon nanotube for the sorption of tetra and hexa valent actinides: Experimental and theoretical insight, RSC Advances, 6 (2016) 39553-39562.
19. N.K. Gupta, A. Sengupta, A. Boda, V.C. Adya, S.M. Ali, Oxidation state selective sorption behavior of plutonium using: N, N-dialkylamide functionalized carbon nanotubes: Experimental study and DFT calculation, RSC Advances, 6 (2016) 78692-78701.
20. S. Pahan, A. Boda, S.M. Ali, Density functional theoretical analysis of structure, bonding, interaction and thermodynamic selectivity of hexavalent uranium (UO22+) and tetravalent plutonium (Pu4+) ion complexes of tetramethyl diglycolamide (TMDGA), Theor. Chem. Acc. 134 (2015) 1-16.
21. A. Klamt, Conductor-like screening model for real solvents: a new approach to the quantitative calculation of solvation phenomena, J. Phys. Chem. 99 (1995) 2224-2235.
22. A. Klamt, G. Schuurmann, COSMO: a new approach to dielectric screening in solvents with explicit expressions for the screening energy and its gradient, J. Chem. Soc. Perkin Trans. 2 (1993) 799-805.
23. ADF, SCM Theoretical chemistry, Vrije Universiteit, Amsterdam, The Netherlands, see http://www. scm. com, 2017.
24. G. te Velde, F.M. Bickelhaupt, E.J. Baerends, C. Fonseca Guerra, S.J.A. van Gisbergen, J.G. Snijders, T. Ziegler, Chemistry with ADF, J. Comput. Chem. 22 (2001) 931-967.

25. K. Binnemans, Interpretation of europium(III) spectra, Coordination Chem. Rev. 295 (2015) 1-45.
26. P. P. Barthelemy, G. R. Choppin, Luminescence study of complexation of europium and dicarboxylic acids, Inorg. Chem. 28 (1989) 3354-3357.
27. C. Reichardt, Solvatochromic dyes as solvent polarity indicators, Chemical reviews, 94 (1994) 2319-2358.
28. C. Reichardt, Polarity of ionic liquids determined empirically by means of solvatochromic pyridinium N-phenolate betaine dyes, Green Chem. 7 (2005) 339-351.
29. C. Reichardt, Solvents and Solvent Effects in Organic Chemistry, Weinheim: Wiley-VCH, 2003.
30. C. Reichardt, Pyridinium N-phenolate betaine dyes as empirical indicators of solvent polarity: Some new findings, Pure Appl. Chem. 76 (2004) 1903−1919.
31. C. Reichardt, Solvents and solvent effects: an introduction, Org. Process Res. Dev. 11 (2007) 105-113.
32. X. Wang, K. Chen, J. Yao, H. Li, Recent progress in studies on polarity of ionic liquids, Sci. China Chem. 59 (2016) 517-525.
33. S. N. Aki, V. K. Brennecke, J. F. A. Samanta, How polar are room-temperature ionic liquids? Chem. Commun. 5 (2001) 413−414.
34. C. Reichardt, E. Harbusch-Gornert, Liebigs Ann. Chem. (1983) 721–743.
35. K. Dimroth, C. Reichardt, T. Siepmann and F. Bohlmann, Justus Liebigs Ann. Chem. 661 (1963) 1–37.
36. S. Spange, C. Lienert, N. Friebe, K. Schreiter, Complementary interpretation of E_T (30) polarity parameters of ionic liquids. Phys. Chem. Chem. Phys. 22 (2020) 9954-9966.

37. M. Potangale, S. Tiwari, Correlation of the empirical polarity parameters of solvate ionic liquids (SILs) with molecular structure. J. Mol. Liq. 297 (2020) 111882.

38. B. R. Mellein, S. N. Aki, R. L. Ladewski, J.F. Brennecke, Solvatochromic studies of ionic liquid/organic mixtures. J. Phys. Chem. B 111 (2007) 131−138.

39. M.N. Kobrak, The relationship between solvent polarity and molar volume in room-temperature ionic liquids, Green Chem. 10 (2008) 80−86.

40. J.L. Anderson, J. Ding, T. Welton, D. W. Armstrong, Characterizing ionic liquids on the basis of multiple solvation interactions, J. Am. Chem. Soc. 124 (2002) 14247−14254.

41. C. Chiappe, C. S. Pomelli, S. Rajamani, Influence of structural variations in cationic and anionic moieties on the polarity of ionic liquids. J. Phys. Chem. B 115 (2011) 9653−9661.

42. K.A. Venkatesan, B. Robert Selvan, M.P. Antony, T.G. Srinivasan, P.R. Vasudeva Rao, Physiochemical and Plutonium Retention Properties of Hydrolytic and Radiolytically Degraded Tri-n-Amylphosphate, Solvent Extr. Ion Exch. 24 (2006) 747–763.

43. J.G. Huddleston, A.E. Visser, W.M. Reichert, H.D. Willauer, G.A. Broker, R.D. Rogers, Characterization and comparison of hydrophilic and hydrophobic room temperature ionic liquids incorporating the imidazolium cation, Green Chem. 3 (2001) 156–164.

44. D.R. MacFarlane, P. Meakin, J. Sun, N. Amini, and M. Forsyth, Pyrrolidinium imides: a new family of molten salts and conductive plastic crystal phases, J. Phys. Chem. B 103 (1999) 4164-4170.

45. J.P. Mikkola, P. Virtanen, R. Sjöholm, Aliquat 336®-a versatile and affordable cation source for an entirely new family of hydrophobic ionic liquids, Green Chem. 8 (2006) 250-255.

46. M.A. Assenine, B. Haddad, A. Paolone, S.A. Brandán, M. Goussem, D. Villemin, M. Boumediene, M. Rahmouni, S. Bresson, Synthesis, thermal properties, vibrational spectra and computational studies of Trioctylmethylammonium bis(trifluoromethylsulfonyl)imide ionic liquid, J. Molec. Stru. 1232 (2021) 130085.
47. S. Kannan, B.G. Vats, I.C. Pius, D.M. Noronha, P.S. Dhami, P.W. Naik, M. Kumar, Extraction and structural studies of an unexplored monoamide, N, N′-dioctyl, α-hydroxy acetamide with lanthanide (III) and actinide (III) ions, Dalton Trans. 43 (2014) 5252-5255.
48. T. Prathibha, B.R. Selvan, K.A. Venkatesan, S. Rajeswari, M.P. Antony, Radiolytic stability of N, N-di-alkyl-2-hydroxyacetamides, J. Radioanal. Nucl. Chem. 311 (2017) 1929-1935.
49. R. Ruhela, S. Panja, B.S. Tomar, M.A. Mahajan, R.M. Sawant, S.C. Tripathi, A.K. Singh, P.M. Gandhi, R.C. Hubli, A.K. Suri, Bis-(2-ethylhexyl) carbamoyl methoxy phenoxy-bis-(2-ethylhexyl) acetamide [BenzoDODA]—first selective extractant for plutonium (IV) recovery (SEPUR) from acidic media, Tetrahedron Letters. 53 (2012) 5434-5436.
50. X. Sun, Y. Ji, F. Hu, B. He, J. Chen, D. Li, The inner synergistic effect of bifunctional ionic liquid extractant for solvent extraction, Talanta 81 (2010) 1877–1883.
51. A.S. Suneesh, K.A. Venkatesan, K.V. Syamala, M.P. Antony, P.R. Vasudeva Rao, Mutual separation of americium (III) and europium (III) using glycolamic acid and thioglycolamic acid, Radiochim. Acta. 100 (2012) 425-430.

Chapter 3: Extraction behavior of uranium in CHON based ligand-ionic liquid system

This chapter deals with the application of room temperature ionic liquid as a diluent for the extraction of uranium. The RTIL used in study is methyl-tri-*n*-octylammonium nitrate [N_{1888}][NO_3]. The solvent extraction behavior of uranium(VI) in the solution of *N,N*-dioctyl-2-hydroxy acetamide (DOHyA) in [N_{1888}][NO_3] is discussed in detail.

3.1. Introduction

In the last two decades, RTILs are being explored as diluents and extractants for possible applications related to spent nuclear fuel reprocessing and waste mangament [1-9]. Essentially, they are explored as potential substitute to molecular diluents (*n*-dodecane) in solvent extraction. The fascinating properties of RTILs over molecular diluents are negligible vapour pressure, high solubility for organic and inorganic species, wide liquid range, highly polar and high solvation capability. Initially, Dai et al. [10] and Visser et al. [11] studied the extraction of group I and group II metal ions by crown ethers present in RTIL. Dietz and co-workers [12-16] studied the extraction behavior of several metal ions of nuclear interest using neutral extractants like crown ether and tri-*n*-butyl phosphate (TBP) present in RTIL medium. The mechanism of extraction in RTIL phase was reported to differ significantly in RTIL medium depending upon the aqueous phase conditions. Ion exchange between target metal ion and RTIL was reported [12,13] as one of the primary mode of metal ion extraction in RTIL phase. Dietz et al. [12-16] proposed that unlike the conventional diluents, RTIL diluents are not "inert" and may pose several implications on the "greenness" of the solvent in solvent extraction processes. Those investigations revealed that ionic liquid diluents provide extraordinary extraction of target metal ion than conventional molecular diluents. The main reasons for high distribution ratio obtained in the RTIL system could be the solvating capability and ionic nature of the ionic liquid in extracted phase.

The role of an "inert" diluent like *n*-dodecane in a solvent extraction procedure is to dissolve the extractant molecule and provide strong hydrophobicity to the organic phase such that the organic phase is immiscible with aqueous medium [17]. In addition, the diluent also solvates the metal-ligand complex formed in organic phase after extraction. The conventional ionic liquids employed for solvent extraction applications are based on alkyl imidazolium cation, for instance, 1-butyl-3-methylimidazolium cation in conjunction with bis(trifluromethylsulphonyl)imide anion results in a hydrophobic ionic liquid, $[C_4mim][NTf_2]$, which makes the ionic liquid immiscible with aqueous medium [5-7]. Moreover, they dissolve a wide range of ligands suitable for solvent extraction applications. However, due to the characteristic ionic nature of ionic liquids, they often undergo cation and anion exchange reaction with target metal ions present in aqueous solutions [12,13]. As a result, these ionic liquids show exceptional extraction of target metal ions, facilitated by a couple of modes, one involving cation exchange and the other, metal-ligand complex formation. In addition, the ionic liquids also stabilize the polar metal-ligand complex by solvation.

Even though the mass transfer of metal ions occurring through the dual mode enhances the extraction of metal ions to a remarkable extent. During ion exchange mode of extraction, ionic liquid is irreversibly lost from the organic phase. In addition, the presence of organic ions in aqueous phase pollutes the aqueous phase and therefore further treatment of aqueous phase becomes difficult. In view of this, it is necessary to choose appropriate cation-anion combinations of the ionic liquid that is devoid of undergoing any ion exchange, but retaining all the good properties of the ionic liquid for excellent solvent extraction application. Moreover, for the separation of target metals from radioactive feed solution, it is desirable to select the ionic liquid, which is made up of CHON-atoms so that the ionic liquid is completely incinerable and the waste disposal of the spent ionic liquid becomes easy. In connection with the CHON-based ionic liquids that are strongly hydrophobic, Mikkola et al. [18] reported the synthesis of ionic liquids containing methyl-tri-*n*-octylammonium cation ($[N_{1888}]^+$) associated with a wide variety of anions for various applications. It should be noted that the $[N_{1888}]^+$ cation is an affordable and versatile source for combining with several anions by means of a simple substitution reaction, as described elsewhere [18], for producing strongly hydrophobic ionic liquids. These ionic liquids have been exploited for various nuclear fuel cycle applications [19-21].

Hydroxyacetamides are regarded as potential candidates for the separation of trivalent actinides (Am(III) and Cm(III)) from nitric acid medium [22,23]. These reagents are similar to diglycolamides, but half the molecular size of diglycolamides containing an alcoholic and amidic moiety in the structure. The advantages of using hydroxyacetamides over diglycolamides for the solvent extraction of trivalent actinides are discussed elsewhere [23]. Rama et al. [24] studied the extraction behavior of trivalent actinides from nitric acid medium in a solution of 2-hydroxy–*N,N*-dioctyl-2-hydroxyacetamide (DOHyA) in $[C_4mim][NTf_2]$ ionic liquid as well as in *n*-dodecane. Extraordinary extraction of Pu(IV) and U(VI) in DOHyA was reported when *n*-dodecane was replaced by $[C_4mim][NTf_2]$ [24]. However, there is no literature available on the extraction of actinides in a solution of DOHyA in $[N_{1888}][NO_3]$ and the role of these types of long chained hydrophobic ionic liquids in augmenting the extraction of actinides has not been understood thoroughly. To unravel the role of $[N_{1888}][NO_3]$, the solvent extraction behavior of uranium (VI) in DOHyA/$[N_{1888}][NO_3]$ was studied and compared with those obtained in *n*-dodecane in this chapter, which was supported by DFT calculations.

Experimental details for the present chapter are presented in section 2.5.1 of chapter 2. The Synthesis of the ionic liquids and extractant are discussed in section 2.6.5, 2.6.6 and 2.6.7 of chapter 2 respectively.

Table. 3.1. Structures of extractant and ionic liquids used for the present study.

Name	Structure
Extractant	
N,N-dioctyl-2-hydroxyacetamide (DOHyA) (R: C_8H_{17})	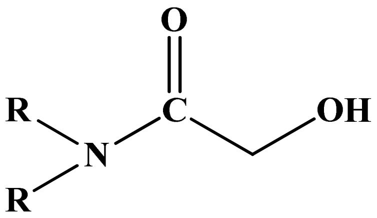
Ionic liquid	
Methyl-tri-*n*-octylammonium nitrate $[N_{1888}][NO_3]$ (R: C_8H_{17})	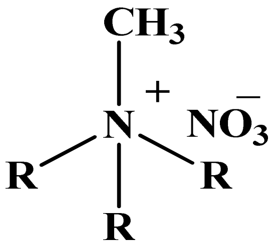
Methyl-tri-*n*-octylammonium bis(trifluoromethylsulfonyl)imide $[N_{1888}][NTf_2]$ (R: C_8H_{17})	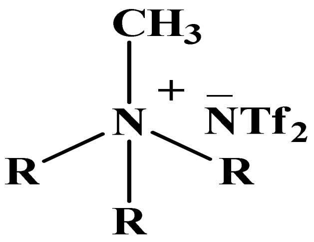

3.2. Results and discussions

3.2.1. *Extraction of U(VI) in DOHyA/n-DD*

N,N-dioctyl-2-Hydroxy acetamide (DOHyA) is a promising ligand for the extraction of trivalent actinides from nitric acid medium. Prathiba et al. [23] studied the extraction behavior of Am(III) and Eu(III) in a solution of DOHyA in *n*-DD and reported that the distribution ratio of these trivalents abruptly increase from the value of 0.1 at 2 M nitric acid, reaches a value ~200 at 4 M nitric acid followed by saturation [23]. However, the extraction behavior of U(VI) in DOHyA/*n*-DD was not reported. Fig. 3.1 shows the variation in the distribution ratio of U(VI) in 0.1 M DOHyA/*n*-DD as a function of nitric acid concentration in aqueous phase. It can be seen that the distribution ratio of U(VI) in organic phase gradually increases with increase in the concentration of nitric acid. The distribution ratio of U(VI) is negligible at 0.1 M nitric acid and the distribution ratio of ~5 is obtained at 7 M nitric acid. Comparing this result with the extraction observed for Am(III) and Eu(III) reported elsewhere [23], the present results show that the selectivity of DOHyA towards U(VI) is poor as compared to the trivalents, Am(III) and Eu(III). Since DOHyA is a neutral ligand, the increase in the distribution ratio of U(VI) observed with increase in the concentration of nitric acid could be attributed to the increase in the formation of neutral $UO_2(NO_3)_2$ complex, followed by the co-ordination of neutral species with DOHyA.

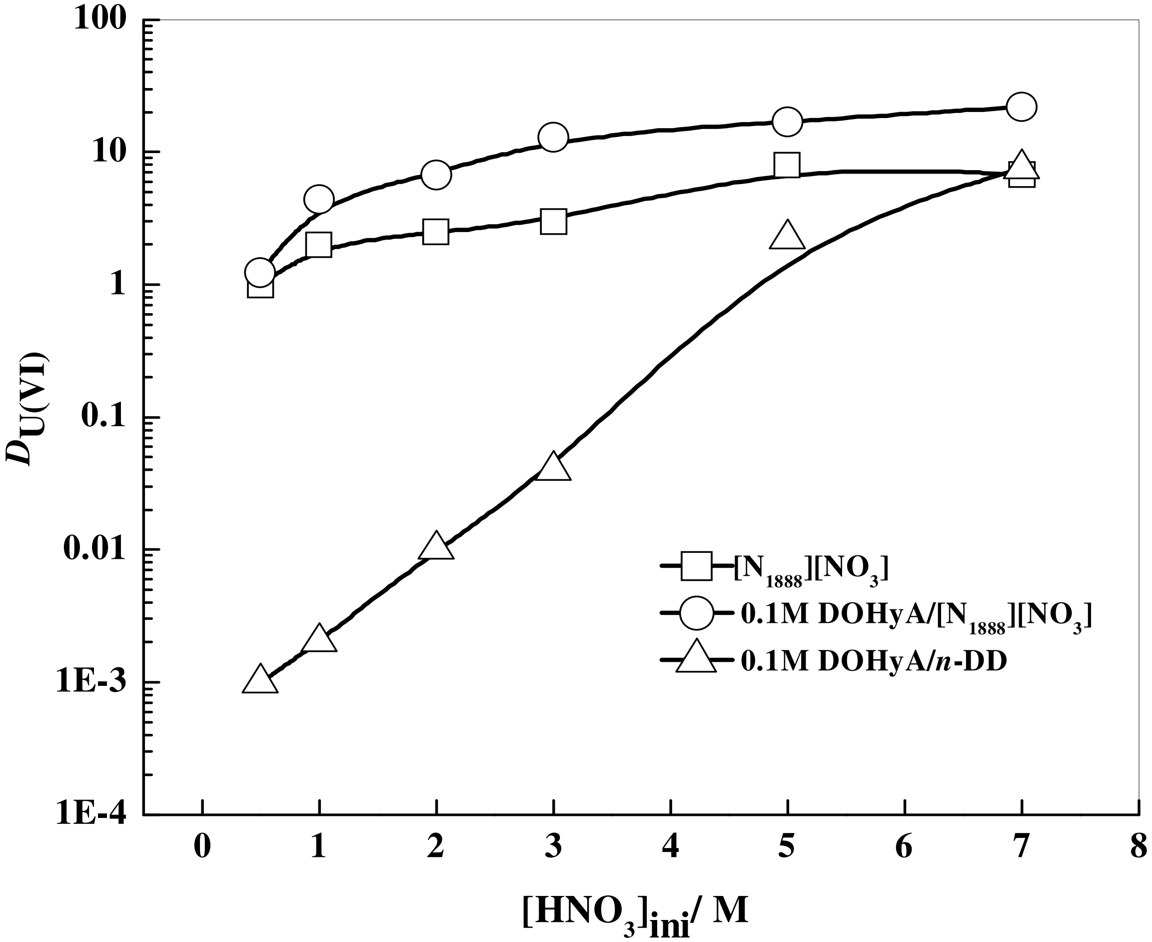

Fig. 3.1. Variation in the distribution ratio of U(VI) in organic phase as a function of nitric acid concentration in aqueous phase. Organic phase: 0.1 M DOHyA/$[N_{1888}][NO_3]$ (or *n*-DD) and $[N_{1888}][NO_3]$ phase alone; Aqueous phase: (0.5-7 M) nitric acid + 4×10^{-4} M U(VI); Equilibration time = 1 hour; Temperature = 298 K; Phase volume ratio = 1.

3.2.2. *Extraction of U(VI) in DOHyA/$[N_{1888}][NO_3]$*

The ionic liquids in conjunction with conventional extractants are shown to influence remarkably the extraction behavior of metal ions in ionic liquid phase during solvent extraction applications [5-7]. It would be interesting to understand how the extraction behavior of U(VI) changes in organic phase upon replacing *n*-dodecane by an ionic liquid $[N_{1888}][NO_3]$. This particular ionic liquid was chosen in the present study owing to the fact that it is completely incinerable and the other interesting features, as discussed above. From Fig. 3.1., it can be seen that the distribution ratios of U(VI) in 0.1 M DOHyA/[N_{1888}][NO_3] are higher than those observed in 0.1 M in DOHyA/*n*-DD at all nitric acid concentrations. This shows that the ionic liquid, [N_{1888}][NO_3], facilitates the extraction of U(VI) in DOHyA/[N_{1888}][NO_3] phase. To understand the role of [N_{1888}][NO_3] in organic phase, it is necessary to understand the extraction behavior of U(VI) in ionic liquid alone.

3.2.3. *Extraction of U(VI) in [N_{1888}][NO_3]*

Actinides such as Pu^{4+} and UO_2^{2+} form anionic complexes with various anions present in aqueous solution [25,26]. These anionic species undergo anionic exchange with ionic liquids such as [N_{1888}][NO_3] and methyl-tri-*n*-octylammonium bis(trifluoromethylsulphonyl)imide ([N_{1888}][NTf_2]) [19,27]. Since nitric acid is employed as aqueous phase in the present study, it is quite likely that the actinides form a wide range of anionic nitrate species in aqueous phase, and their abundances are strongly dependent on the concentration of nitric acid [22,23]. Rout *et al.* [24] studied the extraction behavior of Pu^{4+} in [N_{1888}][NTf_2] and it was reported that the distribution ratio of Pu^{4+} increased with the increase in concentration of nitric acid [24]. The $D_{Pu^{4+}}$ was significant at nitric acid concentrations above 2 M ($D_{Pu^{4+}}$>1) and the distribution ratio of about ~35 was obtained at 6 M nitric acid. This was attributed to the formation of anionic plutonium(IV) species such as $[Pu(NO_3)_5]^-$ and $[Pu(NO_3)_6]^{2-}$ above 2 M nitric acid concentration, followed by the anion exchange of these species with $[NTf_2]^-$ anion of the ionic liquid [25].

In contrast to Pu^{4+}, the abundance of anionic uranyl species, such as $[UO_2(NO_3)_3]^-$ and $[UO_2(NO_3)_4]^{2-}$ is less as compared to anionic plutonium (IV) species at a particular nitric acid concentration due to the characteristic property of UO_2^{2+} ion [26]. Therefore, it is quite likely that the extraction of U(VI) in $[N_{1888}][NO_3]$ or $[N_{1888}][NTf_2]$ would be expected to be less as compared to the extraction of Pu^{4+} observed in these ionic liquids. The extraction behavior of U(VI) in $[N_{1888}][NO_3]$or $[N_{1888}][NTf_2]$ is shown in Fig. 3.2. It can be seen that the distribution ratio of U(VI) increases abruptly with the increase in the concentration of nitric acid followed by a marginal increase in the distribution ratios above 2 M nitric acid. It should be noted that the distribution ratio of U(VI) obtained in case of $[N_{1888}][NO_3]$ is higher than that observed for $[N_{1888}][NTf_2]$. This shows that there is an advantage of using $[N_{1888}][NO_3]$ ionic liquid over $[N_{1888}][NTf_2]$ for the extraction of U(VI) from nitric acid solution. In addition, the loss of NTf_2^- ion encountered during the anion exchange of uranyl species with $[N_{1888}][NTf_2]$ could be avoided by the use of $[N_{1888}][NO_3]$ ionic liquid, since the nitrate ions are common to both organic ($[N_{1888}][NO_3]$) and aqueous phases. Therefore, the contamination of $[NTf_2]^-$ anion during the extraction of anionic uranyl species can be avoided. In view of this, $[N_{1888}][NO_3]$ ionic liquid was employed for the extraction of uranium in the present study.

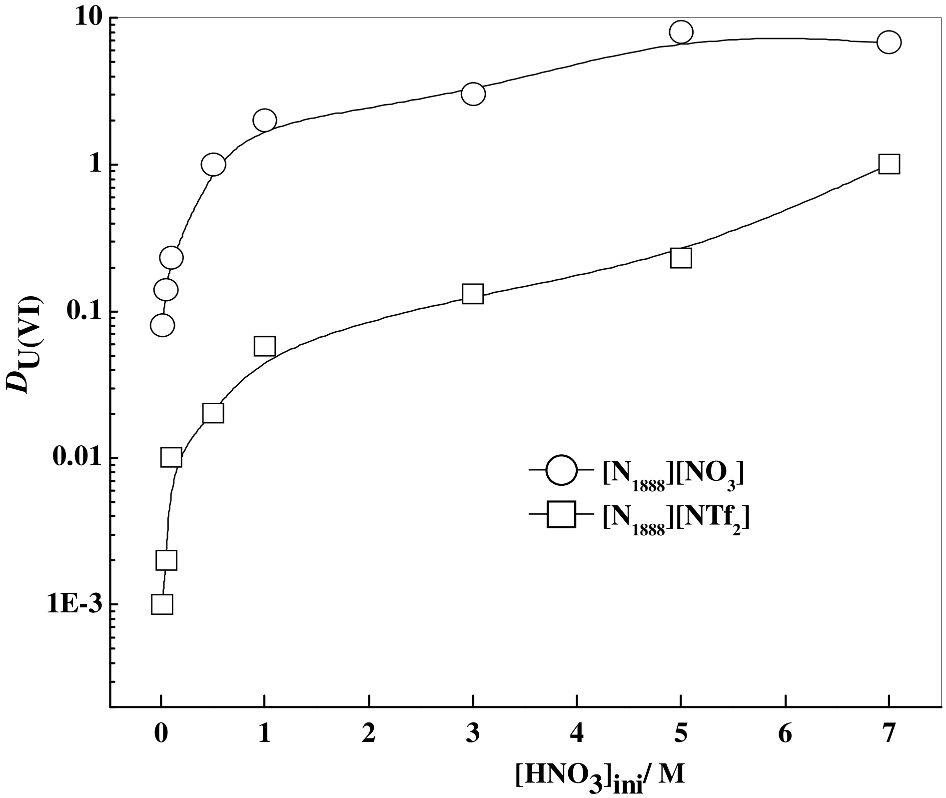

Fig. 3.2. Comparison of the distribution ratio of U(VI) in two different ionic liquid phases studied as a function of nitric acid concentration. Ionic liquid phase: $[N_{1888}][NO_3]$ (or $[N_{1888}][NTf_2]$); Aqueous phase: (0.01-7 M) nitric acid containing 4×10^{-4} M U(VI); Equilibration time = 1 hour; Temperature = 298K; Phase volume ratio = 1.

The extraction behavior of U(VI) in $[N_{1888}][NO_3]$ is included in Fig. 3.1. for comparing these results with those obtained in DOHyA/$[N_{1888}][NO_3]$. It can be seen that the distribution ratios of U(VI) in $[N_{1888}][NO_3]$ are lower than those observed in 0.1 M DOHyA/$[N_{1888}][NO_3]$ at all nitric acid concentrations. This shows that the presence of DOHyA in $[N_{1888}][NO_3]$ facilitates synergistic extraction of U(VI). In order to understand the role of DOHyA and $[N_{1888}][NO_3]$ in the extraction of U(VI) and the mechanism of U(VI) extraction in this ionic liquid medium, the organic phase obtained after extraction was probed by FTIR and Raman spectroscopy discussed below.

3.2.4. Kinetics of extraction

The variation in the distribution ratio of U(VI) as a function of equilibration time is shown in Fig. 3.3. It can be seen that the distribution ratio of U(VI) increases with increase in the duration of equilibration. The variation in the distribution ratio was insignificant after 30 min of equilibration. Therefore, for all extraction studies, the equilibration was carried out for 1 h to ensure the equilibrium was established.

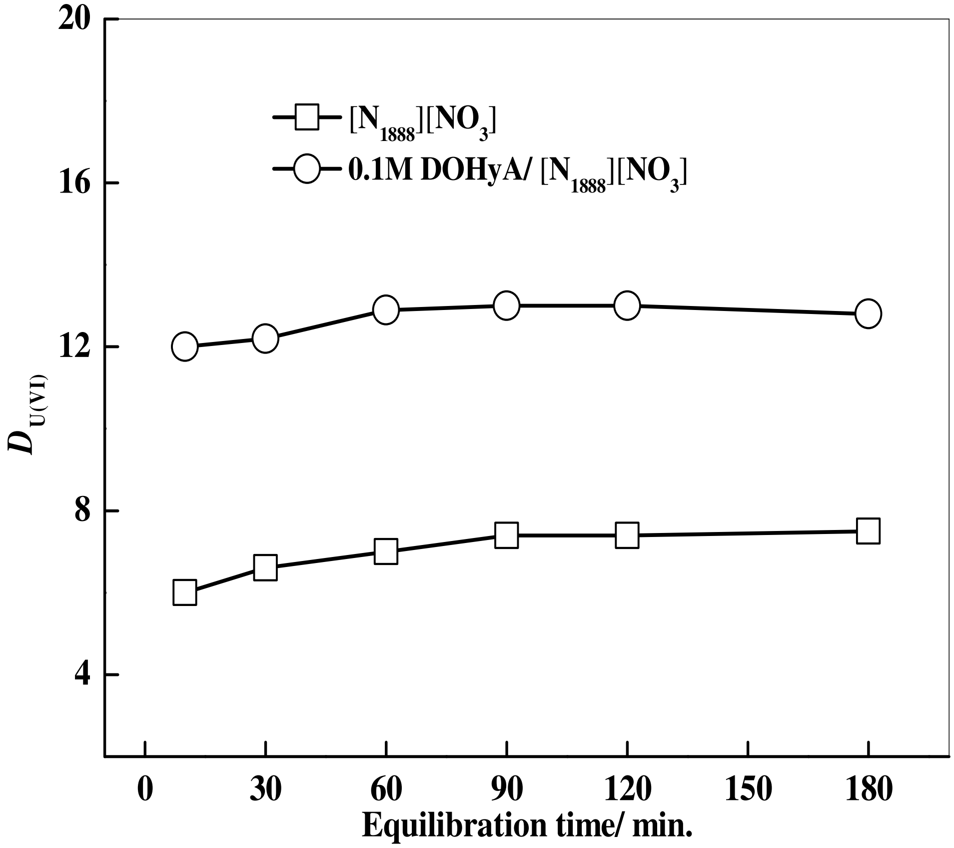

Fig. 3.3. Variation of the distribution ratio of U(VI) as a function of the equilibration time. Organic phase: 0.1M DOHyA/$[N_{1888}][NO_3]$; Aqueous phase: 3M HNO_3 containing $4x10^{-4}$ M of U(VI); Temperature = 298 K; Equilibration time = 10 – 180 minutes; Phase volume ratio = 1.

3.2.5. Extraction Stoichiometry

The extraction of uranium in DOHyA can be represented by equation 3.1. The subscripts "aq" and "IL" denote the aqueous and ionic liquid phases, respectively, and "x" is the number of DOHyA molecules involved in the extraction of uranium.

$$UO_2^{2+}{}_{aq} + 2NO_3^-{}_{aq} + x\,DOHyA_{IL} \Leftrightarrow UO_2(NO_3)_2\,(DOHyA)_{x\ \ IL} \tag{3.1}$$

The equilibrium constant for the above reaction can be represented in equation 3.1.

$$\mathrm{K} = \frac{[\mathrm{UO_2(NO_3)_2(DOHyA)x}]_{\mathrm{IL}}}{[\mathrm{UO_2^{2+}}]_{\mathrm{aq}}[\mathrm{NO_3}]^2_{\mathrm{aq}}\,[\mathrm{DOHyA}]^{\mathrm{x}}_{\mathrm{IL}}} \tag{3.2}$$

Upon rearranging equation 3.1 results in equation 3.2

$$\log D_{U(VI)} = \log \mathrm{K} + 2\log[NO_3]_{aq} + x\ \log[DOHyA]_{IL} \tag{3.3}$$

To determine the number of molecules of DOHyA coordinated to U(VI) in the ionic liquid phase, the effect of DOHyA concentration on the extraction of uranium (VI) in ionic liquid phase was studied. The slope obtained from the plot of log $D_{U(VI)}$ against log [DOHyA] gives the number of molecules of DOHyA coordinated to uranium in the ionic liquid phase. The plot of Fig. 3.4 displays the variation in the distribution ratio of U(VI) as a function of DOHyA concentration in the ionic liquid phase at constant nitric acid concentration in the aqueous phase. It can be seen that the distribution ratio of U(VI) increases with increase in the concentration of DOHyA in ionic liquid phase. Linear regression analysis of the extraction data results in a slope value 1 at all nitric acid concentrations. This shows that about one molecule of DOHyA is involved in the extraction of U(VI) in ionic liquid phase.

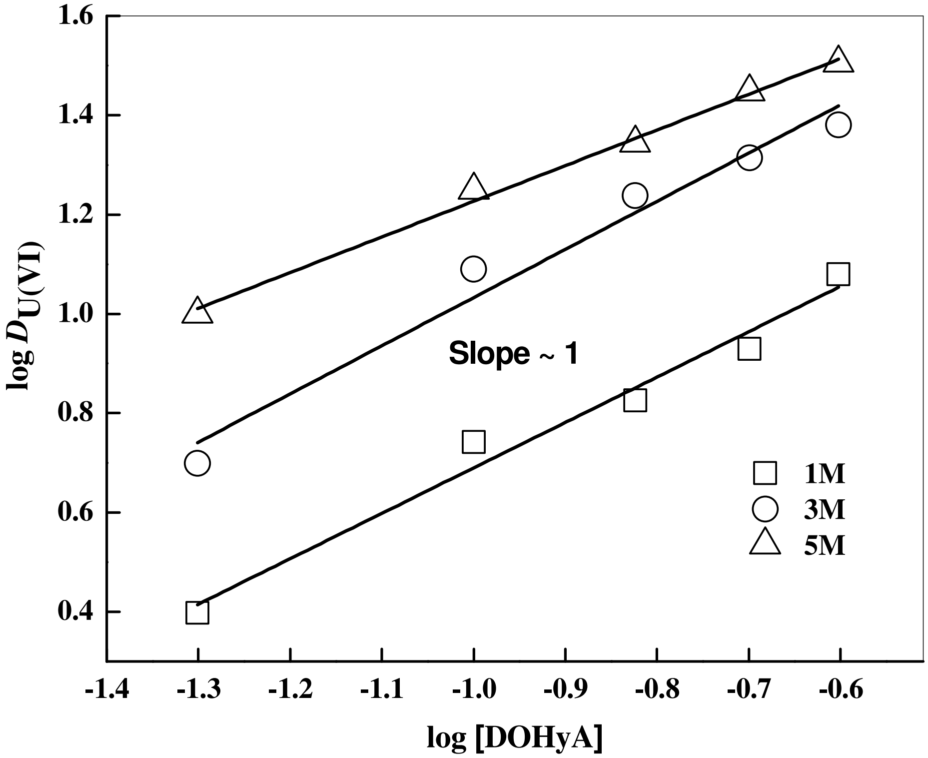

Fig. 3.4. Plot of log$D_{U(VI)}$ against log [DOHyA]. Ionic liquid phase: 0.05-0.25 M DOHyA/[N_{1888}][NO_3]; Aqueous phase: 1-5 M HNO_3 containing 4x10^{-4} M of U(VI); Temperature = 298 K; Equilibration time = 1 hour; Phase volume ratio = 1.

3.2.6. FT-IR Spectroscopy

Fig. 3.5. shows the ATR – FTIR spectrum of 0.1 M DOHyA/[N_{1888}][NO_3] phase recorded after contacting the ionic liquid phase with a solution of U(VI) in 3 M nitric acid. The amount of uranium in nitric acid was varied from 10 to 50 g/L. The spectrum was compared with that obtained (0.1 M DOHyA/[N_{1888}][NO_3]) in the absence of uranium during extraction. It should be noted that increasing the amount of uranium in aqueous phase increases the loading of uranium in organic phase, which is to be discussed in section 3.2.8 The ionic liquid phase (0.1 M DOHyA/[N_{1888}][NO_3]) before U(VI) extraction shows the presence of a transmittance band at 1650 cm^{-1} due to amidic (>C=O) stretching frequency of DOHyA. The intensity of the

transmittance band at 1650 cm^{-1} decrease with increase in the amount of uranium in aqueous phase and the position of the transmittance band is shifted from 1650 cm^{-1} to the lower wave number region 1620 cm^{-1} upon uranium loading in organic phase. The shift of amidic (>C=O) transmittance bands upon uranium loading can happen only when DOHyA is co-ordinated to the uranyl ion in organic phase.

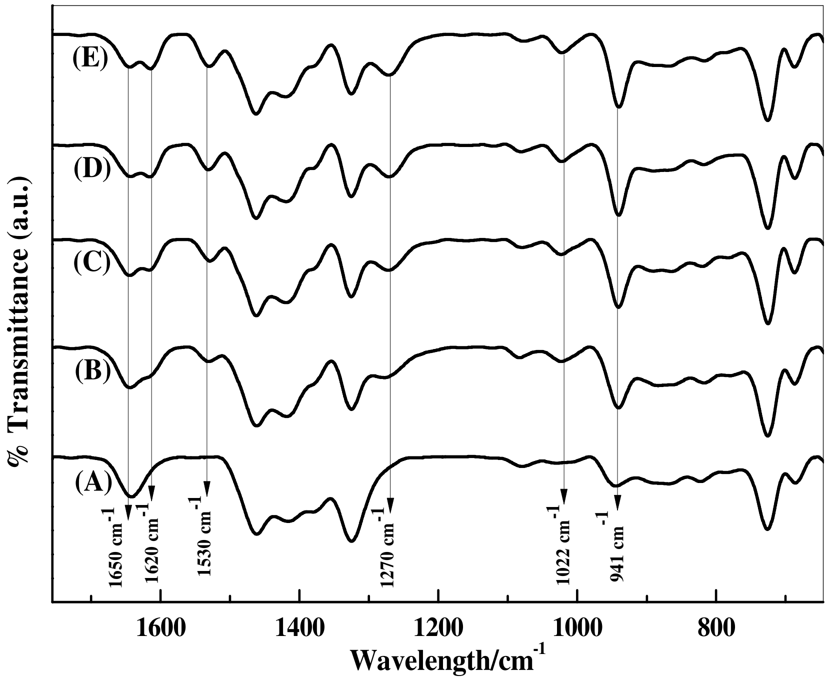

Fig. 3.5. ATR-FTIR spectra of U(VI) loaded ionic liquid phase. Ionic liquid phase: 0.1 M DOHyA/[N_{1888}][NO_3] equilibrated with 3 M HNO_3 (A), 3 M HNO_3 containing 20 g/L U(VI) (B), 3 M HNO_3 containing 30 g/L U(VI) (C), 3 M HNO_3 containing 40 g/L U(VI) (D), 3 M HNO_3 containing 50 g/L U(VI) (E).

The co-ordination of DOHyA with uranyl ion can affect the uranyl ion co-ordination environment, especially the O=U=O asymmetric stretching frequencies, which occurs in the wave number region 950 cm^{-1} to 920 cm^{-1}, depending upon the nature of ligand co-ordinated to the uranyl ion [28]. The co-ordination of weak field ligands like nitrate or TBP to uranyl ion results in a transmittance band at 950 cm^{-1} and the co-ordination of strong field ligands such as chloride results in a band at 920 cm^{-1} [29]. The appearance of the O=U=O asymmetric stretching bands at 941 cm^{-1} indicates that DOHyA is co-ordinated to the uranyl ion. Since DOHyA is a neutral ligand, and based on the above observations, the mechanism shown in equation 3.1 can also be proposed for the extraction of uranium from nitric acid medium.

Conversely, if the mechanism shown in equation 3.1 alone is responsible for the extraction of uranium from nitric acid medium, it is difficult to explain the enhancement of uranium extraction in the presence of $[N_{1888}][NO_3]$, as shown in Fig. 3.1. Therefore, it is quite likely that the cation or anion of the ionic liquid might be involved in the extraction of U(VI) when $[N_{1888}][NO_3]$ was employed for extraction. Among these ions, the nitrate ion of the ionic liquid is expected to play a major role in the extraction of uranium in 0.1 M DOHyA/$[N_{1888}][NO_3]$ phase. To involve the participation of nitrate from organic phase, the mechanism shown in equation 3.4 and 3.5 can be proposed for the extraction of uranium in $[N_{1888}][NO_3]$ medium. The mechanism (equation 3.4) shows that the nitrate ion belongs to $[N_{1888}][NO_3]$ is involved in the formation of neutral uranyl nitrate complex followed by the co-ordination of DOHyA with neutral uranyl nitrate in organic phase.

$$\mathrm{UO_2^{2+}}{}_{aq} + 2NO_3^-{}_{IL} + xDOHyA_{\ IL} \Leftrightarrow UO_2(NO_3)_2(DOHyA)_{x\ \ IL} \tag{3.4}$$

$$2[\mathrm{N_{1888}}]^+_{IL} + 2[\mathrm{NO_3^-}]_{\mathrm{aq}} \Leftrightarrow 2[\mathrm{N_{1888}}][\mathrm{NO_3}]_{IL} \tag{3.5}$$

Due to the supply of nitrate ion from $[N_{1888}][NO_3]$ to uranyl ion, the concentration of $[N_{1888}]^+$ increases in organic phase. Since $[N_{1888}]^+$ ion is strongly hydrophobic, it could not undergo dissolution in aqueous phase, unlike the imidazolium cation based ionic liquids. Instead, the nitrate ion present in aqueous phase is transferred to the organic phase for charge neutralization, as shown in equation 3.5. Therefore, the mechanism shown in equations 3.4 and 3.5 explains the enhancement in the distribution ratio of U(VI) observed in the presence of $[N_{1888}]$

$[NO_3]$. This mechanism is similar to the extraction of U(VI) by crown ether ligand in the presence of lipophilic anions, which usually enhance the distribution ratio of U(VI)in crown ether phase to a significant extent [30]. Since the nitrate ion present in $[N_{1888}][NO_3]$ act similar to "lipophilic anion" in the present case, the distribution ratio of U(VI) in 0.1M DOHyA/$[N_{1888}][NO_3]$ is higher than that observed in the case of $[N_{1888}][NO_3]$.

3.2.7. *Raman Spectroscopy*

The mechanism shown in equation 3.4 and 3.5 indicates that the concentration of "free nitrate" ion that is not co-ordinated to (UO_2^{2+}) is not undergoing any change upon uranium extraction into organic phase. However, the concentration of nitrate ion co-ordinated to uranium, known as the "co-ordinated nitrate", increases with increase in the extraction of uranium in organic phase. The features of the nitrate ion, that is, co-ordinated or un co-ordinated nitrate can be easily monitored by Raman spectroscopy. The symmetric stretching of the "free nitrate" (un co-ordinated) ion gives a Raman band at 1040 cm^{-1}, and the co-ordinated nitrate ion gives a band at 1020 cm^{-1}. The Raman spectrum of the uranium extracted organic phase namely 0.1 M DOHyA in $[N_{1888}][NO_3]$ is recorded at different loadings of uranium, and the results are displayed in Fig. 3.6a. It can be seen that there is a peak appearing at 860 cm^{-1} upon uranium extraction, which is due to the O=U=O symmetric stretching, and the intensity of this peak increases with increase in the concentration of uranium in aqueous phase. This could be due to the increase in the loading of uranium in 0.1 M DOHyA/$[N_{1888}][NO_3]$ phase with increase in the amount of uranium in aqueous phase (to be discussed below). In addition to this, it is important to note that the normalized relative intensity of "free-nitrate" peak at 1040 cm^{-1} decreases marginally and broadens upon increasing the uranium loading in organic phase. At higher loadings of uranium (30 g/L and above), a shoulder at 1020 cm^{-1} appears in the Raman spectrum apart from the 1040 cm^{-1} peak. It should be noted that the "free-nitrate" peak at 1040 cm^{-1} is arising due to the presence of [N$_{1888}$][NO$_3$] and the "co-ordinated nitrate" peak at 1020 cm^{-1} is arising due to the nitrate ions co-ordinated to the uranyl ion. The decrease in the relative intensity of the peak at 1040 cm^{-1} and growth of the shoulder at 1020 cm^{-1} could happen only when the uranyl nitrate undergoes association with [N$_{1888}$][NO$_3$] resulting in the formation of anionic uranyl nitrate complex in organic phase, as shown in equations 3.6 and 3.7.

$$[\mathrm{N}_{1888}][\mathrm{NO}_3]_{IL} + \mathrm{UO}_2(\mathrm{NO}_3)_{2\ aq} \Leftrightarrow [\mathrm{N}_{1888}][\mathrm{UO}_2(\mathrm{NO}_3)_3]_{IL} \tag{3.6}$$

$$2[\mathrm{N}_{1888}][\mathrm{NO}_3]_{IL} + \mathrm{UO}_2\ (\mathrm{NO}_3)_{2\ aq} \Leftrightarrow [N_{1888}][UO_2(NO_3)_4]_{IL} \tag{3.7}$$

Increasing the concentration of uranyl ion in aqueous phase, favours the reactions shown in equation 3.6 and 3.7 and therefore, the intensity of "free-nitrate" peak decreases with increase in the amount of uranium in aqueous phase. Moreover, the intensity of the shoulder peak increases with increase of uranium loading due to the association of nitrate from ionic liquid with uranyl nitrate as shown in equations 3.6 and 3.7.

If anion association is responsible for the extraction of uranium in 0.1 M DOHyA/[N$_{1888}$][NO$_3$], a similar anion association could be expected when [N$_{1888}$][NO$_3$] alone is employed for the extraction of U(VI) from nitric acid medium. The Raman spectrum of the [N$_{1888}$][NO$_3$] phase recorded after contacting the [N$_{1888}$][NO$_3$] with aqueous solution of nitric acid (3 M) containing uranyl nitrate is shown in Fig. 3.6b. It can be seen that the uranyl ion peak namely O=U=O stretching, occurs at 860 cm^{-1} and the "free-nitrate" peak occurs at 1040 cm^{-1} in the Raman spectrum. Again, the intensity of the "free-nitrate" peak decreases marginally and broadening with the increase in the amount of uranium in aqueous phase, similar to those observed in 0.1 M DOHyA/[N$_{1888}$][NO$_3$]. In addition, the shoulder at 1020 cm^{-1} increases with increase in uranium loading in the ionic liquid phase. These observations clearly indicate that uranyl nitrate from aqueous phase undergoes association reaction with the nitrate ion of $[N_{1888}][NO_3]$ phase. As a result, the intensity of "free-nitrate" decreases and the co-ordinated nitrate increases with the increase in the extraction of uranium in organic phase.

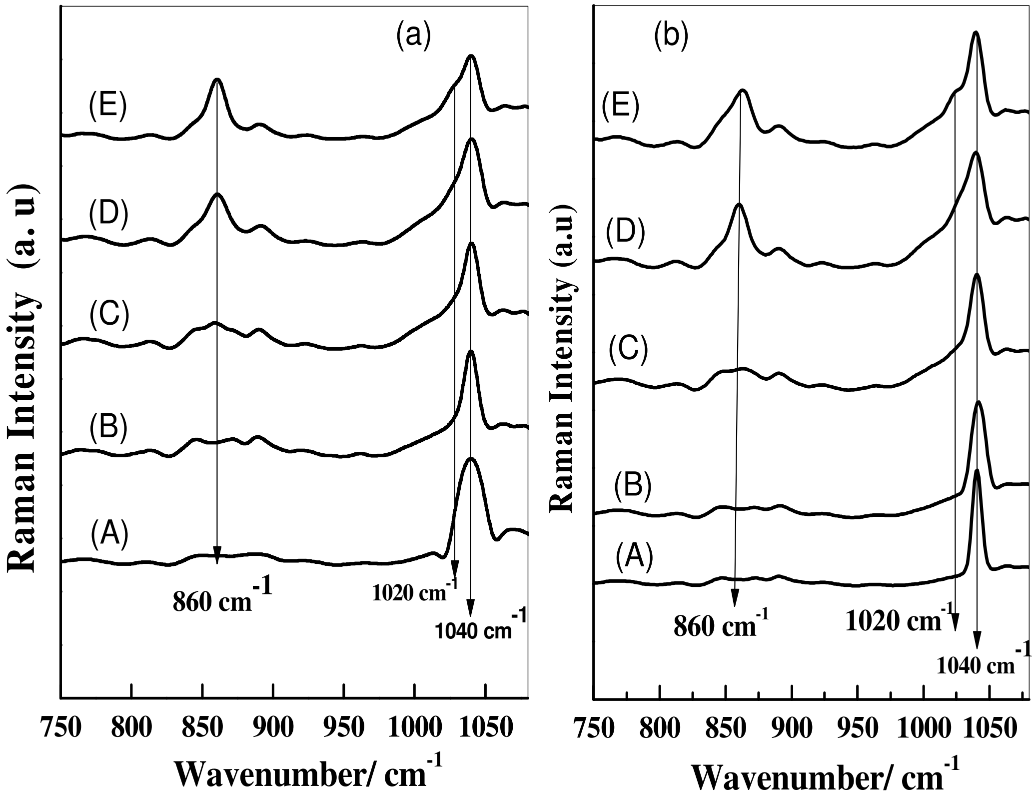

Fig. 3.6a. Raman spectra of U(VI) loaded ionic liquid phases. Ionic liquid phase: 0.1M DOHyA/$[N_{1888}][NO_3]$ (pure) (A), equilibrated with 3 M HNO_3 (B), equilibrated with 3 M HNO_3 containing 10 g/L U(VI) (C), equilibrated with 3 M HNO_3 containing 30 g/L U(VI) (D), equilibrated with 3 M HNO_3 containing 50 g/L U(VI) (E).

Fig. 3.6b. Raman spectrum of U(VI) loaded ionic liquid phases. Ionic liquid phase: pure $[N_{1888}][NO_3]$ (A), equilibrated with 3 M HNO_3 (B), equilibrated with 3 M HNO_3 containing 10 g/L U(VI) (C), equilibrated with 3 M HNO_3 containing 30 g/L U(VI) (D), equilibrated with 3 M HNO_3 containing 50 g/L U(VI) (E).

The FTIR spectrum of the organic phase also shows the growth of transmittance bands at 1530 cm^{-1}, 1270 cm^{-1}, 1022 cm^{-1} upon uranium loading in 0.1 M DOHyA/[N$_{1888}$][NO$_3$] phase (Fig. 3.5.) or [N$_{1888}$][NO$_3$] phase (Fig. 3.7.). These are due to the nitrate ion stretching vibrations, co-ordinated to the uranyl ion. The intensity of these peaks increase with increase in the amount of uranium loaded in organic phase. The results obtained from FTIR and Raman spectroscopy discussed above confirm that the extraction of uranium in 0.1 M DOHyA/[N$_{1888}$][NO$_3$] is occurring through a couple of modes, namely the co-ordination of DOHyA with uranyl nitrate as well as by the association of [N$_{1888}$][NO$_3$] with uranyl nitrate. These two modes are responsible for the extraction of uranium and they seem to occur independent of each other, as shown in equations 3.1, 3.6 and 3.7 As a result, the extraction of uranium observed in 0.1 M DOHyA/[N$_{1888}$][NO$_3$] is much higher than that observed in 0.1 M DOHyA/*n*-DD as well as [N$_{1888}$][NO$_3$] alone. The other bands appearing in IR spectrum are due to the various molecular vibrations of either DOHyA or [N$_{1888}$][NO$_3$] molecule and they are not affected to any significant extent upon uranium extraction in organic phase.

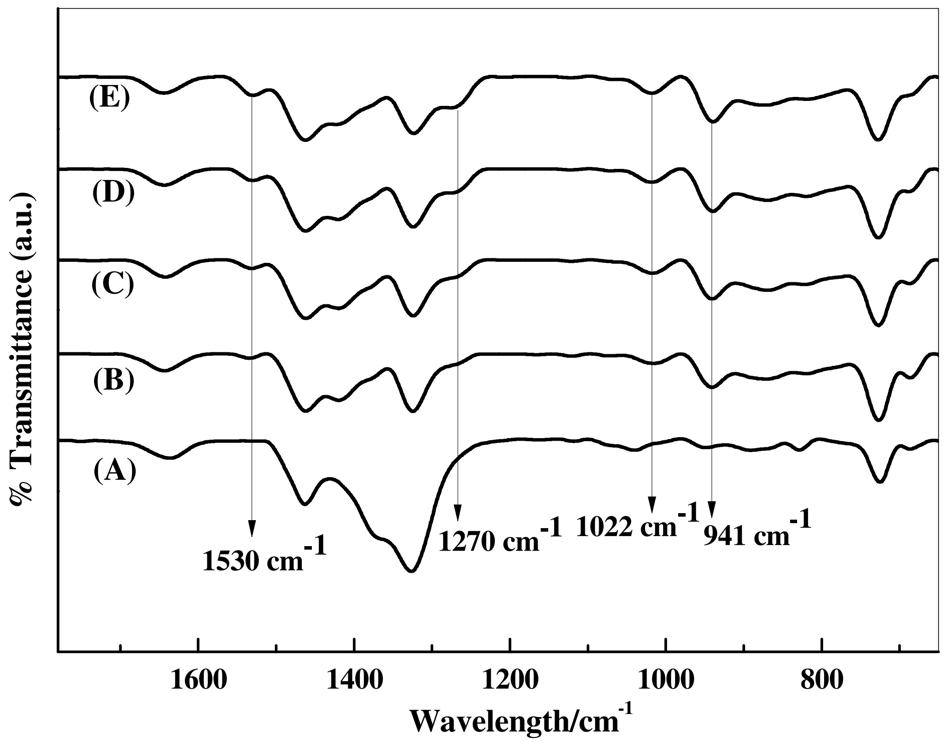

Fig. 3.7. ATR-FTIR spectra of U(VI) loaded ionic liquid phases. Ionic liquid phase: $[N_{1888}][NO_3]$ equilibrated with 3 M HNO_3 (A), equilibrated with 3 M HNO_3 containing 20 g/L U(VI) (B), equilibrated with 3 M HNO_3 containing 30 g/L U(VI) (C), equilibrated with 3 M HNO_3 containing 40 g/L U(VI) (D), equilibrated with 3 M HNO_3 containing 50 g/L U(VI) (E).

3.2.8. *Loading behavior of uranium in organic phase*

It was discussed above that increasing the amount of uranium in aqueous phase increases the loading of uranium in organic phase. To understand this, the extraction behavior of uranium from nitric acid medium was studied in a solution of 0.1 M DOHyA/$[N_{1888}][NO_3]$ or $[N_{1888}][NO_3]$ and the results are shown in Fig. 3.8. It can be seen that the extraction of uranium in ionic liquid phase increases with increase in the amount of uranium in aqueous phase. The extraction of uranium is more in the presence of DOHyA and at higher nitric acid concentrations. It is also observed that a maximum amount of 23 to 25 g/L of uranium could be loaded in ionic liquid phase (0.1 M DOHyA/[N_{1888}][NO_3]) at higher uranium concentration in aqueous phase. This corresponds to the uranium to DOHyA ratio of 1:1 in organic phase.

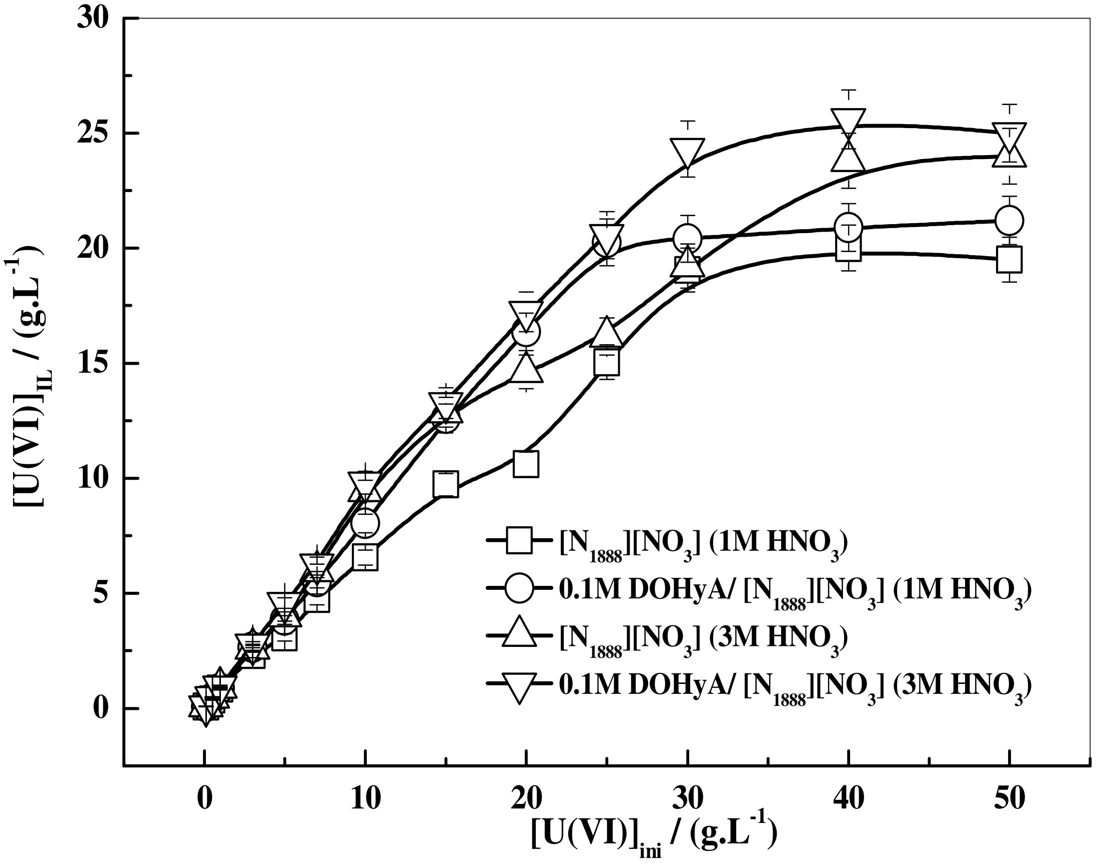

Fig. 3.8. Variation in the loading of U(VI) in the ionic liquid phase as a function of U(VI) concentration in aqueous phase. Ionic liquid phase: 0.1 M DOHyA/[N_{1888}][NO_3] or [N_{1888}][NO_3] alone; Aqueous phase: 1M and 3M nitric acid containing varied concentration of U(VI) (0.1 g/L to 50 g/L), Equilibration time = 1 hour; Temperature = 298 K: Phase volume ratio = 1.

3.2.9. Effect of radiation dose

Since ionic liquid is proposed for the extraction of actinides from fuel solution, the extraction of U(VI) was studied in the gamma-irradiated 0.1M DOHyA/[N_{1888}][NO_3] and [N_{1888}][NO_3]. The results are shown in Fig. 3.9. The ionic liquid phases were irradiated up to 500 kGy absorbed dose and the distribution ratio of U(VI) from 3 M nitric acid medium was measured in the irradiated organic phases. It can be seen from Fig. 3.9. that the distribution ratio of U(VI) was nearly similar irrespective of the absorbed dose in both the ionic liquid phases. Therefore ionic liquid phase is stable towards absorbed dose.

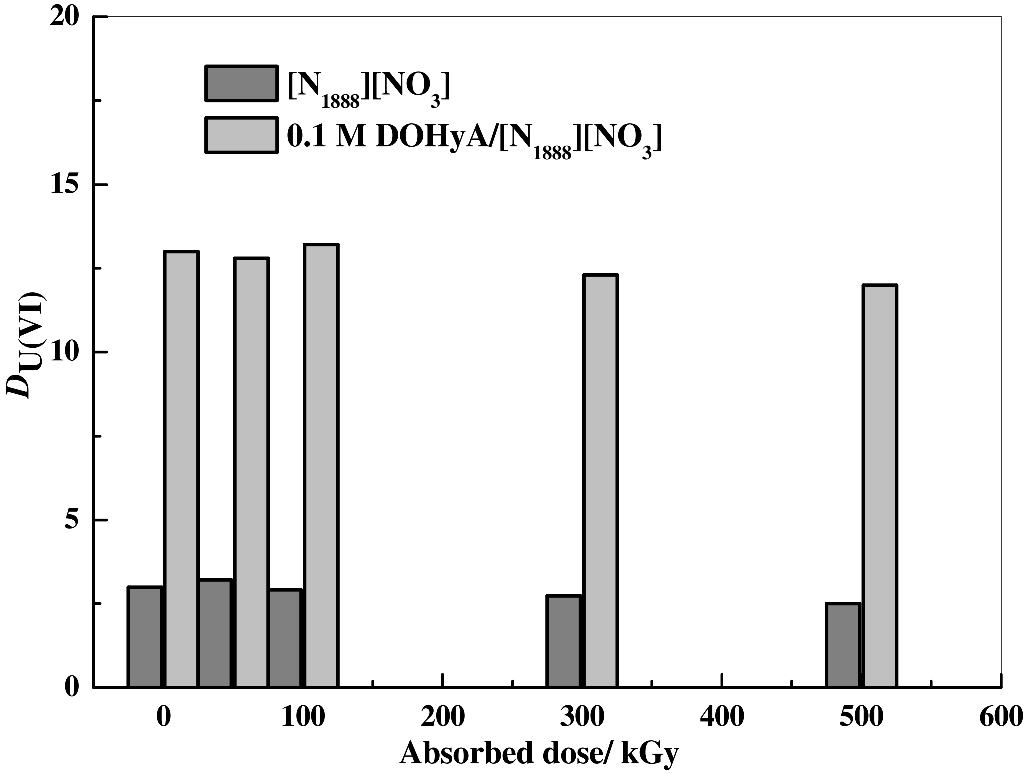

Fig. 3.9. Variation in the distribution ratio of U(VI) as a function of absorbed dose. Ionic liquid phase: 0.1 M DOHyA/[N_{1888}][NO_3] or [N_{1888}][NO_3] alone; Aqueous phase: 3 M HNO_3 containing $4x10^{-4}$ M of U(VI); Absorbed dose: 0 – 500 kGy; Temperature = 298 K; Equilibration time = 1 hour; Phase volume ratio = 1.

3.2.10. Stripping study

The Fig. 3.10 shows the stripping behavior of uranium from the loaded ionic liquid phase using 0.01 M nitric acid. Initially U(VI) was loaded from 3M nitric acid in to the ionic liquid phase and the loaded ionic liquid phase was equilibrated with 0.01M nitric acid phase. Near quantitative recovery of uranium is achieved after five contacts of the organic phase with nitric acid. Therefore, the study shows that the loaded uranium can be quantitatively recovered with dilute nitric acid.

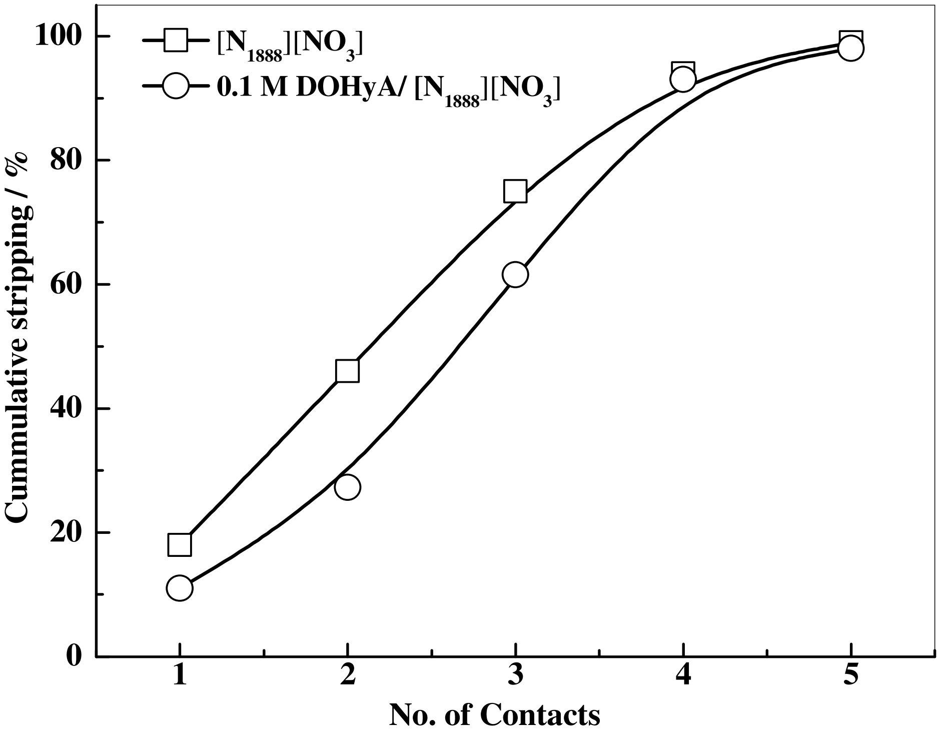

Fig. 3.10. Percentage stripping of U(VI) from the loaded ionic liquid phase. Ionic liquid phase: 0.1 M DOHyA+4x10^{-4} M U(VI); Aqueous phase: 0.01M nitric acid; Temperature = 298 K; Equilibration time = 1 hour; Phase volume ratio = 1.

3.3. Theoretical results

3.3.1. Structural parameters

The optimized structures of free DOHyA (ligand), $[N_{1888}][NO_3]$, $[N_{1888}][NTf_2]$ and the complexes of UO_2^{2+} with the ligand along with nitrate in gas phase are presented in Fig. 3.11. The structural parameters determined from the optimized structures are given in Table. 3.2. The >C=O bond distance in the free DOHyA was determined to be 1.240 Å. In case of $[N_{1888}][UO_2(NO_3)_3(DOHyA)]$and $[UO_2(NO_3)_2(DOHyA)_2]$ complex, the >C=O bond distance was found to be 1.251 Å and 1.258 Å respectively. The increase in bond distance is observed due to the co-ordination of U(VI) ion with amidic O atom. Due to this co-ordination the U=O bond distance was also lengthened from 1.714 Å (free UO_2^{2+} ion) to 1.790 and 1.815 Å for $[N_{1888}][UO_2(NO_3)_3(DOHyA)]$ and $[UO_2(NO_3)_2$ $(DOHyA)_2]$ complexes respectively. The U-O (distance between U and O of ligand) bond distances were determined to be 2.443 Å and 2.381 Å respectively for $[N_{1888}][UO_2(NO_3)_3(DOHyA)]$ and $[UO_2(NO_3)_2(DOHyA)_2]$ complexes.

In $[N_{1888}]_2[UO_2(NO_3)_4]$, the three nitrate ions in the complex were acting as monodentate ligand and one nitrate ion was acting as bidentate ligand with the average U-O ($O-NO_2$) bond distance of 2.423 Å is shown Table. 3.2. The U=O bond distance was lengthened from 1.714 Å (free UO_2^{2+} ion) to 1.796 Å in $[N_{1888}]_2[UO_2(NO_3)_4]$. In $[N_{1888}]_2[UO_2(NO_3)_2(NTf_2)_2]$, the two nitrate ions were found to act as bidentate and the two NTf_2^- ions act as monodentate ligand, with the bond distance of U-O (O-NO2); 2.539 Å and U-O (NTf_2^-); 2.421 Å. The U=O bond distance was lengthened from 1.714 Å (free UO_2^{2+} ion) to 1.786 Å in this case. The N-O (NO_3^- ion) bond distances in the complexes of $[N_{1888}][UO_2(NO_3)_3(DOHyA)]$, $[N_{1888}]_2[UO_2(NO_3)_4]$, $[UO_2(NO_3)_2(DOHyA)_2]$, and $[N_{1888}]_2[UO_2(NO_3)_2(NTf_2)_2]$ were 1.287, 1.294, 1.290 and 1.273 Å respectively (1.268 Å for free NO_3^-).

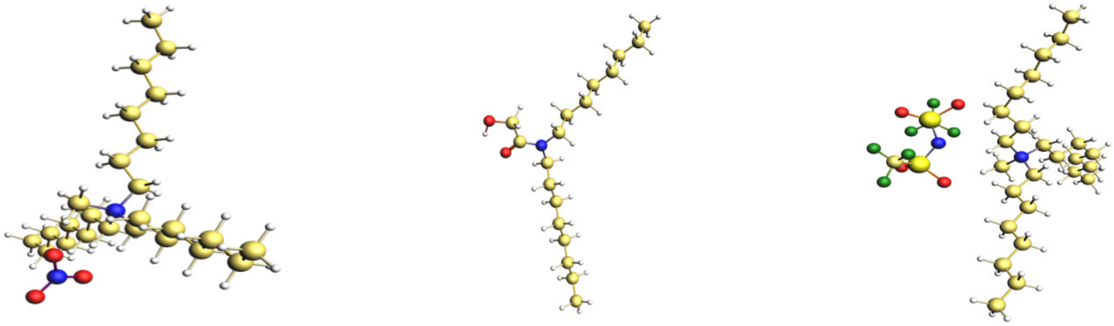

$[N_{1888}][NO_3]$ DOHyA $[N_{1888}][NTf_2]$

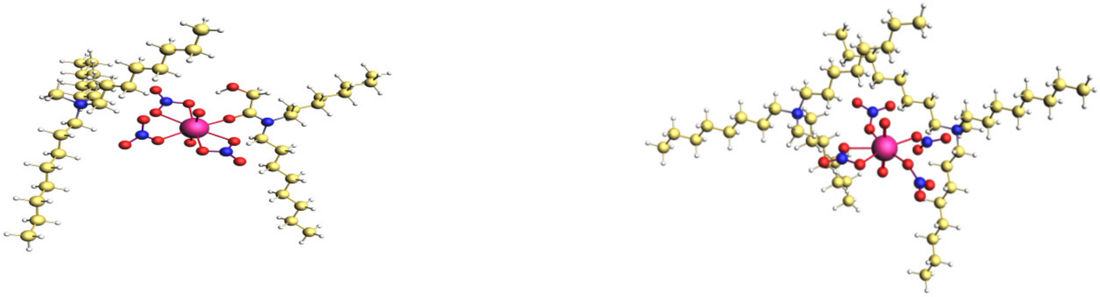

$N_{1888}][UO_2(NO_3)_3$ (DOHyA)] $[N_{1888}]_2[UO_2(NO_3)_4]$

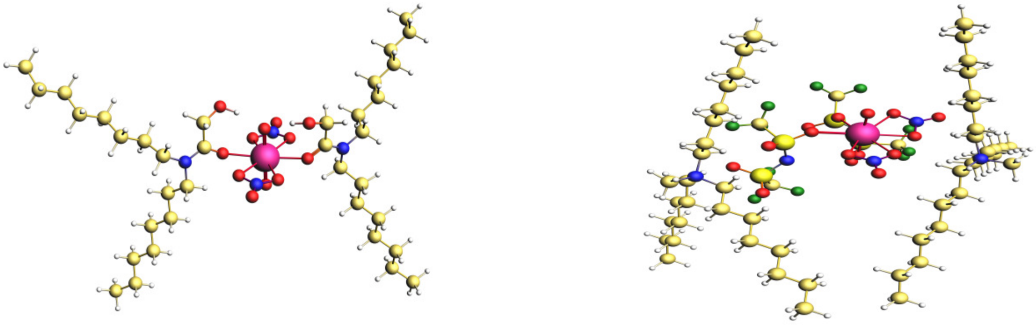

$UO_2(NO_3)_2$ $(DOHyA)_2$ $[N_{1888}]_2[UO_2(NO_3)_2(NTf_2)]$

Fig. 3.11. Optimized structures of DOHyA, $[N_{1888}][NO_3]$, $[N_{1888}][NTf_2]$ and complexes of U(VI) with DOHyA at BP/SVP level of theory.

Table. 3.2. The bond length of the uranyl complexes determined BP86/SVP level of theory in gas phase.

Complex	Bond lengths / Å		
	U-O (O=U=O)	U-O (O=C)	U-O (O-NO$_2$)
[N$_{1888}$] [UO$_2$(NO$_3$)$_3$(DOHyA)]	1.790	2.443	2.503
[N$_{1888}$]$_2$ [UO$_2$(NO$_3$)$_4$]	1.796	-	2.423
UO$_2$(NO$_3$)$_2$ (DOHyA)$_2$	1.815	2.389	2.489
[N$_{1888}$]$_2$ [UO$_2$(NO$_3$)$_2$(NTf$_2$)$_2$]	1.786	-	2.539

3.3.2. Bonding parameters

The calculated values of charge on uranium atom and the orbital's population from the natural population analysis were given in Table. 3.3. From the calculated values it is observed that there is increase in the f- and d-orbital population values which indicates the participation of d- and f-orbitals of U atom in the complex formation. The charge (q_U) on uranium was found to be lower in case of [UO$_2$(NO$_3$)$_2$ (DOHyA)$_2$] (1.712) and [N$_{1888}$][UO$_2$(NO$_3$)$_3$(DOHyA)] (1.749) as compared to [N$_{1888}$]$_2$[UO$_2$(NO$_3$)$_4$] (1.820) and [N$_{1888}$]$_2$[UO$_2$(NO$_3$)$_2$(NTf$_2$)] (1.800). This indicates that there is a charge transfer likely from ligand to metal atom, which is reflected in the increase population of f-orbital in these complexes. In the case of U(VI) complexation with ionic liquid without ligand [N$_{1888}$]$_2$ [UO$_2$(NO$_3$)$_4$], the more atomic charge (q_U) was observed on uranium atom compared to the complexes containing the ligand, which was also further reflected in the lower f-population values in the case of [N$_{1888}$]$_2$[UO$_2$(NO$_3$)$_4$]. Further, the values of electron density (ρ_c), Laplacian ($\nabla^2\rho_c$) and total energy density (H) were determined from the Bader analysis. The calculated values are presented in Table. 3.4, which helps to understand the nature of interactions in the complexes formed. From Table. 3.4, it can be observed that the

$\nabla^2\rho_c>0$ and H < 0 for U-O (O of C=O or NO_3^-) in all the complexes. These values specify the presence of partial covalent interactions between U and donor O atoms [31].

Table. 3.3. Charge and orbital occupation values of uranium after complexing with the extractant and ionic liquids at the B3LYP/TZVP level of theory.

Complex	Charge (q_U)	s	p	d	f
$[N_{1888}]\ [UO_2(NO_3)_3(DOHyA)]$	1.749	4.177	11.781	11.508	2.778
$[N_{1888}]_2\ [UO_2(NO_3)_4]$	1.820	4.162	11.775	11.502	2.734
$UO_2(NO_3)_2\ (DOHyA)_2$	1.712	4.714	11.801	11.494	2.811
$[N_{1888}]_2\ [UO_2(NO_3)_2(NTf_2)_2]$	1.800	4.171	11.777	11.480	2.765

Table. 3.4. Calculated electron density (ρ_c), Laplacian ($\nabla^2\rho_c$) and total energy density (H) of U(VI) complexes with extractant (DoHyA) and ionic liquids ($[N_{1888}][NO_3]$ or $[N_{1888}][NTF_2]$) at the B3LYP/TZP/ZORA level of theory.

Complex	**BCP**	**ρ_c(e/au^3)**	**$\nabla^2\rho_c$ (e/au^5)**	**H**
$[N_{1888}]\ [UO_2(NO_3)_3(DOHyA)]$	U-O (UO2)	0.2871	0.3774	-0.3272
	U-O (NO3)	0.0316	0.1879	-0.0645
	U-O (C=O)	0.0521	0.2276	-0.0191
$[N_{1888}]_2\ [UO_2(NO_3)_4]$	U-O (UO2)	0.2825	0.3787	-0.3178
	U-O (NO3)	0.0625	0.2337	-0.0097
$UO_2(NO_3)_2$ (2 DOHyA)	U-O (UO2)	0.2709	0.3663	-0.0322
	U-O (NO3)	0.0568	0.1865	-0.0863
	U-O (C=O)	0.0603	0.2402	-0.0662
$[N_{1888}]_2\ [UO_2(NO_3)_2(NTf_2)_2]$	U-O (UO2)	0.2895	0.3764	-0.3326
	U-O (NO3)	0.0994	0.1728	-0.0049
	U-O (NTf_2)	0.0575	0.2313	-0.0056

3.3.3. Thermodynamics of complexation in gas and solvent phase

The stoichiometry of metal-ligand complexation in organic phase was determined from the slope analysis of the experimental data and it was determined to be 1:1 (Metal : Ligand) in ionic liquid (see section 3.2.5) phase. The stoichiometry of uranium to DOHyA in *n*-DD was presumed as 1:2, since most of the amide based ligands exhibited the uranium:amide stoichiometry of 1:2 [32,33]. Accordingly, the stoichiometric reactions are represented in equations 3.8 to 3.11.

$$UO_2^{2+}{}_{(aq)} + 2NO_3^-{}_{(aq)} + DOHyA_{(IL)} + [N_{1888}][NO_3]_{(IL)} \rightarrow [N_{1888}]\,[UO_2(NO_3)_3(DOHyA)]_{(IL)} \quad (3.8)$$

$$UO_2^{2+}{}_{(aq)} + 2NO_3^-{}_{(aq)} + 2DOHyA_{(n\text{-DD})} \rightarrow UO_2(NO_3)_2(DOHyA)_{2(n\text{-DD})} \quad (3.9)$$

$$UO_2^{2+}{}_{(aq)} + 2NO_3^-{}_{(aq)} + 2\,[N_{1888}][NO_3]_{(IL)} \rightarrow [N_{1888}]_2[UO_2(NO_3)_4]_{(IL)} \quad (3.10)$$

$$UO_2^{2+}{}_{(aq)} + 2NO_3^-{}_{(aq)} + 2\,[N_{1888}][NTf_2]_{(IL)} \rightarrow [N_{1888}]_2\,[UO_2(NO_3)_2(NTf_2)_2]_{(IL)} \quad (3.11)$$

The behavior of co-ordination of uranium with ligands in gas phase can be explained by determining the binding energy (ΔE_g) of the complexes. For instance, the ΔE_g for the coordination of uranium shown in equation 3.8 and 3.9 can be described by equations 3.12 and 3.13. A similar equation can be written for equations 3.10 and 3.11.

$$\Delta E_g(U) = E_{[N1888][UO2(NO3)3(DOHyA)]} - [E_{UO22+} + 2E_{NO3-} + E_{[N888][NO3]}] \quad (3.12)$$

$$\Delta E_g(U) = E_{[UO2(NO3)22(DOHyA)]} - [E_{UO22+} + 2E_{NO3-} + 2E_{DOHyA}] \quad (3.13)$$

The calculated values of binding energy (ΔE) are presented in Table. 3.5. It is observed that the ΔE of UO_2^{2+} ion with DOHyA and $[N_{1888}][NO_3]$ is -560.267 kcal/mol and UO_2^{2+} ion towards DOHyA i.e -546.608 kcal/mol. The calculated binding energies follows the order $[N_{1888}]$ $[UO_2(NO_3)_3(DOHyA)]$ >$[N_{1888}]_2$ $[UO_2(NO_3)_4]$ > $UO_2(NO_3)_2$ $(DOHyA)_2$> $[N_{1888}]_2$ $[UO_2(NO_3)_2(NTf_2)_2]$, which is in line with the experimental observations discussed in section 3.2.1 and 3.2.2.

Although the gas phase ΔE values showed the experimental trends, it is always desirable to perform the solvent phase calculations as the metal ions are extracted from the aqueous phase to organic phase. The calculated ΔE values in the solvent phase are presented in Table. 3.6. It is observed that the binding energy of UO_2^{2+} ion towards DOHyA in $[N_{1888}][NO_3]$ medium is -119.915 kcal/mol, which is more than that of DOHyA in *n*-dodecane medium is -108.478 kcal/mol. Similarly, with ionic liquids the ΔE values are determined to be -116.916 kcal/mol ($[N_{1888}]_2[UO_2(NO_3)_4]$) and -106.132 kcal/mol ($[N_{1888}]_2[UO_2(NO_3)_2(NTf_2)]$) respectively. The results are found to be similar to those observed in gas phase. However, the addition of solvation effects consideribly lowered the magnitude of ΔE values due to solvation effects.

Table. 3.5. The energetic values of complexes of UO_2^{2+} with ligand and ionic liquids determined by B3LYP/TZVP level of theory in the gas phase.

Complex	ΔE (kcal/mol)	ΔH (kcal/mol)	ΔG (kcal/mol)
$[N_{1888}]\ [UO_2(NO_3)_3(DOHyA)]$	-560.267	-555.779	-509.779
$[N_{1888}]_2\ [UO_2(NO_3)_4]$	-559.509	-556.086	-511.805
$UO_2(NO_3)_2\ (DOHyA)_2$	-546.608	-541.267	-497.267
$[N_{1888}]_2\ [UO_2(NO_3)_2(NTf_2)_2]$	-544.132	-538.333	-495.382

Further, the thermodynamic properties of the four complexes by incorporating thermal corrections (ΔH and ΔG) were computed and the values are shown in Table. 3.5 and 3.6. The free energy of complexation values (ΔG) trend determined in gas phase for the studied complexes is $[N_{1888}]_2\ [UO_2(NO_3)_4]$ > $N_{1888}]\ [UO_2(NO_3)_3(DOHyA)]$ > $UO_2(NO_3)_2(DOHyA)_2$> $[N_{1888}]_2\ [UO_2(NO_3)_2(NTf_2)_2]$, which is slightly different from the observed trend of ΔE values (Table. 3.5). However, the free energy of complextaion values (ΔG) in the solvent phase (Table

3.6) follows the similar trend as binding energy in the solvent phase i.e $[N_{1888}]$ $[UO_2(NO_3)_3(DOHyA)]$ > $[N_{1888}]_2[UO_2(NO_3)_4]$ > $UO_2(NO_3)_2(DOHyA)_2$> $[N_{1888}]_2$ $[UO_2(NO_3)_2(NTf_2)_2]$, which is in line with the experimental observations .

Table. 3.6. The energetic values of complexes of UO_2^{2+} with ligand and ionic liquids determined by B3LYP/TZVP level of theory in the solvent phase.

Complex	ΔE (kcal/mol)	ΔH (kcal/mol)	ΔG (kcal/mol)
$[N_{1888}]$ $[UO_2(NO_3)_3(DOHyA)]$	-119.915	-120.444	-74.737
$[N_{1888}]_2$ $[UO_2(NO_3)_4]$	-116.916	-118.804	-74.523
$UO_2(NO_3)_2$ $(DOHyA)_2$	-108.478	-108.447	-64.448
$[N_{1888}]_2$ $[UO_2(NO_3)_2(NTf_2)_2]$	-106.132	-105.644	-62.693

Since the ionic liquids composed of the combination of cation and anion there is possibility of ion exchange mechanism when contacted with the aqueous phase containing various ions. For instance, the ion exchange reaction between uranyl ion and the ions of ionic liquid medium reaction can be modeled as follows.

$$UO_2(NO_3)_3{}^-{}_{aq} + NO_3{}^-{}_{IL} \rightarrow UO_2(NO_3)_3{}^-{}_{IL} + NO_3{}^-{}_{aq} \quad (3.14)$$

$$UO_2(NO_3)_3{}^-{}_{aq} + NTf_2{}^-{}_{IL} \rightarrow UO_2(NO_3)_3{}^-{}_{IL} + NTf_2{}^-{}_{aq} \quad (3.15)$$

$$UO_2(NO_3)^+{}_{aq} + N_{1888(IL)}{}^+ \rightarrow UO_2(NO_3)^+{}_{IL} + N_{1888(aq)}{}^+ \quad (3.16)$$

$$UO_2{}^+{}_{aq} + N_{1888(IL)}{}^+ \rightarrow UO_2{}^+{}_{IL} + N_{1888(aq)}{}^+ \quad (3.17)$$

The feasibility of ion exchange can be explained by the Gibbs energy change of complexation of metal ion. Therefore the solvent phase free energy was calculated for the exchange reactions of equations 3.14 to 3.17 by using equation 3.18.

$$\Delta G_{ext}(U) = E_{[UO2(NO3)3]-/(aq)} + E_{[NO3]-/(IL)} - (E_{UO2(NO3)3-/(aq)} + E_{NO3-/(IL)}) + RT\text{-}T\Delta S \quad (3.18)$$

The calculated values of Gibbs energy change for the complexation of uranium in the ionic liquid phase during the anion exchange of $UO_2(NO_3)_3^-$ ion with nitrate of $[N_{1888}][NO_3]$ (equation 3.14) is -1.245 kcal/mol, which is slightly higher than the exchange with NTf_2^- of $[N_{1888}][NTf_2]$ medium (equation 3.15), whose value is -0.423 kcal/mol. This indicates that the anion exchange of uranyl nitrate is more feasible in $[N_{1888}][NO_3]$ than $[N_{1888}][NTf_2]$. The Gibbs energy change for the cation exchange of UO_2^{2+} with the cation of ionic liquid is 14.686 kcal/mol for $[N_{1888}][NO_3]$ medium and 27.281 kcal/mol for $[N_{1888}][NTf_2]$ medium. Similarly for $[UO_2(NO_3)]^+$ exchange these values are 3.146 for $[N_{1888}][NO_3]$ medium and 5.816 kcal/mol $[N_{1888}][NTf_2]$ medium respectively. The positve energy change indicates that the cation exchange mechanism was not feasible.

3.3.4. FT-IR Results

From DFT calculations, the calculated C=O, stretching frequency values of the free DOHyA, NO_3^- and UO_2^{2+} were determined to be 1697, 1428 and 1094 cm^{-1}, as shown in Table. 3.7. The stretching frequencies of C=O are shifted from 1697 to 1646 and 1605 cm^{-1} in the case of $[N_{1888}][UO_2(NO_3)_3(DOHyA)]$and $UO_2(NO_3)_2(DOHyA)_2$ complexes respectively due to the interaction of UO_2^{2+} ion with amidic oxygen atom. The stretching frequencies of U=O are shifted from 1094 to 928 and 893 cm^{-1} for $[N_{1888}][UO_2(NO_3)_3(DOHyA)]$and $UO_2(NO_3)_2(DOHyA)_2$ complexes respectively. Similarly, the nitrate ion ($O\text{-}NO_2$) stretching frequencies are shifted from 1428 cm^{-1} to 1333 and 1373 cm^{-1} for $[N_{1888}][UO_2(NO_3)_3(DOHyA)]$ and $UO_2(NO_3)_2(DOHyA)_2$ complexes respectively. In the other two complexes $[N_{1888}]_2[UO_2(NO_3)_4]$ and $[N_{1888}]_2[UO_2(NO_3)_2(NTf_2)_2]$ complexes, lowering of the stretching frequencies of nitrate ion 1348 and 1390 cm^{-1} are observed. These results are in line with experimental observations as discussed in section 3.2.6 and 3.2.7.

Table. 3.7. Calculated vibrational frequencies of different complexes at BP/SVP level of theory.

Complex	Stretching frequencies / cm^{-1}		
	U-O (O=U=O)	U-O (O=C)	U-O (O-NO_2)
$[N_{1888}]$ $[UO_2(NO_3)_3(DOHyA)]$	928	1646	1333
$[N_{1888}]_2$ $[UO_2(NO_3)_4]$	917	-	1348
$UO_2(NO_3)_2$ $(DOHyA)_2$	893	1605	1373
$[N_{1888}]_2$ $[UO_2(NO_3)_2(NTf_2)_2]$	940	-	1390

3.4. Summary

The extraction of U(VI) in organic phases followed in the order of DOHyA/*n*-DD << $[N_{1888}][NO_3]$ < DOHyA/$[N_{1888}][NO_3]$, indicating that $[N_{1888}][NO_3]$ and DOHyA were involved in the extraction of U(VI) in the ionic liquid medium. From FTIR and Raman spectroscopy, the shift in the amidic carbonyl bands from 1650 cm^{-1} to 1620 cm^{-1} confirmed the participation of DOHyA in the extraction of uranium in DOHyA/$[N_{1888}][NO_3]$ medium, similar to *n*-DD system. However, the growth of 1020 cm^{-1} shoulder at the expense of 1040 cm^{-1} intensity confirmed uranyl nitrate underwent nitrate ion association with $[N_{1888}][NO_3]$. Therefore, it appears that uranyl nitrate was extracted into DOHyA/$[N_{1888}][NO_3]$ phase by two different modes, seems to be independent of each other. They are U(VI) extraction through (a) the co-ordinate complex formation with DOHyA, and (b) through the association reaction of uranyl nitrate with nitrate ion of ionic liquid. The extraction of U(VI) in both $[N_{1888}][NO_3]$ and 0.1M DOHyA/$[N_{1888}][NO_3]$ was similar, both under unirradiated and irradiated conditions. The quantitative stripping of lodeded U(VI) from ionic liquid phase was achieved in 4 to 5 contacts with dilute nitric acid. From DFT calculations, natural population analysis showed that there is participation of d- and f-orbitals of U atom in the complex formation with the ligand DOHyA and ionic liquids. Further, from the AIM calculation there is partial covalent character was observed between U and donor O atoms. The calculated values of Gibbs energy of complexation of U(VI) with DOHyA and ionic liquids in the solvent phase using DFT are in line with the experimentally determined complexation of UO_2^{2+} ion with the extractant and ionic liquid. Based on the DFT calculations, it was established that the cation exchange mechanism by both the ionic liquids $[N_{1888}][NO_3]$ and $[N_{1888}][NTf_2]$ was not feasible, but anion exchange mechanism was feasible.

References

1. X. Sun, H. Luo, S. Dai, Ionic liquids-based extraction: a promising strategy for the advanced nuclear fuel cycle, Chem. Rev. 112 (2011) 2100-2128.
2. L. Chen, Y. Wang, X. Yuan, Y. Ren, N. Liu, L. Yuan, W. Feng, Highly selective extraction of uranium from nitric acid medium with phosphine oxide functionalized pillar [5] arenes in room temperature ionic liquid, Sep. Purif. Technol. 192 (2018) 152-159.
3. N.K. Gupta, Ionic liquids for TRansUranic Extraction (TRUEX)—Recent developments in nuclear waste management: A review, J. Mol. Liq. 269 (2018) 72-91.
4. B.B. Mishra, N. Devi, Solvent extraction and separation of europium (III) using a phosphonium ionic liquid and an organophosphorus extractant-A comparative study, J. Mol. Liq. 271 (2018) 389-396.
5. P.K. Mohapatra, Actinide ion extraction using room temperature ionic liquids: opportunities and challenges for nuclear fuel cycle applications, Dalton Trans. 46 (2017) 1730-1747.
6. T. Sun, Y. Zhang, Q. Wu, J. Chen, L. Xia, C. Xu, Comparative study on the extraction of trivalent americium and europium by CMPO in imidazolium-based ionic liquids and dodecane, Solvent Extr. Ion Exch. 35 (2017) 408-422.
7. P.R. Vasudeva Rao, K.A. Venkatesan, Alok Rout, T.G. Srinivasan, K. Nagarajan, Potential applications of room temperature ionic liquids for fission products and actinide separation, Sep. Sci. Technol. 47 (2012) 204-222.
8. I. Billard, A. Ouadi, C. Gaillard, Liquid–liquid extraction of actinides, lanthanides, and fission products by use of ionic liquids: from discovery to understanding, Anal. Bioanal. Chem. 400 (2011) 1555-1566.

9. H.H. Sung, R.N. Menchavez, Y.M. Koo, Reprocessing of spent nuclear waste using ionic liquids. Korean J. Chem. Eng. 27 (5) (2010) 1360-1365.

10. S. Dai, Y.H Ju, C.E Barnes, Solvent extraction of strontium nitrate by a crown ether using room-temperature ionic liquids, Journal of the Chemical Society, Dalton Trans. 1 (1999) 1201-1202.

11. A.E. Visser, R.P. Swatloski, W.M. Reichert, S.T. Griffin, R.D. Rogers, Traditional extractants in non-traditional solvents: Group 1 and 2 extraction by crown ethers in room temperature ionic liquids, Ind. Eng. Chem. Res. 39 (2000) 3596 – 3604.

12. M.L. Dietz, D.C. Stepinski, Anion concentration-dependent partitioning mechanism in the extraction of uranium into room-temperature ionic liquids, Talanta 75 (2008) 598 - 603.

13. M.L. Dietz, Ionic liquids as extraction solvents: Where do we stand?, Sep. Sci. Technol. 41 (2006) 2047-2063.

14. M.L. Dietz, J.A. Dzielawa, I.L. Blake, A. Young, M.P. Jensen, Influence of solvent structural variations on the mechanism of facilitated ion transfer into room temperature ionic liquids, Green Chem. 5 (2003) 682 - 685.

15. M.L. Dietz, J.A. Dzielawa, Ion-exchange as a mode of cation transfer into room temperature ionic liquids containing crown ethers: implications for the ‘greenness’ of ionic liquids as diluents in liquid–liquid extraction, Chem. Commun. (2001) 2124-2125.

16. D.C. Stepinski, M.P. Jensen, J.A. Dzielawa, M.L. Dietz, Synergistic effects in the facilitated transfer of metal ions into room-temperature ionic liquids, Green Chem. 7 (2005) 151 – 157.

17. J. Swanson, Purex process flowsheets, Science and technology of tributyl phosphate, (1984) 55.

18. J.P. Mikkola, P. Virtanen, R Sojholm, Aliquat 336-a versatile and affordable cation source for an entirely new of hydrophobic ionic liquids, Green Chem. 8 (2006) 250-255.

19. Alok Rout, K. Chatterjee, K.A. Venkatesan, K.K. Sahu, M.P. Antony, P.R. Vasudeva Rao, Solvent extraction of plutonium(IV) in monoamide - Ammonium ionic liquid mixture, Sep. Purif. Technol. 159 (2016) 43-49.

20. Alok Rout, K.A. Venkatesan, M.P. Antony, P.R. Vasudeva Rao, Liquid-Liquid extraction of americium(III) using a completely incenerable ionic liquid system, Sep. Purif. Technol. 158 (2016) 137-143.

21. B. Mahanty, A. Bhattacharyya, P.K. Mohapatra, Separation of neptunium (IV) from actinides by solid phase extraction using a resin containing Aliquat 336, J. Chromatogr. A 1564 (2018) 94-101.

22. S. Kannan, B.G. Vats, I.C. Pius, D.M. Noronha, P.S. Dhami, P.W. Naik, M. Kumar, Extraction and structural studies of an unexplored monoamide, N, N′-dioctyl, α-hydroxy acetamide with lanthanide (III) and actinide (III) ions, Dalton Trans. 43 (2014) 5252-5255.

23. T. Prathibha, R. Kumaresan, B.R. Selvan, K.A. Venkatesan, M.P. Antony, P.R.V. Rao, N,N-dialkyl-2-hydroxyacetamides for modifier-free separation of trivalent actinides from nitric acid medium, Radiochim. Acta 104 (2016) 173-181.

24. R. Rama, Alok Rout, K. Venkatesan, M. Antony, Room temperature ionic liquid system for the mutual separation of Pu (IV) from other actinides using 2-hydroxy acetamide extractant, Sep. Purif. Technol. 196 (2018) 166-173.

25. A.J. Ryan, E. Wheelwright, Recovery and purification of plutonium by anion exchange, Ind. Eng. Chem. 51 (1959) 60-65.

26. G.T. Seaborg, J.J. Katz, L.R. Morss, The Chemistry of the Actinide Elements, Springer Science & Business Media, 2012.

27. A. Landgren, J. Liljenzin, Extraction behaviour of technetium and actinides in the Aliquat-336/nitric acid system, Solvent Extr. Ion Exch. 17 (1999) 1387-1401.

28. K. Ohwada, T. Ishihara, Infra-red spectrophotometry of uranyl nitrate/tri-n-butyl phosphate in organic solvents, J. Inorg. Nucl. Chem. 28 (1966) 2343-2345.

29. M. Gal, P. Goggin, J. Mink, Vibrational spectroscopic studies of uranyl complexes in aqueous and non-aqueous solutions, Spectrochimica Acta Part A: Molecular Spectroscopy, 48 (1992) 121-132.

30. P.K. Mohapatra, V. Manchanda, Ion-pair extraction of uranyl ion from aqueous medium using crown ethers, Talanta 47 (1998) 1271-1278.

31. W. Koch, G. Frenking, J. Gauss, D. Cremer, J.R. Collins, Helium chemistry: theoretical predictions and experimental challenge, J. Am. Chem. Soc.109 (1987) 5917-5934.

32. K. McCann, B.J. Mincher, N.C. Schmitt, J.C. Braley, Hexavalent actinide extraction using N, N-dialkyl amides, Ind. Eng. Chem.Res. 56 (2017) 6515-6519.

33. P.K. Verma, P.N. Pathak, N. Kumari, B. Sadhu, M. Sundararajan, V.K. Aswal, P.K. Mohapatra, Effect of successive alkylation of N, N-dialkyl amides on the complexation behavior of uranium and thorium: solvent extraction, small angle neutron scattering, and computational studies, J. Phys. Chem. B 118 (2014) 14388-14396.

Chapter 4: Extraction behavior of Eu(III) and Zr(IV) in ammonium ionic liquids

Ionic liquids are being considered as a potential candidate for replacing the traditional molecular diluents in a solvent extraction application [1-7]. The conventional ionic liquid employed for solvent extraction applications are 1-alkyl-3-methyl imidazolium bis(trifluoromethylsulphonyl)imide ([$C_n$mim][NTf_2]) has several drawbacks, such as significant solubility of ionic liquid in aqueous phase, undergo cation exchange with several ions present in the aqueous solution during solvent extraction etc [2-4]. The cation exchange of [$C_n$mim][NTf_2] ionic liquids results in the loss of ionic liquid from organic phase, leading to the contamination or pollution of the aqueous feed solution by ionic liquid. The loss of ionic liquid from organic phase leads to reduction in recycling ability of the ionic liquid for the subsequent solvent extraction application. In view of this, it is recommended to replace the conventional imidazolium based ionic liquids by strongly hydrophobic ionic liquids which are made up of alkyl ammonium cations. Alkyl ammonium ion based ionic liquids ($[R_4N]^+$; R $\geq$ butyl) are strongly hydrophobic as compared to imidazolim ionic liquids due to the presence of four bulky alkyl chains attached to the cationic nitrogen atom [8]. Since these ionic liquids are strongly hydrophobic they do not undergo cation exchange with other ions present in aqueous phase [9-11].

In the present chapter, tri-butyl-methyl ammonium bis(trifluoromethylsulfonyl)imide ([N_{1444}][NTf_2]) ionic liquid was studied as a diluent and results on the solvent extraction of Eu(III) and Zr(IV) in RTIL medium containing molecular extractants was reported. This chapter is divided into two parts (part A and part B). Part I discusses the solvent extraction and complexation behavior of Eu(III) in molecular extractants such as tetra-2-ethylhexyldiglycolamide (T2EHDGA) or carbamoylphospinoxide (CMPO) dissolved in alkylammonium bis(trifluoromethylsulfonylimide). In part II, the studies on the extraction behavior of Zr(IV) using 2-ethylhexylbenzodioxodiamide (BD) dissolved in alkyl ammonium bis(trifluoromethylsulfonyl)imide ionic liquid was studied.

PART A: Europium(III) complexation behavior in ammonium ionic liquid medium containing neutral extractants

4.1. Introduction

High level liquid waste (HLLW) is generated during reprocessing of spent nuclear fuels. It is composed of trivalent actinides (Am(III), Cm(III)), lanthanides (Ln(III)), fission products and corrosion products in 3-4 M nitric acid medium [12,13]. Partitioning of trivalent actinides and transmutation into short lived or stable products has been suggested for the safe disposal of HLLW [12,13]. A number of reagents based on carbamoylmethylphosphinoxide (CMPO), diamides, and diglycolamides [17] have been suggested for the separation of trivalent actinides and lanthanides from HLLW [14,15].The method involves the solvent extraction of trivalent metal ions from HLLW into the solution of diglycolamide in *n*-dodecane medium. For instance a solution of 0.2 M *N,N,N',N'*-tetra(2-ethylhexyl)diglycolamide (T2EHDGA) in *n*-DD has been proposed for solvent extraction application [15,16]. However the reagent, T2EHDGA, has several drawbacks such as poor solubility of polar extractant in a non polar diluent *n*-dodecane, and third phase formation (splitting of organic phase) during the course of solvent extraction. Several authors have maneuvered this problem by adding phase modifiers to the organic phase, even though the organic phase without the addition of modifiers was preferable [4-7]. Another way to overcome the problem of third phase formation is to use ionic liquid diluent in place of molecular diluent *n*-dodecane [8]. Since the ionic liquids are comprised entirely of ions, unlike molecular *n*-dodecane, they stabilize the polar extractants, and polar metal-solvates (metal-ligand complexes) in ionic liquid phase [9-19]. In view of this, ionic liquids have been proposed for the extraction of metal ions, where in the posibility of third phase formation is quite insignificant [19].

In view of this, the results on the extraction behavior of Eu(III) from nitric acid medium in to a solution of T2EHDGA or CMPO dissolved in [N_{1444}][NTf_2] is reported in this chapter. *Experimental details for the present chapter (part A) are presented in the section 2.5.2 of the chapter 2. The synthesis of ionic liquid employed in the present study was discussed in section 2.6.4.*

Table. 4.1. Structure of molecular extractant and RTIL used in part A of chapter 4.

Name	Structure
Extractant	
N,N,N',N'-tetra-2-ethylhexyldiglycolamide (T2EHDGA)	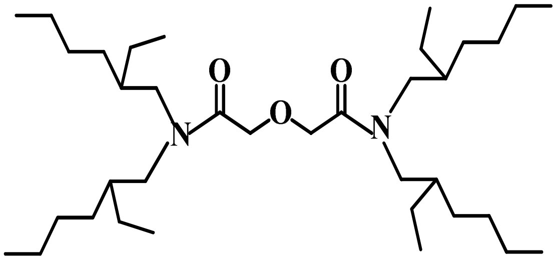
Octyl-phenyl-*N,N*-diisobutylcarbamoylmethyl phosphinoxide (CMPO)	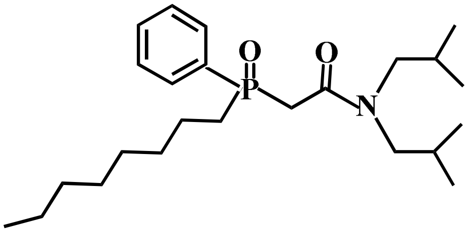
Ionic liquid	
Tri-butyl-methyl ammonium bis(trifluoromethylsulfonyl)imide [N_{1444}][NTf_2] (R: C_4H_9)	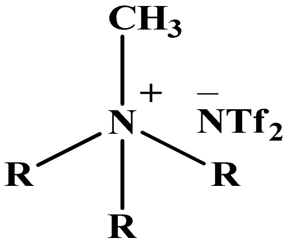

4.2. Results and discussions

4.2.1. Effect of nitric acid concentration

Fig. 4.1. shows the variation in the distribution ratio of Eu(III) in T2EHDGA (or CMPO)/[N_{1444}][NTf_2] as a function of nitric acid concentration. The extraction of Eu(III) observed in presence of T2EHDGA and CMPO was compared with those obtained in [N_{1444}][NTf_2] ionic liquid alone. As expected, the extraction of Eu(III) in [N_{1444}][NTf_2] is insignificant at all acidities, which is due to the absence of functional group in [N_{1444}][NTf_2]. However, the distribution ratio of Eu(III) increases remarkably upon adding T2EHDGA (or CMPO) to [N_{1444}][NTf_2] phase at all nitric acid concentrations. The extraction of Eu(III) in 0.05M T2EHDGA (0.05M CMPO)/[N_{1444}][NTf_2] phase is significantly high ($D_{Eu(III)}$ >100) especially at higher acidities (~3M), which is indeed desirable for the extraction of trivalent actinides and lanthanides from nuclear waste. It can be seen from Fig. 4.1., that the distribution ratio of Eu(III) decreases with increase in the concentration of nitric acid. The decreasing trend with increase in the concentration of nitric acid is usually attributed to the cation exchange mechanism of ionic liquid [17,20-24]. Since Eu(III) is not extractable by [N_{1444}][NTf_2], the observed decreasing trend in Fig. 4.1. could be attributed to the competition between H^+ and Eu(III) ion for co-ordination with ligand in ionic liquid phase. A similar behavior was also reported in the literature for the extraction of Am(III) in a solution of, *N,N*-dioctyl-(4-trihexylammonium)butyramide bis(trifluoromethylsulfonyl)imide ([AmDOA][NTf_2]) task specific ionic liquid in [N_{1444}][NTf_2] [25].

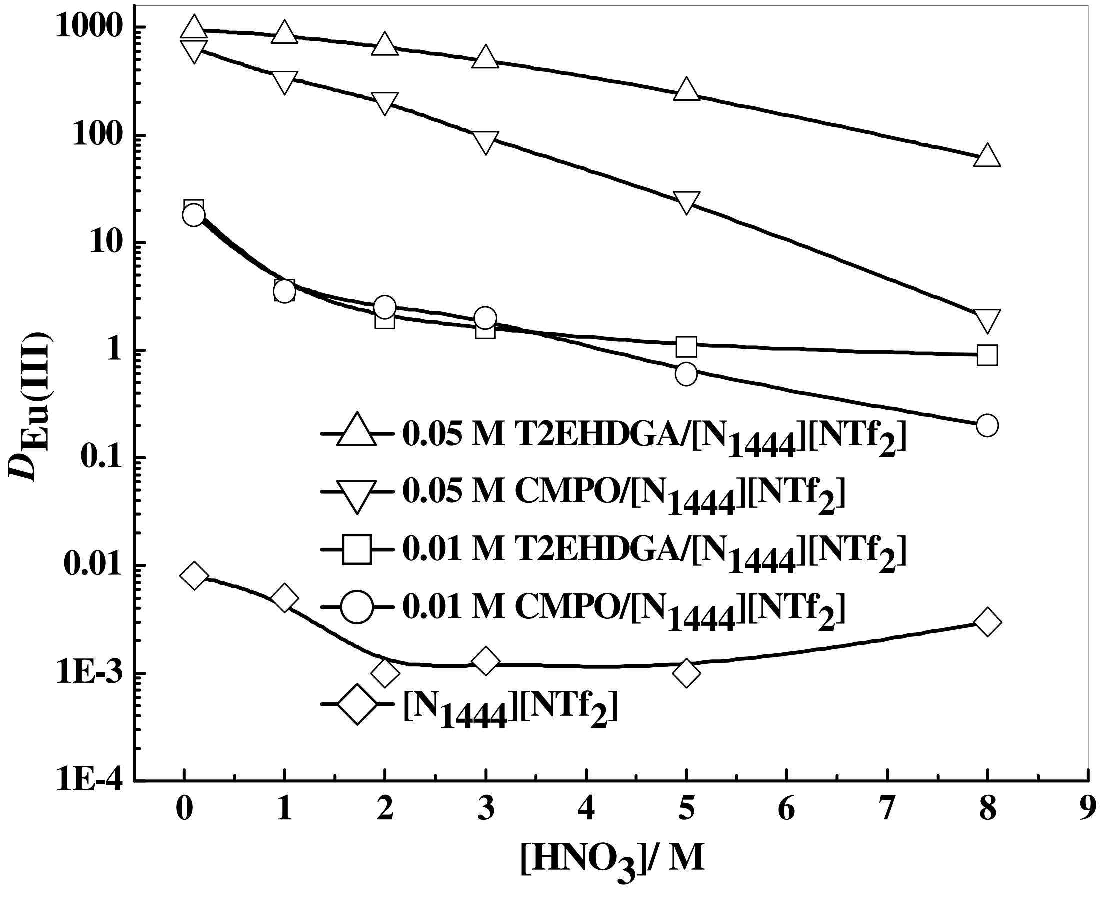

Fig. 4.1. Variation in the distribution ratio of Eu(III) as a function of the nitric acid concentration in the aqueous phase. Ionic liquid phase: 0.05 M T2EHDGA (or CMPO)/$[N_{1444}][NTf_2]$ or $[N_{1444}][NTf_2]$ alone; Aqueous phase: 0.1 – 8.0 M HNO_3 spiked with $^{152+154}$Eu tracer Temperature = 298 K; Equilibration time = 1 hour; Phase volume ratio = 1.

To understand the extraction of nitric acid in ionic liquid phase, the extraction behavior of nitric acid with 0.05 M T2EHDGA (or CMPO)/$[N_{1444}][NTf_2]$ as well as in $[N_{1444}][NTf_2]$ was investigated and the results are displayed in Fig. 4.2. It can be seen that the extraction of nitric acid in organic phase increases with increase in the concentration of nitric acid in aqueous phase from 0.1 to 8.0 M, irrespective of the nature of the organic phase. As expected, the presence of T2EHDGA (or CMPO) in $[N_{1444}][NTf_2]$ phase increased the extraction of nitric acid, which is due to the protonation of the carbonyl functional groups present in the two extractant moieties.

The nitric acid extraction follows the order: T2EHDGA/[N_{1444}][NTf_2] > CMPO/[N_{1444}][NTf_2] > [N_{1444}][NTf_2].

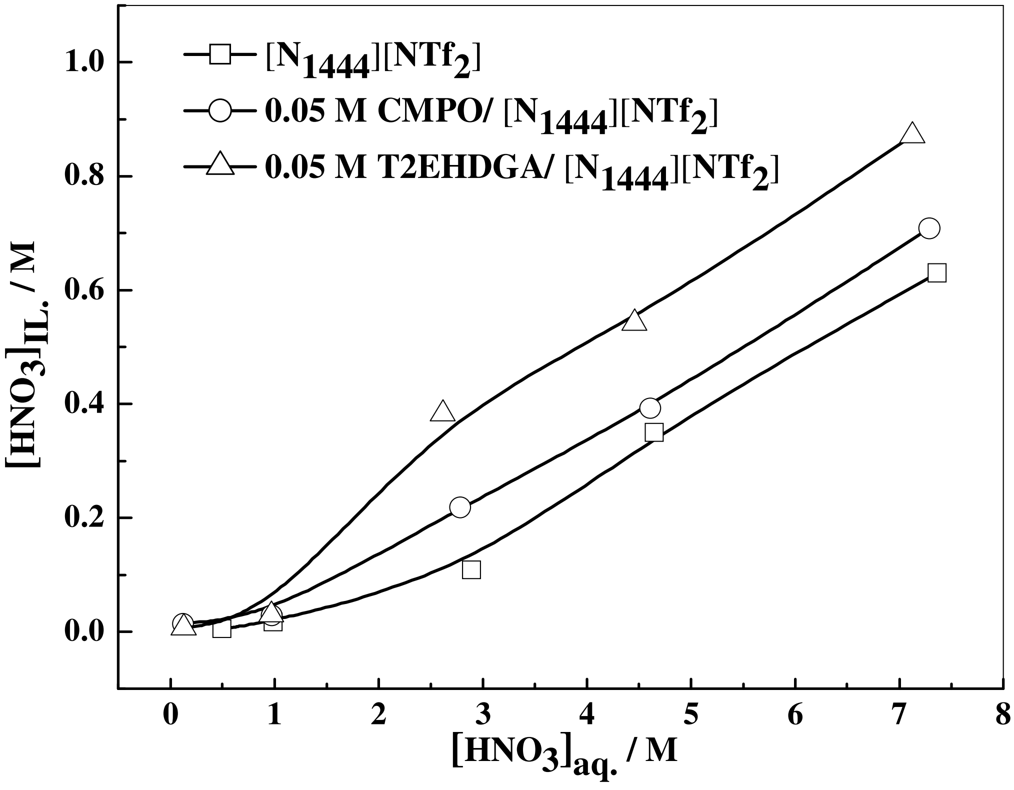

Fig. 4.2. Extraction of nitric acid in ionic liquid phase as a function of equilibrium concentration of nitric acid in aqueous phase. Ionic liquid phase: 0.05 M T2EHDGA(or CMPO)/[N_{1444}][NTf_2] or [N_{1444}][NTf_2] alone; Aqueous phase: 0.1 – 8.0 M HNO_3 Temperature = 298 K; Equilibration time = 1 hour; Phase volume ratio = 1.

4.2.2. ATR-FTIR Spectroscopy

To confirm the protonation of nitric acid with T2EHDGA or CMPO phase, the ATR-FTIR spectrum of 0.05 M T2EHDGA (or CMPO)/[N_{1444}][NTf_2] was recorded after contacting the ionic liquid phase with various concentrations of nitric acid, and the results are displayed in Fig. 4.3. It can be seen that the transmittance bands occurring at 1651 cm^{-1} and 1635 cm^{-1} are due to the stretching frequency of amidic C=O group present in T2EHDGA and CMPO respectively (Fig. 4.3A and 4.3B). The transmittance band of C=O in case of T2EHDGA is shifted from

1651 cm^{-1} to1633 cm^{-1} (Fig. 4.3A), upon equilibration with 1M nitric acid, and broadened further with increase in the concentration of nitric acid. In contrast to this, there is a marginal shift in the carbonyl peak of CMPO at 1635 cm^{-1} upon acid (1M) equilibration (Fig. 4.3B). However, broadening of transmittance bands upon increasing the concentration of nitric acid is also observed in case of CMPO. The peak at 1264 cm^{-1} due to P=O group present in CMPO is not presented in the Fig. 4.3B. as the intensity of P=O transmittance band is minimal and masked by other transmittance bands. The above findings clearly suggest that the extraction of nitric acid results in the protonation of the amidic C=O group in T2EHDGA as well as CMPO.

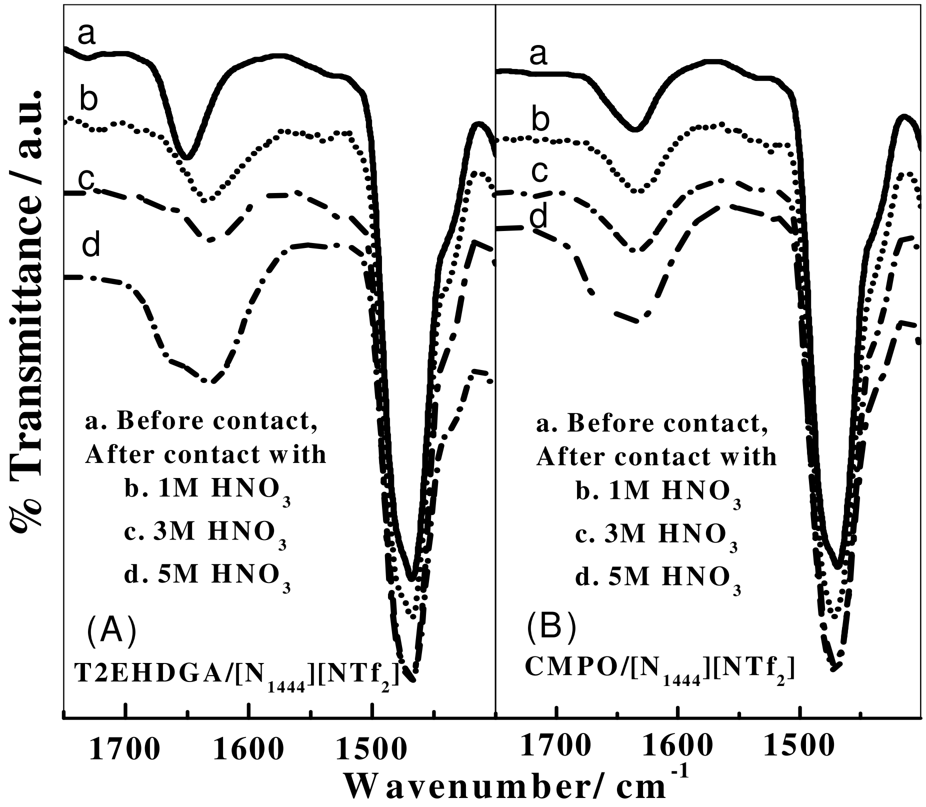

Fig. 4.3. ATR-FTIR spectra of ionic liquid phase recorded before and after nitric acid equilibration. Ionic liquid phase: 0.05 M T2EHDGA (or CMPO)/[N_{1444}][NTf_2]; Aqueous phase: 0-5 M HNO_3; Temperature = 298 K; Equilibration time = 1 hour; Phase volume ratio = 1.

To confirm the co-ordination of T2EHDGA or CMPO with Eu(III) the ATR-FTIR spectra of the organic phase 0.05 M T2EHDGA (or CMPO)/[N_{1444}][NTf_2] were recorded after contacting the aqueous phase containing Eu(III) nitrate solution in 3 M nitric acid and the results are shown in Fig. 4.4. The amount of Eu(III) in the aqueous phase was varied from 1 to 10 g.L^{-1}. It can be seen that the transmittance band occurring at 1630 cm^{-1} is due to the protonated amidic carbonyl group. The ATR-FTIR spectra of the ionic liquid phase recorded after contacting the 0.05 M T2EHDGA (or CMPO)/[N_{1444}][NTf_2] with Eu(III) solution in 3 M nitric acid shows further broadening at 1630 cm^{-1} and partial shifting to 1590 cm^{-1} in both TEHDGA and CMPO cases. The appearance of a transmittance bands at 1590 cm^{-1} is due to the co-ordination of Eu(III) with the amidic carbonyl group of T2EHDGA and CMPO, leading to the shift of amidic C= O stretching frequencies from 1630 cm^{-1} to 1590 cm^{-1}. A similar behavior was also reported during the extraction of Nd(III) from nitric acid medium by a solution of diglycolamide in *n*-dodecane [26].

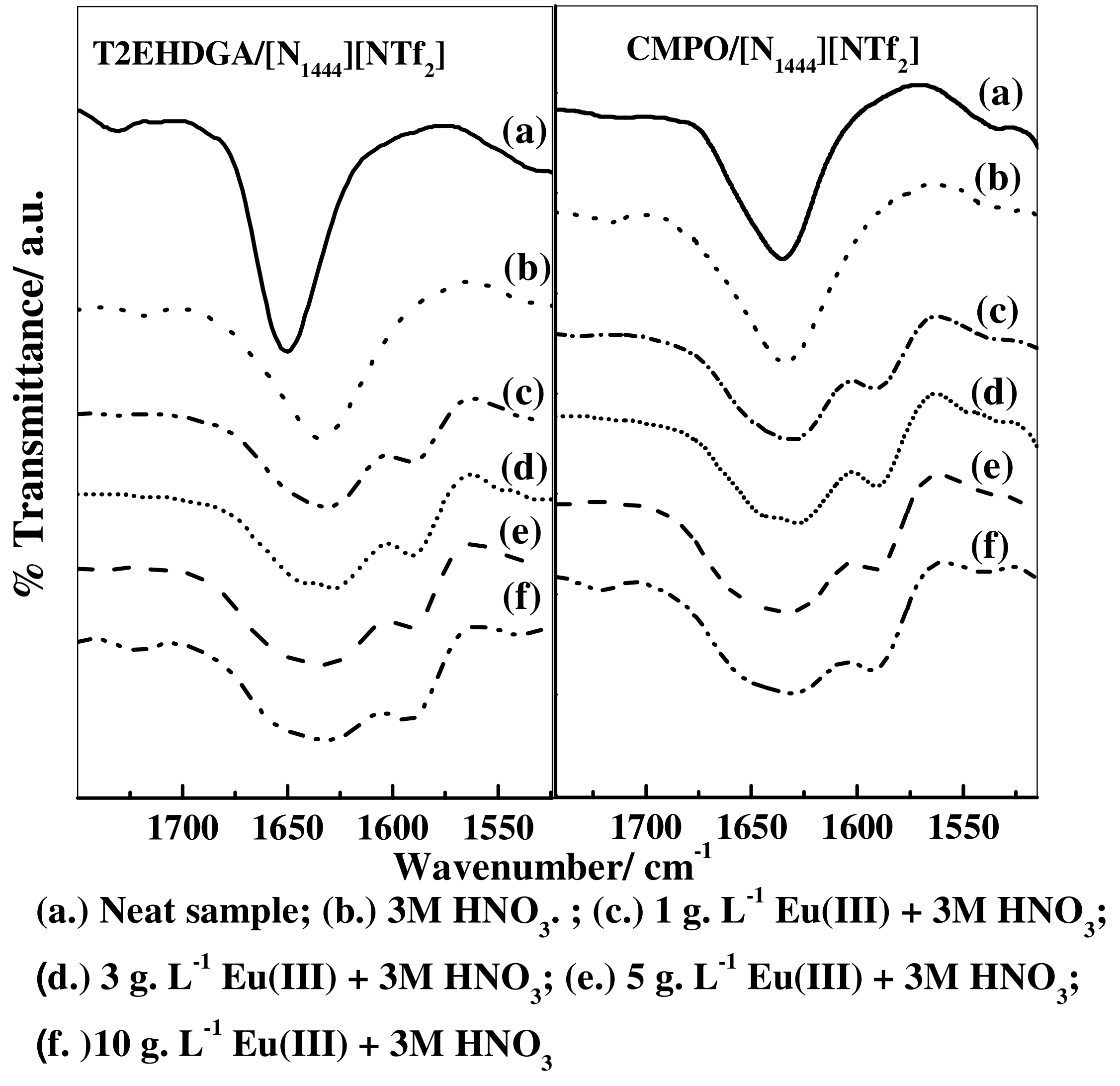

Fig 4.4. ATR-FTIR spectra of ionic liquid phase recorded after contacting the organic phase with 3 M nitric acid containing Eu(III) ion (1-10g.L^{-1}). Ionic liquid phase: 0.05 M T2EHDGA (or CMPO)/[N$_{1444}$][NTf$_2$]; Aqueous phase: 3 M HNO$_3$ containing Eu(III) (1-10 g.L^{-1}); Temperature = 298 K; Equilibration time = 1 hour; Phase volume ratio = 1.

4.2.3. Aggregation behavior of ionic liquid phase

Even though, a large number of reports are available in literature [1-11] on the separation of metal ions from the aqueous phase using ionic liquid as medium, the studies on aggregate formation in the ionic liquid phase during the solvent extraction of metal ion is very limited [25]. Therefore, studies have been carried out on the aggregation behavior of the ionic liquid phase during the extraction of Eu(III) from nitric acid medium. The aggregation behavior in ionic liquid was studied by dynamic light scattering measurements described elsewhere [25]. The self aggregation behavior of neat $[N_{1444}][NTf_2]$ is shown in Fig. 4.5. It can be seen that the average aggregate size of $[N_{1444}][NTf_2]$ is about 0.8 nm. The self-aggregation observed in $[N_{1444}][NTf_2]$ indicates that the cation and anion of the ionic liquid are held together by strong attractive forces. Addition of T2EHDGA or CMPO (both 0.05M) to $[N_{1444}][NTf_2]$ increases the average aggregate size and their distribution in the resultant solution is shown in Fig. 4.5. This could be due to the interaction between the polar amidic carbonyl group of T2EHDGA and CMPO with the cation of the ionic liquid. Since T2EHDGA contains a couple of amidic carbonyl groups and relatively more polar as compared to CMPO, the interaction of $[N_{1444}]^+$ with T2EHDGA seems to be more as compared to CMPO. As a result the average aggregate size formed in T2EHDGA phase is more than CMPO phase. In addition, FWHM of the aggregate distribution is more for T2EHDGA as compared to CMPO. This again indicates the formation of aggregates of different sizes is more in T2EHDGA as compared to CMPO phase.

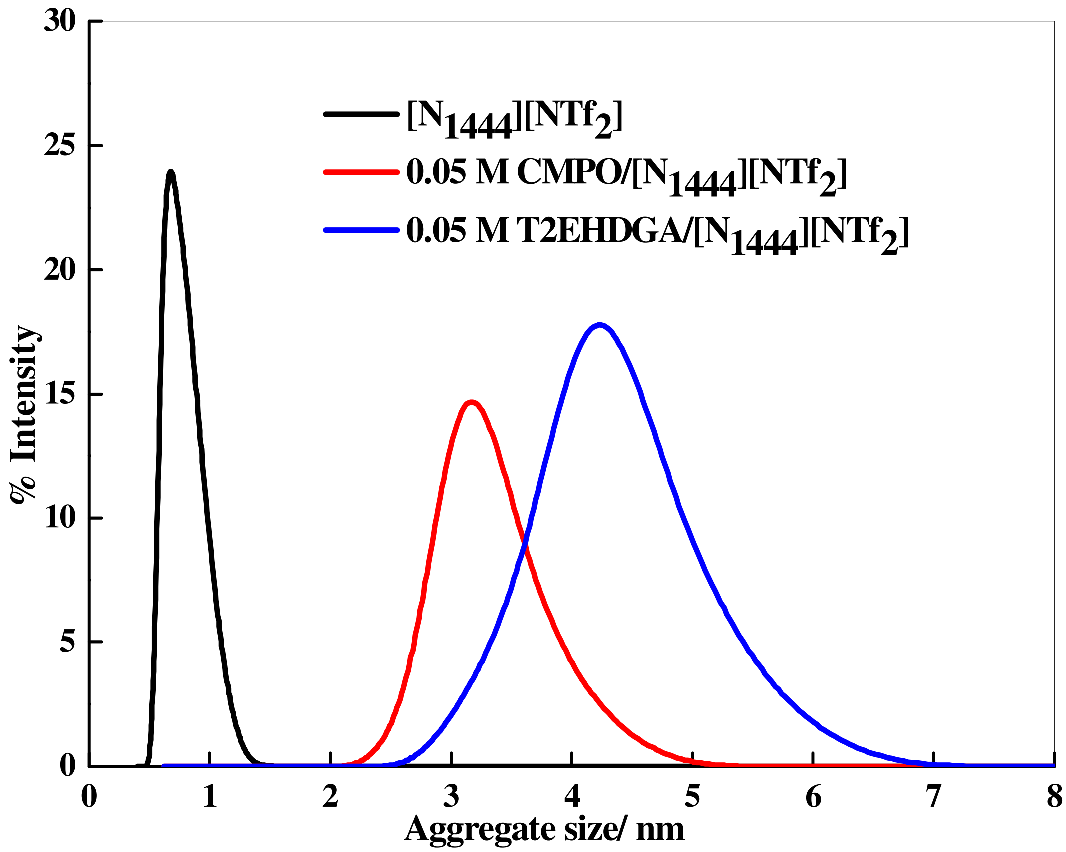

Fig. 4.5. Aggregate distribution in the ionic liquid phase before extraction. Ionic liquid phase: [N_{1444}][NTf_2] alone or 0.05 M T2EHDGA (or CMPO)/[N_{1444}][NTf_2]; Temperature = 298 K.

The variation in the aggregation behavior of 0.05 M T2EHDGA (or CMPO) in [N_{1444}][NTf_2] was recorded after contacting the ionic liquid phase with nitric acid and the results are displayed in the Fig. 4.6. The concentration of nitric acid was varied from 1 to 5 M in aqueous phase and the concentration of nitric acid extracted into ionic liquid phase was discussed in section 4.2.1. It can be seen from Fig. 4.6. that the aggregate size and their distribution in ionic liquid phase increases with increase in the concentration of nitric acid in aqueous phase. This could be due to the extraction of nitric acid, that protonates the T2EHDGA and CMPO molecules in ionic liquid. The Protonation of T2EHDGA or CMPO in ionic liquid phase makes the molecule more polar and facilitates the aggregation of protonated species in ionic liquid phase, as discussed elsewhere [26-28]. The reports on the aggregation behavior of diglycolamides in *n*-dodecane medium also show a similar feature that the aggregate size increases upon protonation and extraction of metal ions in organic phase [28]. Since the increase in the concentration of nitric acid in aqueous phase increases the extraction of nitric acid into ionic liquid phase and facilitate aggregation, the aggregate size and their distribution in ionic liquid phase increased with increase in the concentration of nitric acid in aqueous phase as shown in Fig. 4.6A and 4.6B for T2EHDGA and CMPO phases respectively. It should be noted that due to high ionic nature and good solvating ability of the ionic liquid phase, the undesirable third phase formation was not observed even after equilibrating the ionic liquid phase, T2EHDGA/$[N_{1444}][NTF_2]$ or CMPO/$[N_{1444}][NTF_2]$ with concentrated nitric acid. In contrast to this, the third phase formation was reported in a conventional *n*-dodecane phase, when 0.2 M T2EHDGA/*n*-DD was contacted with 4 M nitric acid [15]. Similarly, 0.2 M CMPO/*n*-DD forms third phase formation upon equilibration with 0.5 M nitric acid [29]. Therefore, the study showed that the employment of ionic liquid diluent in place of the conventional diluent *n*-dodecane can prevent the undesirable third phase formation.

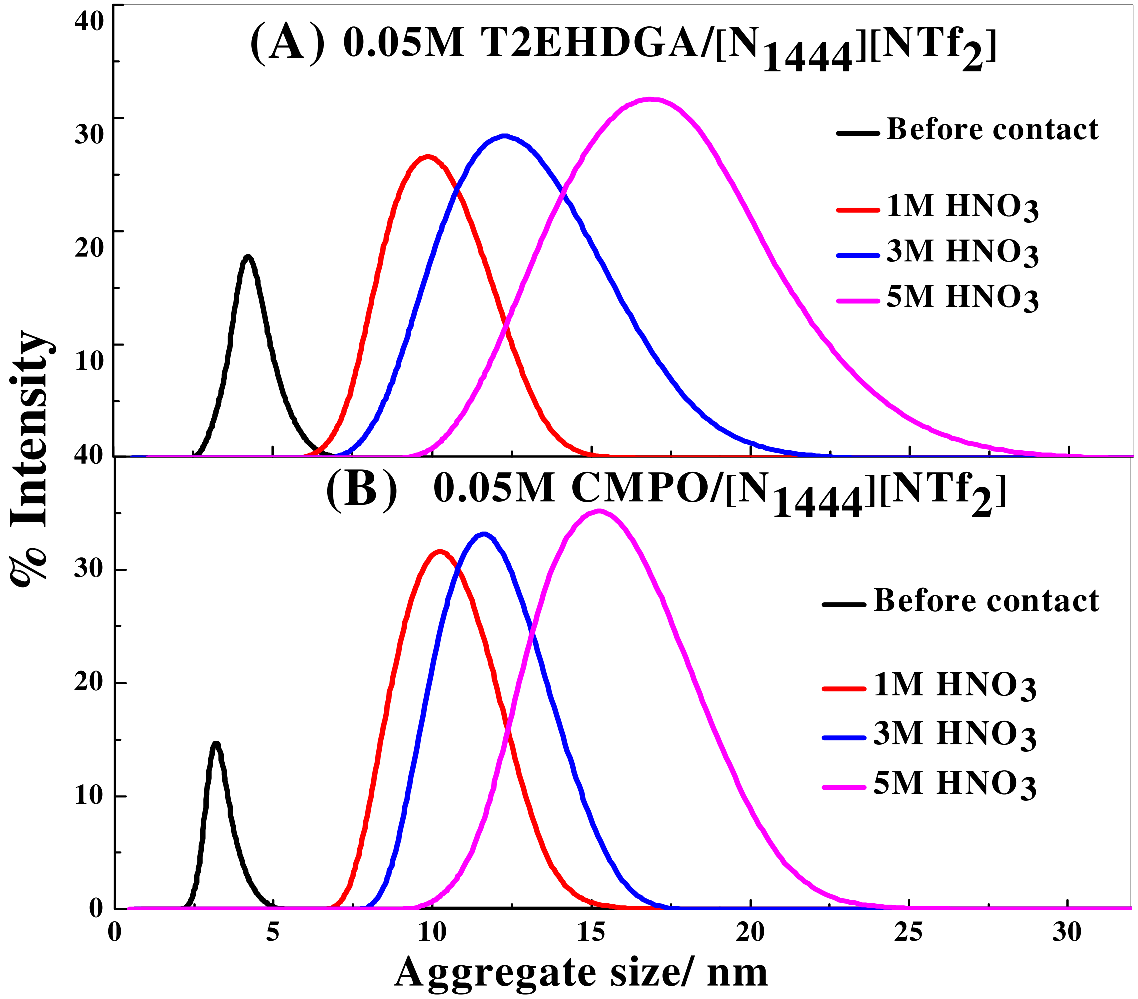

Fig. 4.6. Aggregate distribution in the ionic liquid phase recorded after contacting the ionic liquid phase with nitric acid. Ionic liquid phase: 0.05 M T2EHDGA (or CMPO)/[N_{1444}][NTf_2]; Aqueous phase: 0 -5 M HNO_3; Temperature = 298 K; Phase volume ratio = 1.

It would be interesting to compare the aggregate formation behavior observed in the present study with those reported in literature for the conventional diluent (*n*-DD) []. The literature survey reveals that few reports on the aggregation behavior of CMPO in *n*-DD are available, whereas the aggregation behavior of T2EHDGA was reported in 0.2 M T2EHDGA/*n*-

DD [26,28]. However, in the present study, we employed a solution of 0.05 M T2EHDGA/[N_{1444}][NTf_2] owing to the higher distribution ratio of Eu(III) (>100) achieved in ionic liquid phase as compared to *n*-DD under similar conditions [15]. Nevertheless, it is desirable to compare the aggregation behavior of the organic phase observed in 0.05 M T2EHDGA/[N_{1444}][NTf_2] with those reported in 0.2 M T2EHDGA/*n*-DD. T2EHDGA undergoes self-aggregation in *n*-DD medium with the average self aggregate size of 2 nm for 0.2 M T2EHDGA/*n*-DD [26] solution. However, the self-aggregation behavior of T2EHDGA (or CMPO) in [N_{1444}][NTf_2] could not be determined, since [N_{1444}][NTf_2] itself undergoes self-aggreagation (unlike n-dodecane) as discussed above. The aggregate size observed for 0.05 M T2EHDGA/ [N_{1444}][NTf_2] was 4.2 nm (Fig. 4.6). It should be noted that the average aggregate size observed for 0.05M T2EHDGA/[N_{1444}][NTf_2] was more (4.2 nm) than that observed for 0.2M T2EHDGA/*n*-DD (2 nm) [26], even though the concentration of T2EHDGA employed was less in ionic liquid phase.

The average aggregate size reported for the nitric acid extracted 0.2 M T2EHDGA/*n*-DD phase, increased with increase in the concentration of nitric acid in aqueous phase. It was reported that the aggregate size increased from 3.1 nm to 18 nm when 0.2M T2EHDGA/*n*-DD was contacted with 1 M and 3 M nitric acid respectively [26,28], whereas in 0.05 M T2EHDGA/[N_{1444}][NTf_2], the average aggregate size increases from 10 nm to 17 nm with the increase of nitric acid from 1 M to 3 M as shown in Fig 4.6. Beyond 3 M nitric acid, when 0.2 M T2EHDGA/*n*-DD was contacted with 4 M nitric acid, third phase formation in organic phase (splitting of organic phase) was observed. This is an undesirable event during the course of solvent extraction and it occurs essentially due to the poor solubility of the polar aggregates in *n*-DD phase. This indicates that there is a critical size exists for the aggregates to dissolve in *n*-

dodecane phase and above that critical size the organic phase undergoes splitting. The critical size for the aggregate size was determined to be 28 nm in case of 0.2 M T2EHDGA/*n*-DD [26]. In contrast to this, there was no third phase formation observed in case of 0.05 M T2EHDGA/[N_{1444}][NTf_2] and the third phase was not observed even after equilibrating the ionic liquid phase with concentrated nitric acid. This shows that the ionic liquid stabilizes the aggregates formed in organic phase irrespective of the aggregate size due to the polar nature of ionic liquid as compared to the non polar nature of *n*-DD.

4.2.4 Aggregation behavior in Eu(III) extracted phase

The variation in the distribution ratio of Eu(III) in a solution of 0.05M T2EHDGA (or CMPO)/[N_{1444}][NTf_2] at different initial concentration of Eu(III) in 3M nitric acid is shown in Table. 4.2. It can be seen that the extraction of Eu(III) in T2EHDGA and CMPO phase increases with increase in the concentration initial concentration of Eu(III) in aqueous phase. The amount of Eu(III) extracted into T2EHDGA phase is more than that observed in CMPO phase at a specific concentration of Eu(III) in aqueous phase. Fig. 4.7. shows the variation in the aggregation size of 0.05M T2EHDGA (or CMPO)/[N_{1444}][NTf_2] recorded, after containing the ionic liquid phase with Eu(III) nitrate solution in 3M nitric acid. It can be seen that the average aggregate size increases and their distribution in ionic liquid phase increases with increase in the amount of Eu(III) loading in aqueous phase. Increasing the concentration of Eu(III) in aqueous phase increases the extraction of Eu(III) as shown in Table. 4.2. The extraction of Eu(III) occurs through the co-ordination of T2EHDGA and CMPO molecules with Eu(III). The co-ordination of Eu(III) with T2EHDGA or CMPO increases the polarity of the metal-solvate complex and facilitates the aggregation of these metal-solvates in ionic liquid phase. The mechanistic sequence of changes that occur during the course of solvent extraction of nitric acid and metal ion is described elsewhere [11, 25]. Therefore, the average aggregate size and its distribution in ionic liquid phase increases with increase in the extraction of Eu(III) in ionic liquid phase as shown in Fig. 4.7. The average aggregate size increases from 12.8 nm to 25.2 nm and from 13.5 nm to 35 nm with increase in Eu(III) concentration from 1 g.L^{-1} to 10 g.L^{-1} in the aqueous phase in case of 0.05M T2EHDGA/[N$_{1444}$][NTf$_2$] and 0.05M CMPO/[N$_{1444}$][NTf$_2$] respectively. It should be noted that there was no third phase formation in both solutions.

Table. 4.2. Extraction of Eu(III) into the ionic liquid phase as a function of Eu(III) concentration in the initial solution. Ionic liquid phase: 0.05 M CMPO (or 0.05M T2EHDGA/[N$_{1444}$][NTf$_2$]); Aqueous phase: 3 M HNO$_3$ + (1-10) g.L^{-1} Eu(III); Equilibration time = 1 hour; Temperature = 298K; Phase volume ratio = 1.

[Eu(III)]$_{ini}$ (g.L^{-1})	[Eu(III)]$_{eq.,IL}$ (g.L^{-1})	[Eu(III)]$_{eq.,IL}$ (g.L^{-1})
	0.05 M CMPO/ [N$_{1444}$][NTf$_2$]	0.05 M T2EHDGA/ [N$_{1444}$][NTf$_2$]
1	0.8	0.99
3	1.06	2.14
5	1.16	2.16
10	1.2	2.2

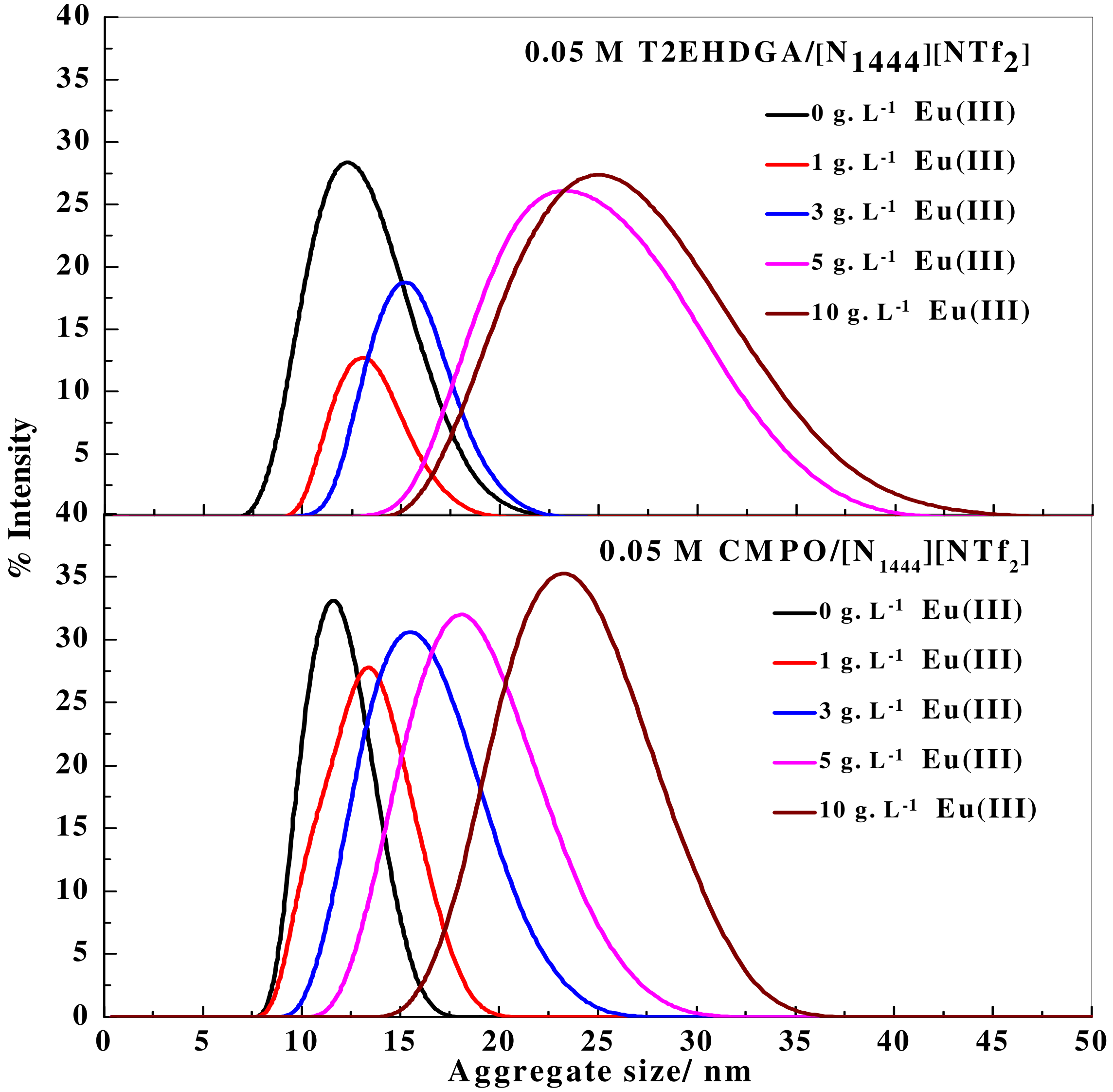

Fig. 4.7. Aggregate distribution in organic phase recorded after contacting the organic phase with a solution of Eu(III) in 3 M nitric acid. Ionic liquid phase: 0.05 M T2EHDGA (or CMPO)/[N_{1444}][NTf_2]; Aqueous phase: 3 M HNO_3 + 1-10 g.L^{-1} Eu(III) ; Temperature = 298 K; Phase volume ratio = 1.

4.2.5. Extraction Stoichiometry

The extraction of europium in T2EHDGA or CMPO can be represented by equation 4.1. The subscripts “aq” and “IL” denote the aqueous and ionic liquid phases respectively. L is the ligand namely, T2EHDGA or CMPO employed and “x” is the number of ligand molecules involved in the extraction of europium.

$$Eu^{3+}{}_{aq} + 3NO_3^-{}_{aq} + x\,L_{IL} \Leftrightarrow Eu\ (NO_3)_3\,(L)_{x\ \ IL} \tag{4.1}$$

The equilibrium constant for the above reaction can be represented in equation 4.1.

$$\mathrm{K_{ex}} = \frac{[\mathrm{Eu(NO_3)_3(L)x}]_{\mathrm{IL}}}{[\mathrm{Eu^{3+}}]_{\mathrm{aq}}[\mathrm{NO_3}]^3_{\mathrm{aq}}\,[\mathrm{L}]^{\mathrm{x}}_{\mathrm{IL}}} \tag{4.2}$$

Upon rearranging equation 4.1 results in equation 4.2

$$\log D_{Eu(III)} = \log K_{ex} + 3\log[NO_3^-]_{aq} + x\ \log[L]_{IL} \tag{4.3}$$

To determine the number of molecules of ligand coordinated to Eu(III) in the ionic liquid phase, the effect of ligand concentration on the extraction of europium (III) in the ionic liquid phase was studied. The slope obtained from the plot of log $D_{Eu(III)}$ against log [ligand] gives the number of molecules of ligand coordinated to europium in the ionic liquid phase. The plot of Fig. 4.8. displays the variation in the distribution ratio of Eu(III) as a function of ligand concentration in the ionic liquid phase at constant nitric acid concentration in the aqueous phase. It can be seen that the distribution ratio of Eu(III) increases with increase in the concentration of ligand in the ionic liquid phase. A linear regression of the extraction data resulted in a straight line with a slope of 2.8 and 2.3 for T2EHDGA and CMPO respectively. This shows that around ~ 3 molecules of T2EHDGA and ~ 2 molecules of CMPO are co-ordinated to Eu(III) in ionic liquid phase. Since $[N_{1444}][NTf_2]$ does not participate in the extraction of Eu(III) at 3 M nitric acid, as shown in Fig. 4.1. Therefore observed extraction could be attributed essentially to the metal-ligand cordination mechanism, in which three molecules of T2EHDGA and two molecules of CMPO are co-ordinated to Eu(III).

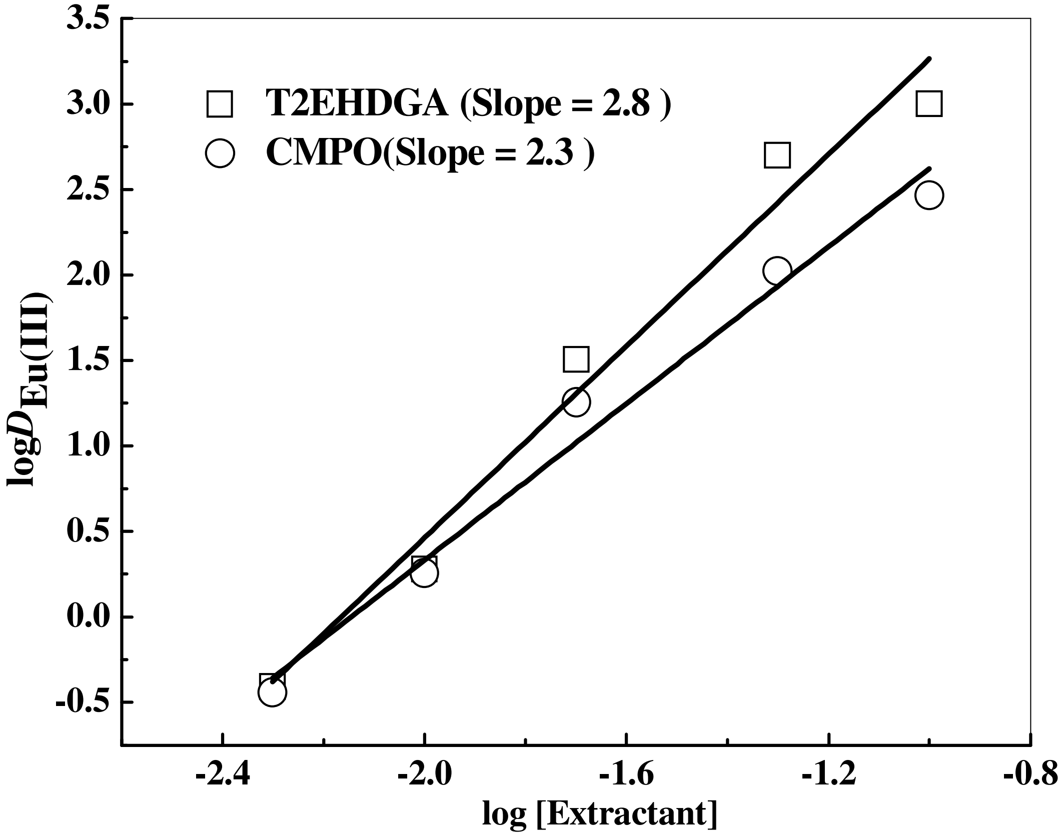

Fig. 4.8. Plot of $\log D_{Eu}$ against log [extractant]. Ionic liquid phase: 0.005 – 0.1 M T2EHDGA (or CMPO)/$[N_{1444}][NTf_2]$; Aqueous phase: 3 M HNO_3 spiked with $^{(152+154)}$Eu tracer; Temperature = 298 K; Equilibration time = 1 hour; Phase volume ratio = 1.

4.2.6. Luminescence Spectra

The luminescence spectra of Eu(III) in T2EHDGA (or CMPO)/[N_{1444}][NTf_2] phase was recorded to understand the co-ordination environment of Eu(III) in the extracted ionic liquid phase [30]. The Eu(III) in the extracted phase was excited by Xe source and thethe emission spectrum of Eu(III) present in the extracted ionic liquid phase was shown in Fig. 4.9. The emission spectra of the extracted phase was compared with the emission spectra of Eu(III) in aqueous phase at two different nitric acid concentrations namely, 1 M and 3 M. The emission band at 615 nm ($^5D_0 \rightarrow {}^7F_2$) is due to electric dipole transition and is extremely sensitive to the ligand environment around Eu(III) and the corresponding magnetic dipole transition occurs at 592 nm ($^5D_0 \rightarrow {}^7F_1$) which is independent of ligand environment. The intensity of peak corresponding to electric dipole (the peak at 615 nm) is always less intense than that corresponding to the magnetic dipole (the peak at 592 nm) in the presence of water wherein the Eu(III) ion exists in the form of $[Eu(H_2O)_9]^{3+}$ complex [30]. Alok *et al.* studied the Eu(III) luminescence in ionic liquid medium, and reported that the Eu(III) luminescence intensity of peak at 615 nm is lower than 592 nm intensity at 0.1 M nitric acid [30]. Under such condition the number of water molecules associated with Eu(III) in the co-ordination sphere was determined to be ~8.5. However, the intensity of 615 nm peak increased with increase in the concentration of nitric acid from 1-3 M as compared to the increase observed at 592 nm. This can be attributed to the formation of $[Eu(NO_3)_n(H_2O)_{9-n}]^{3-n}$ complex leading to the expulsion of water molecules from $[Eu(H_2O)_9]^{3+}$.

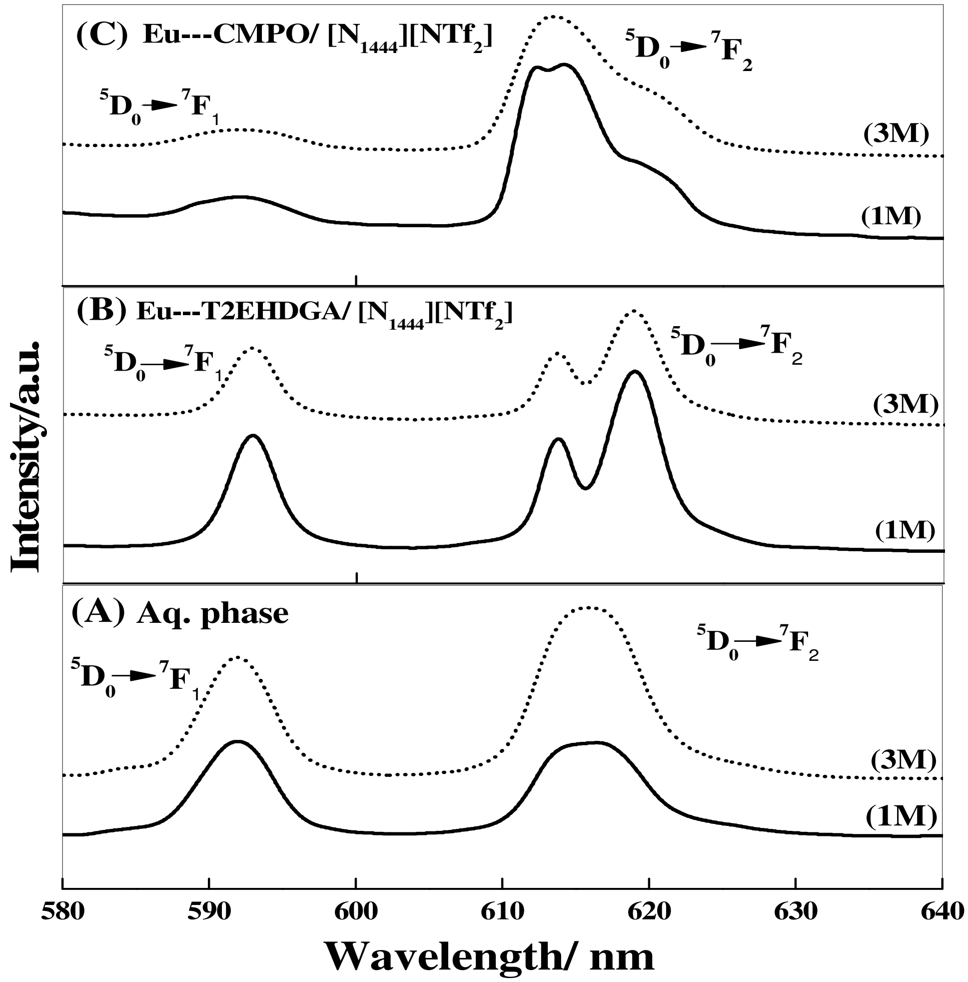

Fig. 4.9. Emission spectra of Eu(III) in the aqueous and ionic liquid phases. Ionic liquid phase: 0.05 M T2EHDGA (or CMPO)/[N_{1444}][NTf_2]; Aqueous phase: 10^{-3} M Eu(III) in 3 M HNO_3; Temperature = 298 K; Equilibration time = 1 hour; Phase volume ratio = 1.

The asymmetry factor (I_{615}/I_{592}), which is a measure of the degree of decrease in the symmetry around Eu(III) ion was determined to be 0.9 and 1.2 at 1 M and 3 M HNO_3 are shown in Table. 4.3. The increase in the magnitude of asymmetric factor indicates the substitution of H_2O molecules by nitrate ion in the coordination sphere of $[Eu(H_2O)_9]^{3+}$ leading to the decrease in the symmetry environment of the resultant complex. Fig. 4.9B and 4.9C shows the emission spectrum of Eu(III) present in ionic liquid phase. The spectrum was recorded after the extraction of Eu(III) from 1 M or 3 M nitric acid medium by a solution of 0.05 M T2EHDGA (or CMPO) in $[N_{1444}][NTf_2]$. It can be seen that the emission intensity at 615 nm is more intense than the intensity observed at 592 nm. This is apparently due to decrease in symmetry of $[Eu(H_2O)_9]^{3+}$ complex caused by the coordination of NO_3^- ion, T2EHDGA or CMPO molecules in place of water molecules coordination sphere of Eu(III) ion in ionic liquid phase.

Table. 4.3. Peak intensity ratio, decay time, and number of inner sphere water molecules associated in the Eu(III) complex aqueous and ionic liquid phases.

Eu(III) phase	I_{615}/I_{592}		τ (ms)		N_{H2O}	
	1 M HNO_3	3 M HNO_3	1 M HNO_3	3 M HNO_3	1 M HNO_3	3 M HNO_3
Aqueous	0.9	1.2	120	124	8	7.5
T2EHDGA/ $[N_{1444}][NTf_2]$	1.42	1.24	1516	1496	0.05	0.1
CMPO/ $[N_{1444}][NTf_2]$	2.11	1.62	1191	1109	0.18	0.2

The decay profile of luminescence at 615 nm was monitored and the results are displayed in the Fig. 4.10. The data were fitted using a first order exponential decay and the life time of luminiscene (τ) obtained from the fitting are shown in Table 4.3. It can be seen that the life time (τ) of Eu(III) increases by an order upon extraction of Eu(III) into ionic liquid phase as compared to that observed in 1 M and 3 M HNO_3. The presence of water molecules in the co-ordination sphere of Eu(III) lowers the life time of luminescence [31]. The increase in luminescence life time observed upon extraction into ionic liquid phase could be attributed to the co-ordination of the T2EHDGA or CMPO with Eu(III) leading to the expulsion of water molecules from the coordination sphere of Eu(III) in ionic liquid phase. From the life time measurements, the number of water molecules (N_{H2O}) coordinated to Eu(III) was determined [30,31] and the values are displayed in Table. 4.3. It can be seen from Table. 4.3. that the number of water molecules coordinated to Eu(III) at 1 M and 3 M nitric acid is about 8 and 7.5 respectively. At 0.1 M HNO_3, the number of water molecules coordinated to Eu(III) was reported to be 9. This shows the increasing the concentration of HNO_3 decreases the water molecules coordinated to Eu(III) which could be due to the formation of $[Eu(NO_3)_n(H_2O)_{9-n}]^{3-n}$ in the aqueous phase. Extraction of Eu(III) from aqueous phase results in the coordination in the coordination of Eu(III) by T2EHDGA and CMPO leading to the expulsion of water molecules from the coordination sphere. Therefore, the number of water molecules coordinated to Eu(III) decrease remarkably to ~0.1 upon extraction in both systems.

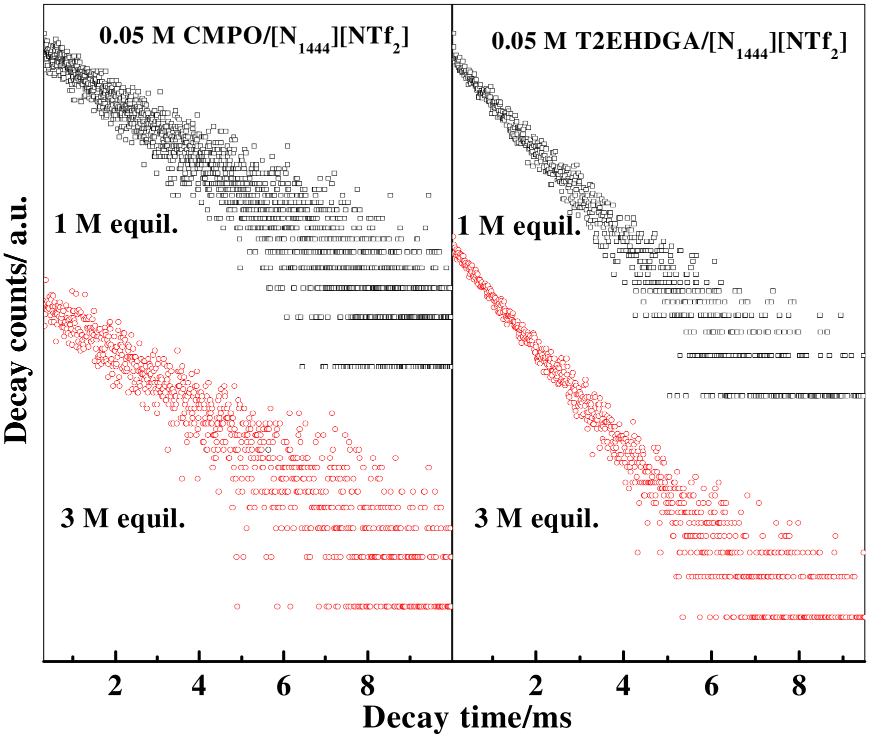

Fig. 4.10. Decay profile of Eu(III) in ionic liquid phase. Ionic liquid phase: 0.05 M T2EHDGA (or CMPO)/$[N_{1444}][NTf_2]$; Aqueous phase: 10^{-3} M Eu(III) in 3 M HNO_3; Temperature = 298 K; Equilibration time = 1 hour; Phase volume ratio = 1.

4.2.7. Effect of radiation dose

When ionic liquid is proposed for the separation of trivalent actinides and lanthanides from nuclear waste, it is necessary to study the effect of gamma radiation on the extraction behavior of Eu(III). In this context, the ionic liquid phase, 0.05 M T2EHDGA/[N_{1444}][NTf_2] and 0.05M CMPO/[N_{1444}][NTf_2] were irradiated up to 500 kGy absorbed dose and the distribution ratio of Eu(III) in the irradiated ionic liquid phase was determined. The extraction of Eu(III) was carried out from 3 M HNO_3. The results are displayed in Fig. 4.10. It is quite interesting to observe that the distribution ratio of Eu(III) in 0.05 M T2EHDGA/[N_{1444}][NTf_2] is not changing with increase of absorbed dose. On the contrary, the distribution ratio of Eu(III) in 0.05 M CMPO/[N_{1444}][NTf_2] decreases with increase of absorbed dose. In general, the irradiation of organic molecules causes degradation of organics present in ionic liquid phase. The degraded solvent phase in some cases extract the metal ion much more than the undegraded solvent phase and in other cases the degraded solvent extract less than the undegraded solvent phase [32,33]. Usually when the organic phase is composed of diglycolamide or amide, the irradiation of organic phase results in the formation of innocuous degradation products that are washable (soluble in aqueous phase) from organic phase [15]. In view of this, the distribution ratio of Eu(III) decrease with increase of absorbed dose. However, the insignificant variation in the distribution ratio of Eu(III) with increase of absorbed dose observed in present study indicates that the degradation products of T2EHDGA formed in ionic liquid medium also extracts Eu(III) from aqueous phase. In addition, it also indicates that these degradation products do not seem to dissolve in aqueous phase [15]. The literature reports suggest that one of the degradation product of diglycolamides named as *N,N*-dialkyl-2-hydroxyacetamide (R_2NCOCH_2OH) can also extract the trivalent actinides and lanthanides from nitric acid medium to a remarkable extent [34,35].

These degraded products are hydrophobic and dissolve easily in ionic liquid phase phase [34,35]. Therefore, the study shows that degradation products of T2EHDGA, i.e., *N,N*-bis(2-ethylhexyl)glycolamide (DEHHyA) in combination with T2EHDGA might be participating in the extraction of Eu(III) synergistically and thus variation in the distribution ratio of Eu(III) in ionic liquid phase with increase of absorbed dose is insignificant. In contrast to T2EHDGA degradation, the distribution ratio of Eu(III) in radiolytically degraded CMPO/[N_{1444}][NTf_2] decreases with increase of absorbed dose, as expected. This shows the degradation of CMPO in ionic liquid phase does not extract Eu(III) and the distribution ratio of Eu(III) decreases with increase of absorbed dose.

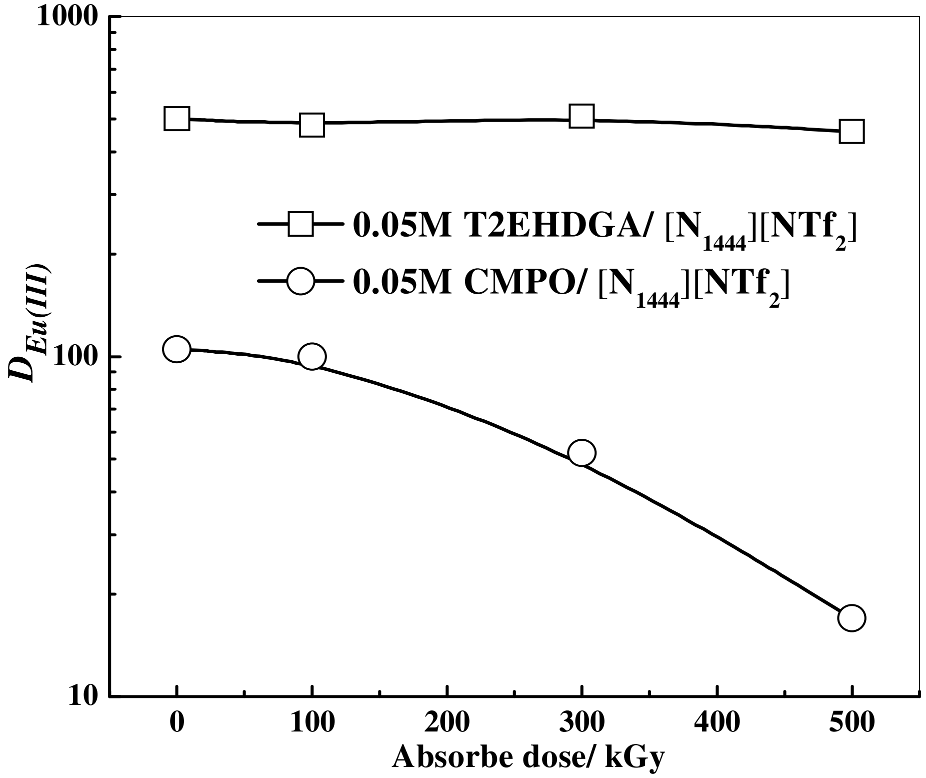

Fig. 4.11. Variation in the distribution ratio of Eu(III) as a function of absorbed dose. Ionic liquid phase: 0.05 M T2EHDGA (or CMPO)/[N_{1444}][NTf_2] irradiated to various dose levels; Aqueous phase: 3 M HNO_3 spiked with $^{(152+154)}$Eu tracer; Temperature = 298 K; Equilibration time = 1 hour; Phase volume ratio = 1.

4.3. Summary

The distribution ratio of Eu(III) decreased with increase in the concentration of nitric acid in both T2EHDGA and CMPO in $[N_{1444}][NTf_2]$. The extraction mechanism suggests that three molecules of T2EHDGA and two molecules of CMPO were involved in the complex formation with europium(III) in ionic liquid phase. The ionic liquid undergoes self-aggregation in organic phase and the average size of nitric acid or Eu(III) extracted aggregates formed in organic phase increased with increase in the concentration of nitric acid as well as Eu(III) in the aqueous phase. Luminescence spectroscopy study confirms the coordination of T2EHDGA and CMPO in the first coordination sphere of europium (III). The radiolytic stability of ionic liquid phase (T2EHDGA (or CMPO)/ $[N_{1444}][NTf_2]$)) was stable up to 500 kGy absorbed dose and there was marginal change in the distribution ratio of Eu(III) in ionic liquid phase with absorbed dose in both the cases.

PART B: Selective separation of zirconium(IV) from uranium(VI) using dioxoamide ligand present in ammonium ionic liquid medium: An application towards spent metallic fuel reprocessing

4.4. Introduction

The metallic alloy composed of U-Zr and U-Pu-Zr was as a fuel for fast reactors [36,37] to achieve high breeding ratio in a short span of time. About 6 to 10 % of zirconium has been added to these metallic actinides (U & Pu) to increase the melting temperature of the resultant U-Zr alloy and U-Pu-Zr alloy [36,37]. The addition of zirconium to actinides also increases thermal-mechanical stability of alloy. Reprocessing of the spent metallic fuel by an aqueous route results in the generation of a dissolver solution in nitric acid medium containing significant amount of zirconium along with the actinides such as uranium, plutonium, neptunium and americium and several fission products formed upon irradiation [37]. About 60 % of the zirconium present in the fuel dissolves in nitric acid medium, while the rest zirconium remains as an insoluble residue along with some fission products such as molybdenum, during the dissolution of spent metallic nuclear fuel [38].

The chemistry of zirconium in the dissolver solution is very complex. Essentially it exists as the tetravalent zirconium(IV) ion in nitric acid medium and depending upon the acidity, concentration of zirconium, temperature, and ageing, the zirconium(IV) undergoes polymerization reaction in aqueous nitric acid medium [39,40]. At nitric acid concentrations above 4M, the Zr(IV) partially exists in the form of $[Zr(OH)_4(H_2O)_6]^{8+}$ and at lower nitric acid concentration (< 4M), Zr(IV) exists in the form of an octamer [39,40]. The concentration of Zr(IV) in the dissolver solution generated from metallic fuel reprocessing is estimated to be ~0.06 M (~ 5.5 g/L), which is about 5 to 10 times higher than the concentration of Zr(IV) in dissolver solution generated from the reprocessing of spent oxide fuels [38]. The presence of zirconium in the dissolver solution poses several challenges during the separation of uranium and plutonium by PUREX process, trivalent actinide-lanthanide group separation and actinide-lanthanide mutual separation [41,42]. Therefore, it is desirable to separate zirconium from nitric acid medium prior to the PUREX process. The literature reports of diamides are promising ligands for selective separation of tetravalent metal ions from aqueous medium [43,44]. The advantages of using benzodioxodiamides (BenzoDODA) were discussed elsewhere [43,44]. The ligand employed for the extraction of zirconium and uranium was an amide molecule, and the coordinating site was amidic carbonyl moiety (>C=O), which was a hard base donor. Therefore, the amide easily coordinates with hard acid tetravalent zirconium (HSAB principle). In addition the ionic potential (charge to radius ratio) of zirconium was higher than uranium. Therefore, the extraction behavior of Zr(IV) from nitric acid medium was studied in a solution of $[N_{1444}][NTf_2]$ and 2-ethylhexyl benzodioxodiamide (BD) and the decyl-derivative of benzodioxodiamide (BDD) in $[N_{1444}][NTf_2]$ and the results obtained from these studies are reported in this chapter.

Experimental details for the part B of chapter 4 are presented in the section 2.5.3 of the chapter 2. The synthesis of extractant and ionic liquid employed in the present study are discussed in section 2.6.8 and 2.6.4 of chapter 2 respectively.

Table. 4.4. Structure of molecular extractant and RTIL used in part B of chapter 4.

Name	Structure
Extractant	
BenzoDODA R= 2-Ethylhexyl corresponds BD R= Decyl corresponds BDD	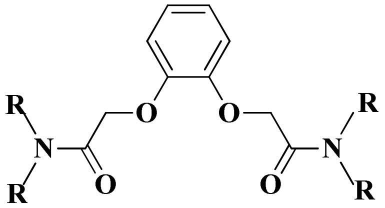
Ionic liquid	
Methyltributylammonium bis(trifluoromethylsulfonyl)imide $[N_{1444}][NTf_2]$ (R: C_4H_9)	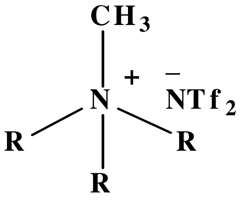

4.5. Results and discussions

4.5.1. Effect of nitric acid concentration

The extraction of Zr(IV) was studied as a function of nitric acid concentration in aqueous phase and the results are shown in Fig. 4.12. It can be seen from Fig. 4.12. that the extraction of Zr(IV) in $[N_{1444}][NTf_2]$ is negligible, which is due to the absence of functional group in $[N_{1444}][NTf_2]$. However the addition of small amount of BD to $[N_{1444}][NTf_2]$ increases the distribution ratio of Zr(IV) to a significant extent. Therefore, the distribution ratio of Zr(IV) in 0.05 M BD/$[N_{1444}][NTf_2]$ increases from 1 at 0.1 M nitric acid to the value of about 100 at 5 M nitric acid concentration. Comparison of the distribution ratio of Zr(IV) obtained in 0.05 M BD/ $[N_{1444}][NTf_2]$ with those obtained in 0.05 M BD/*n*-DD , shown in the same figure, indicates that the presence of ionic liquid in conjunction with BD increases the distribution ratio of zirconium to a significant extent. The $D_{Zr(IV)}$ in 0.05 M BD/*n*-DD increases from 0.2 to the value of 10 with the increase in the concentration of nitric acid from 0.1 to 5 M. In contrast to the imidazolium cation, [46] the use of hydrophobic $[N_{1444}]^+$ ion increases the $D_{Zr(IV)}$ with increase in the concentration of nitric acid, similar to those observed in *n*-dodecane phase [44]. It is quiet likely that the mechanism of Zr(IV) extraction in 0.05 M BD/$[N_{1444}][NTf_2]$ could be similar to the solvation-type mechanism reported for the extraction of Zr(IV) in *n*-dodecane medium containing neutral extractants like BD. However, the presence of ionic liquid $[N_{1444}][NTf_2]$ provides higher distribution ratio of Zr(IV) in ionic liquid medium than those observed in *n*-dodecane.

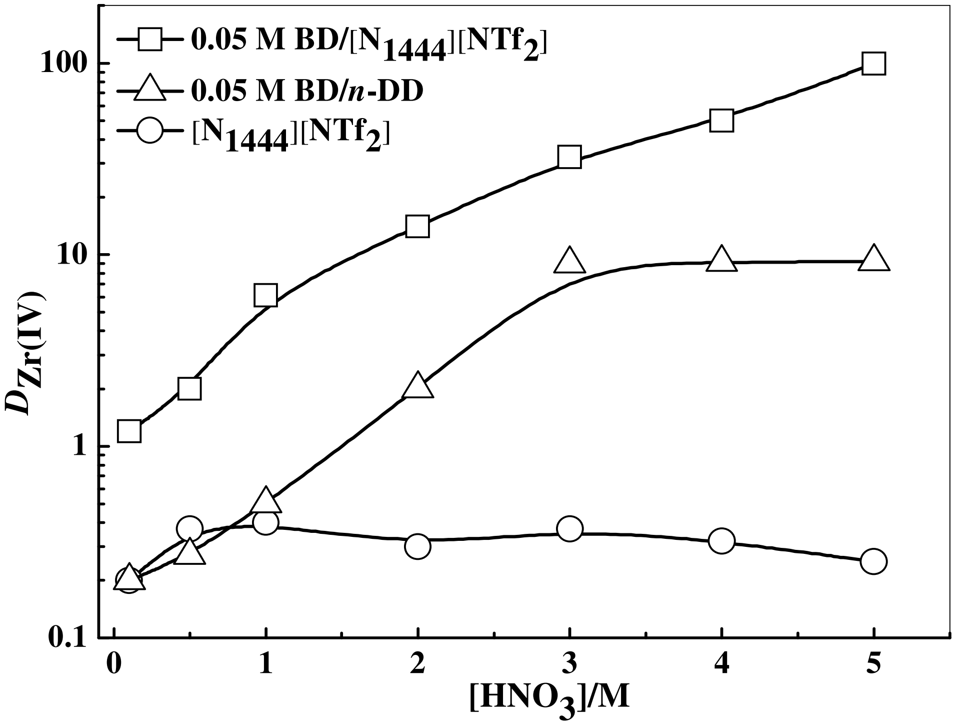

Fig. 4.12. Variation in the distribution ratio of Zr(IV) as a function of the nitric acid concentration in the aqueous phase. Ionic liquid phase: 0.05 M BD/ $[N_{1444}][NTf_2]$ (or *n*-DD) or $[N_{1444}][NTf_2]$ alone; Aqueous phase: 0.1 M – 8.0 M $[HNO_3]$; [Zr(IV)] = 1 g/L; Temperature = 298 K; Equilibration time = 1 hour; Phase volume ratio = 1.

4.5.2. Extraction kinetics

The rate of extraction of zirconium(IV) from 3 M nitric acid medium was studied in a solution of 0.05 M BD/ $[N_{1444}][NTf_2]$ and the results on the variation in the distribution ratio of Zr(IV) as a function of duration of equilibration is shown in Fig. 4.13. It can be seen that the distribution ratio of Zr(IV) increase with increase in the duration of equilibration up to 60 minutes. Thereafter, the variation in the $D_{Zr(IV)}$ is negligible in the rest of the period. Therefore, it can be presumed that the equilibrium is established in 1 hour. However, all equilibration studies were carried for 2 hour to ensure the establishment of equilibrium in the experimental solution.

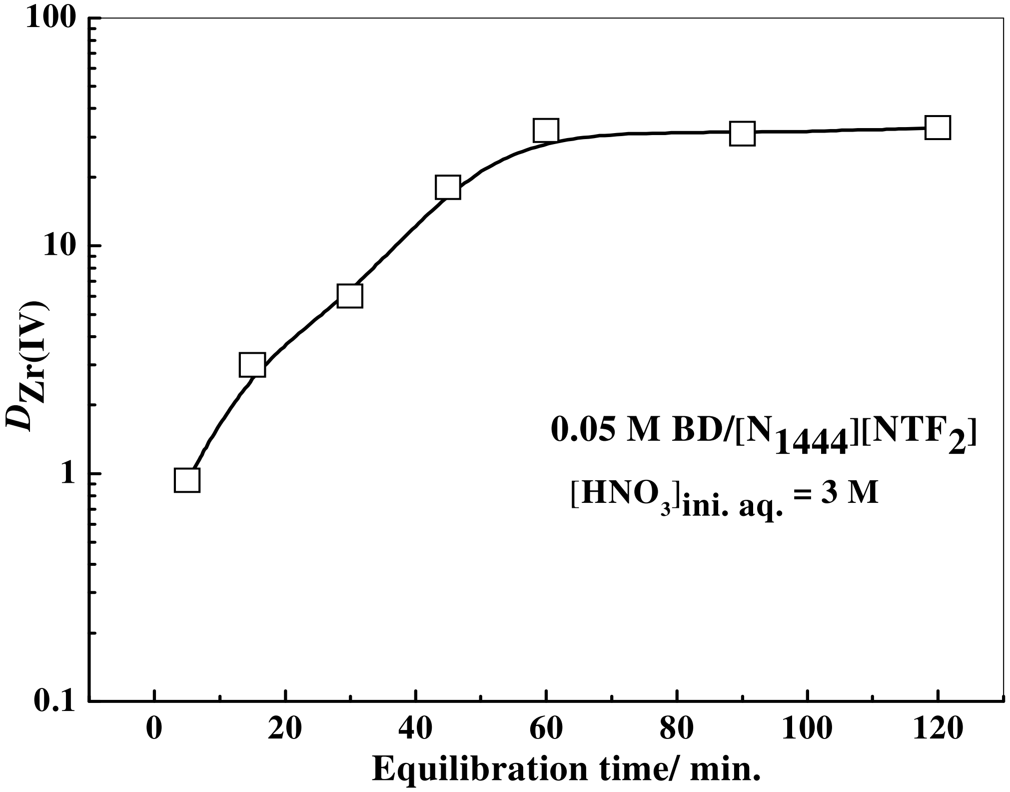

Fig. 4.13. Variation in the distribution ratio of Zr(IV) as a function of the Equilibration time. Ionic liquid phase: 0.05 M BD/ $[N_{1444}][NTf_2]$; Aqueous phase: 3.0 M $[HNO_3]$; [Zr(IV)] = 1 g/L; Temperature = 298 K; Equilibration time = 10-120 minutes; Phase volume ratio = 1.

4.5.3. Extraction stoichiometry

The extraction of zirconium in BD can be represented by equation 4.4. The subscripts "aq" and "IL" denote the aqueous and ionic liquid phases respectively and "x" is the number of BD molecules involved in the extraction of zirconium.

$$\mathrm{Zr^{4+}_{(aq)} + 4NO^{-}_{3(aq)} + x\ BD \Leftrightarrow Zr(NO_3)_4(BD)_{x\,(\mathit{IL})}} \tag{4.4}$$

The equilibrium constant for the above reaction can be represented in equation 4.5.

$$\mathrm{K} = \frac{\mathrm{[Zr(NO_3)_4(BD)x]_{IL}}}{\mathrm{[Zr^{4+}]_{aq}[NO_3]^4_{aq}\,[BD]^x_{IL}}} \tag{4.5}$$

Upon rearranging equation 4.5 results in equation 4.6

$$\log D_{Zr(IV)} = \log \mathrm{K} + 4\log[NO_3]_{aq} + x\ \log[BD]_{IL} \tag{4.6}$$

To determine the number of molecules of BD coordinated to Zr(IV) in the ionic liquid phase, the effect of BD concentration on the extraction of zirconium (IV) in the ionic liquid phase was studied. The slope obtained from the plot of log $D_{U(VI)}$ against log [BD] gives the number of molecules of BD coordinated to uranium in the ionic liquid phase. The plot of Figure 4.14 displays the variation in the distribution ratio of U(VI) as a function of BD concentration in the ionic liquid phase at constant nitric acid concentration in the aqueous phase. It can be seen that the distribution ratio of Zr(IV) increases with increase in the concentration of BD in the ionic liquid phase. Linear regression analysis of the extraction data results in a slope value 2.1. This shows that about two molecules of BD is involved in the extraction of Zr(IV) in the ionic liquid phase.

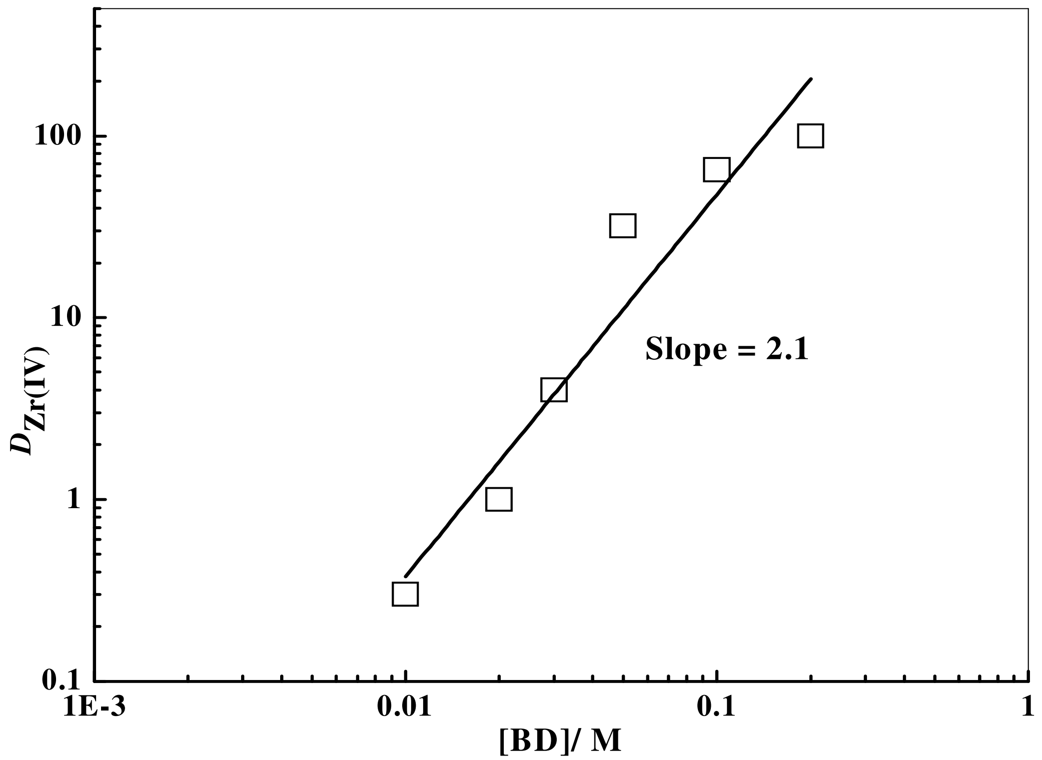

Fig. 4.14. Plot of log$D_{Zr(IV)}$ against log [extractant]. Ionic liquid phase: 0.01 M – 0.2 M BD/[N_{1444}][NTf_2]; Aqueous phase: 3 M [HNO_3] and [Zr(IV)]= 1 g/L; Temperature = 298 K; Equilibration time = 1 hour; Phase volume ratio = 1.

4.5.4. Extraction of Zr(IV) and U(VI)

Fig. 4.15. shows the variation in the distribution ratio of uranium(VI) in 0.05 M BD/ [N_{1444}][NTf_2] and the separation factor of zirconium over uranium as a function of nitric acid concentration in aqueous phase. The distribution ratio of uranium was compared with the distribution ratio of zirconium in the Fig. 4.15. It is interesting to note that the distribution ratio of uranium in 0.05 M BD/ [N_{1444}][NTf_2] is significantly small as compared to the $D_{Zr(IV)}$ values. The $D_{U(VI)}$ increases from 0.45 to 0.9 with increasing the nitric acid concentration from 0.1 M to 5 M. As a result, the separation factor achieved for zirconium over uranium varies from the value 2 to ~100 with increase in the concentration of nitric acid for 0.1 M to 5 M. The magnitude of

separation factor indicates separation of zirconium from uranium. Therefore, the solvent phase, i.e., BD/ $[N_{1444}][NTf_2]$ in ionic liquid can be regarded as a promising candidate for the separation of zirconium from metallic fuel dissolver solution.

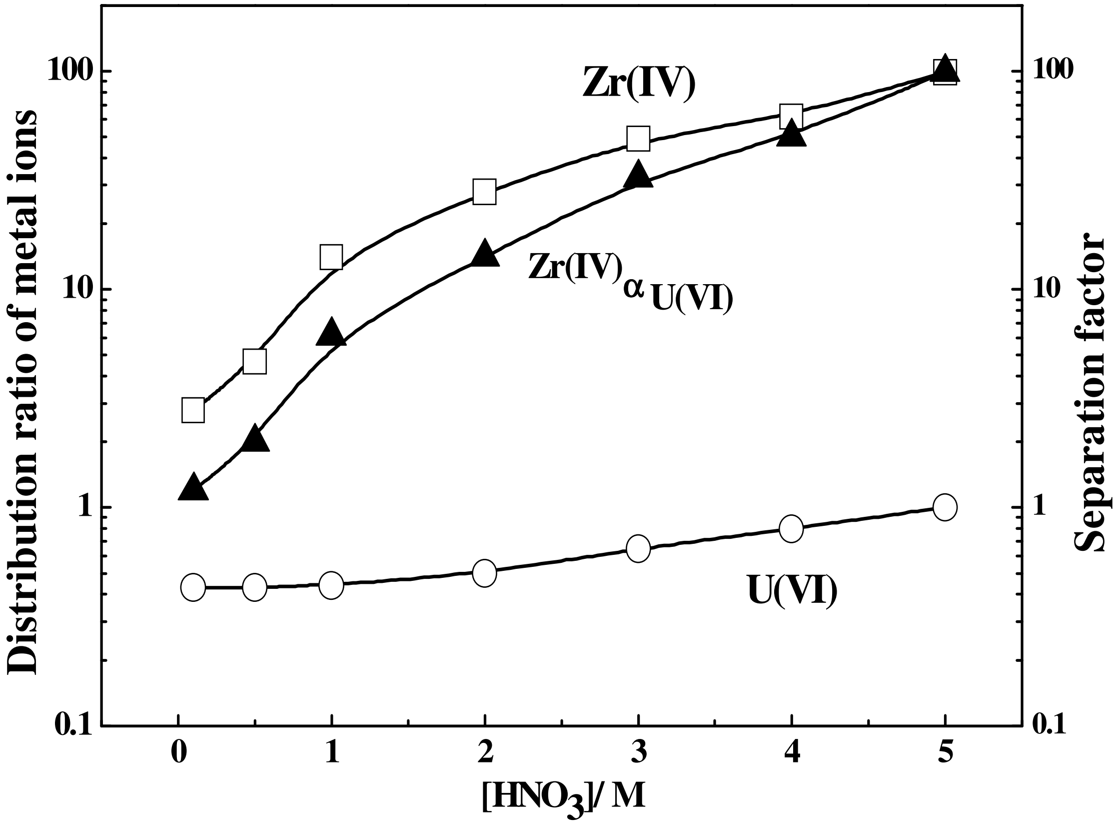

Fig. 4.15. Variation in the distribution ratio of Metal ions (Zr(IV) and U(VI)) as a function of the nitric acid concentration in the aqueous phase. Ionic liquid phase: 0.05 M BD/ $[N_{1444}][NTf_2]$; Aqueous phase: 0.1 M – 8.0 M $[HNO_3]$; [Zr(IV)] = 1 g/L; Temperature = 298 K; Equilibration time = 1 hour; Phase volume ratio = 1.

4.5.5. Effect of co-extraction of uranium(VI)

Since the dissolver solution is likely to contain significant amount of uranium along with Zr(IV), the variation in the distribution ratio of zirconium as a function of uranium concentration in 3M nitric acid was studied in a solution of 0.05 M BD/ $[N_{1444}][NTf_2]$. The amount of zirconium in aqueous phase was fixed at 1g/L and the amount of uranium was varied from 1 g/L to 16 g/L. It can be seen that the distribution ratio of zirconium decreases abruptly from 75 to the value of 2 with increase in the amount of uranium from 1 g/L to 3 g/L. Further increase in the amount of uranium upto 16 g/L does not vary the distribution ratio of zirconium to any significant extent. Fig. 4.16. also shows the percentage extraction of zirconium at different amounts of uranium in aqueous phase. More than 65 % of Zr(IV) is extracted into 0.05 M BD/ $[N_{1444}][NTf_2]$ phase at 16 g/L of uranium in aqueous phase.

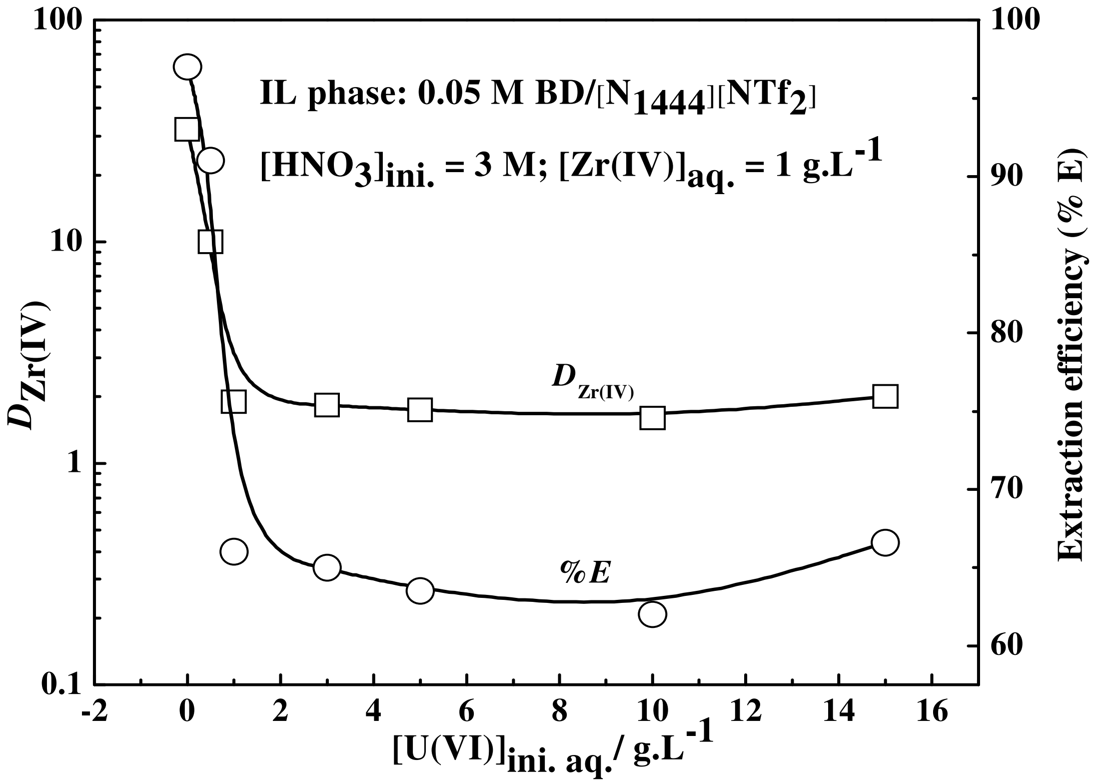

Fig. 4.16. Variation in the distribution ratio of Zr(IV) as a function of the Uranium metal ion concentration in the aqueous phase. Ionic liquid phase: 0.05 M BD/ $[N_{1444}][NTf_2]$; Aqueous phase: 1 g/L Zr(IV) + 0-15 g/L U(VI) in 3.0 M $[HNO_3]$; [Zr(IV)] = 1 g/L; Temperature = 298 K; Equilibration time = 1 hour; Phase volume ratio = 1.

4.5.6. Loading of Zr(IV) as a function of [HNO_3]

The extraction isotherm of Zr(IV) in 0.05 M BD/ [N_{1444}][NTf_2] is shown in Fig. 4.17. It can be seen that the loading of zirconium in ionic liquid phase increases with increase in the amount of zirconium present in aqueous phase. The saturation in the loading of zirconium occurs when the amount of zirconium in aqueous phase reaches about 16 g/L, at which the amount of zirconium loaded in 0.05 M BD/ [N_{1444}][NTf_2] is about 4 g/L, which corresponds to loading of 0.05 M Zr(IV) in ionic liquid phase. This indicates the formation of a 1:1 complex of Zr(IV) with BD in ionic liquid phase. However, the zirconium to BD stoichiometry of 1:2 was obtained when $D_{Zr(IV)}$ was plotted against the concentration of BD, as shown in Fig. 4.14. It should be noted that the linear relation yielding the stoichiometry 1:2 was obtained (Fig. 4.14.), when the amount of zirconium in aqueous phase was fixed at 1 g/L (0.01M) and the concentration of BD in ionic liquid phase was varied. In contrast to this, the zirconium extraction isotherm was obtained by varying the concentration of Zr(IV) in aqueous phase at a fixed concentration of BD (0.05M) in ionic liquid phase. Under such condition, it is quite likely that the stoichiometry of zirconium to BD could change to accommodate the loaded zirconium, which happens at higher amounts of Zr(IV) in aqueous phase. It should be noted that the 1:1 stoichiometry of zirconium to BD is obtained only when the amount of zirconium in aqueous phase exceeds the value of 16 g/L zirconium in aqueous phase. Therefore, the results indicate that the stoichiometry of Zr(IV) to BD can change depends upon the loading of Zr(IV) in ionic liquid phase.

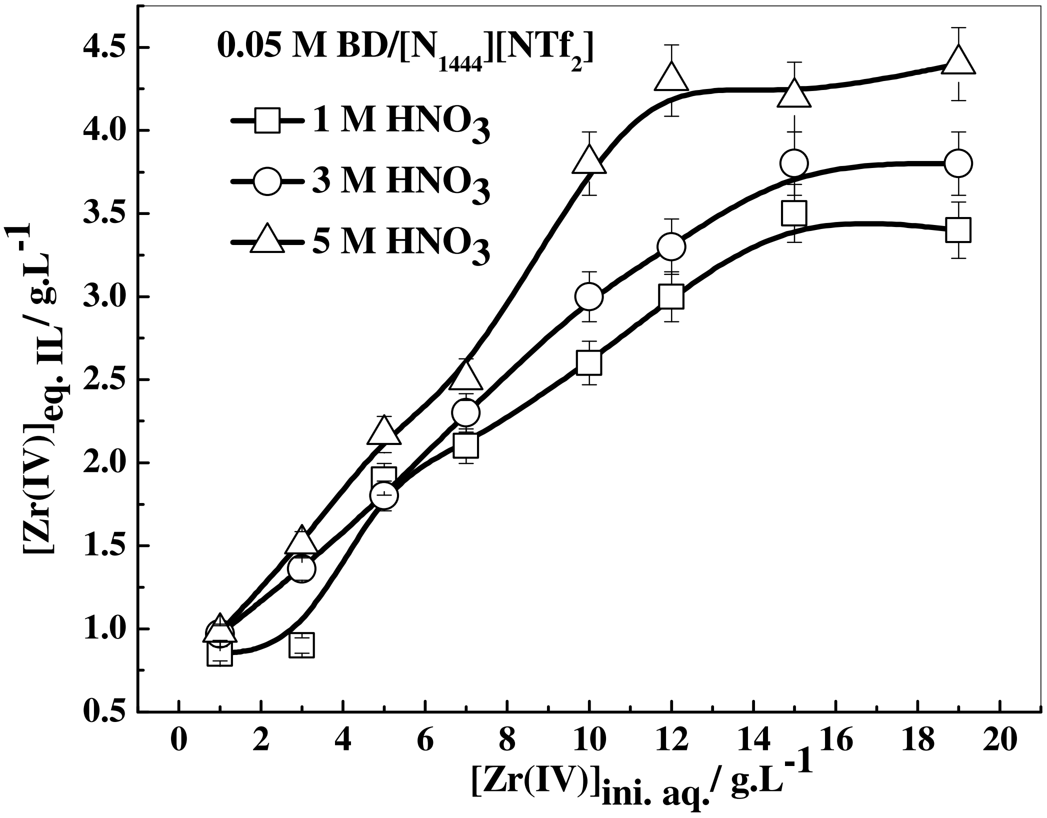

Fig. 4.17. Amount of Zr(IV) loaded into ionic liquid phase after extraction as a function of the initial Zr(IV) concentration. Ionic liquid phase: 0.05 M BD/ $[N_{1444}][NTf_2]$; Aqueous phase: 1.0-3.0 M $[HNO_3]$; [Zr(IV)] = 1-19 g/L; Temperature = 298 K; Equilibration time = 1 hour; Phase volume ratio = 1.

4.5.7. Effect of Temperature

The effect of temperature on the distribution ratio of zirconium was studied and the results on the variation in the logarithmic value of the distribution ratio against reciprocal temperature (1/T) are shown in Fig. 4.18. The extraction of zirconium was carried out from 3 M nitric acid medium in 0.05 M BD in $[N_{1444}][NTf_2]$. It is observed that the distribution ratio of Zr(IV) increases with 1/T, indicating the exothermic nature of extraction. The enthalpy change accompanied by the extraction of Zr(IV) in 0.05 M BD/ $[N_{1444}][NTf_2]$ can be determined from the slope of linear fit shown in Fig. 4.19, according to the van’t Hoff relation of the form shown in equation 4.6. The enthalpy change (ΔH_{total}) was determined to be - 44 kJ.mol^{-1}. This indicates that the equilibrium reaction shown in equation 4.4 for the extraction of zirconium is driven by enthalpy change.

$$\frac{\partial \ln D_{Zr(IV)}}{\partial (1/T)} = -\frac{\Delta H_{total}}{R} \tag{4.6}$$

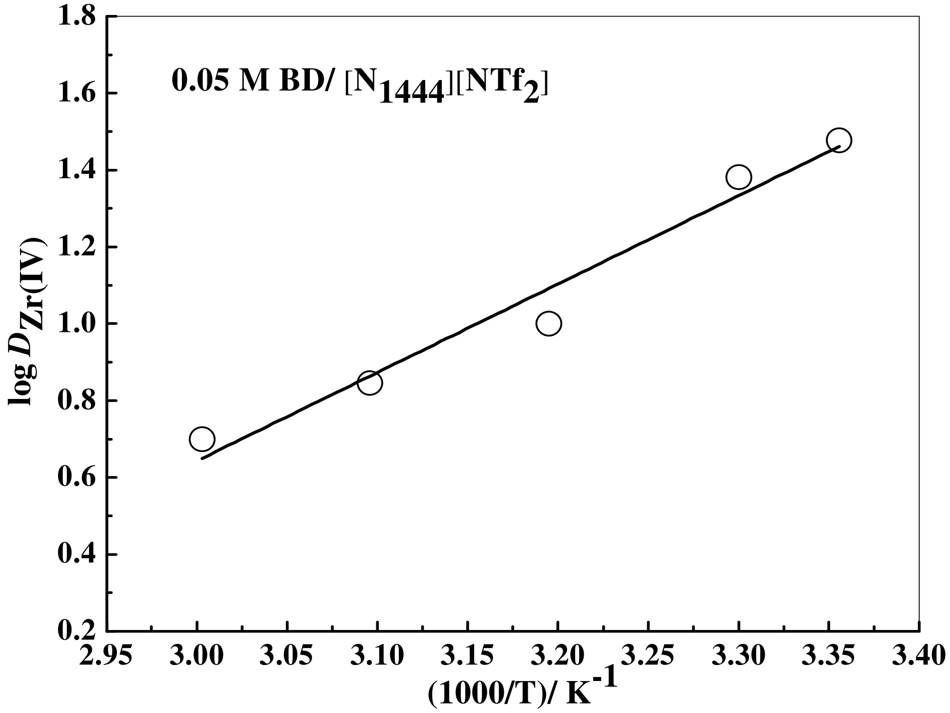

Fig. 4.18. Effect of temperature on the distribution ratio of Zr(IV) in ionic liquid phase. Ionic liquid phase: 0.05 M BD/ [N_{1444}][NTf_2]; Aqueous phase: 3.0 M [HNO_3]; [Zr(IV)] = 1 g/L; Temperature = 298 K; Equilibration time = 1 hour; Phase volume ratio = 1.

4.5.8. Effect of alkyl group attached to ligand and ammonium moiety of RTIL

Fig. 4.19. shows the comparison in the distribution ratio of zirconium as a function of nitric acid concentration in benzodioxodiamide derivatives present in different ionic liquids. The ionic liquids chosen for comparison are [N_{1444}][NTf_2] and methyltrioctylammonium bis(trifluoromethylsulfonyl)imide ([N_{1888}][NTf_2]). Similarly the benzodioxodiamide derivatives chosen for comparison are 2-ethylhexyl and the decyl-derivatives of benzodioxodiamide. The

decyl derivative is abbreviated as BDD. It can be seen that the distribution ratio of Zr(IV) increases in all cases with increase in the concentration of nitric acid, as expected. However, the distribution ratio of Zr(IV) increase in the order of 0.05 M BD/ $[N_{1888}][NTf_2]$ < 0.05 M BDD/ $[N_{1444}][NTf_2]$ < 0.05 M BD/ $[N_{1444}][NTf_2]$. The results indicates that increasing the chain length of alkyl group attached to the amidic nitrogen atom of benzodioxodiamide decreases the distribution ratio of zirconium at all nitric acid concentrations. The decrease in distribution ratio upon increasing the chain length of alkyl group attached to either to ionic liquid or to benzodioxodiamide indicates that the steric hindrance of the alkyl group could be the governing factor for the extraction of zirconium in ionic liquid phase.

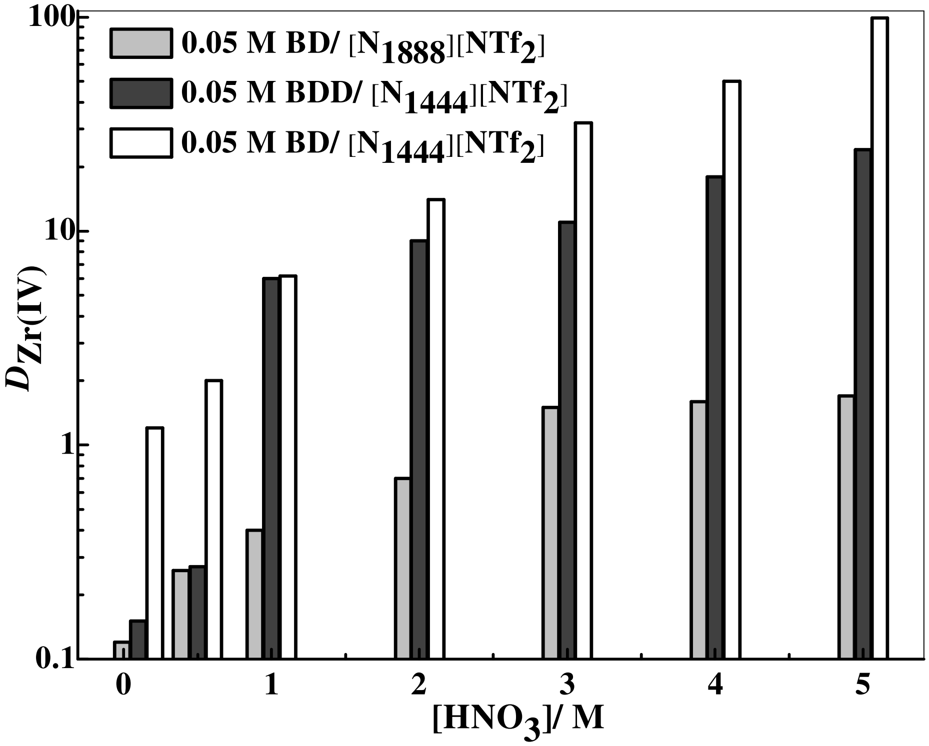

Fig. 4.19. Variation in the distribution ratio of Zr(IV) as a function of the nitric acid concentration in the aqueous phase. Ionic liquid phase: 0.05 M BD (or BDD) /$[N_{1444}][NTf_2]$ (or $[N_{1888}][NTf_2]$); Aqueous phase: 0.1 M – 8.0 M $[HNO_3]$; [Zr(IV)] = 1 g/L; Temperature = 298 K; Equilibration time = 1 hour; Phase volume ratio = 1.

4.6. Summary

The extraction of Zr(IV) in $[N_{1444}][NTf_2]$ was negligible, but the addition of ligand (BD) to $[N_{1444}][NTf_2]$, the distribution ratio of Zr(IV) increased as a function of nitric acid concentration. The extraction trend of Zr(IV) observed in ionic liquid and n-dodecane medium were similar, suggesting that the mechanism of Zr(IV) extraction in both the cases could be similar. However, the $D_{Zr(IV)}$ values were higher in ionic liquid medium as compared to n-dodecane. The linear dependence of $D_{Zr((IV))}$) on [BD] with a slope of 2.1, suggested that 2 molecules of BD were involved in the extraction of Zr(IV) in ionic liquid phase. In contrast, the saturation in the loading of Zr(IV) observed in the extraction of Zr(IV) isotherm suggested a molecule of BD was coordinated to Zr(IV) at higher Zr(IV) loading. The results showed that the stoichiometry of Zr(IV) to BD could change from 1:2 to 1:1 depending upon loading of Zr(IV) in ionic liquid phase. The extraction of Zr(IV) in 0.05 M BD/ $[N_{1444}][NTf_2]$ was driven by enthalpy, and the enthalpy change accompanied by the extraction of zirconium was determined to be -44 $kJ.mol^{-1}$. The distribution ratio of U(VI) in 0.05 M BD/ $[N_{1444}][NTf_2]$ was significantly low as compared to $D_{Zr(IV)}$ values at all nitric acid concentrations, leading to the separation factor of zirconium over uranium varying from 2 to 100 with increase in the concentration of nitric acid from 0.1 to 5 M. The distribution ratio of Zr(IV) decreased abruptly with increase in the amount of uranium from 1 to 3 g/L, followed by saturation in the $D_{Zr(IV)}$ values. More than 65 % of Zr(IV) was extracted into 0.05 M BD/ $[N_{1444}][NTf_2]$ phase even at 16 g/L of uranium in aqueous phase. The magnitude of separation factor shows the possibility of separation of zirconiumm from uranium matrix present in nitric acid medium.

References

1. Sung Ho Ha, R.N. Menchavez, Y.M. Koo, Reprocessing of spent nuclear waste using ionic liquids. Korean J. Chem. Eng. 27 (2010) 1360-1365.
2. T. Sun, Y. Zhang, Q. Wu, J. Chen, L. Xia, C. Xu, Comparative study on the extraction of trivalent americium and europium by CMPO in imidazolium-based ionic liquids and dodecane, Solvent Extr. Ion Exch. 35 (2017) 408-422.
3. P.K. Mohapatra, Actinide ion extraction using room temperature ionic liquids: opportunities and challenges for nuclear fuel cycle applications, Dalton Trans. 46 (2017) 1730-1747.
4. P.R. Vasudeva Rao, K.A. Venkatesan, Alok Rout, T.G. Srinivasan, K. Nagarajan. Potential applications of room temperature ionic liquids for fission products and actinide separation, Sep. Sci. Technol. 47 (2012) 204-222.
5. L. Chen, Y. Wang, X. Yuan, Y. Ren, N. Liu, L. Yuan, W. Feng, Highly selective extraction of uranium from nitric acid medium with phosphine oxide functionalized pillar [5] arenes in room temperature ionic liquid, Sep. Purif. Technol. 192 (2018) 152-159.
6. N.K. Gupta, Ionic liquids for TRansUranic Extraction (TRUEX)—Recent developments in nuclear waste management: A review, J. Mol. Liq. 269 (2018) 72-91.
7. B.B. Mishra, N. Devi, Solvent extraction and separation of europium (III) using a phosphonium ionic liquid and an organophosphorus extractant-A comparative study, J. Mol. Liq. 271 (2018) 389-396.
8. J.P. Mikkola, P Virtanen, R Sojholm, Aliquat 336- a versatile and affordable cation source for an entirely new of hydrophobic ionic liquids, Green Chem. 8 (2006) 250-255.

9. Alok Rout, K. Chatterjee, K.A. Venkatesan, M.P. Antony, P.R. Vasudeva Rao, Solvent extraction of plutonium(IV) in monoamide-ammonium ionic liquid mixture, Sep. Purif. Technol. 159 (2016) 43-49.

10. M. Van de Voorde, K. Van Hecke, K. Binnemans, T. Cardinaels, Separation of samarium and europium by solvent extraction with an undiluted quaternary ammonium ionic liquid: towards high-purity medical samarium, RSC Adv. 8 (2018) 20077-20086.

11. Alok Rout, K. Chatterjee, K. A. Venkatesan, P. R. Vasudeva Rao, Liquid-Liquid extraction of americium(III) using a completely incenerable ionic liquid system, Sep. Purif. Technol. 158 (2016) 137-143.

12. Assessment of partitioning processes for transmutation of actinides. IAEA TECDOC CD series, IAEA-TECDOC-CD-1648, 2010.

13. S.A. Ansari, P.N. Pathak, P.K. Mojhapatra, V.K. Manchanda, Aqueous Partitioning of Minor Actinides by Different Processes, Sep. Purif. Rev. 40 (2011) 43–76.

14. B.A. Moyer, Ion Exchange and Solvent Extraction. A series of Advances, Volume 19. CRC Press, Taylor and Francis Group 2010.

15. S.A. Ansari, P.N. Pathak, P.K. Mohapatra, V.K. Manchanda, Chemistry of Diglycolamides: Promising Extractants for Actinide Partitioning, Chem. Rev. 112 (2012) 1751–1772.

16. P. Deepika, K. N. Sabharwal, T. G. Srinivasan, P. R. Vasudeva Rao, Studies on the Use of *N,N,N´,N´*-Tetra(2-ethylhexyl) Diglycolamide (TEHDGA) for Actinide Partitioning. I: Investigation on Third-Phase Formation and Extraction Behavior, Solvent Extr. Ion Exch. 28 (2) (2010)184-201.

17. Y. Sasaki, Y. Sugo, S. Suzuki, S. Tachimori, The Novel Extractants, Diglycolamide, for the extraction of lanthanides and actinides in HNO_3-*n*-Dodecane system, Solvent Extr. Ion Exch. 19 (2001) 91–103.

18. R.B. Gujar, S.A. Ansari, P.K. Mohapatra, V.K. Manchanda, Development of T2EHDGA Based Process for Actinide Partitioning. Part I: Batch Studies for Process Optimization, Solvent Extr. Ion Exch. 28 (2010) 350–366.

19. Alok Rout, K.A. Venkatesan, T.G. Srinivasan, P.R. Vasudeva Rao, Extraction and third phase formation behavior of Eu(III) in CMPO–TBP extractants present in room temperature ionic liquid, Sep. Purif. Technol. 76 (2011) 238–243.

20. S. Murakami, M. Matsumiya, T. Yamada, Extraction of Pr(III), Nd(III) and Dy(III) from HTFSA Aqueous Solution by TODGA/Phosphonium-Based Ionic Liquids, Solvent Extr. Ion Exch. 34 (2016) 172-187.

21. M. Panigrahi, M. Grabda, D. Kozak, A.K. Dorai, E. Shibata, J. Kawamura, T. Nakamura, Liquid–liquid extraction of neodymium ions from aqueous solutions of $NdCl_3$ by phosphonium-based ionic liquids, Sep. Purif. Technol. 171 (2016) 263-269.

22. R. Zarrougui, R. Mdimagh, N. Raouafi, Highly efficient extraction and selective separation of uranium (VI) from transition metals using new class of undiluted ionic liquids based on H-phosphonate anions, J. Hazard. Mater. 342 (2018) 464-476.

23. I.A. Shkrob, T.W. Marin, M.P. Jensen, Ionic Liquid Based Separations of Trivalent Lanthanide and Actinide Ions, Ind. Eng. Chem. Res. 53 (2014) 3641–3653.

24. M. Gras, N. Papaiconomou, E. Chainet, F. Tedjar, I. Billard Separation of cerium(III) from lanthanum(III), neodymium(III) and praseodymium(III) by oxidation and liquid-liquid extraction using ionic liquids, Sep. Purif. Technol. 178 (2017) 169-177.

25. Alok Rout, K.A.Venkatesan, M.P. Antony, Ammonium based amide functionalized task specific ionic liquid for actinide separation, Solvent Extr. Ion Exch. 36 (2018) 558-573.

26. K.R. Swami, A.S. Suneesh, R. Kumerasan, K.A. Venkatesan, M.P. Antony, Dynamic Light Scattering and FTIR Spectroscopic Investigations on the Reverse Micelles Produced During the Extraction of Nd(III) and Nitric Acid in Tetra Ethylhexyl Diglycolamide, ChemistrySelect 2 (2017) 11177 – 11186.

27. P.K. Verma, P.N. Pathak, P.K. Mohapatra, V.K. Aswal, B. Sadhu, M. Sundararajan, An Insight into Third-Phase Formation during the Extraction of Thorium Nitrate: Evidence for Aggregate Formation from Small-Angle Neutron Scattering and Validation by Computational Studies, J. Phys. Chem. B 117 (2013) 9821–9828.

28. K. Rama Swami, R. Kumaresan, K.A. Venkatesan, M.P. Antony, Minimizing the aggregation of diglycolamide reverse micelles in the n-dodecane phase with bis-(2-ethylhexyl)phosphoric acid “reactive” phase modifier, New. J. Chem. 42 (2018) 8891-8899.

29. W. Liansheng, M. Casarci, G.M. Gasparini, The extraction of Eu(III) from acidic media by octylphenyl-N,N-diisobutylcarbamoylmethylphosphine oxide, Solvent Extr. Ion Exch. 8(1) (1990) 49-64.

30. Alok Rout, S. Kumar, K. A. Venkatesan, S. Maji, M. P. Antony, Complexation of Eu(III) in a Completely Incinerable Ionic Liquid System: A Luminescence Spectroscopy Approach, ChemistrySelect 3 (2018) 3029-3035.

31. K. Binnemans, Interpretation of europium(III) spectra, Coordination Chem. Rev. 295 (2015) 1-45.

32. R.G. Schuler, C.B. Bowers Jr, J. E. Smith Jr, V. Van Brunt, M.W. Davis Jr, The extraction of Cesium and strontium from acidic high activity nuclear waste using a PUREX process compatible organic extractant, Solvent Extr. Ion Exch. 3 (1985) 567-604.

33. E. Aneheim, C. Ekberg, A. Fermvik, M.R. St J. Foreman, B. Grűner, Z. Hájkova, M. Kvicalova, A TBP/BTBP-based GANEX Separation Process—Part 2: Ageing, Hydrolytic, and Radiolytic Stability, Solvent Extr. Ion Exch. 29 (2011) 157–175.

34. P. Sinharoy, D.P. Nair, J.N. Sharma, K. Banerjee, Effect of degradation products of TEHDGA on actinide partitioning process, Sep. Purif. Technol. 161 (2016) 32-37.

35. T. Prathibha, R. Kumaresan, K.A. Vekatesan, M.P. Antony, P.R. Vasudeva Rao, N,N-dialkyl-2-hydroxyacetamides for modifier-free separation of trivalent actinides from nitric acid medium, Radiochim. Acta 104 (3) (2016) 173–181.

36. C.B Lee, J.S. Cheon, S.H. Kim, J.Y. Park, H.K. Joo, Metal fuel development and verifcation for proto type generation IV sodiumcooled fast reactor, Nucl. Eng. Technol. 48 (2016) 1096–1108.

37. C. Laue, D. Gates-Anderson, T. Fitch, Dissolution of metallic uranium and its alloys, J. Radioanal. Nucl. Chem. 261 (3) (2004) 709–717.

38. B. Sreenivasulu, A. Suresh, N. Sivaraman, M. Joseph, Dissolution and characterization studies on U–Zr and U–Pu–Zr alloys in nitric acid medium, J. Radioanal. Nucl. Chem. 311 (2017) 789–800.

39. J.V. Holders, A review of the solvent extraction process chemistry of fission products, Radiochim. Acta. 25 (1978) 171–180.

40. F.R. Bruce, Progress in Nuclear Energy: The behavior of fission products in solvent extraction processes. In: F.R. Bruce, J.M. Fletcher, H.H. Hyman, J.J. Katz, (eds) Series III Process chemistry, Vol I, McGraw-Hill, New York (1956).

41. D.D. Sood, S.K. Patil, Chemistry of nuclear fuel reprocessing: Current status, J. Radioanal. Nucl. Chem. 203 (1996) 547–573.

42. J. Garraway, P.D. Wilson, Coextraction of pertechnetate and zirconium by tri-n-butyl phosphate, J. Less Common Metals.106 (1985) 183–192.

43. R. Ruhela, S. Panja, B.S. Tomar, M.A. Mahajan, R.M. Sawant, S.C. Tripathi, A.K. Singh, P.M. Gandhi, R.C. Hubli, A.K. Suri, Bis-(2-ethylhexyl) carbamoyl methoxy phenoxy-bis-(2-ethylhexyl) acetamide [BenzoDODA]—first selective extractant for plutonium (IV) recovery (SEPUR) from acidic media, Tetrahedron Lett.53 (2012) 5434-5436.

44. R. Ruhela, S. Panja, B.S. Tomar, A.K. Singh, S.C. Tripathi, P.M. Gandhi, R.C. Hubli, liquid-liquid extraction studies for the separation and recovery of plutonium from acidic medium with novel ligand Benzodioxodiamide (BenzoDODA), Sep. Purif. Technol. 124 (2014) 49-53.

45. M.L. Dietz, Ionic liquids as extraction solvents: where do we stand?, Sep. Sci. Technol. 41 (2006) 2047 -2063.

46. J.G. Huddleston, A.E. Visser, W.M. Reichert, H.D. Willauer, G.A. Broker, R.D. Rogers, Characterization and Comparison of Hydrophilic and Hydrophobic Room Temperature Ionic Liquids Incorporating the Imidazolium Cation, Green Chem. 3 (2001) 156–164.

Chapter 5: Studies related to aggregation behavior and empirical polarity index of ionic liquid phase

This chapter deals the aggregation behavior and the empirical polarity index of the ionic liquid phase containing nitric acid and metal-ligand complexes. This chapter is divided into three parts and each part is described below

PART 1: Probing the absence of third phase formation during the extraction of trivalent metal ions in an ionic liquid medium

5.1. Introduction

The separation of the target metal from aqueous phase is industrially carried out by a solvent extraction procedure [1,2]. The solvent phase is usually composed of a polar ligand diluted in an inert molecular diluent medium, such as *n*-dodecane [1,2]. Due to the polar nature of the ligand, they tend to undergo aggregation in organic phase. The extraction of metal ion from aqueous phase results in the formation of metal-ligand complex in organic phase [1,2]. Since the polarity of such metal-ligand complex is more as compared to the ligand itself, these complexes tend to undergo aggregation further in organic phase due to polar-polar interactions [4-7]. Apart from such interactions, the aggregates also interact efficiently with *n*-dodecane by Van der Waals forces. Therefore the aggregates are distributed homogeneously in *n*-dodecane, as long as these interactions are strong as compared to the polar-polar interactions. However at a particular metal loading in organic phase the polar-polar interactions among the aggregates are sufficiently strong as compared to the Van der Waals interactions, the aggregates undergo demixing in organic phase and expelled out as third phase during the course of solvent extraction.

Third phase formation is an undesirable event in a solvent extraction procedure and it is of serious concern when fissile metal ions are concentrated during third phase formation [8]. The causes of third phase formation in a counter-current solvent extraction procedure are described elsewhere [8]. Few options are available for preventing the third phase formation [9-11]. The first option is to design a ligand that increases the Van der Waals interaction of the aggregate with molecular diluent. Another way is to add phase modifiers that minimize the polarity imparted on the metal-ligand complex, or stabilize the polar metal-ligand complex. Both these options, in fact, shift the third phase formation limit to a higher value, such that there is no undesirable event in the operating process condition. Alternatively, the best method for preventing the third phase formation is to employ strongly polar diluent in place of a molecular diluent for stabilizing the polar metal-ligand complex. One such candidate is the room temperature ionic liquid (RTIL), which is an organic salt, melt at temperatures lower than 373 K [12,26-29].

From solvent extraction point of view, the literature shows that the traditional ligands in conjunction with the ionic liquid were shown to exhibit extraordinary extraction of actinides and lanthanides. In this direction a large number of reports have been reported in literature making use of the properties indicated above for solvent extraction application in last two decade [13-20]. However, the polar nature of the ionic liquid has not been tapped so far for preventing the third phase formation during the course of solvent extraction. The loading behavior of Eu(III) in a solution of carbamoylmethylphoshine oxide (CMPO) in 1-butyl-3-methylimidazolium bis(trifluoromethylsulphonyl)imide ($[C_4mim][NTF_2]$) ionic liquid was discussed elsewhere [21,24]. Generally the ligand CMPO was prone to form third phase even with dilute nitric acid and therefore it required a large concentration of phase modifier, such as tri-*n*-butyl phosphate (TBP), in *n*-dodecane phase for maneuvering third phase formation [22,23]. However, the third phase formation was not observed in ionic liquid phase even at the stoichiometric level of loading of Eu(III) in CMPO and TODGA in ionic liquid phase was discussed elsewhere [21,24]. Nevertheless, the role of ionic liquid in preventing the third phase formation was unknown.

To unravel the puzzle and to understand the role of ionic liquid in preventing the third phase formation, the extraction behavior of Am(III) and Nd(III) was studied in a solution of tetra (2-ethylhexyl) diglycolamide (T2EHDGA) or CMPO present in tri-*n*-octylmethylammonium nitrate

$[N_{1888}][NO_3]$. The ligands T2EHDGA and CMPO were regarded as promising extractants for the group separation of trivalent actinides and lanthanides from high-level nuclear waste [22,25,30]. To understand the insights of the extracted phase, dynamic light scattering (DLS) experiments were performed in the ionic liquid phase obtained after extraction of trivalent metal ion and compared the results with those obtained before extraction. In view of this, the results on the extraction and aggregation behavior of Am(III) and Nd(III) from nitric acid medium in a solution of T2EHDGA or CMPO in $[N_{1888}][NO_3]$ is reported in this chapter.

Experimental details for the present chapter (part 1) are presented in the section 2.5.4 of the chapter 2. The synthesis of ionic liquid was discussed in section 2.6.6 chapter 2 respectively.

Table. 5.1. Structure of molecular extractant and RTIL used in part I of chapter 5.

Name	Structure
Extractant	
N,N,N',N'-tetra(2-ethylhexyl)diglycolamide (T2EHDGA)	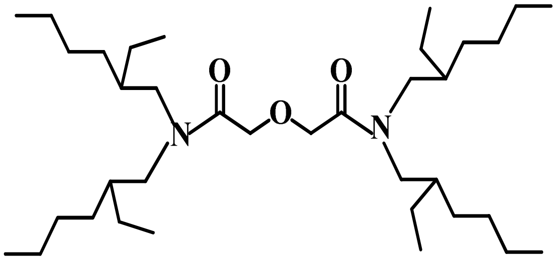
Octyl-phenyl-*N,N*-diisobutylcarbamoylmethyl phosphinoxide (CMPO)	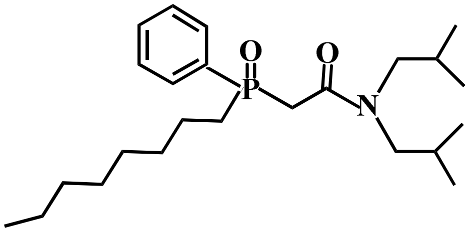
Ionic liquid	
Methyl-tri-*n*-octylammonium nitrate $[N_{1888}][NO_3]$ (R: C_8H_{17})	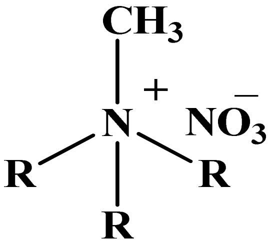

5.2. Results and discussions

5.2.1. Effect of nitric acid concentration

Fig. 5.1. shows the variation in the % extraction of Am(III) in 0.1 M T2EHDGA (or CMPO)/[N_{1888}][NO_3] as a function of nitric acid concentration. The extraction of Am(III) observed in presence of T2EHDGA and CMPO was compared with those obtained in [N_{1888}][NO_3] ionic liquid alone. It can be seen that the extraction of Am(III) increases from a negligible value (< 1 % extraction) at 0.01M nitric acid in both cases to the value of > 99 % extraction in case of T2EHDGA and ~80 % extraction in case of CMPO at 5 M nitric acid. The extraction trend observed in the present study is similar to the extraction observed in case of molecular diluent system composed of T2EHDGA or CMPO in *n*-dodecane [10, 22, 23]. This shows that the role of [N_{1888}][NO_3] during the extraction of Am(III) seems to be similar to *n*-dodecane. However, it is important to realize that both T2EHDGA and CMPO in *n*-dodecane medium gives a third phase, when contacted with Am(III) solution in nitric acid, as discussed elsewhere [23, 34]. Moreover, the 0.2 M T2EHDGA and 0.2 M CMPO in *n*-dodecane forms third phase even with nitric acid having a concentration of 4 M and 1 M respectively [23, 34]. It was reported that the third phase formation was facilitated when the stoichiometry of T2EHDGA to HNO_3 exceeded 1:1.2 in organic phase [34].

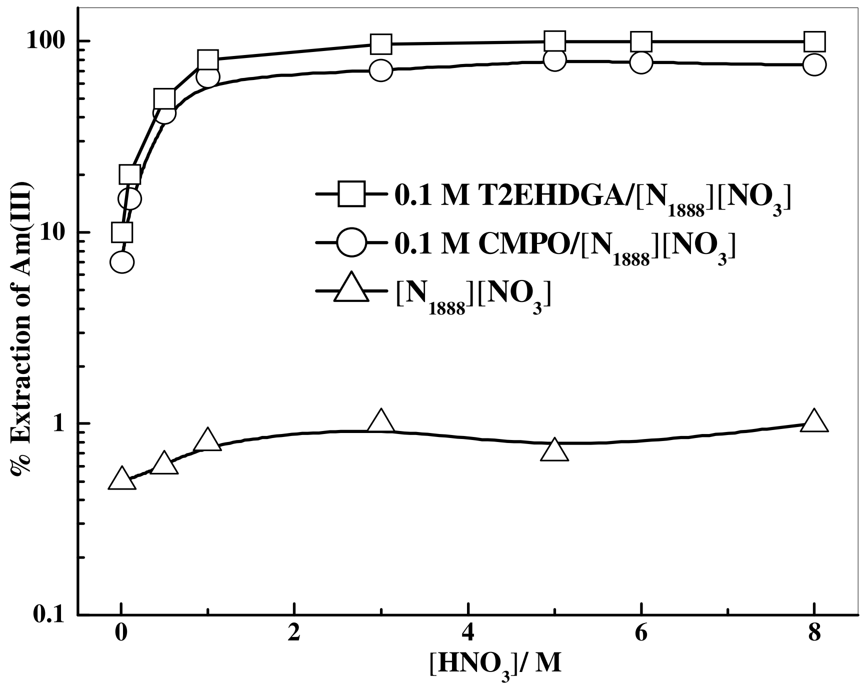

Fig. 5.1. Variation in the percentage extraction Am (III) as a function of the nitric acid concentration in the aqueous phase. Ionic liquid phase: 0.1 M T2EHDGA (or CMPO)/[N_{1888}][NO_3] or [N_{1888}][NO_3] alone; Aqueous phase: 0.01-8.0 M HNO_3 spiked with ^{241}Am tracer; Temperature = 298 K; Equilibration time = 1 h ; Phase volume ratio = 1.

To understand the extraction of nitric acid in ionic liquid phase, the extraction behavior of nitric acid with 0.1 M T2EHDGA (or CMPO)/[N_{1888}][NO_3] as well as in [N_{1888}][NO_3] was investigated and the results are displayed in Fig. 5.2. It can be seen that the extraction of nitric acid in ionic liquid phase increases with increase in the concentration of nitric acid in aqueous phase from 0.1 to 8.0 M, irrespective of the nature of the ionic liquid phase. As expected, the presence of T2EHDGA (or CMPO) in [N_{1888}][NO_3] phase increased the extraction of nitric acid, which is due to the protonation of the carbonyl functional groups present in the two extractant moieties. The nitric acid extraction follows the order: T2EHDGA/[N_{1888}][NO_3] > CMPO/[N_{1888}][NO_3] > [N_{1888}][NO_3]. These results indicate that concentration of nitric acid extracted into organic phase is significantly large as compared to those observed in molecular diluent systems [23, 34]. This is due to the extraction of nitric acid by $[N_{1888}][NO_3]$ itself as indicated in Fig.5.2. Nevertheless, it was realized there was no third phase formation in both T2EHDGA and CMPO phases even after contacting the T2EHDGA (or CMPO)/$[N_{1888}][NO_3]$ solutions with 8 M nitric acid. This shows that ionic liquid employed in the present study is playing a vital role in eliminating the third phase formation. This can be understood by probing the aggregation behavior of the ionic liquid phase obtained after the extraction of nitric acid. In view of this, dynamic light scattering experiments were performed in the ionic liquid phase obtained before and after the extraction of nitric acid and Nd(III) present in nitric acid. The Nd(III) was regarded as a lanthanide representative for the trivalent metal ion present in the nuclear waste, and it is formed in significant amounts in a fission reaction.

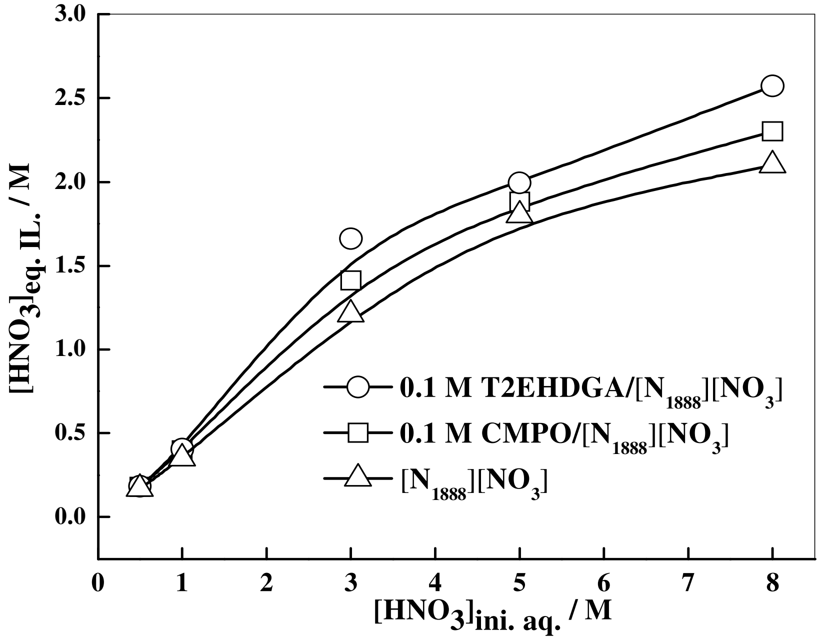

Fig. 5.2. Extraction of nitric acid in ionic liquid phase as a function of initial concentration of nitric acid in aqueous phase. Ionic liquid phase: 0.1 M T2EHDGA (or CMPO)/$[N_{1888}][NO_3]$ or $[N_{1888}][NO_3]$ alone; Aqueous phase: 0.01-8.0 M HNO_3 Temperature = 298 K; Equilibration time = 1 h; Phase volume ratio = 1.

5.2.2. Aggregation behavior of T2EHDGA or CMPO in [N_{1888}][NO_3]

Fig. 5.3. shows the aggregate distribution of the ionic liquid [N_{1888}][NO_3] and its solution with T2EHDGA and CMPO. It is interesting to note that [N_{1888}][NO_3] itself undergoes aggregation with the average aggregate size of 20 nm. The self aggregation of [N_{1888}][NO_3] could be due to the strong columbic interaction between the cation and anion of the ionic liquid. The addition of T2EHDGA and CMPO to [N_{1888}][NO_3] increases the average aggregate size and their distribution in solution. The increase in the average aggregate size with the addition of T2EHDGA or CMPO could be due to the associative interaction between the ligand and cationic part of the ionic liquid, as discussed elsewhere [35]. Therefore, it is expected that increasing the concentration of T2EHDGA or CMPO in ionic liquid phase could increase the aggregate size and their distribution in ionic liquid phase. Fig. 5.3. also shows the variation in the aggregate distribution in ionic liquid phase as a function of T2EHDGA or CMPO concentration in ionic liquid phase. It can be seen that the aggregate size and their distribution in ionic liquid phase increases with increase in the concentration of T2EHDGA and CMPO from 0.1 M to 0.3M, which is in line with the expectation.

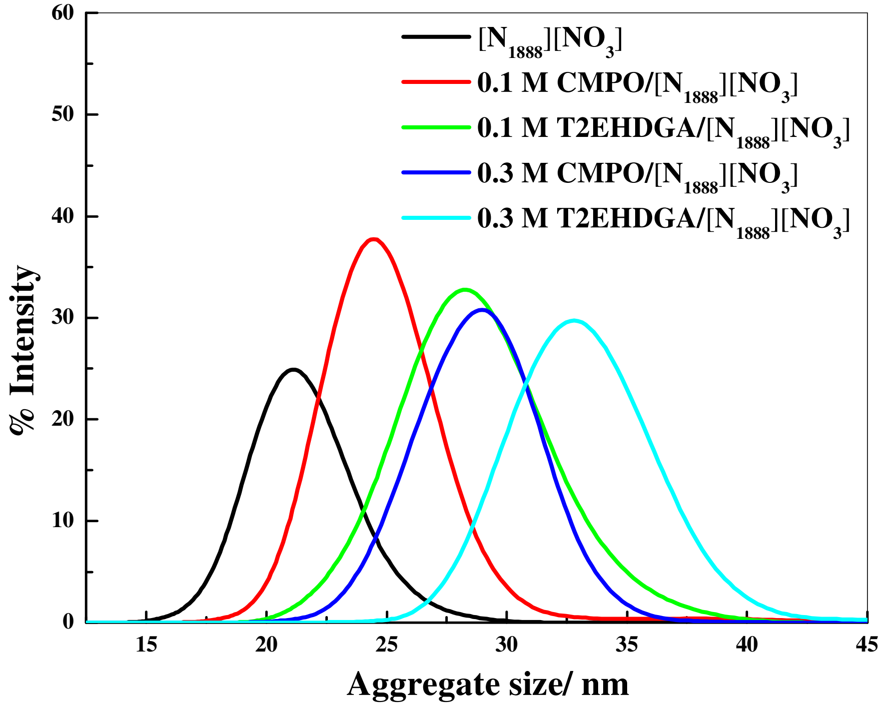

Fig. 5.3. Aggregate distribution in the ionic liquid phase before extraction. Ionic liquid phase: 0.1 M or 0.3 M T2EHDGA (or CMPO)/[N_{1888}][NO_3] and [N_{1888}][NO_3] alone; Temperature = 298 K.

5.2.3. Aggregation behavior of ionic liquid phase after HNO_3 extraction

Since the extraction of trivalent metal ion is carried out from nitric acid medium, it is important to understand the aggregation behavior of the ionic liquid phase and its solution with T2EHDGA and CMPO after contacting with nitric acid. The ligands T2EHDGA and CMPO in a molecular diluent, *n*-dodecane, forms third phase with nitric acid itself. For instance, 0.2 M T2EHDGA and 0.2 M CMPO forms third phase when contacted with nitric acid concentrations above 4 M and 2 M respectively [23,34]. Therefore, the DLS experiments were performed initially with [N_{1888}][NO_3] the ionic liquid phase after contacting with nitric acid. The results are shown in Fig. 5.4. It is interesting to note that the average aggregate size and its distribution in ionic liquid phase decreases with increase in the concentration of nitric acid in aqueous phase.

This could be due to the extraction of nitric acid by ionic liquid phase that seems to minimize the interaction between the cation and anion of the ionic liquid and neighboring ions. From Fig. 5.2. it was noted that the extraction of nitric acid in ionic liquid phase increased with increase in the concentration of nitric acid in aqueous phase.

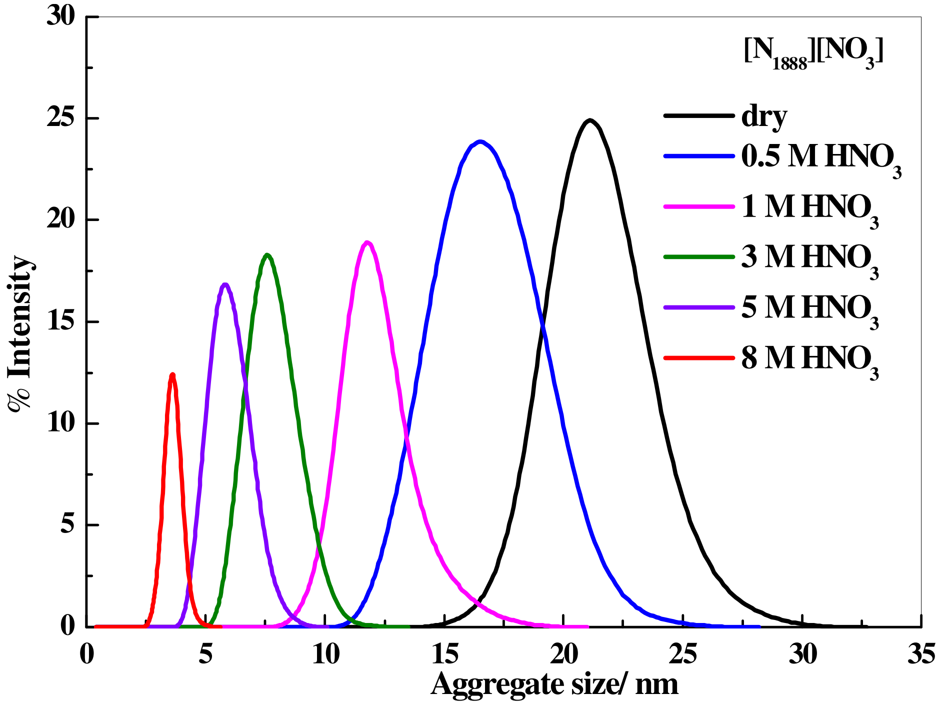

Fig. 5.4. Aggregate distribution in [N_{1888}][NO_3] before and after nitric acid extraction. Ionic liquid phase: [N_{1888}][NO_3]; Aqueous phase: 0.5 – 8 M HNO_3; Temperature = 298 K; Equilibration time = 1 hour; Phase volume ratio = 1.

A similar behavior was also observed in a solution of 0.1 M T2EHDGA (or CMPO)/ [N_{1888}][NO_3] after contacting with nitric acid. For instance Fig. 5.5. shows the comparison in the aggregate distribution observed in the solution of 0.1 M T2EHDGA (or CMPO)/[N_{1888}][NO_3] before and after contacting with 3 M nitric acid. It can be seen that the aggregate size and its distribution in ionic liquid phase is lowered from the average aggregate size of 30 nm for 0.1 M T2EHDGA/[N_{1888}][NO_3] and 25 nm for 0.1 M CMPO/[N_{1888}][NO_3] and to the value of 15 nm and 12 nm respectively after contacting the ionic liquid solution with 3 M nitric acid. In contrast to this observation, the aggregate size and their distribution of T2EHDGA in *n*-dodecane phase was reported to increase after contacting the organic phase (T2EHDGA/*n*-DD) with nitric acid [6,7]. Moreover the aggregate size in *n*-DD phase was reported to increase with increase in the concentration of nitric acid [6,7]. When the organic phase contained a critical aggregate size at a particular concentration of nitric acid, the aggregates underwent demixing in *n*-dodecane, which consequently led to third phase formation [6,7].

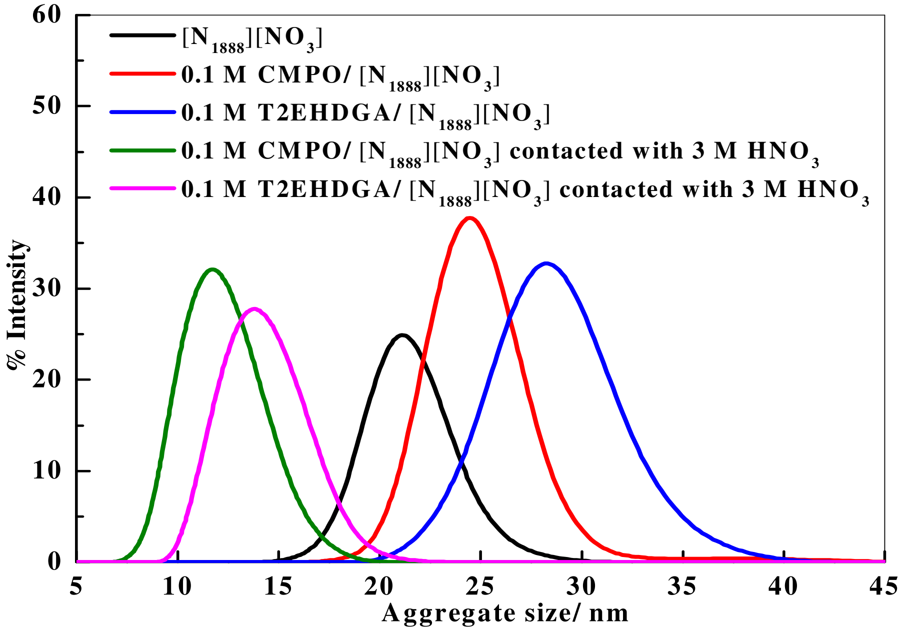

Fig. 5.5. Aggregate distribution in the ionic liquid phase before and after contacting with nitric acid. Ionic liquid phase: 0.1M T2EHDGA (or CMPO)/$[N_{1888}][NO_3]$ and $[N_{1888}][NO_3]$ alone; Aqueous phase: 3M HNO_3; Temperature = 298K; Equilibration time = 1hour; Phase volume ratio = 1.

In contrast to the observation reported in *n*-dodecane, the scenario of increase in the aggregate size with increase in the concentration of nitric acid does not arise in the present ionic liquid phase, since the aggregate size decreased with increase in the concentration of nitric acid. This is due to the fact that the aggregates formed upon equilibration of nitric acid are strongly polar and they seem to be stabilized by the polar nature of ionic liquid. Stabilization of aggregates result in the dispersion of polar aggregates and lowering of average aggregate size and its distribution in ionic liquid phase. Fig. 5.6. shows the variation in the average aggregate size of the ionic liquid phase containing 0.1 M T2EHDGA (or CMPO)/$[N_{1888}][NO_3]$ recorded after contacting the ionic liquid phase with different concentration of nitric acid. It can be seen that the aggregate size decreases with increase in the concentration of nitric acid, as expected.

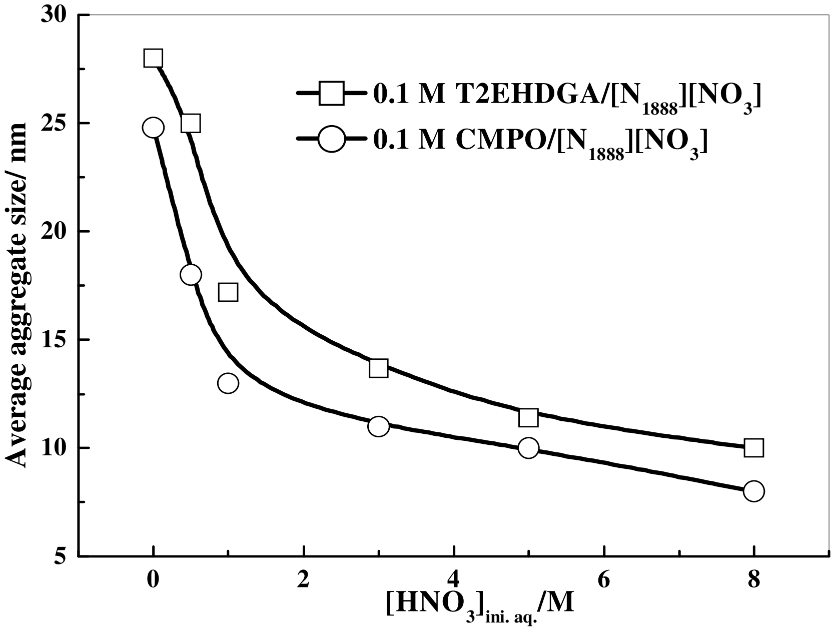

Fig. 5.6. Variation in the aggregate size as a function of nitric acid concentration. Ionic liquid phase: 0.1M T2EHDGA (or CMPO)/$[N_{1888}][NO_3]$; Aqueous phase: 0.5-8 M HNO_3; Temperature = 298 K; Equilibration time = 1 hour; Phase volume ratio = 1.

5.2.4. Effect of T2EHDGA or CMPO concentration on aggregation behavior

Fig. 5.7. shows the variation in the aggregate distribution as a function of T2EHDGA and CMPO concentration in ionic liquid phase. The aggregate distribution was recorded after contacting the ionic liquid phase with 3 M nitric acid. In this case, the average aggregate size and its distribution in ionic liquid phase increased with increase in the concentration of T2EHDGA or

CMPO in ionic liquid phase. This shows that the addition of extractant to ionic liquid facilitates aggregation, perhaps, due to the higher extraction of nitric acid in ionic liquid phase. Protonation of T2EHDGA or CMPO increases the polarity of the protonated species in ionic liquid phase and therefore the aggregate size increased with increase in the concentration of T2EHDGA and CMPO in ionic liquid phase.

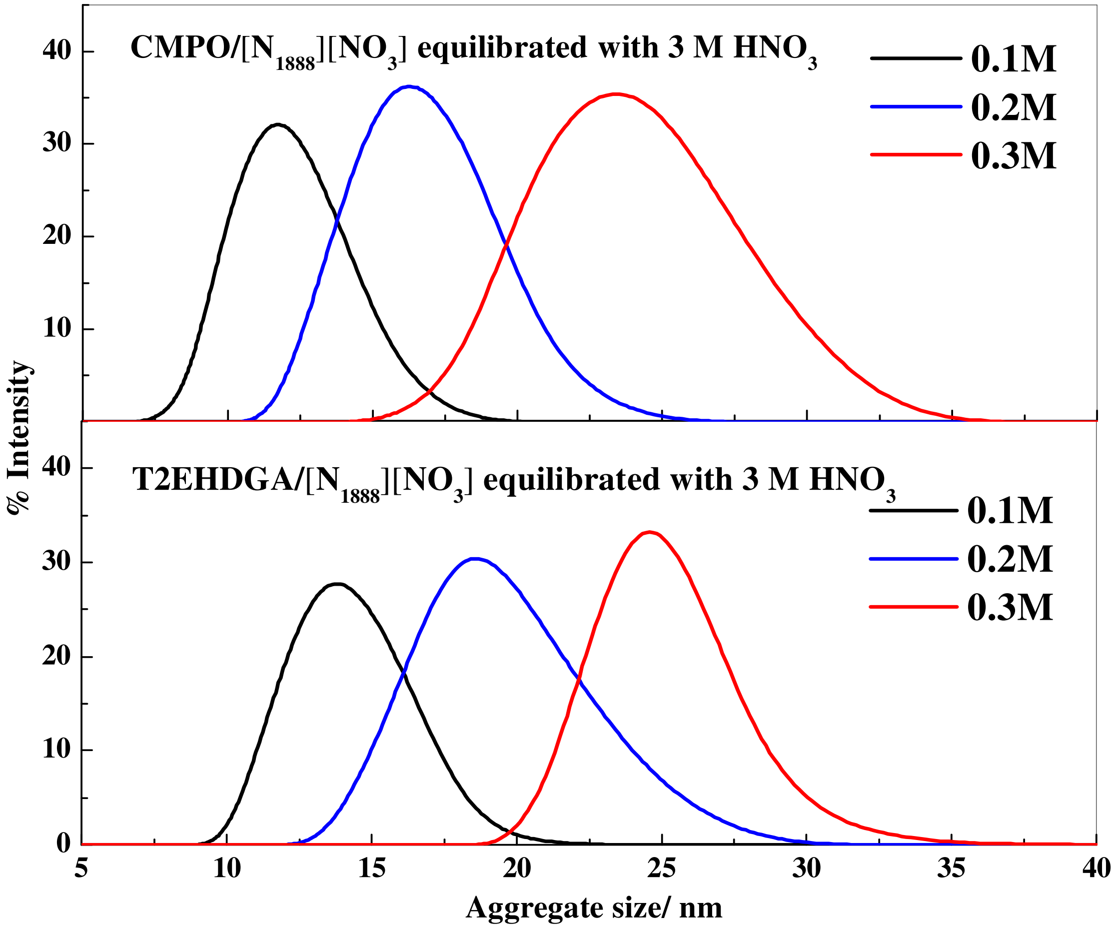

Fig. 5.7. Aggregate distribution in the organic phase as a function of extractant concentration obtained after contacting with 3 M nitric acid. Ionic liquid phase: T2EHDGA (or CMPO)/[N_{1888}][NO_3]; Aqueous phase: 3 M HNO_3; Temperature = 298 K; Equilibration time = 1 hour; Phase volume ratio = 1.

Fig. 5.8. shows the amount of HNO_3 extracted into ionic liquid phase at various concentrations T2EHDGA and CMPO. It can be seen that the quantity of nitric acid extracted into ionic liquid phase increases with increase in the concentration of T2EHDGA and CMPO in ionic liquid phase. As a result, the average aggregate size also increases with increase in the concentration of extractant in ionic liquid phase. However, it is important to note that there was no third phase formation in all cases even though the average aggregate size was about 25 nm. In contrast, the T2EHDGA in *n*-dodecane was reported to form third phase when the average aggregate size exceeds the value of 30 nm [6,7].

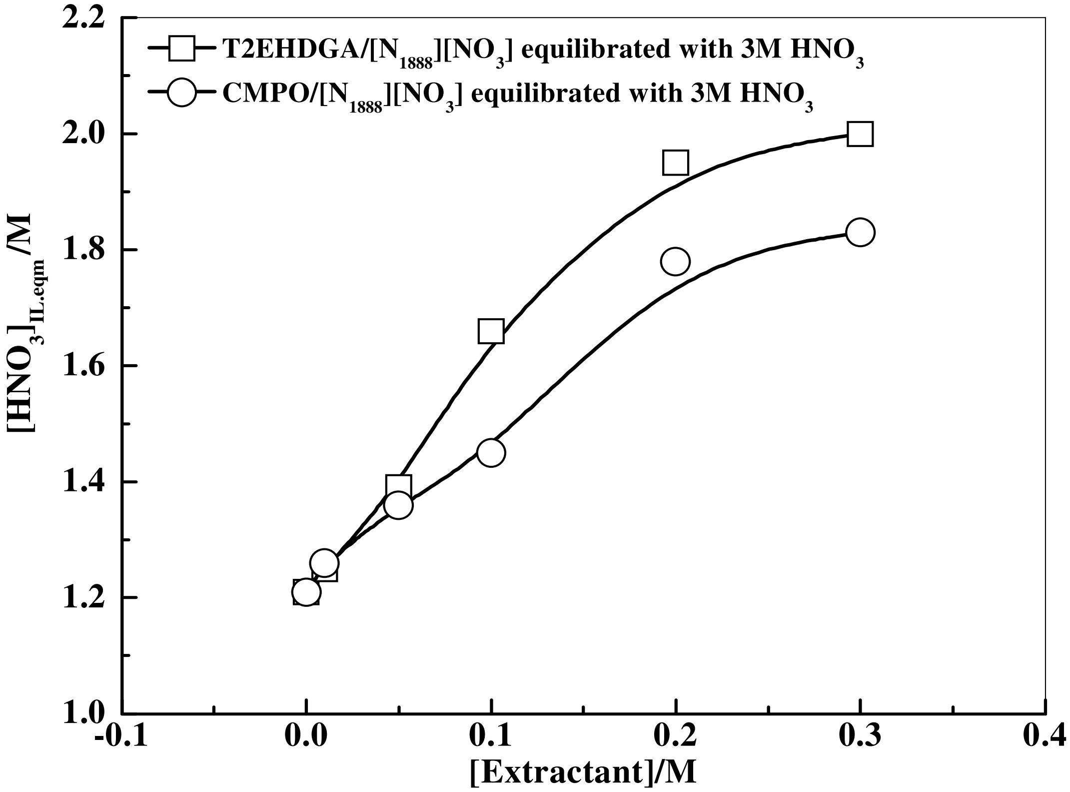

Fig. 5.8. Nitric acid extraction as a function of the extractant concentration in the ionic liquid phase. Ionic liquid phase: (0.01-0.3 M) T2EHDGA (or CMPO)/[N_{1888}][NO_3]; Aqueous phase: 3 M HNO_3;Temperature = 298 K; Equilibration time = 1 h; Phase volume ratio = 1.

5.2.5. Aggregation behavior in Nd(III) extracted phase

The study shows that increase in the protonation of the ligand present in [N_{1888}][NO_3] phase increases the aggregate size of the resultant solution. Therefore, it is quite likely that increasing the co-ordination of the ligand by the metal ion would also increase the average aggregate size. To confirm this, the extraction behavior of Nd(III) from 3 M nitric acid medium was studied in a solution of 0.1 M T2EHDGA (or CMPO)/[N_{1888}][NO_3]. The concentration of Nd(III) in aqueous phase was varied from 0.5 to 5 g/L. The ionic liquid phase obtained after the extraction was subjected to DLS studies. The aggregate distribution is shown in Fig. 5.9 and the amount of Nd(III) extracted into ionic liquid phase is also shown in the Fig. 5.9. It can be seen that the extraction of Nd(III) in ionic liquid phase increases with increase in the concentration of Nd(III) in aqueous phase. In addition, it is also noted that the aggregate size and its distribution in ionic liquid phase increases with increase in the loading of Nd(III) in ionic liquid phase. This could be due to the co-ordination of Nd(III) by T2EHDGA and CMPO that increases the polarity of the Nd(III)-ligand complex. As a result, these complexes undergo aggregation in [N_{1888}][NO_3] phase. A similar behavior was also reported by several authors in *n*-dodecane phase [6, 7]. These observations confirm that co-ordination of the ligand either by Nd(III) or a proton increases the average aggregate size and their distribution in ionic liquid phase. However, it should be noted that there was no third phase formation even after contacting the ionic liquid phase with an aqueous solution contacting 5 g/L Nd(III) in 3M nitric acid, where as the T2EHDGA or CMPO in *n*-dodecane forms third phase when contacted with 3M nitric acid solution containing traces of Nd(III) [23, 34]. It is worthwhile to mention here that the concentration of trivalent metal ions present in nuclear waste (0.6 g/L in 3-4 M nitric acid) was about an order lower than the concentration of Nd(III) (5 g/L) employed for extraction in the present system [36]. All these observations again confirm that the polar Nd(III)-ligand complex formed in ionic liquid phase was stabilized by $[N_{1888}][NO_3]$.

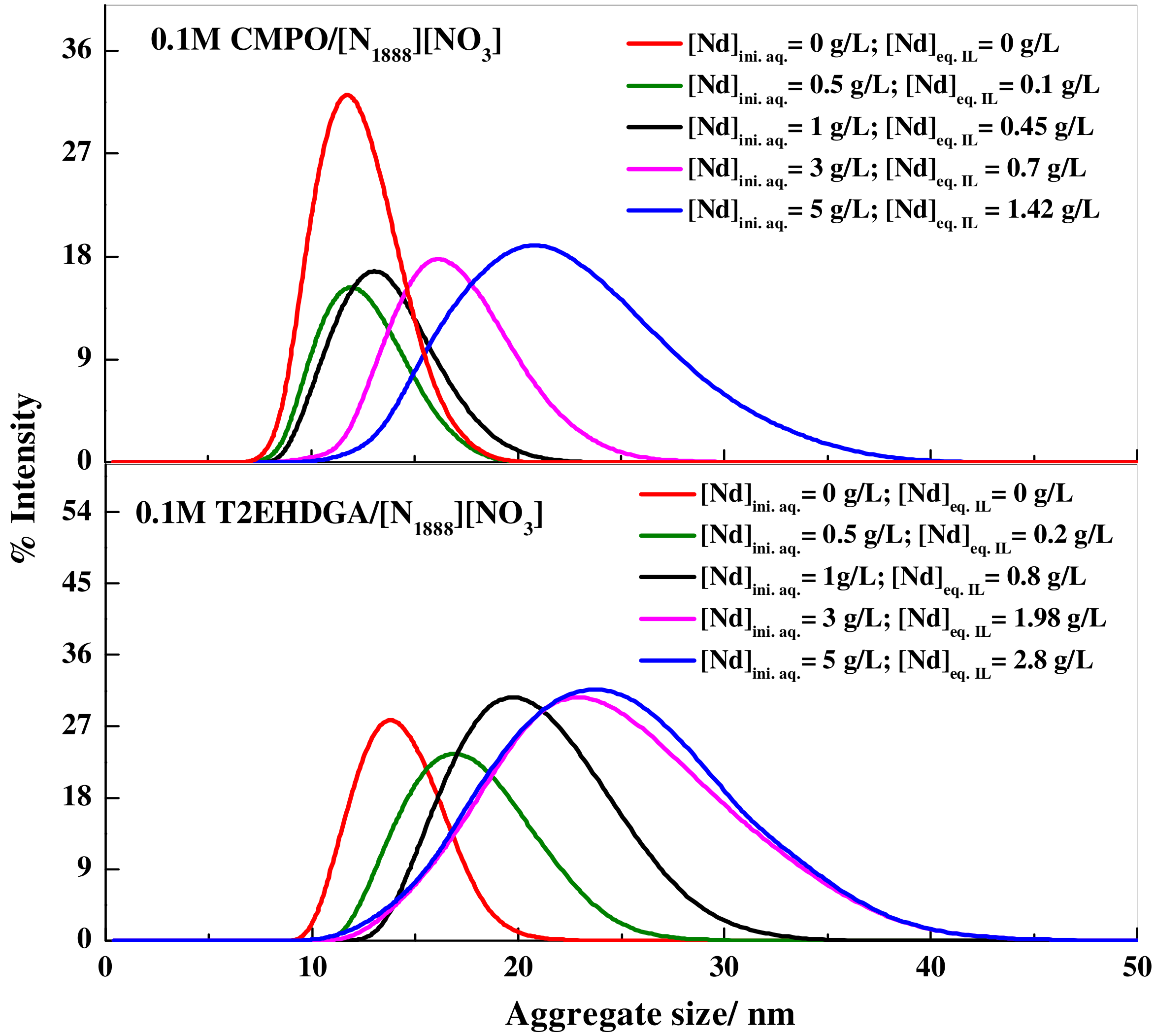

Fig. 5.9. Aggregate distribution in ionic liquid phase as a function of Nd(III) concentration in the aqueous phase. Ionic liquid phase: 0.1M T2EHDGA (or CMPO)/$[N_{1888}][NO_3]$; Aqueous phase: 3 M HNO_3 + varied Nd(III) concentration; Temperature = 298 K; Equilibration time = 1 hour; Phase volume ratio = 1.

5.2.6. Extraction Stoichiometry

The extraction of americium in T2EHDGA or CMPO can be represented by equation 5.1. The subscripts "aq" and "IL" denote the aqueous and ionic liquid phases respectively. L is the ligand T2EHDGA or CMPO employed and "x" is the number of ligand molecules involved in the extraction of europium.

$$Am^{3+}_{aq} + 3NO^{-}_{3\,aq} + x\,L_{IL} \Leftrightarrow Am\ (NO_3)_3\,(L)_{x\ \ IL} \tag{5.1}$$

The equilibrium constant for the above reaction can be represented in equation 5.1.

$$\mathrm{K_{ex}} = \frac{[\mathrm{Am(NO_3)_3(L)x}]_{\mathrm{IL}}}{[\mathrm{Am^{3+}}]_{\mathrm{aq}}[\mathrm{NO_3}]^{3}_{\mathrm{aq}}\,[\mathrm{L}]^{\mathrm{x}}_{\mathrm{IL}}} \tag{5.2}$$

Upon rearranging equation 5.1 results in equation 5.2

$$\log D_{Am(III)} = \log K_{ex} + 3\log[NO_3^{\ -}]_{aq} + x\ \log[L]_{IL} \tag{5.3}$$

To confirm the co-ordination and the stoichiometry of trivalent metal-ligand complex formed in ionic liquid phase, the effect of ligand concentration on the extraction of Am(III) was studied at various concentrations of nitric acid and the results are displayed in Fig. 5.10. The slope obtained from the plot of log $D_{Am(III)}$ against log [ligand] gives the number of molecules of ligand coordinated to Am(III) in the ionic liquid phase. It can be seen that the distribution ratio of Am(III) increases with increase in the concentration of ligand in the ionic liquid phase. Linear regression analysis of the extraction data results in a slope values ranging from 1.7 to 2 for all nitric acid concentrations. This shows that about two molecules of ligand is involved in the extraction of Am(III) in the ionic liquid phase.

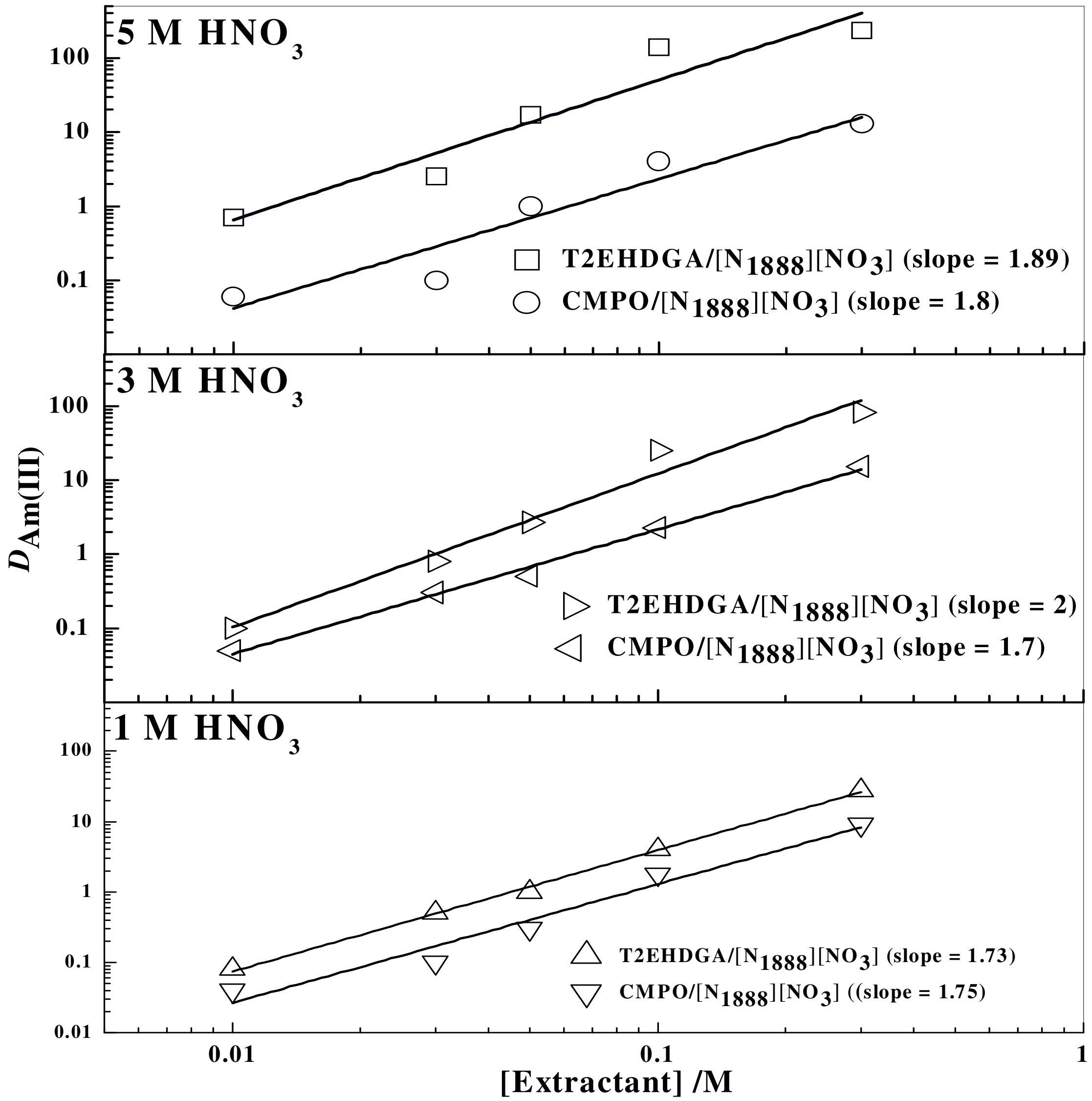

Fig. 5.10. Variation in the distribution ratio of Am(III) as a function of extractant concentration. Ionic liquid phase: 0.01–0.3 M T2EHDGA (or CMPO)/[N_{1888}][NO_3]; Aqueous phase: 3 M HNO_3 spiked with ^{241}Am tracer; Temperature = 298K; Equilibration time = 1 hour; Phase volume ratio = 1.

5.2.7. Effect of Nitrate ion concentration

Fig. 5.11. shows the variation in the distribution ratio of Am(III) in 0.1 M T2EHDGA (or CMPO)/[N_{1888}][NO_3], studied as a function of nitrate ion concentration in aqueous phase. Since T2EHDGA and CMPO are a neutral ligands, it is expected that 3 molecules of nitrate should be co-ordinated to Am(III) during the extraction of Am(III) in ionic liquid phase. From Fig. 5.11., it is observed that the distribution ratio of Am(III) increases with increase in the concentration of nitrate ion (in the form of $NaNO_3$), as expected. However, linear regression of the extraction data gave a slope value 2 instead of the expected 3. A similar behavior was also reported elsewhere [ ] when Am(III) was extracted into the ionic liquid phase containing TODGA in [N_{1888}][NO_3]. Based on this result, the plausible mechanism for the extraction of Am(III) in the ionic liquid phase as shown in equation 5.4 and 5.5.

$$([N_{1888}][NO_3])_{IL.} + HNO_{3aq.} \Leftrightarrow ([N_{1888}][NO_3]\cdot HNO_3)_{IL.} \qquad (5.4)$$

$$Am(III)_{aq.} + 2(L)_{IL.} + 2\,NO^-_{3\,aq} + H^+_{IL.} + NO^-_{3\,IL.} \Leftrightarrow [Am(L)_2(NO_3)_3]_{IL.} + H^+_{aq.} \qquad (5.5)$$

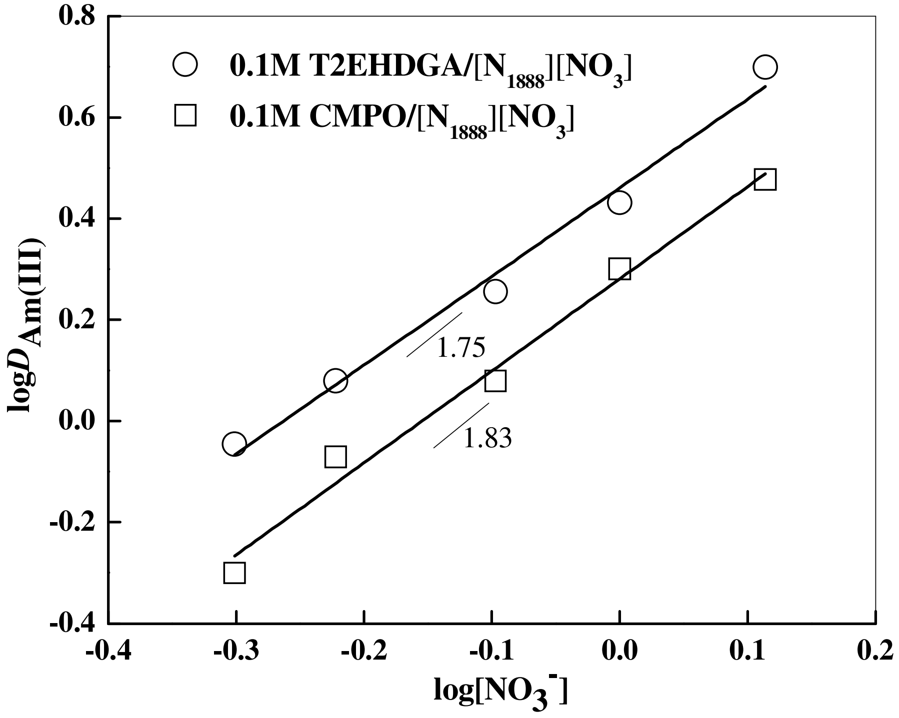

Fig. 5.11. Variation in the plot of logD_{Am} as a function of log [NO_3^-]. Ionic liquid phase: 0.1 M T2EHDGA (or CMPO)/[N_{1888}][NO_3]; Aqueous phase: 3 M HNO_3 + (0.1–0.8 M) $NaNO_3$ spiked with ^{241}Am tracer; Temperature = 298 K; Equilibration time = 1 hour; Phase volume ratio = 1.

5.2.8. Effect of radiation dose

If the ionic liquid phase is proposed for the extraction of Am(III) from HLLW, it is quite likely that the extractant molecules could undergo radiolytic degradation leading to the decrease in the distribution ratios of Am(III). The radiolytic degradation of T2EHDGA and CMPO in *n*-dodecane medium was discussed elsewhere [37-41]. It was reported that the distribution ratio of trivalent metal ion decrease significantly with increase of absorbed dose. Moreover, the presence of *n*-dodecane sensitizes or increases the degradation of T2EHDGA. Therefore, it would be interesting to understand the effect of gamma irradiation on the radiolytic degradation of T2EHDGA and CMPO present in [N_{1888}][NO_3] phase. The radiolytic degradation was studied by measuring the distribution ratio of Am(III) in the radiolytically degraded 0.1M T2EHDGA or

0.1M CMPO/ [N_{1888}][NO_3] phase. The results on the variation in the distribution ratio of Am(III) as a function of absorbed gamma dose varied upto 500 kGy is shown in Fig. 5.12. Unlike the results reported in case of *n*-dodecane, the distribution ratio of Am(III) in the degraded T2EHDGA/[N_{1888}][NO_3] and CMPO/[N_{1888}][NO_3] remains nearly constant irrespective of the absorbed dose. This indicates that T2EHDGA and CMPO in [N_{1888}][NO_3] does not seem to be affected by gamma radiation, perhaps the gamma dose seems to be absorbed essentially [N_{1888}][NO_3]. In contrast, the presence of *n*-dodecane sensitizes the degradation of the ligands co-existing with *n*-dodecane. Therefore, it appears from the degradation studies that [N_{1888}][NO_3] seem to protect the ligands co-existing in the solution and perhaps [N_{1888}][NO_3] may be undergoing sacrificial degradation.

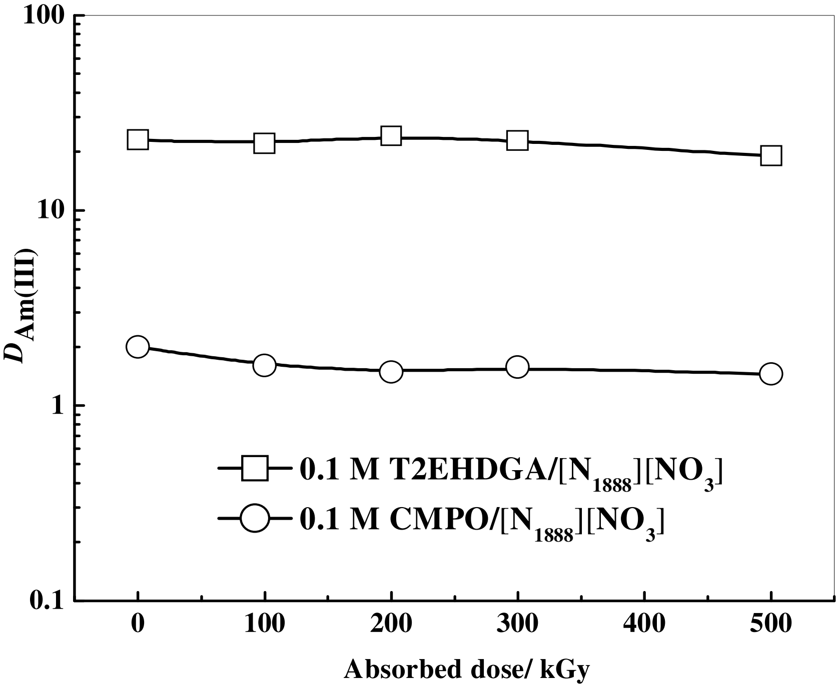

Fig. 5.12. Variation in the distribution ratio of Am(III) as a function of absorbed dose. Ionic liquid phase: 0.1 M T2EHDGA (or CMPO)/[N_{1888}][NO_3]; Aqueous phase: 3 M HNO_3 spiked with ^{241}Am tracer; Absorbed dose: 0–500 kGy; Temperature = 298 K; Equilibration time = 1 hour; Phase volume ratio = 1.

5.3. Summary

The extraction behavior of Am(III) and Nd(III) from nitric acid medium was studied in a solution of T2EHDGA or CMPO in $[N_{1888}][NO_3]$ ionic liquid and probing the ionic liquid phase to dynamic light scattering studies to understand the absence of third phase formation in these systems. The extraction of Am(III) in $[N_{1888}][NO_3]$ was negligible at all nitric acid concentrations investigated in the present study. Addition of T2EHDGA and CMPO increased in the extraction of Am(III) and the extraction trend was quite similar to *n*-dodecane. About two molecules of T2EHDGA or CMPO were involved in the extraction of Am(III) and a molecule of NO_3^- ion seem to participate in the extraction of Am(III). Even though the extraction trend of trivalent metal ion in T2EHDGA or CMPO in $[N_{1888}][NO_3]$ was similar to *n*-dodecane, it was realized that the third phase formation behavior in ionic liquid phase was significantly different. The extraction of nitric acid in ionic liquid phase was quite high and it was an order higher than the stoichiometry required for the formation of 1:1 ligand to HNO_3 protanated complex. Third phase was not observed even at the loading of 1.4 g/L Nd(III) in case of 0.1 M CMPO and 2.8 g/L of Nd(III) in case of 0.1 M T2EHDGA in $[N_{1888}][NO_3]$ medium. In contrast, the third phase formation was reported when the stoichiometry of T2EHDGA:HNO_3 exceeded 1:1.2, and after contacting the T2EHDGA or CMPO solution in *n*-dodecane with 3 M nitric acid solution containing traces of Nd(III).

To understand the absence of third phase formation in ionic liquid system, dynamic light scattering studies were performed and the results revealed that ionic liquid itself formed aggregates with the average size of 20 nm. The Addition of T2EHDGA and CMPO to $[N_{1888}][NO_3]$ increased the average aggregate size and their distribution in ionic liquid. The important understanding of the present study was that the aggregate size decreased with increase in the extraction of nitric acid in ionic liquid phase, which was observed in the presence as well as in the absence of ligands. This observation was in contrast to the conventional *n*-dodecane systems, where in the aggregate size increased with increase in the loading of nitric acid in organic phase. The decrease in the average aggregate size observed in ionic liquid phase was attributed to the reduced interaction of cations and anions of the ionic liquid phase. The increase in the concentration of ligand or loading of Nd(III) in ionic liquid phase increased the aggregation of metal-ligand complexes in ionic liquid phase. However, the third phase formation was not observed in all cases.

All these observations pointout that the polar metal-ligand aggregates are stabilized by the polar nature of $[N_{1888}][NO_3]$. The question of third phase formation did not arise in the present ionic liquid, as the size of aggregates lowered upon extraction of nitric acid. As a result, the aggregates formed in ionic liquid phase were much smaller than those observed in *n*-dodecane phase under similar conditions. Therefore, it was possible to load significant amount of Nd(III) in ionic liquid phase without the concern of third phase formation. The radiation stability of the ionic liquid phase was also studied and the results revealed that the distribution ratio of Am(III) was unaltered even at the absorbed gamma dose 500 kGy. The absence of third phase formation and the stability of the ligand towards gamma radiation in ionic liquid medium confirm that ionic liquids are promising candidates for nuclear fuel cycle applications**.**

PART 2: Aggregation behavior of ionic liquid in molecular liquid medium

5.4. Introduction

The liquid organic phase employed in a solvent extraction process is composed of a metal specific ligand diluted in an inert diluent, like *n*-dodecane [43,44]. The main purpose of the ligand is to co-ordinate with the target metal ion, and the one of the main roles of a diluent is to dissolve the ligand and make the organic phase immiscible with aqueous phase, so that the target metal is separated from the host of other metal ions present in aqueous phase. Therefore, the ligands employed in solvent extraction are designed to encompass a polar moiety, to coordinate with metal ion, as well as non-polar alkyl chain moiety to dissolve the polar ligand in a non-polar *n*-dodecane [6,7]. Since the ligands contain both polar and non-polar moieties in a molecule, they are regarded as amphiphiles. When such amphipiles are dissolved in *n*-dodecane, the ligands tend to undergo self-aggregation due to polar-polar interactions [45]. The degree of self-aggregation depends upon the polarity of the co-ordinating site and the interaction between the alkyl moiety of the ligand with *n*-dodecane. The polar-polar interactions of the ligand facilitate self aggregation, while the interaction between the alkyl group of the ligand with *n*-dodecane (known as Van der Waals interaction) facilitate, dispersion of the ligand in *n*-dodecane medium [6,7]. The extraction of metal ion into organic phase results in the co-ordination of metal ion with ligands, known as the metal-solvates. Since the metal-solvates are more polar than the ligand, the extraction of metal ions facilitates the aggregation of metal-solvates and merger of existing aggregates in organic phase [46-51]. As a result, a number of aggregates of different size are formed in organic phase and undergo distribution in organic phase.

In the two decades, room temperature ionic liquids (RTILs) have been explored as diluent in a solvent extraction procedure [52-66]. They have been suggested as an alternative to n-dodecane. RTILs are organic salts molten at temperatures lower than or equal to 373 K [52]. The studies reported in literature show that the traditional ligands in conjunction with room temperature ionic liquids exhibit extraordinary extraction of metal ions from aqueous phase [53]. In addition, RTILs are reported to prevent the undesirable event in a solvent extraction procedure, namely the third phase formation during the course of extraction [18,19], since the polar nature of RTILs stabilize the polar metal-ligand complexes formed in organic phase. Literature reports also indicate that ionic liquid containing quaternary ammonium cation associated with a strongly hydrophobic anion has been developed and exploited for various applications in the separation of actinides and lanthanides from nitric acid solutions [64-66]. Unlike the conventional imidazolium ionic liquids, the properties of these ammonium ionic liquids associated with hydrophobic anions are very unique. For instance, these ammonium cation and the hydrophobic anion based ionic liquids which is used in the present study, are again strongly polar, yet they are miscible in *n*-paraffins [64]. The miscibility of ammonium ionic liquids in *n*-dodecane has been exploited for various applications in nuclear fuel cycle, since *n*-dodecane has been accepted as a diluent in nuclear fuel cycle application [60-64].

In this context, we also exploited the miscibility of quaternary ammonium ionic liquid containing hydrophobic anion such as tri-*n*-octylmethylammonium bis(2-ethylhexyl)phosphate [N_{1888}][D2EHP] and tri-*n*-octylmethylammonium bis(2-ethylhexyl)diglycolamide [N_{1888}][DGA], in *n*-dodecane phase, and studied the extraction behavior of Eu(III) from nitric acid medium [60]. Similarly, the [N_{1888}][D2EHP] was explored as phase modifier to modulate the extraction properties of the PUREX solvent, namely 1.1 M tri-*n*-butylphosphate (TBP) in *n*-DD for the extraction of uranium and plutonium [16]. Even though a large number of quaternary ammonium ionic liquids, or in general ionic liquids, have been explored for the extraction of actinides and fission products, the aggregation behavior of ionic liquid in *n*-dodecane and how the aggregation pattern changes upon nitric acid and metal ion extraction in to ionic liquid phase has not been explored so far. Understanding the aggregation behavior of organic phase is very much essential for understanding the insights of solvent extraction and third phase formation [48,49]. In view of this, the present paper deals with the investigations on the aggregation behavior of $[N_{1888}]$[D2EHP] in *n*-dodecane medium. The aggregation behavior of $[N_{1888}]$[D2EHP] has been studied as a function of various parameters such as concentration of $[N_{1888}]$[D2EHP] in *n*-DD, aqueous phase nitric acid and Nd(III) concentration etc. The results obtained from these studies are reported in this part of chapter 5.

In view of this, the results on the aggregation behavior of $[N_{1888}]$[D2EHP]/n-DD was studied as a function of various experimental parameters such as concentration of $[N_{1888}]$[D2EHP], feed acidity, concentration of metal ion in the aqueous phase and temperature etc. is reported in this chapter.

Experimental details for the present chapter (part 2) are presented in the section 2.5.5 of the chapter 2. The synthesis of ionic liquid is discussed in section 2.6.9 of chapter 2 respectively.

Table. 5.2. Structure of ionic liquid used in part II of chapter 5

Name	Structure
Ionic liquid	
Methyl-tri-*n*-octyl ammonium bis(2-ethylhexyl) phosphate $[N_{1888}][D2EHP]$	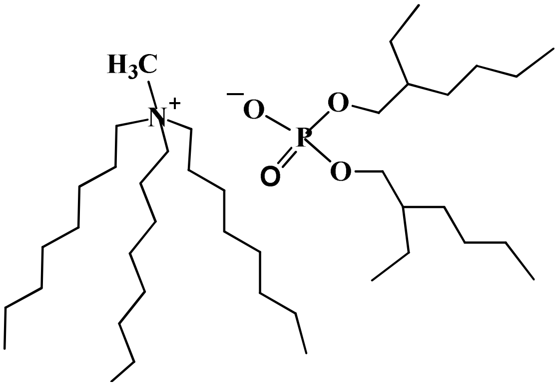

5.5. Results and discussions

5.5.1. Aggregation behavior of $[N_{1888}][D2EHP]$ in n-DD

Room temperature Ionic liquids completely comprise ions [16,17]. When ionic liquids are dissolved in a non-polar medium, such as *n*-dodecane, they tend to undergo aggregation due to the interaction between the cations and anions of the ionic liquid. In addition, the non-polar nature of *n*-dodecane favours the mutual interaction between the ions present in the ionic liquid. The aggregation behavior of $[N_{1888}][D2EHP]$ in *n*-DD at various concentrations of $[N_{1888}][D2EHP]$ is shown in Fig. 5.13. It can be seen that the intensity of aggregates and their distribution in *n*-DD increases with increase in the concentration of $[N_{1888}][D2EHP]$ in *n*-DD. The average aggregate size increases from 0.7 nm at 0.01 M $[N_{1888}][D2EHP]$ to 18 nm at 0.1 M $[N_{1888}][D2EHP]$. A 30-fold increase in the average aggregate size is observed for the 10-fold increase in the concentration of $[N_{1888}][D2EHP]$/*n*-DD. The intensity and FWHM of aggregates initially increases with increase in the concentration of $[N_{1888}][D2EHP]$, and above 0.07 M

[N_{1888}][D2EHP] in *n*-DD the increase in intensity of aggregates is small, where as the FWHM increases significantly with increase in the concentration of [N_{1888}][D2EHP].

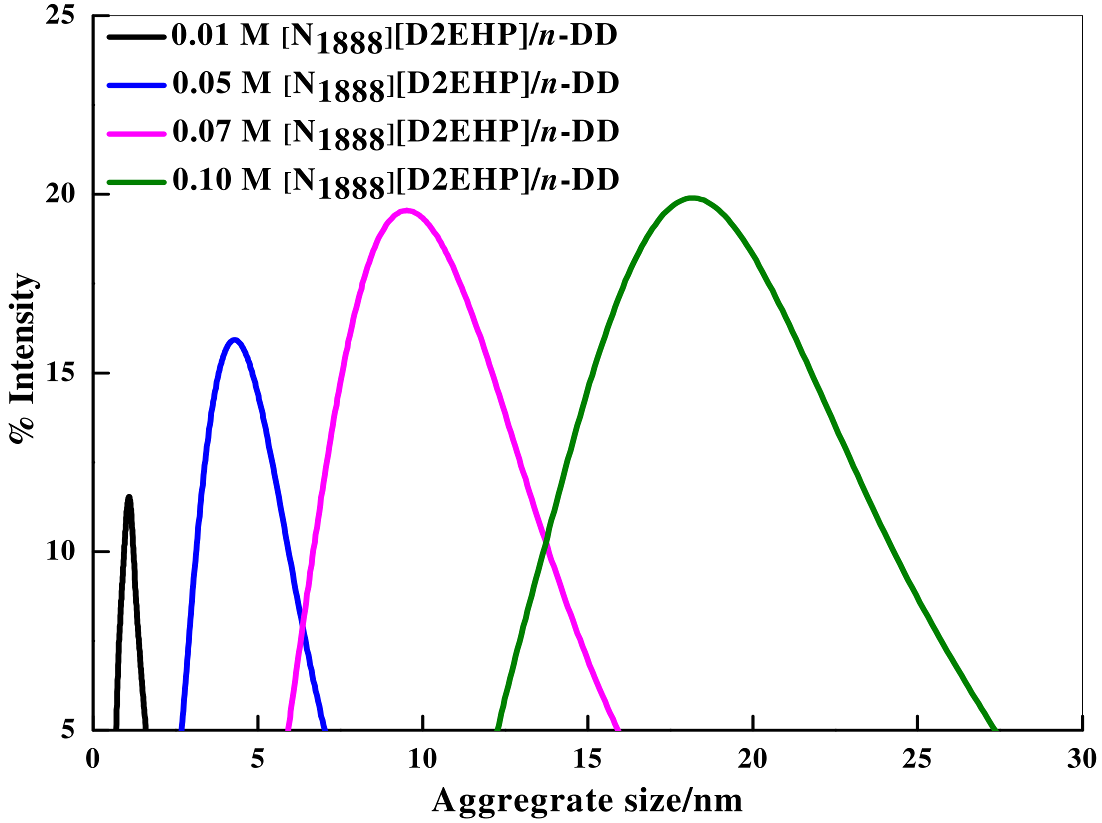

Fig. 5.13. Variation in the aggregate size as a function of the concentration of [N_{1888}][D2EHP] in *n*-dodecane. Organic phase: 0.01 – 0.1 M [N_{1888}][D2EHP] in *n*-DD; Temperature = 298 K.

5.5.2. Effect of [HNO_3] on aggregation of organic phase

The ionic liquid [N_{1888}][D2EHP] was proposed for the mutual separation of lanthanides and actinides from dilute nitric acid medium ranging from 10^{-3} M to 0.5 M [16]. When ionic liquid phase is contacted with aqueous phase, it is quite likely that significant amount of nitric acid could be extracted into the organic phase and the aggregation behavior of organic phase is therefore, likely to change with respect to the concentration of nitric acid. The extraction behavior of nitric acid in a solution of 0.05 M [N_{1888}][D2EHP]/*n*-DD is shown in Fig. 5.14. It can be seen that the extraction of nitric acid increases with increase in the concentration of nitric acid in aqueous phase.

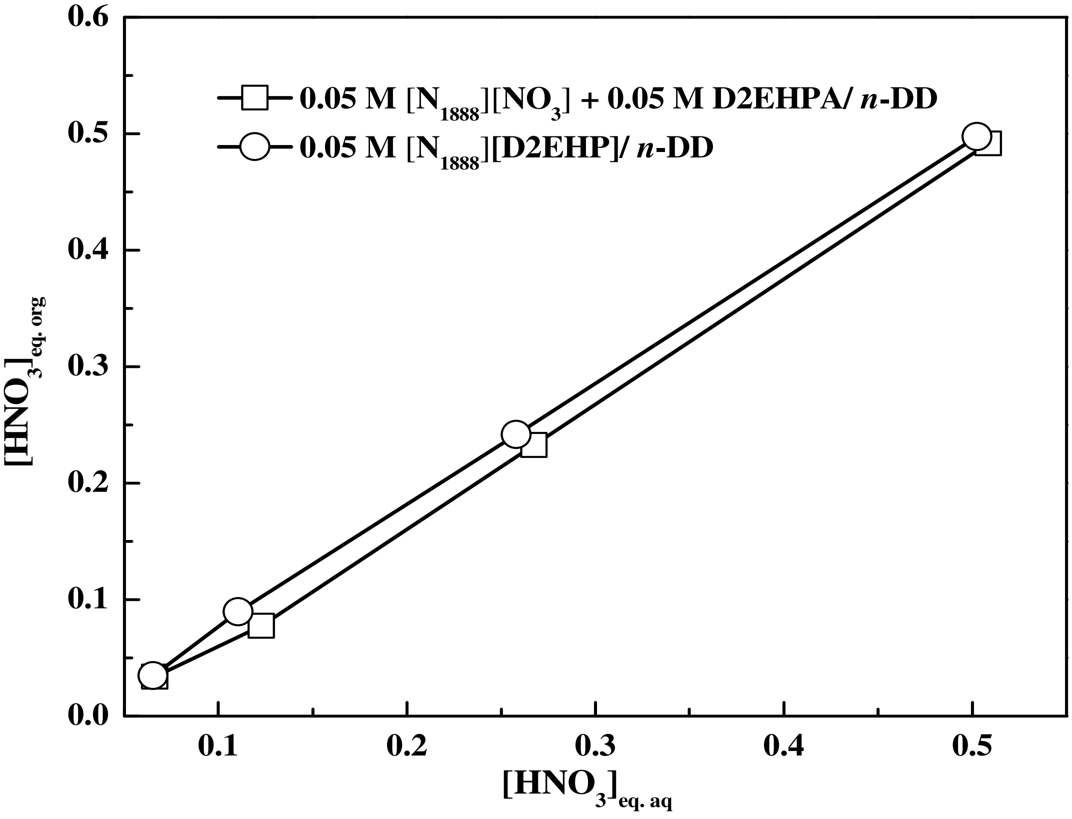

Fig. 5.14. Acid extraction by [N_{1888}][D2EHP] and the mixture of its precursors. Organic phase: 0.05 M [N_{1888}][D2EHP] (0.05 M [N_{1888}][NO_3] + 0.05 M D2EHPA)/*n*-DD; Aqueous phase: 0.01 to 0.5 M; Equilibration time = 1 hour; Temperature = 298 K.

The concentration of nitric acid extracted into organic phase is about 0.05 M, when the equilibrium concentration of nitric acid is 0.1 M and the concentration of nitric acid in organic phase reaches a value of 0.4 M, when the equilibrium concentration of nitric acid in aqueous phase is 0.43 M. The extracted nitric acid present in organic phase can react with [N_{1888}][D2EHP] and convert [N_{1888}][D2EHP] into its precursors namely tri-*n*-octylmethylammonium nitrate

($[N_{1888}][NO_3]$) and bis(2-ethylhexyl)phosphoric acid (D2EHPA) by the reaction shown in equation 5.6 was reported in the literature [53,54]. It should be noted that bis(2-ethylhexyl)phosphoric acid is represented as D2EHPA and its conjugate anion is represented as D2EHP. Fig. 5.15. also shows the variation in the acid extraction of the precursors 0.05 M $[N_{1888}][NO_3]$ + 0.05 M D2EHPA in *n*-dodecane. It can be seen that the extraction values are comparable with that of 0.05 M $[N_{1888}]$[D2EHP]/*n*-DD.

$$[N_{1888}][\text{D2EHP}] + HNO_3 \Leftrightarrow [N_{1888}][NO_3] + \text{D2EHPA} \tag{5.6}$$

The ease of reaction shown in equation 5.6 depends upon the concentration of nitric acid and the pK_a of D2EHPA. In view of the formation of $[N_{1888}][NO_3]$ and D2EHPA, it is quite likely that the aggregation behavior of the organic phase could change after contacting with nitric acid. Therefore, the aggregation behavior of 0.05 M $[N_{1888}]$[D2EHP]/*n*-DD after contacting the organic phase with nitric acid was studied and the results are shown in Fig. 5.15. The concentration of nitric acid was varied from 10^{-3} M to 0.5 M. It can be seen that the average aggregate size increases with increase in the concentration of nitric acid in aqueous phase. The increase in average aggregate size could be attributed to the increase in the extraction of nitric acid. The extracted nitric acid then reacts with $[N_{1888}]$[D2EHP] resulting in the formation of the precursors namely $[N_{1888}][NO_3]$ and D2EHPA, by the reaction shown in equation 5.6 and these precursors seem to associate together, forming an adduct as shown in Fig. 5.16. It should be noted the average size of adduct is expected to be more than the average molecular size of ionic liquid. In view of this, the aggregate size determined in organic phase after contacting with nitric acid is more. Increasing the concentration of nitric acid increases the adduct formation and their mutual interaction between adducts. Therefore, the average aggregate size observed in organic phase increases with increase in the concentration of nitric acid in aqueous phase.

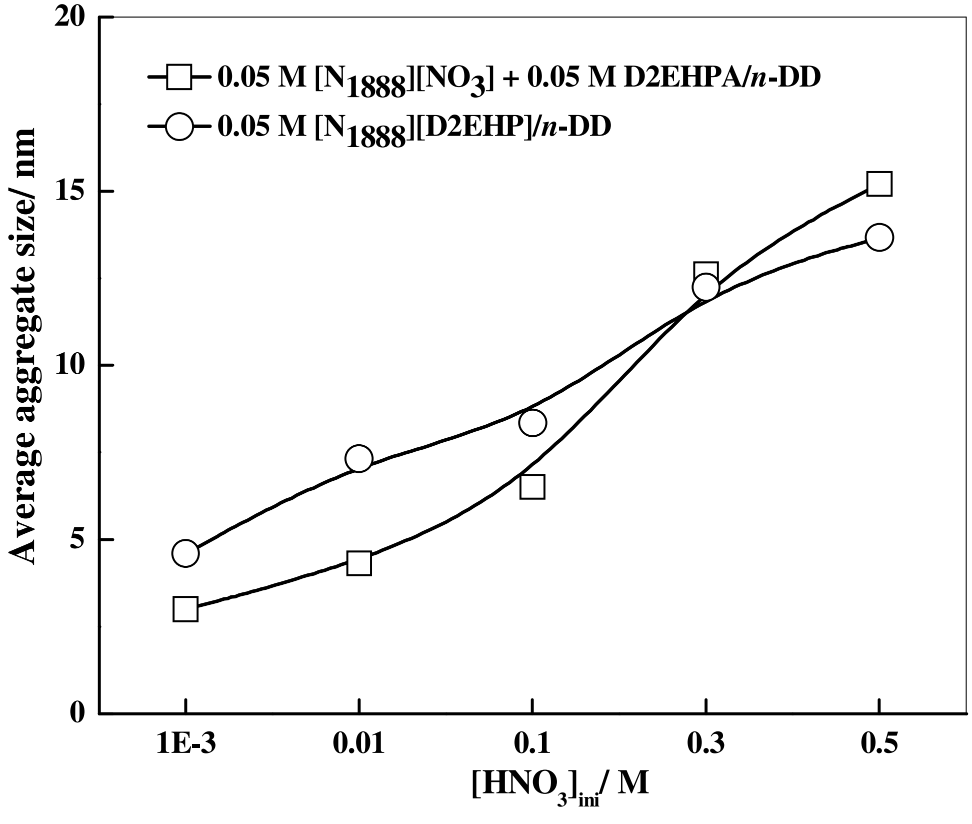

Fig. 5.15. Variation in the aggregate size as a function of the concentration of nitric acid. Organic phase: 0.05 M $[N_{1888}]$[D2EHP]/*n*-DD or 0.05 M $[N_{1888}][NO_3]$+0.05 M D2EHPA /*n*-DD ; Aqueous phase: 0.001 - 0.5 M HNO_3; Equilibration time = 1 hour; Temperature = 298 K.

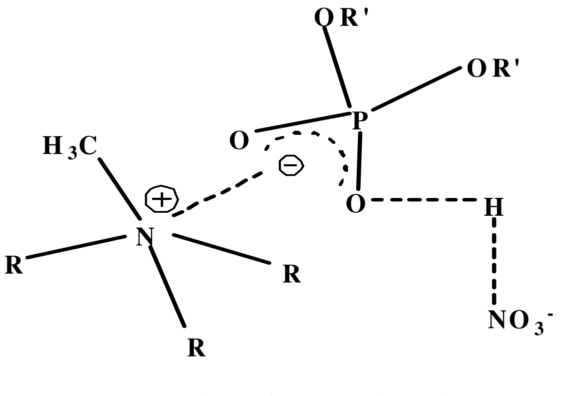

(R = Octyl; R' = 2(ethyl)hexyl)

Fig. 5.16. Proposed structure of adduct formation upon nitric acid extraction by $[N_{1888}]$[D2EHP].

Furthermore, the extraction of water could be accompanied by the extraction of nitric acid depending upon the concentration of nitric acid present in aqueous phase. For this purpose, the amount of water content present in the 0.05 M [N_{1888}][D2EHP]/*n*-DD phase was measured as a function of nitric acid concentration. The water content in 0.05 M [N_{1888}][D2EHP]/*n*-DD, obtained after extraction, decreases from 0.42 wt% to 0.02 wt% with the increase in the concentration of nitric acid from 0.001 M to 0.5 M. At low nitric acid concentrations, ionic liquid organic phase exits in the form of [N_{1888}][D2EHP]. Since the ionic liquid is completely comprising of ions, some amount of water (0.42 wt%) is extracted in to organic phase for hydration. As the concentration of nitric acid is increased, the adduct formation, shown in Fig. 5.16. increases, and since the size of the adduct is higher than [N_{1888}][D2EHP], as discussed above (Fig. 5.16.), the water required for hydration in organic phase decreases. Moreover, when the concentration of nitric acid in aqueous phase is more than the concentration of ionic liquid (that is above 0.05 M nitric acid), the ionic strength is more in aqueous phase. Under such conditions, the water is retained in aqueous phase. Therefore, the water content in 0.05 M [N_{1888}][D2EHP]/*n*-DD phase, obtained after extraction, decreases with the increase in the concentration of nitric acid.

5.5.3. Aggregation of precursors of [N_{1888}][D2EHP]

It is learnt that any factor that increases the concentration of [N_{1888}][NO_3] and D2EHPA (equation 5.6) increases the formation of adduct. The adduct formation between [N_{1888}][NO_3] and D2EHPA can be studied by the measurement of aggregate size at a fixed concentration of [N_{1888}][NO_3] while varying the concentration of D2EHPA vice versa. The results on the aggregation behavior of a solution of [N_{1888}][NO_3] + D2EHPA/*n*-DD are shown in Fig. 5.17. The concentration of [N_{1888}][NO_3] was fixed at 0.05 M and the concentration of D2EHPA was varied from 0.01 to 0.1 M in Fig. 5.17a. It can be seen that average aggregate size increases with increase in the concentration of D2EHPA. A similar behavior is also observed (Fig. 5.17b) when the concentration of D2EHPA is fixed at 0.05 M and the concentration of $[N_{1888}][NO_3]$ is varied from 0.01 to 0.1 M. However, it should be noted that the intensities observed in Fig. 5.17a and Fig. 5.17b. are quite different since the individual concentrations of D2EHPA and $[N_{1888}][NO_3]$ employed in the solution are different and therefore their aggregation behavior in the solution is also different. It is interesting to note that the intensity of aggregate is higher, when the concentration of $[N_{1888}][NO_3]$ and D2EHPA are equal. This indicates the aggregates of the particular type namely $[N_{1888}][NO_3]$- - -D2EHPA (Fig. 5.16) are formed in significant abundance at this concentration.

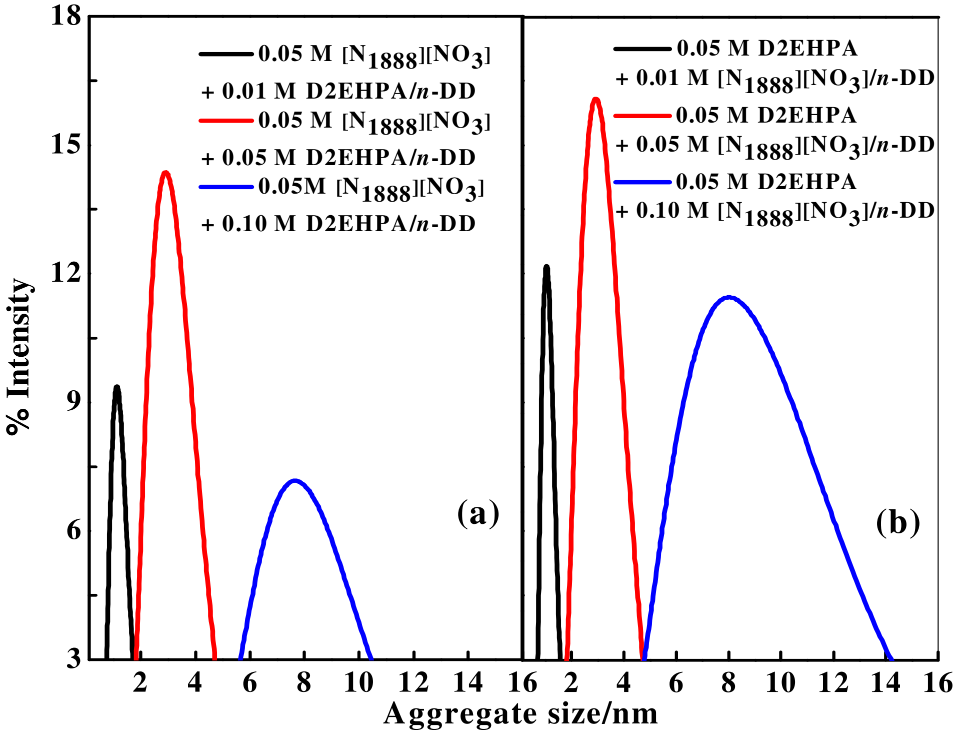

Fig. 5.17. Variation in the aggregate size as a function of the concentration of precursors. Organic phase: $[N_{1888}][NO_3]$ + D2EHPA/*n*-DD; Temperature = 298 K.

5.5.4. Aggregation behavior of Nd(III) extracted ionic liquid phase

Since [N_{1888}][D2EHP] is soluble in *n*-DD, a number of studies have been reported in literature on the extraction of Ln(III)/An(III) from dilute nitric acid medium in the solution of [N_{1888}][D2EHP] in *n*-DD [ ]. Therefore, it is essential to understand the aggregation behavior of the extracted phase containing lanthanide ion. For this purpose, the extraction of the lanthanide representative, Nd(III) ion, was carried out in a solution 0.05 M [N_{1888}][D2EHP]/*n*-DD from nitric acid medium and the organic phase obtained after extraction was subjected to DLS measurements. The average aggregate size obtained from DLS measurements was plotted as a function of nitric acid concentration in aqueous phase is shown in Fig. 5.18. The aggregate size was compared with those obtained in the absence of Nd(III) in ionic liquid phase, i.e., the average aggregate of 0.05 M [N_{1888}][D2EHP]/*n*-DD obtained after containing the ionic liquid phase with nitric acid medium alone. It can be seen that the aggregate size of Nd(III) extracted ionic liquid phase was marginally higher than those obtained in the absence of Nd(III) and the average aggregate size increases with increase in the concentration of nitric acid in ionic liquid phase. This indicates that the extraction of Nd(III) and nitric acid in ionic liquid phase facilitates the aggregation of [N_{1888}][D2EHP] in *n*-DD phase.

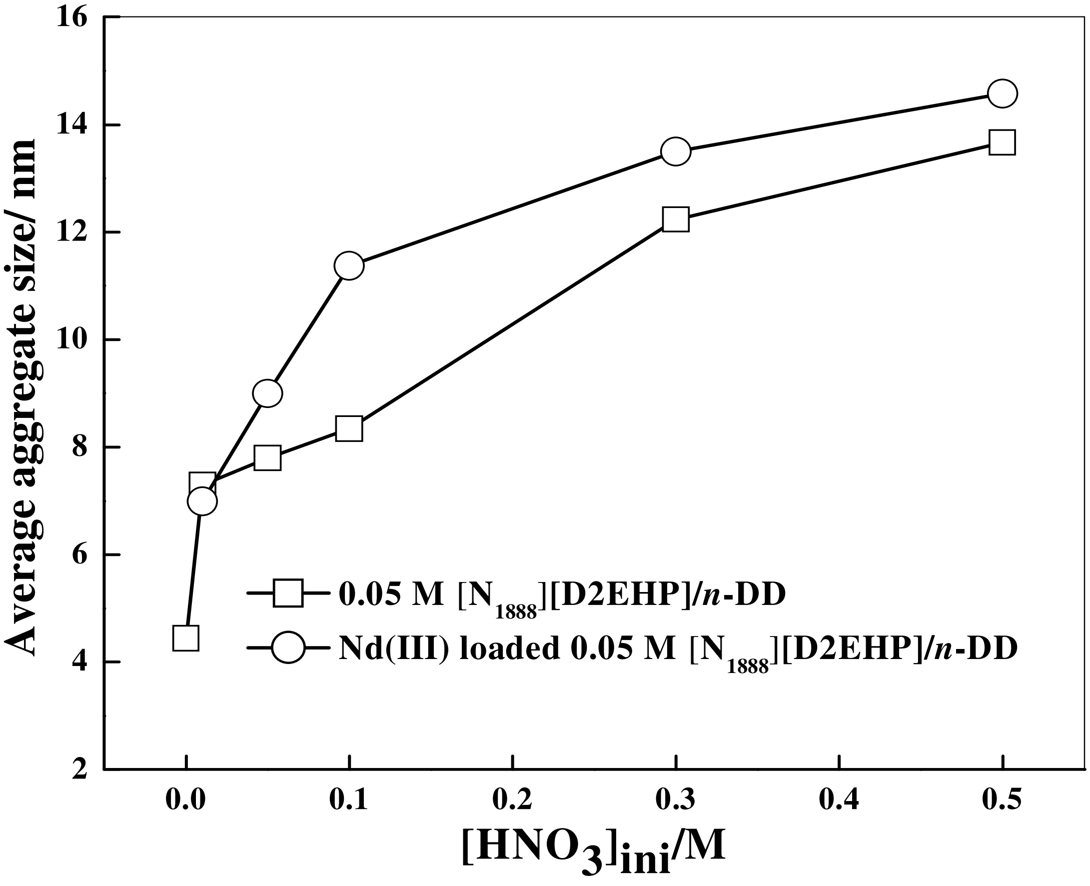

Fig. 5.18. Variation in the average aggregate size as a function of initial concentration of nitric acid in aqueous phase. Organic phase: 0.05M $[N_{1888}]$[D2EHP] in *n*-DD; Aqueous phase: 0.001 to 0.5 M HNO_3 + 1 g/L Nd(III); Equilibration time = 1 hour; Temperature = 298 K.

Fig. 5.19. shows the aggregation behavior of 0.05 M $[N_{1888}]$[D2EHP]/*n*-DD obtained after contacting the ionic liquid phase with a solution of Nd(III) in a 0.1 M nitric acid. The concentration of Nd(III) in aqueous phase was varied from 1 g/L to 5 g/L. It can be seen that the average aggregate size increases with increase in the loading Nd(III) in organic phase. The average aggregate size increases from 4.2 nm in case of 0.05 M $[N_{1888}]$[D2EHP]/*n*-DD before equilibration, to 20 nm upon contacting the organic phase with 5 g/L Nd(III) in 0.1 M nitric acid. This could be due to the increase in loading of Nd(III) with increase in Nd(III) concentration in

aqueous phase. The amount of Nd(III) loaded in the organic phase upon equilibration is given in the parenthesis in Fig. 5.19. The results show that the co-ordination of Nd(III) with [N_{1888}][D2EHP] seems to increase the polarity of organic phase and facilitates the aggregation. In addition to the increase in average aggregate size, the aggregate size distribution also increases with increase in the loading of Nd(III) in organic phase. This indicates a large number of aggregates of different sizes are formed upon Nd(III) extraction in organic phase.

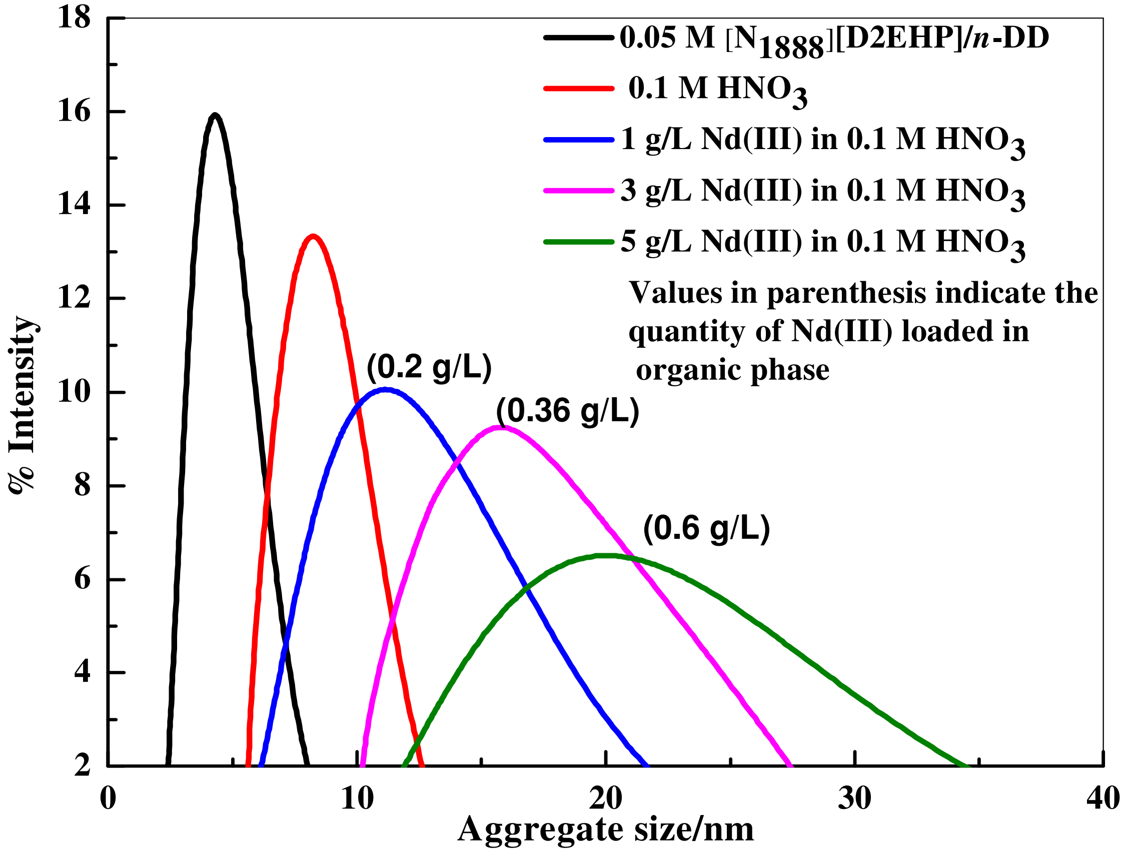

Fig. 5.19. Variation in the aggregate size as a function of the concentration of Nd(III) in aqueous phase. Organic phase: 0.05 M [N_{1888}][D2EHP] in *n*-DD; Aqueous phase: 0.1 M nitric acid and Nd(III) in 0.1 M HNO_3; Equilibration time = 1 hour; Temperature = 298 K.

5.5.5. Effect of Temperature on aggregation

Fig. 5.20. shows the aggregation behavior of 0.05 M [N_{1888}][D2EHP]/*n*-DD as a function of temperature. It can be seen that the aggregate size and aggregate decreases with increase of temperature, as expected [6,7]. This could be due to increase in the dispersion of [N_{1888}][D2EHP] in *n*-DD phase with increase of temperature.

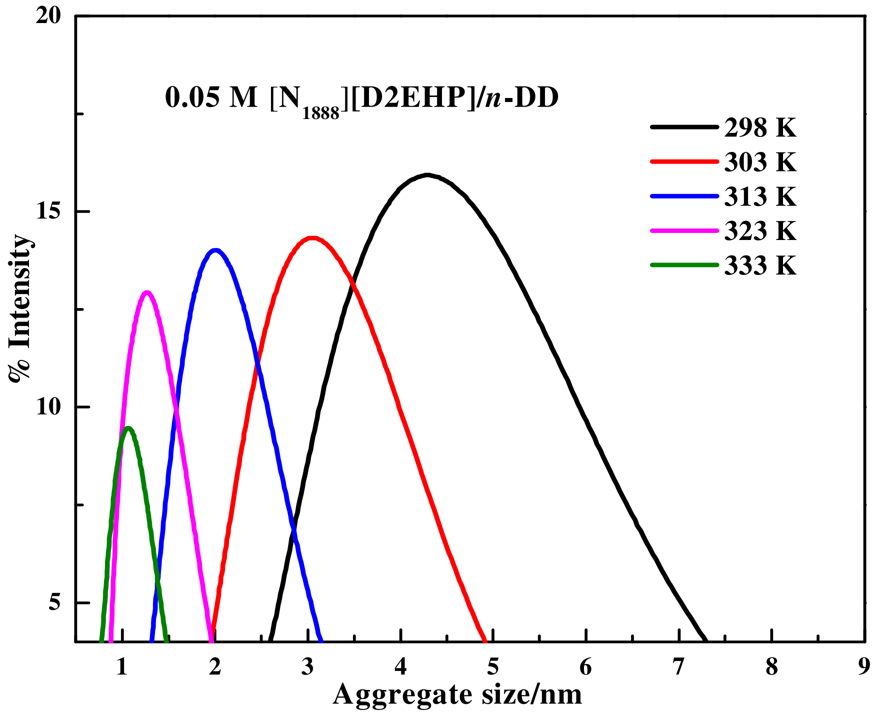

Fig. 5.20. Variation in the aggregate size as a function of temperature. Organic phase: 0.05 M [N_{1888}][D2EHP] in *n*-DD; Temperature = 298-333 K.

5.6. Summary

The dynamic light scattering studies were performed in an ionic liquid phase containing [N_{1888}][D2EHP] in *n*-dodecane. The results revealed that [N_{1888}][D2EHP] undergo aggregation in *n*-dodecane medium, due to the interaction between the cation and anion of the ionic liquid. A 30 fold increase in the average aggregate size was observed with 10-fold increase in the concentration of [N_{1888}][D2EHP]. Beyond 0.07 M concentration of [N_{1888}][D2EHP] in *n*-dodecane, the aggregate distribution in *n*-dodecane phase was more. Contacting the *n*-dodecane phase containing [N_{1888}][D2EHP] with nitric acid resulted in the formation of its precursor namely, [N_{1888}][NO_3] and D2EHPA. These precursors seem to associate together and forms an adduct. In view of the formation of adduct, the aggregate size determined after contacting with nitric acid was more. Since, the precursors enhance the formation of adduct, the addition of one component of the precursor increases the adduct formation, and the aggregates of particular type (1:1 adduct) was maximum, when the concentration of precursors were equal. Increasing the loading of Nd(III) increased the average aggregate size as well as the aggregate distribution. However, the increase of temperature decreased the average aggregate size due to dispersion of [N_{1888}][D2EHP] in *n*-dodecane.

PART 3: Normalized polarity indices of tri-*n*-butyl phosphate complexes in ionic liquid using Reichardt's dye as polarity probe

5.7. Introduction

Liquid-liquid extraction has been adopted for the separation of target metal ion from aqueous solution. In this method, the organic phase is contacted with the aqueous phase containing the target metal and other interfering metal ions in a acidic solution. The organic phase is usually composed of a ligand known as an extractant dissolved in a hydrophobic media, known as the diluent. The diluent is usually the *n*-paraffin (*n*-dodecane) or alkyl substituted aromatics [67,68]. The purpose of the ligand is to coordinate with the target metal ion present in aqueous phase and facilitate the mass transfer of target metal ion into organic phase. Therefore, the ligands employed for liquid-liquid extraction contain organic polar functional groups such as phosphoryl (>P=O) and amidic (R_2N-C=O) groups covalently linked to the hydrophobic alkyl group. The objective of diluents is to dissolve the ligand in organic phase and make the organic phase strongly hydrophobic (immiscible with aqueous phase) such that the target metal is separated from aqueous phase upon liquid-liquid extraction. Another important role of the diluent is to stabilize the polar metal-ligand complex formed upon extraction in organic phase to avoid undesirable third phase formation. Since the diluent is strongly hydrophobic and the metal-ligand complex present in the organic phase is polar, the complex tends tend to undergo reverse micellar aggregation in organic phase depending upon the degree of loading of metal ion in organic phase [69,70]. Extensive aggregation of reverse micelles results in the splitting of organic phase into two phases, known as a third phase formation, which can occur during the course of solvent extraction [5,71].

In the last couple of decades, room temperature ionic liquids (RTILs) have been explored as diluents in liquid-liquid extraction [72-79]. The third phase formation in ionic liquid systems have not been observed or reported so far, which is otherwise observed in *n*-dodecane diluents. In view of this, a number of studies have been reported in literature that use ionic liquid as diluent during the extraction of lanthanides and actinides using the customary ligands that are prone to form third phase in n-dodecane medium upon metal ion extraction [74-78]. The stability of the polar metal-ligand complex in ionic liquid phase depends upon the degree of interaction between the ionic liquid and metal-ligand complex, which in turn depends upon the polarity of the ionic liquid medium, as discussed in part 1 and part II of chapter 5. The polarity of the organic compound can be regarded as the overall solvation capability or solvation power of the organic compound in stabilizing the metal-ligand complex in organic phase [80-82]. The solvation capability depends upon the specific and nonspecific interactions, intermolecular interactions of metal-ligand complex and metal-ligand-solvent in organic phase. Since ionic liquids are comprised entirely of ions, when ionic liquid serves as a diluents in organic phase, it could dramatically increase polarity of organic phase. Determining the polarity of the organic phase is a challenging job and so far only indirect methods have been suggested for measuring the polarity of the medium [82-86]. Among the various methods the most easiest method is to use solvatochromic probes such as pyridinium-N-phenolate betaine dye, known as Reichardt's dye N(30) or solvatochromic betaine dye, for the measurement of polarity of the medium [84,85]. The Reichardt's dye exhibits the maximum absorption (λ_{max}) in the visible region and depending upon the polarity of medium the position of λ_{max} is different. In the recent past several reports are available dealing with the determination of the normalized polarity values of RTILs using Reichardt's dye as solvatochromic probe [84]. However the polarity of the organic solution containing the nitric acid in ionic liquid, ligand in ionic liquid, and metal-ligand complexes in ionic liquid medium etc. have not been explored so far. In fact, the polarity of the organic phase obtained after liquid-liquid extraction is important for understanding the insights of solvent extraction as well as third phase formation discussed above. The ionic liquids employed for extraction and polarity measurements were N-butyl-N-methyl imadazoliumbis(trifluoromethylsulfonyl)imide [C_4mim][NTf_2], N-butyl-N-methyl pyrrolidinium bis(trifluoromethylsulfonyl)imide [C_4mpyr][NTf_2], N-butyl-N-methyl pipyridinium bis(trifluoromethylsulfonyl)imide [C_4mpip][NTf_2]. Since these ionic liquids were used as diluents in the extraction of actinides using trialkyl phosphates [72], the polarity of organic phase was measured as a function of concentration of ionic liquid, aqueous phase nitric acid concentration, metal ion concentration in ionic liquid phase etc.

Therefore, the results on the polarity index of ionic liquid phase was studied as a function of various experimental parameters such as concentration of ionic liquid, feed acidity, concentration of metal ion in the ionic liquid phase etc. is reported in this chapter.

Experimental details for the present chapter (part 3) are presented in the section 2.5.6 of the chapter 2. The synthesis of ionic liquids are discussed in section 2.6.1, 2.6.2 and 2.6.3 of chapter 2 respectively.

Table. 5.3. Structure of extractant and ionic liquid used for the present study.

Name	Structure
Solvatochromic probe	
Reichardt's dye	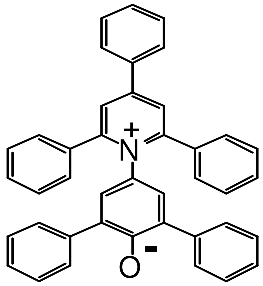
Extractant	
Tri-*n*-butyl phosphate	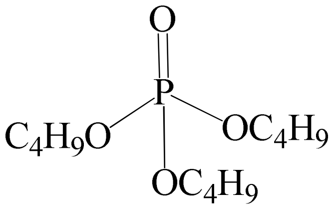
Ionic liquid	
1-Butyl-3-methylimidazolium bis(trifluoromethylsulfonyl)imide	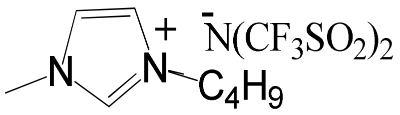
1-Butyl-1-methylpyrrolidinium bis(trifluoromethylsulfonyl)imide	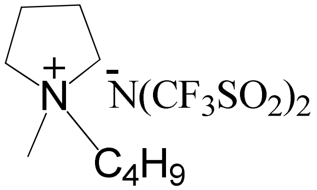
1-Butyl-1-methylpiperdinium bis(trifluoromethylsulfonyl)imide	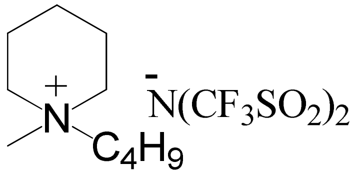

5.8. Results and discussions

5.8.1. Polarity of ionic liquid

Room temperature ionic liquids comprise entirely of ions. When a small quantity of ionic liquid is added to the organic solvent such as acetonitrile, alcohol etc. the polarity of the organic medium is affected dramatically by the interaction occuring between the ionic liquid and solvent medium [86]. Fig. 5.21. shows the visible absorption spectrum of Reichardt's dye in acetonitrile medium in presence and absence of ionic liquids such as $[C_4mim][NTf_2]$, $[C_4mpyr][NTf_2]$ and $[C_4mpip][NTf_2]$. The concentration of ionic liquid in the solution was varied from to 0.02 to 0.35 M. It is observed that the addition of ionic liquid in acetonitrile shifts the λ_{max} hypsochromically (blue shift) with increasing the concentration of ionic liquid [82]. From the measurement of λ_{max} the dimension less normalized polarity value (E_T^N) was determined using equations 5.7 and 5.8 and the values are displayed in Fig. 5.22. as a function of ionic liquid concentration. It can be seen that E_T^N increases with increase in the concentration of ionic liquid in acetonitrile. The normalized polarity of acetonitrile was determined to be 0.472 which was in good agreement with E_T^N value reported in literature [82]. Addition of 0.35 M ionic liquid increases the E_T^N 0.472 to 0.566 for $[C_4mim][NTf_2]$. Similarly for $[C_4mpyr][NTf_2]$, E_T^N increases from 0.472 to 0.506, and for $[C_4mpip][NTf_2]$ from 0.472 to 0.506. It is interesting to note that the E_T^N values follows the order $[C_4mim][NTf_2] > [C_4mpyr][NTf_2] > [C_4mpip][NTf_2]$. Higher polarity observed in case of $[C_4mim][NTf_2]$ is due to presence of π-electrons in the imidazolium ring which seems to polarize the medium in which it is present. The reason for the higher E_T^N value for $[C_4mpyr][NTf_2]$ as compared to $[C_4mpip][NTf_2]$ perhaps could be due to small size of pyrrolidinium cation, which seems to induce more polarity changes in the medium.

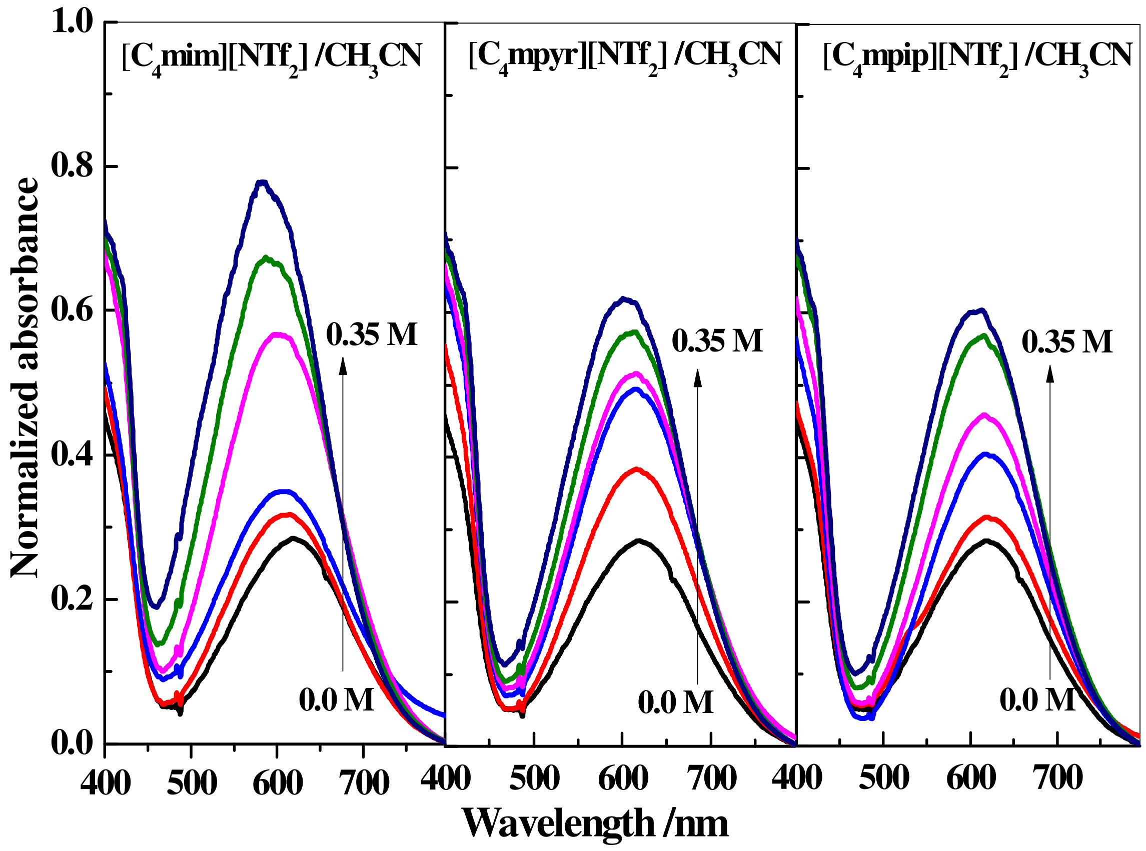

Fig. 5.21. Visible absorption spectra of ionic liquid phase as a function of the concentration of ionic liquid. Ionic liquid phase: 0.02-0.35 M ionic liquid in acetonitrile containing Reichardt's dye; Temperature = 298 K.

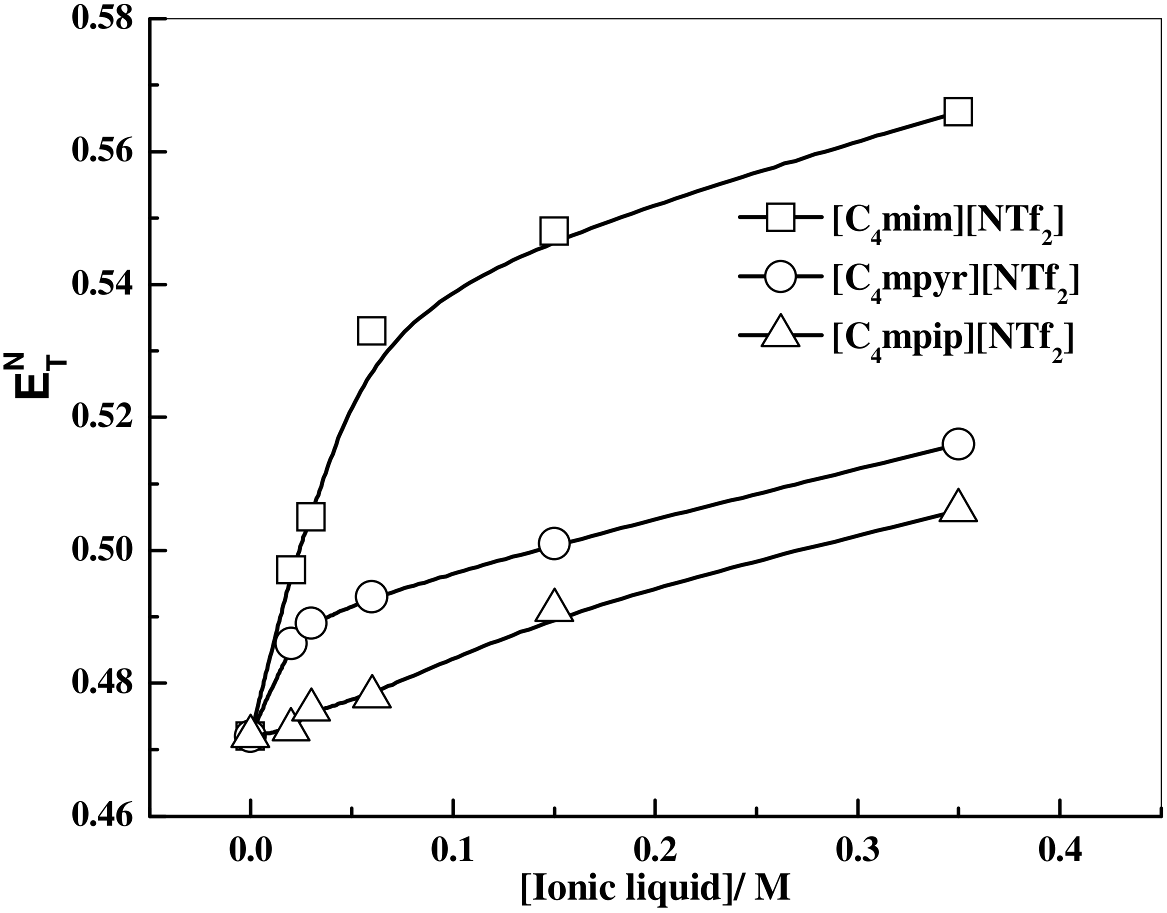

Fig. 5.22. Variation in the polarity as a function of the volume of ionic liquid. Ionic liquid phase: 0.02-0.35 M ionic liquid in acetonitrile ; Temperature = 298 K.

The magnitude of normalized polarity value also depends upon the presence of foreign cation and anions present in the medium. Fig. 5.23. shows the variation in E_T^N of [C$_4$mim][NTf$_2$] as a function of 1-butyl-3-methylimadazolium chloride [C$_4$mim][Cl] and lithiumbis(trifluoromethylsulfonyl)imide (LiNTf$_2$) concentration. In [C$_4$mim][Cl] the cation is same as that present in [C$_4$mim][NTf$_2$] but anion is different and in LiNTf$_2$ the cation is different. It is interesting to note that the addition of [C$_4$mim][Cl] decreases the E_T^N of [C$_4$mim][NTf$_2$]. In literature the E_T^N value of [C$_4$mim][Cl] is reported to be significantly lower than that observed for [C$_4$mim][NTf$_2$] [82]. Therefore, the addition of [C$_4$mim][Cl] to [C$_4$mim][NTf$_2$] decreases the polarity with increase in the concentration of [C$_4$mim][Cl], perhaps due to the weighted average of their polarity values. In addition the presence of Cl$^-$ ion in ionic liquid is reported to form hydrogen bonding with imadazolium C$_2$-H atom as shown in Fig. 5.23. As a result, the polarity induced in the medium decreases and E_T^N values of ionic liquid phase decreases with addition of [C$_4$mim][Cl] [87]. In contast, LiNTf$_2$ contains a smaller cation (Li$^+$) induces more polarity to the ionic liquid phase and therefore the E_T^N value increases with increase in the concentration of LiNTf$_2$.

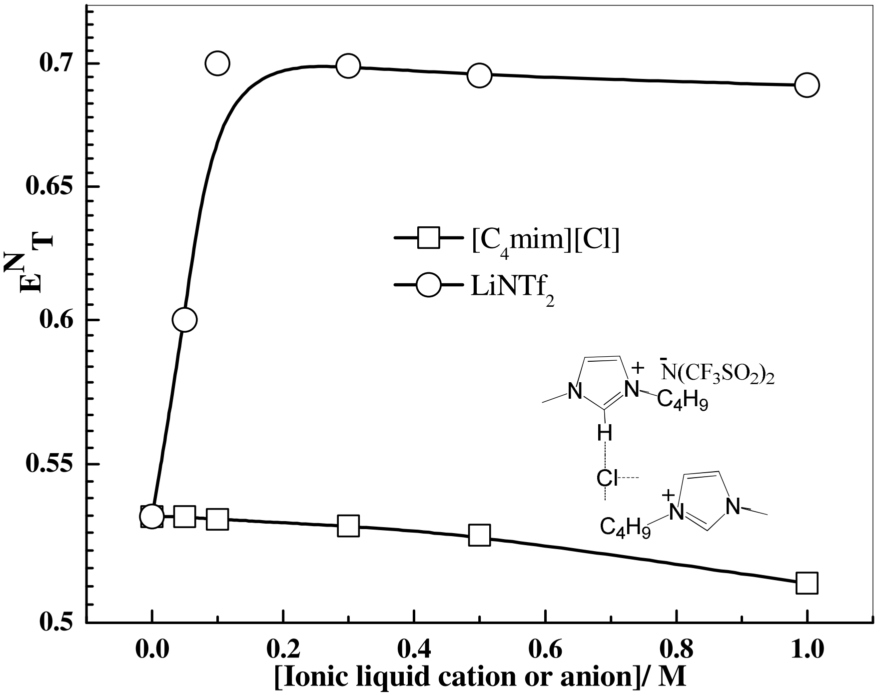

Fig. 5.23. Variation in the polarity as a function of the concentration of ionic liquid cation or anion. Ionic liquid phase: 0.05-1.0 M [C$_4$mim][Cl](or LiNTf$_2$)/[C$_4$mim][NTf$_2$]; Temperature = 298 K.

5.8.2. Polarity of acid and metal nitrate loaded ionic liquid phase

Ionic liquid is employed for the extraction of metal ions from nitric acid feed solution. During this contact significant amount of nitric acid is also co-extracted into the ionic liquid phase. As a result the polarity of the ionic liquid phase could change with respect to the nitric acid concentration in ionic liquid phase. Fig. 5.24. shows the variation in the polarity of the ionic liquid phase as a function of initial nitric acid concentration in aqueous phase. It can be seen that E_T^N values increases with increase in the concentration of nitric acid.

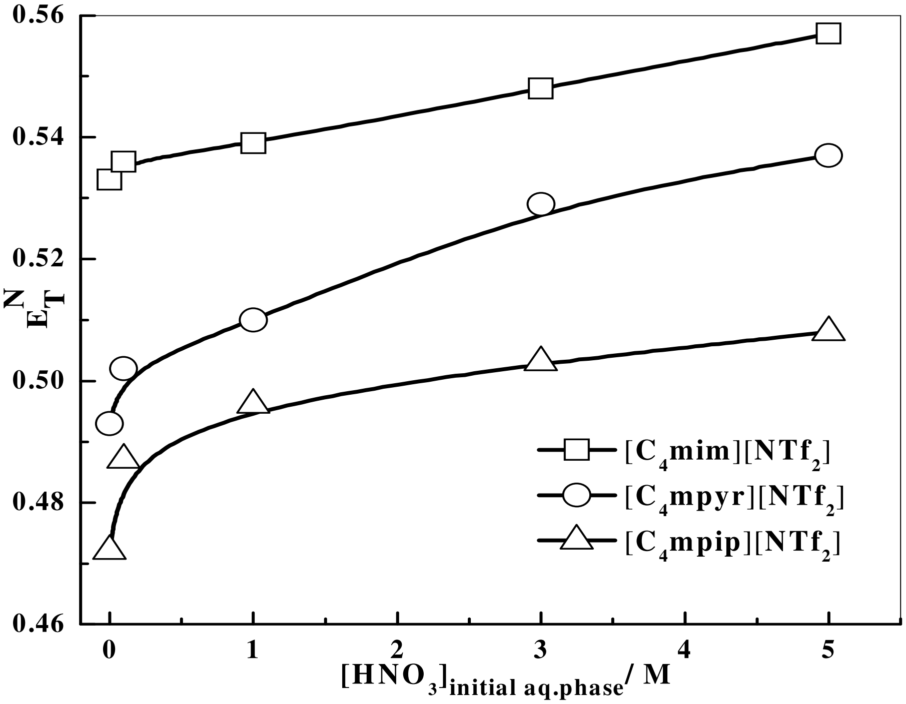

Fig. 5.24. Variation in the polarity as a function of the nitric acid concentration. Ionic liquid phase: $[C_4mim][NTf_2]$, $[C_4mpyr][NTf_2]$ and $[C_4mpip][NTf_2]$. Aqueous phase: 0.1-5.0 M HNO_3; Equilibration time = 1 h; Temperature = 298 K.

Similar to nitric acid, the neodymium nitrate and uranyl nitrate were dissolved in different ionic liquid and the polarity of ionic liquid phase determined at various concentrations of added metal nitrate, the results are shown in Fig. 5.25. and 5.26. It is observed that the E_T^N value increases with increase in the amount of neodymium nitrate and uranyl nitrate present in ionic liquid phase as expected.

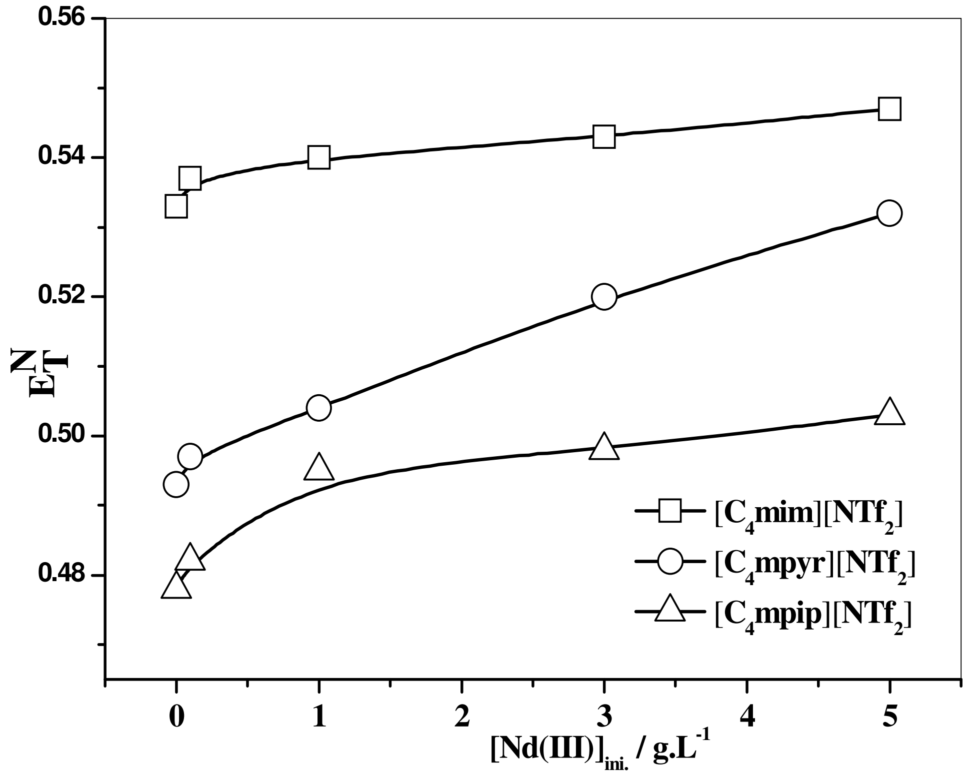

Fig. 5.25. Variation in the polarity as a function of the concentration of [Nd(III)]. Ionic liquid phase: [C_4mim][NTf_2], [C_4mpyr][NTf_2] and [C_4mpip][NTf_2]; Temperature = 298 K.

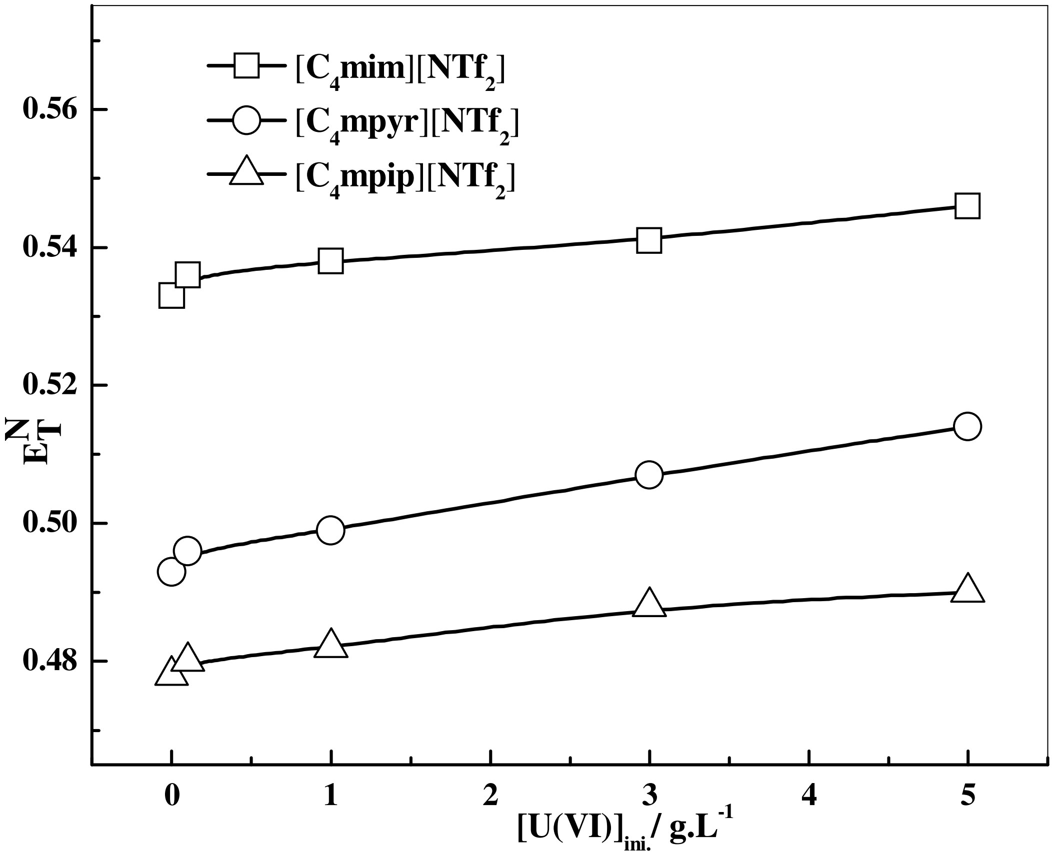

Fig. 5.26. Variation in the polarity as a function of the concentration of [U(VI)]. Ionic liquid phase: [C_4mim][NTf_2], [C_4mpyr][NTf_2] and [C_4mpip][NTf_2]; Temperature = 298 K.

5.8.3. Polarity of ionic liquid phase containing extractant

The organic phase employed for liquid-liquid extraction is composed of a ligand present in a diluent such as *n*-dodecane or ionic liquid. Since tri-*n*-butyl phosphate has been employed for the extraction of actinides from nitric acid solution, the polarity of the tri-*n*-butyl phosphate in ionic liquid phase was determined and the results are displayed in Fig. 5.27. It is observed that E_T^N values decrease with increase in the concentration of tri-*n*-butyl phosphate in ionic liquid phase. Since TBP is less polar as compared to the ionic liquid, increasing the concentration of TBP in ionic liquid imparts less polarity to the organic phase. As a result the E_T^N values decreases with increase in the concentration of TBP. Moreover the E_T^N values follows the order TBP/[C$_4$mim][NTf$_2$] > TBP/[C$_4$mpyr][NTf$_2$] > TBP/[C$_4$mpip][NTf$_2$] at a particular concentration of TBP, which is in line with the polarity variations shown in Fig. 5.22.

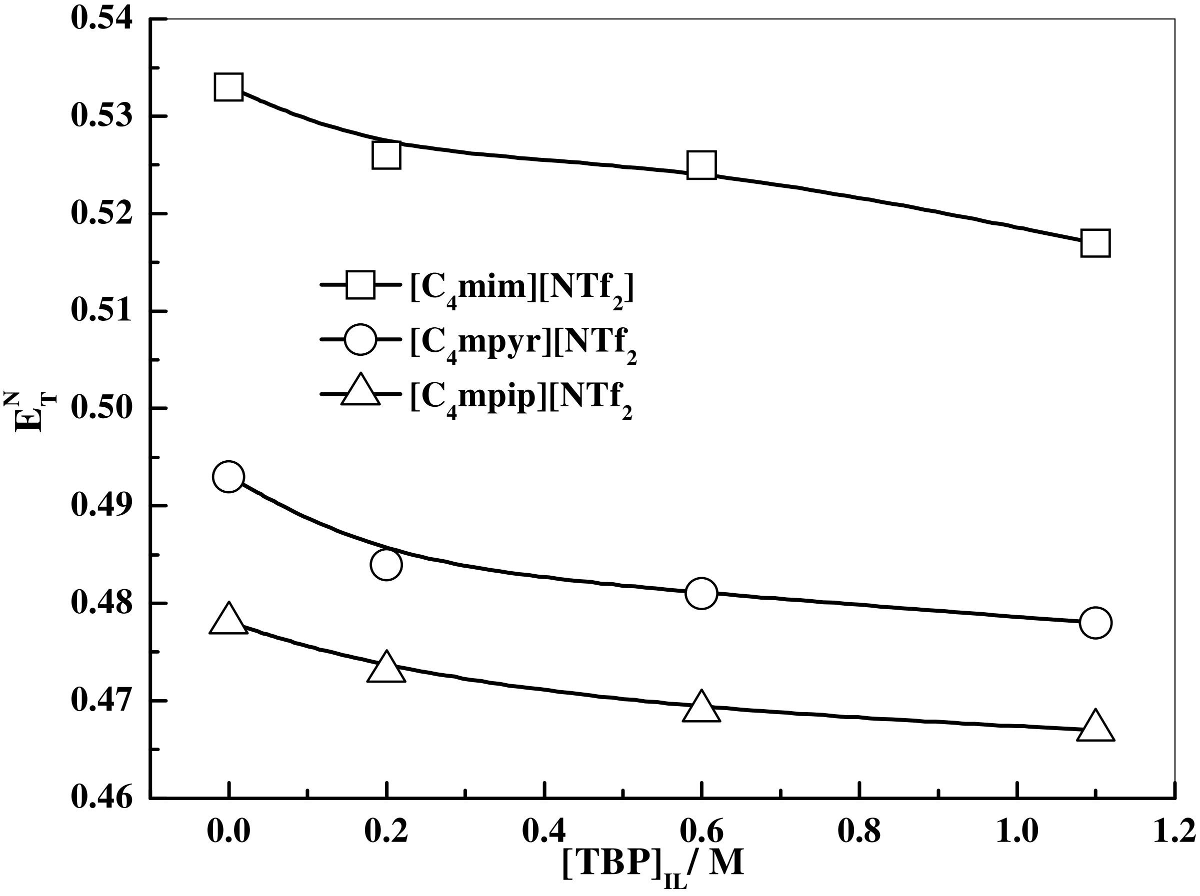

Fig. 5.27. Variation in the polarity as a function of the concentration of TBP. Ionic liquid phase: TBP/[C$_4$mim][NTf$_2$] (or [C$_4$mpyr][NTf$_2$] or [C$_4$mpip][NTf$_2$]); Temperature = 298 K.

5.8.4. Polarity of ionic liquid phase containing metal-ligand complex

The variation in the E_T^N of organic phase as a function of neodymium nitrate loading in the organic phase containing 1.1 M TBP/ ionic liquid is shown in Fig. 5.28(a). Since Nd(NO$_3$)$_3$ was dissolved in ionic liquid, the E_T^N values increases with increase in the amount of neodymium present in ionic liquid phase as discussed in Fig. 5.25. Similarly, the uranyl nitrate was dissolved in ionic liquid phase containing 1.1 M TBP/ionic liquid and the results are shown in Fig. 5.28(b). It is observed that, the E_T^N values increase with increase in the amount of uranium present in ionic liquid.

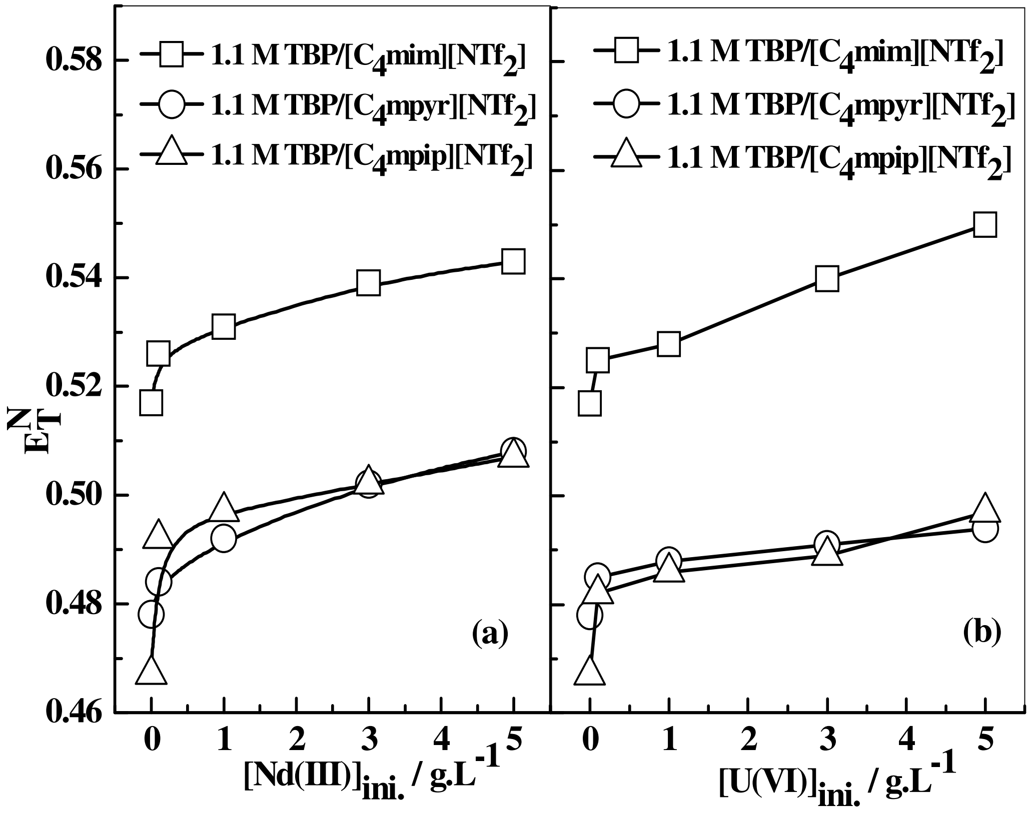

Fig. 5.28. Variation in the polarity as a function of the concentration of (a) Nd(III) and (b) U(VI). Ionic liquid phase: 1.1 M TBP/[C_4mim][NTf_2] (or [C_4mpyr][NTf_2] or [C_4mpip][NTf_2]); Temperature = 298 K.

Fig. 5.29. shows the variation in the E_T^N value as a function of the amount of different metal ions dissolved in the organic phase. The metal nitrates added to 1.1 M TBP/[C_4mim][NTf_2] were thorium nitrate, neodymium nitrate, uranyl nitrate. It can be seen that E_T^N values increase with increase in the amount of metal nitrate present in the ionic liquid phase as expected. Even

though the added metal nitrate coordinates with TBP, the E_T^N values increase with increase in the metal ion concentration. This could be due to the higher polarity of the respective metal-ligand complex that induces more polarity to the ionic liquid phase.

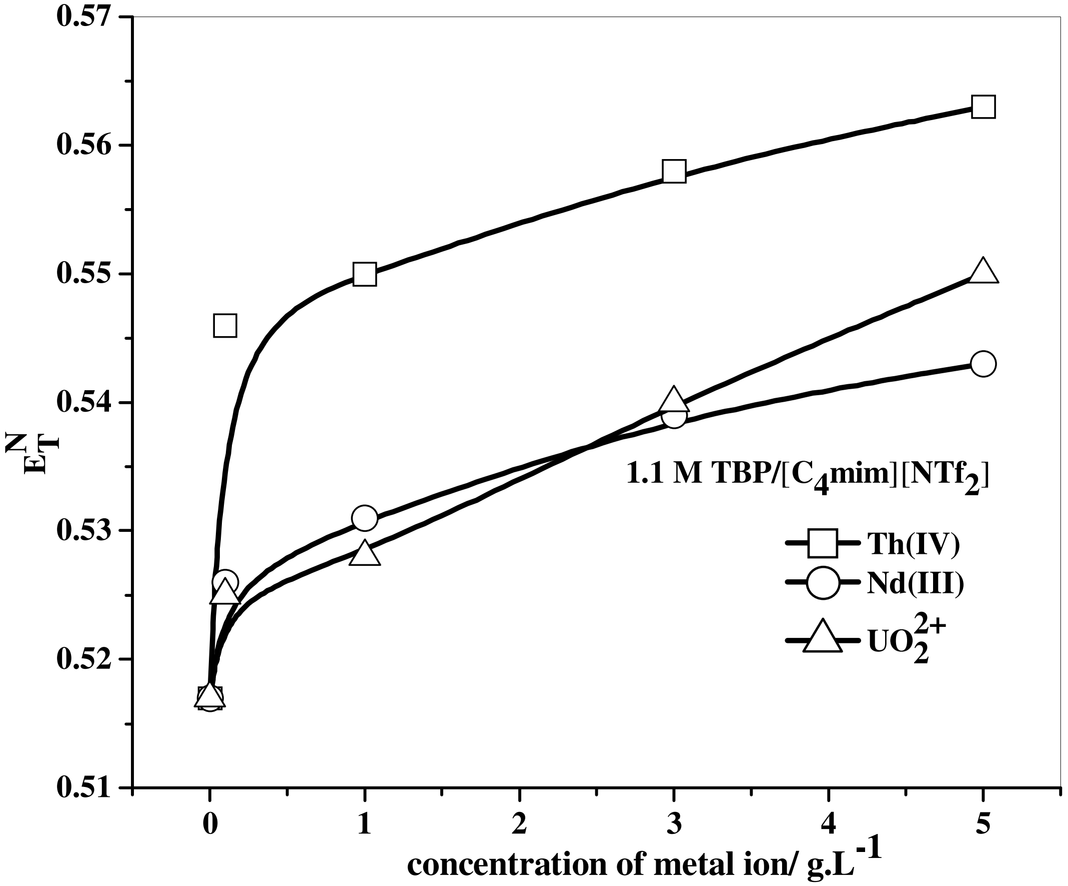

Fig. 5.29. Variation in the polarity as a function of the concentration of metal ion concentration. Ionic liquid phase: 1.1 M TBP/[C_4mim][NTf_2]; Temperature = 298 K.

5.9. Summary

The spectrophotometric measurements were performed in Reichardt's dye in acetonitrile solution containing [C_4mim][NTf_2], [C_4mpyr][NTf_2] and [C_4mpip][NTf_2], nitric acid, TBP and metal ions such as Th^{+4}, Nd^{+3}, UO_2^{2+}. The normalized polarity of the organic phase was measured using Reichardt's dye as the polarity probe. The results revealed that the normalized polarity of ionic liquid phase increased with the increase in the concentration of ionic liquid, nitric acid and other metal nitrates in acetonitrile. In the presence of TBP, the normalized polarity of ionic liquid phase decreased with increase in the concentration of TBP. When the solution containing metal nitrate in TBP/ionic liquid, the normalized polarity of ionic liquid phase increased with increase in the concentration of metal ion.

References

1. J. Rydberg, C. Musikas, G.R. Choppin, Solvent Extraction Principles and Practice. Marcel Dekker, Inc. New York, 1992.
2. B.A. Moyer, Ion Exchange and Solvent Extraction. A series of Advances, Volume 19. CRC Press, Taylor and Francis Group 2010.
3. R. Chiarizia, V. Urban, P. Thiyagarajan, A.W. Herlinger, SANS study of aggregation of the complexs formed by selected metal cations and P,P'-Di(2-ethylhexyl) ethane - and butane - diphosphoric acid, Solvent Extr. Ion Exch.17 (1999) 1171 – 1194.
4. P.N. Pathak, S.A. Ansari, S. Kumar, B.S. Tomar, V.K. Manchanda, Dynamic light scattering study on the aggregation behaviour of N,N,N’,N’-tetraoctyldiglycolamide (TODGA) and its correlation with the extraction behavior of metal ions, J. Colloid and Interface Sci. 342 (2010)114–118.
5. P.K. Verma, P.N. Pathak, P.K. Mohapatra, V.K. Aswal, B. Sadhu, M. Sundararajan, An Insight into Third-Phase Formation during the Extraction of Thorium Nitrate: Evidence for Aggregate Formation from Small-Angle Neutron Scattering and Validation by Computational Studies, J. Phys. Chem. B 117 (2013) 9821–9828.
6. K.R. Swami, K.A. Venkatesan, M.P. Antony, Aggregation Behavior of Alkyldiglycolamides in n-Dodecane Medium during the Extraction of Nd(III) and Nitric Acid, Ind. Eng. Chem. Res. 57 (2018) 13490-13497.
7. K.R. Swami, R. Kumaresan, K.A. Venkatesan, M.P. Antony, Minimizing the aggregation of diglycolamide reverse micelles in the: n -dodecane phase with bis-(2-ethylhexyl)phosphoric acid "reactive" phase modifier, New J. Chem. 42 (2018) 8891-8899.

8. K.R. Swami, R. Kumaresan, K.A. Venkatesan, M.P. Antony, Minimizing the aggregation of diglycolamide reverse micelles in the n-dodecane phase with bis-(2-ethylhexyl)phosphoric acid "reactive" phase modifier, New. J. Chem. 42 (2018) 8891-8899.

9. P.R. Vasudev Rao, Z. Kolarik, A review of third phase formation in extraction of actinides by neutral organophosphorus extractants, Solvent Extr. Ion Exch. 14 (1996) 955-993.

10. R.B. Gujar, S.A. Ansari, P.K. Mohapatra, V.K. Manchanda, Development of T2EHDGA based process for actinide partitioning. part I: Batch studies for process optimization, Solvent Extr. Ion Exch. 28 (2010) 350-366.

11. S.A. Ansari, P.N. Pathak, P.K. Mohapatra, V.K. Manchanda, Chemistry of Diglycolamides: Promising Extractants for Actinide Partitioning, C*hem. Rev*. 112 (2012) 1751–1772.

12. J. Ravi, K.A. Venkatesan, M.P. Antony, T.G. Srinivasan, P.R. Vasudeva Rao, Feasibility of Using Di-Dodecyl-Di-Octyl Diglycolamide for Partitioning of Minor Actinides from Fast Reactor High-Level Liquid Waste, Solvent Extr. Ion Exch. 32 (2014) 424–436.

13. N.V. Plechkova, K.R. Seddon, Applications of ionic liquids in the chemical industry, Chem. Soc. Rev. 37 (2008) 123-150.

14. I.A. Shkrob, T.W. Marin, M.P. Jensen, Ionic Liquid Based Separations of Trivalent Lanthanide and Actinide Ions, Ind. Eng. Chem. Res. 53 (2014) 3641–3653.

15. P. Sun, K. Huang, W. Song, Z. Gao, H. Liu, Separation of rare earths from the transition metals using a novel ionic liquid-based aqueous two phase system: Towards green and

efficient recycling of rare earths from the NdFeB magnets, Ind. Eng. Chem. Res. 57 (2018) 16934-16943.

16. Alok Rout, K.A. Venkatesan, T.G. Srinivasan, P.R. Vasudeva Rao, Tuning the extractive properties of Purex solvent using room temperature ionic liquid, Sep. Sci. Technol**.** 48 (17) (2013) 2576-2581.

17. Alok Rout, K. Chatterjee, K.A. Venkatesan, M.P. Antony, P.R. Vasudeva Rao, Solvent extraction of plutonium(IV) in monoamide-ammonium ionic liquid mixture. Sep. Purif. Technol. 159 (2016) 43-49.

18. P.K. Mohapatra, Actinide ion extraction using room temperature ionic liquids: opportunities and challenges for nuclear fuel cycle applications, Dalton Trans. 46 (2017) 1730-1747.

19. N.K. Gupta, Ionic liquids for TRansUranic Extraction (TRUEX)—Recent developments in nuclear waste management: A review. J. Mol. Liq. 269 (2018) 72-91.

20. R. Zarrougui, R. Mdimagh, N. Raouafic, Highly efficient extraction and selective separation of uranium (VI) from transition metals using new class of undiluted ionic liquids based on H-phosphonate anions, J. Hazard. Mater. 342 (2018) 464-476.

21. D. Ternova, A. Ouadi, V. Mazan, S. Georg, M. Boltoeva, V. Kalchenko, S. Miroshnichenko, I. Billard, C. Gaillard, New Ionic Liquid Based on the CMPO Pattern for the Sequential Extraction of U(VI), Am(III) and Eu(III), J. Solution Chem. 47 (2018) 1309-1325.

22. Alok Rout, K.A. Venkatesan, T.G. Srinivasan, P.R. Vasudeva Rao, Extraction and third phase formation behavior of Eu(III) in CMPO–TBP extractants present in room temperature ionic liquid, Sep. Purif. Technol. 76 (2011) 238–243.

23. W. Liansheng, M. Casarci, G.M. Gasparini, The extraction of Eu(III) from acidic media by octyl(phenyl)-N,N-diisobutyl carbamoyl methylphosphinoxide, Solvent Extr. Ion Exch. 8 (1990) 49-64.

24. A. Suresh, C.V.S. Brahmananda Rao, K.N. Sabharwal, T.G. Srinivasan, P.R. Vasudeva Rao, Third phase formation in the extraction of Nd (III) by octyl(phenyl)-N,N-diisobutyl carbamoyl methylphosphinoxide (OΦCMPO), Solvent Extr. Ion Exch. 17 (1999) 73-78.

25. R. Rama. Alok Rout. K.A. Venkatesan, M.P. Antony, P.R. Vasudeva Rao, Loading behavior of Eu(III) at high aqueous concentrations in diglycolamide/ionic liquid systems. J. Radioanal. Nucl. Chem. 308 (2016) 835–842.

26. S.A. Ansari, P.N. Pathak, P.K. Mohapatra, V.K. Manchanda, Aqueous Partitioning of Minor Actinides by Different Processes, Sep. Purif. Rev. 40 (2011) 43–76.

27. D. Dupont, D. Depuydt, K. Binnemans, Overview of the effect of salts on biphasic ionic liquid/water solvent extraction systems: anion exchange, mutual solubility, and thermomorphic properties, J Phys Chem B. 119 (2015) 6747-6757.

28. X. Sun, Y. Ji, L. Guo, J. Chen, D. Li, A novel ammonium ionic liquid based extraction strategy for separating scandium from yttrium and lanthanides, Sep. Purif. Technol.81 (2011) 25-30.

29. Alok Rout, K.A. Venkatesan, M.P. Antony, P.R. Vasudeva Rao, Liquid–Liquid extraction of americium (III) using a completely incenerable ionic liquid system, Sep. Purif. Technol. 58 (2016) 137-143.

30. Z. Li, X. Li, S. Raiguel, K. Binnemans, Separation of transition metals from rare earths by non-aqueous solvent extraction from ethylene glycol solutions using Aliquat 336, Sep. Purif. Technol. 201 (2018) 318-326.

31. Y. Sasaki, Y. Sugo, S. Suzuki, S. Tachimori, The novel extractants, diglycolamides, for the extraction of lanthanides and actinides in HNO_3-n-dodecane system. Solvent Extr. Ion Exch. 19 (2001) 91–103.

32. G. Koch, Reprocessing by quaternary ammonium nitrates: laboratory studies. In Solvent Extraction Chemistry of Metals; Mckay, H. A. C.; Healy, T. V.; Jenkins, I. L.; Naylor, A., Eds.; MacMillan: London, UK, (1996) 247−266.

33. A. Cao, Light scattering. Recent applications. Anal. Lett. 36 (2003) 3185.

34. Finsy, R., Particle sizing by quasi-elastic light scattering. Adv. Colloid Interface Sci. 52 (1994) 79.

35. K. Ramaswamy, A.S. Suneesh, R. Kumerasan, K.A. Venkatesan, M.P. Antony, Dynamic Light Scattering and FTIR Spectroscopic Investigations on the Reverse Micelles Produced During the Extraction of Nd(III) and Nitric Acid in Tetra Ethylhexyl Diglycolamide, ChemistrySelect. 2 (2017) 11177 – 11186.

36. Alok Rout, S. Mishra, K.A. Venkatesan, M.P. Antony, N.K. Pandey, S. Subramanian, Physicochemical and radiolytic degradation properties of dihexyloctanmide-imidazolium ionic liquid, J. Mol. Liq. 99 (2017) 93-99.

37. K.A. Venkatesan, R. Kumaresan, M.P. Antony, T. Kumar, T.G. Srinivasan, and P.R. Vasudeva Rao, Characterization of high active waste (155 GWd/Te) arising from fast reactor fuel reprocessing, Radiochim. Acta. 100 (2012) 843–849.

38. P. Zsabka, K.V. Hecke, L. Adriaensen, A. Wilden, G. Modolo, M. Verwerft, K. Binnemans, T. Cardinaels, Solvent extraction of Am(III), Cm(III) and Ln(III) ions from simulated highly active raffinate solutions by TODGA diluted in Aliquat-336 nitrate ionic liquid, Solvent Extr. Ion Exch, 36 (2018) 519-541.

39. P. Deepika, K. Sabharwal, K.N. Sabharwal, T.G. Srinivasan, P.R. Vasudeva Rao, Studies on the use of *N,N,N′,N′*-Tetra(2-Ethylhexyl)Diglycolamide (TEHDGA) for Actinide Partitioning II: Investigation on Radiolytic Stability, Solvent Extr. Ion Exch. 29 (2011) 230-246.

40. R.B. Gujar, S.A. Ansari, A. Bhattacharyya, P.K. Mohapatra, A.S. Kanekar, P.N. Pathak, V.K. Manchanda, Studies on the radiolytic stability of *N*,*N*,*N*’,N’-tetra-2-ethylhexyl diglycolamide in *n*-dodecane solution containing different phase modifiers, J. Radioanal. Nucl. Chem. 288 (2011) 621–627.

41. K.L. Nash, P.G. Rickert, E.P. Horwitz, Degradation of TRUEX –Dodecane process solvent, Solvent Extr. Ion Exch. 7 (2007) 655 - 677.

42. K.L. Nash, R.C. Gatrone, G.A. Clark, P.G. Rickert, E.P. Horwitz, Hydrolytic and radiolytic degradation of OφD (iB) CMPO: Continuing studies, Sep. Sci. Technol. 23 (1988) 1355-1372.

43. J. Rydberg, ed. Solvent extraction principles and practice, revised and expanded. CRC Press, 2004.

44. B.A. Moyer, Ion Exchange and Solvent Extraction. A series of Advances, Volume 19. CRC Press, Taylor and Francis Group 2010.

45. R. Chiarizia, A. Briand, M.P. Jensen, P. Thiyagarajan, Sans Study of Reverse Micelles Formed upon the Extraction of Inorganic Acids by TBP in *n*-Octane, Solvent Extr. Ion Exch. 26 (2008) 333.

46. N.M. Vaghela, N.V. Sastry, V.K. Aswal, Surface active and aggregation behavior of methylimidazolium-based ionic liquids of type [$C_n$mim][X], n= 4, 6, 8 and [X]= Cl^-, Br^-, and I^- in water, Colloid Polym. Sci. 289 (2011) 309.

47. W. Kang, B. Dong, Y. Gao, L. Zheng, Aggregation behavior of long-chain imidazolium ionic liquids in ethyl ammonium nitrate, Colloid Polym. Sci. 288 (2010) 1225.

48. P.N. Pathak, S.A. Ansari, P.K. Mohapatra, V.K. Manchanda, A.K. Patra, V.K. Aswal, Role of alkyl chain branching on aggregation behavior of two symmetrical diglycolamides: small angle neutron scattering studies, J. Colloid Interface Sci. 393 (2012) 347-351.

49. P.N. Pathak, S.A. Ansari, P.K. Mohapatra, S. Kumar, B.S. Tomar, V.K. Manchanda, Dynamic light scattering study on the aggregation behaviour of *N,N,N',N'*-tetraoctyl diglycolamide (TODGA) and its correlation with the extraction behaviour of metal ions, J. Colloid Interface Sci. 342 (2010) 114-118.

50. N. Kumari, P.N. Pathak, Dynamic light scattering studies on the aggregation behavior of tributyl phosphate and straight chain dialkyl amides during thorium extraction, J. Ind. Eng. Chem. 20 (2014)1382–1387.

51. P.K. Verma, P.N. Pathak, P.K. Mohapatra, V.K. Aswal, B. Sadhu, M. Sundararajan, An Insight into Third-Phase Formation during the Extraction of Thorium Nitrate: Evidence for Aggregate Formation from Small-Angle Neutron Scattering and Validation by Computational Studies, J. Phys. Chem. B, 117 (2013) 9821–9828.

52. Alok Rout, K.A. Venkatesan, T. G. Srinivasan, P.R. Vasudeva Rao, Tuning the Extractive Properties of Purex Solvent using Room Temperature Ionic Liquid, Sep. Sci. Technol. 48 (2013) 2576-2581.

53. R.S.C. Bose, R. Kumaresan, K.A. Venkatesan, R.L. Gardas, M.P. Antony, P.R. Vasudeva Rao, Insights Into the Extraction of Am(III) by Aliquat-336 Based Ionic Liquids, Sep. Sci. Technol. 49 (2014) 2338–2345.

54. R. Rama, R. Kumerasan, K.A. Venkatesan, P.R. Vasudeva Rao, Insights into the extraction behavior of U(VI) in Aliquat-336 based ionic liquids, Radiochim. Acta 102 (2014) 1009-1016

55. N.V. Plechkova, K.R. Seddon, Applications of ionic liquids in the chemical industry, Chem. Soc. Rev. 37 (2008) 123-150

56. P.R. Vasudeva Rao, K.A. Venkatesan, Alok Rout, T.G. Srinivasan, K. Nagarajan, Potential Applications of Room Temperature Ionic Liquids for Fission Products and Actinide Separation, Sep. Sci. Technol. 47 (2012) 204-222.

57. Alok Rout, K.A.Venkatesan, M.P. Antony, P.R. Vasudeva Rao, Actinide ion extraction using room temperature ionic liquids: opportunities and challenges for nuclear fuel cycle applications, Sep. Purif. Technol. 158 (2016)137-143.

58. Alok Rout, E. Rezende Souza, K. Binnemans, Solvent extraction of europium(III) to a fluorine-free ionic liquid phase with a diglycolamic acid extractant, RSC Adv. 4 (2014) 11899–11906.

59. Alok Rout, K.A. Venkatesan, T.G. Srinivasan, P.R. Vasudeva Rao, Separation of plutonium(IV) from uranium(VI) using phosphonate-based task-specific ionic liquid, Desalin. Water Treat. 38 (2012) 179-183.

60. Alok Rout, K. Binnemans, Solvent Extraction of Neodymium(III) by Functionalized Ionic Liquid Trioctylmethylammonium Dioctyl Diglycolamate in Fluorine-free Ionic Liquid Diluent, Ind. Eng. Chem. Res. 53(2014)6500-6508.

61. Alok Rout, K.A. Venkatesan, T.G. Srinivasan, P.R. Vasudeva Rao, Ionic liquid extractants in molecular diluents: Extraction behavior of europium (III) in quaternary ammonium-based ionic liquids, Sep. Purif. Technol. 95 (2012) 26-31.

62. X.Q. Sun, H.M. Luo, S. Dai, Ionic Liquids-Based Extraction: A Promising Strategy for the Advanced Nuclear Fuel Cycle, Chem. Rev.112 (2012) 2100-2128.
63. X. Sun, Y. Ji, F. Hu, Bo He, Ji Chen, D. Li, The inner synergistic effect of bifunctional ionic liquid extractant for solvent extraction, Talanta 81 (2010) 1877–1883.
64. H. Mehdi, K. Binnemans, K. V. Hecke, L.V. Meervelt, P. Nockemann, Hydrophobic ionic liquids with strongly coordinating anions, Chem. Commun. 46 (2010) 234-236.
65. E. Padhan, K. Sarangi, Recovery of Nd and Pr from NdFeB magnet leachates with bi-functional ionic liquids based on Aliquat 336 and Cyanex 272, Hydrometallurgy 167 (2017) 134-140.
66. Alok Rout, K. A. Venkatesan, T. G. Srinivasan, P. R. Vasudeva Rao, Room temperature ionic liquid diluent for the mutual separation of europium(III) from americium(III), Sep. Purif. Technol. 81 (2011) 109-115.
67. J. Rydberg, M. Cox, C. Musikas, G.R. Choppin, Solvent Extraction Principles and Practice, (2004).
68. V.S. Kislik, Solvent extraction: classical and novel approaches. Elsevier 2012.
69. P.N. Pathak, S.A. Ansari, S. Kumar, B.S. Tomar, V.K. Manchanda, Dynamic light scattering study on the aggregation behaviour of N,N,N′,N′-tetraoctyl diglycolamide (TODGA) and its correlation with the extraction behaviour of metal ions, J. Colloid and Interface Sci. 342 (2010) 114-118.
70. P. Deepika, K.N. Sabharwal, T.G. Srinivasan, P.R. Vasudeva Rao, Studies on the use of N,N,N',N'-Tetra(2-ethylhexyl) diglycolamide (TEHDGA) for actinide partitioning. I: Investigation on third-phase formation and extraction behavior, Solvent Extr. Ion Exch. 28 (2010) 184-201.

71. J.G. Huddleston, A.E. Visser, W.M. Reichert, H.D. Willauer, G.A. Broker, R.D. Rogers, Characterization and comparison of hydrophilic and hydrophobic room temperature ionic liquids incorporating the imidazolium cation, Green Chem. 3 (2001) 156-164.
72. P. Giridhar, K.A. Venkatesan, T.G. Srinivasan, P.R. Vasudeva Rao, Extraction of uranium(VI) from nitric acid medium by 1.1 M tri-n-butylphosphate in ionic liquid diluent, J. Radioanal. Nucl. Chem. 265 (2005) 31-38.
73. M.L. Dietz, Ionic liquids as extraction solvents: Where do we stand?, Sep. Sci. Technol. 41 (2006) 2047-2063.
74. Y. Shen, S. Wang, L. Zhu, J. Wang, W. Wu, Extraction of Th (IV) from an HNO_3 solution by diglycolamide in ionic liquids, Ind. Eng. Chem. Res. 50 (2011) 13990-13996.
75. Alok Rout, K.A. Venkatesan, T.G. Srinivasan, P.R. Vasudeva Rao, Extraction behavior of actinides and fission products in amide functionalized ionic liquid, Sep. Purif. Technol. 97 (2012) 164-171.
76. X. Sun, H. Luo, S. Dai, Ionic liquids-based extraction: A promising strategy for the advanced nuclear fuel cycle, Chem. Rev. 112 (2012) 2100-2128.
77. Z. Kolarik, Ionic Liquids: How Far Do they Extend the Potential of Solvent Extraction of f-Elements?, Solvent Extr. Ion Exch. 31 (2013) 24-60.
78. P.K. Mohapatra, P. Kandwal, M. Iqbal, J. Huskens, M.S. Murali, W. Verboom, A novel CMPO-functionalized task specific ionic liquid: Synthesis, extraction and spectroscopic investigations of actinide and lanthanide complexes, Dalton Trans. 42 (2013) 4343-4347.
79. J. Wang, J. Zhao, D. Feng, X. Kang, Y. Sun, L. Zhao, H. Liang, Enhancing extraction ability by rational design of phosphoryl functionalized ionic liquids and mechanistic investigation on neodymium (III) extraction, J. Rare Earths 34 (2016) 83-90.

80. M.A. Ab Rani, A. Brant, L. Crowhurst, A. Dolan, M. Lui, N.H. Hassan, J. Hallett, P. Hunt, H. Niedermeyer, J. Perez-Arlandis, Understanding the polarity of ionic liquids, Phys. Chem. Chem. Phys. 13 (2011) 16831-16840.

81. R.M. Couto, C. Lourenço, P.C. Simões, L.C. Branco, Task specific ionic liquids as polarity shifting additives of common organic solvents, New J. Chem. 38 (2014) 5559-5565.

82. N. Li, Y.a. Gao, L. Zheng, J. Zhang, L. Yu, X. Li, Studies on the micropolarities of bmimBF4/TX-100/toluene ionic liquid microemulsions and their behaviors characterized by UV− Visible spectroscopy, Langmuir 23 (2007) 1091-1097.

83. J. Canongia Lopes, M.F. Costa Gomes, P. Husson, A.A. Pádua, L.P.N. Rebelo, S. Sarraute, M. Tariq, Polarity, viscosity, and ionic conductivity of liquid mixtures containing $[C_4C_1im][Ntf_2]$ and a molecular component, J. Phys. Chem. B 115 (2011) 6088-6099.

84. C. Reichardt, Solvatochromic dyes as solvent polarity indicators, Chem. Rev. 94 (1994) 2319-2358.

85. C. Reichardt, Polarity of ionic liquids determined empirically by means of solvatochromic pyridinium N-phenolate betaine dyes, Green Chem. 7 (2005) 339-351.

86. P.A. Pires, O.A. El Seoud, V.G. Machado, J.s.C. de Jesus, C.E. de Melo, J.L. Buske, A.P. Cardozo, Understanding Solvation: Comparison of Reichardt's Solvatochromic Probe and Related Molecular "Core" Structures, J. Chem. Eng. Data 64 (2019) 2213-2220.

87. S. Zhang, X. Qi, X. Ma, L. Lu, Y. Deng, Hydroxyl ionic liquids: the differentiating effect of hydroxyl on polarity due to ionic hydrogen bonds between hydroxyl and anions, J. Phys. Chem. B 114 (2010) 3912-3920.

Chapter 6: Radiolytic stability and thermophysical properties of ionic liquid solvent system

This chapter deals the radiolytic stability and thermophysical properties of the ionic liquid phase containing *N,N,N',N'*-tetra(2-ethylhexyl)diglycolamide (T2EHDGA)/methyltri-*n*-octylammonium nitrate ($[N_{1888}][NO_3]$) and bis(2-ethylhexyl)phosphoric acid (D2EHPA) or bis(2-ethylhexyl)diglycolamic acid (HDEHDGA)/$[C_4mim][NTf_2]$. This chapter is divided into two parts and each part is described below

PART I: Investigations on the radiolytic stability of incinerable CHON based ionic liquid containing diglycolamide

6.1. Introduction

In the last two decade, room temperature ionic liquids (RTILs) have been extensively studied for the separation of metal ions, both radioactive and non-radioactive, from aqueous solution composed of nitric acid and hydrochloric acid medium [1-4]. Initially, the ionic liquids are employed as an alternative to the traditional diluent *n*-dodecane (*n*-DD) in solvent extraction application and later they were also employed as an extractant [5-14]. The ionic liquids employed for solvent extraction applications usually contained 1-alkyl-3-methylimidazolium $[C_nmim]^+$ cation and an anion. To make the ionic liquid hydrophobic, suitable for solvent extraction application as a diluent, the $[C_nmim]^+$ cation was combined with the hydrophobic anions such as $[PF_6]^-$ anion, and studied for the extraction of metal ions in conjunction with traditional extractants [15,16]. Soon, it was realized that the resultant ionic liquid, $[C_nmim][PF_6]$, was unsuitable for solvent extraction applications, due to inherent property of the ionic liquid to undergo cation and anion exchange as well as the hydrolytic degradation of PF_6^- to produce phosphoric acid and HF [17-19]. Later, it was suggested to replace the $[PF_6]^-$ anion by a stable bis(trifluoromethylsulfonyl)imide, ($[NTf_2]^-$) ion. The resultant ionic liquid $[C_nmim][NTf_2]$ was strongly hydrophobic and it was studied extensively for solvent extraction applications in the last two decades [1-10].

Eventhough $[C_nmim][NTf_2]$ could avoid the hydrolytic degradation, of the ionic liquid to a large extent, the inherent properties of the ionic liquid namely the cation and anion exchange behavior with the different ions present in aqueous phase could not be avoided [1-4]. Nevertheless, exhaustive studies have been carried out using this ionic liquid till date in conjunction with a number of ligands suitable, not only for the toxic heavy metal ions but also for the radioactive metal ions [1-10]. When the solvent phase (ligand + diluent) is proposed for the treatment of radioactive solutions, it is necessary to evaluate the radiation stability of the solvent phase. In this context the radiation stability of the $[C_n\text{mim}][NTf_2]$ ionic liquid has been studied by several authors over the last two decades and published reviews on the radiation chemistry of ionic liquids [20-22]. The reports revealed that $[NTf_2]^-$ ionic liquids undergo radiolytic degradation yielding significant amount of the aqueous soluble products such as F^-, SO_4^{2-}, CF_3SO_3H, etc. [20] It should be noted that all these degradation products are undesirable for employing $[NTf_2]^-$ ionic liquids for solvent extraction applications in nuclear fuel cycle. Nevertheless, several authors continued the studies with ionic liquids containing P, F and S atoms in the cation or anionic part of the ionic liquid, perhaps owing to the extraordinary extraction of radioactive metal ions, when ionic liquids are employed in conjunction with traditional ligands [1]. Therefore, the limitations of these conventional ionic liquids have been disregarded, when compared to extraordinary extraction achieved in ionic liquid medium.

In recent past, the ionic liquids containing quaternary alkyl ammonium cations namely instance methyltrioctylammonium cation $[N_{1888}]^+$ are becoming popular for the extraction of radioactive metal ions in nuclear fuel cycle [23-27]. The important features of these quaternary alkyl ammonium ionic liquids suitable for nuclear fuel cycle applications are (a) they are made up of C and N atoms, obeying the CHON-principle; (b) strongly hydrophobic and therefore they do not undergo cation exchange; (c) the viscosity of the aqueous equilibrated quaternary alkyl ammonium ionic liquid is less than 100 mP.s, which can be acceptable for solvent extraction application; (d) unlike *n*-dodecane, the use of ionic liquids in general, and quaternary ammonium ionic liquid in particular, do not result in third phase formation [28, 29]. It should be noted that the anion associated with $[N_{1888}]^+$ ion usually undergoes anion exchange with anions present in aqueous phase. However, when the $[N_{1888}]^+$ is combined with $[NO_3]^-$ anion, the resultant ionic liquid, $[N_{1888}][NO_3]$ [35] can be regarded as acceptable for nuclear fuel cycle applications, since the feed solution for reprocessing applications is composed of nitric acid medium [25, 26, 28]. Therefore the anion NO_3^- is “akin” to reprocessing feed solutions, while the anions containing F, S and P atoms are regarded as “alien” ions for reprocessing applications. Moreover, the radiation chemistry and radiolytic degradation of nitrate extracted phases have been well established, since the reprocessing applications always involve nitric acid, and sodium nitrate feed solutions [30-32].

In view of the several advantages described above $[N_{1888}][NO_3]$ ionic liquid, it is necessary to investigate the radiolytic stability of the ionic liquid and the possible changes in the extraction and stripping behavior of metal ions upon γ-irradiation. Therefore the objective of the part I in chapter 6 is to report the results on the extraction behavior of Am(III) and Nd(III) in $[N_{1888}][NO_3]$ medium and in a solution of tetra-2-ethylhexyl diglycolamide (T2EHDGA) present in $[N_{1888}][NO_3]$. The diglycolamide, T2EHDGA, is regarded as a promising candidate for trivalent actinide partitioning [33, 34]. The organic phase was γ-irradiated upto 500 kGy and subjected the irradiated solution for the extraction of Am(III) and Nd(III) from nitric acid medium. The irradiated organic phase was further probed by FTIR spectroscopy to understand the nature of radiolytic degradation products.

Experimental details for the present chapter are presented in section 2.5.7 of chapter 2. The synthesis of the ionic liquid was discussed in section 2.6.6 of chapter 2 respectively.

Table. 6.1. Structure of molecular extractant and RTIL used in part I of chapter 6.

Name	Structure
Extractant	
N,N,N',N'-tetra(2-ethylhexyl) diglycolamide (T2EHDGA)	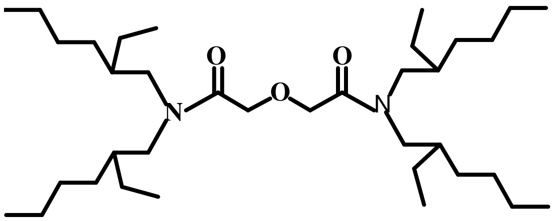
Ionic liquid	
Methyl-tri-*n*-octylammonium nitrate $[N_{1888}][NO_3]$ (R: C_8H_{17})	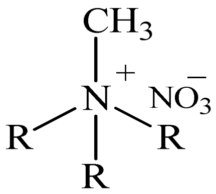

6.2. Results and discussions

6.2.1. Extraction of Am(III) in 0.1 M T2EHDGA/[N_{1888}][NO_3]

Diglycolamides undergo radiolytic degradation to produce innocuous degradation products [36-38]. Since these degradation products are aqueous soluble, they do not interfere in the recovery of actinides from the loaded organic phase. However, the degradation products of phosphoryl reagents such as tri-*n*-butyl phosphate interfere in stripping of actinides from the loaded organic phase and retain significant quantity of actinides [31, 32, 39]. Generally, it was reported that the radiolytic degradation of diglycolamides decrease the distribution ratio of actinides with increase of absorbed dose [36-38]. Fig. 6.1A shows the variation in the distribution ratio of Am(III) in the solution of irradiated 0.1 M T2EHDGA/*n*-DD as a function of absorbed γ-dose. The distribution ratio of Am(III) was measured at different concentrations of nitric acid. It can be seen that the distribution ratio of Am(III) decreases with increase of absorbed dose, as expected. This was attributed to the formation of aqueous soluble degradation products that results in the decrease in the concentration of T2EHDGA with absorbed dose [36-38]. Since the distribution ratio of Am(III) increases with increase in the concentration of nitric acid, $D_{Am(III)}$ at a particular γ-dose is more for 3 M nitric acid followed by 1 M and 0.5 M.

Under similar conditions, the distribution ratio of Am(III) was measured in an irradiated solution of 0.1 M T2EHDGA/[N_{1888}][NO_3]. The results are shown in Fig. 6.1B are in contrast to the decrease in distribution ratio of Am(III) observed for *n*-DD phase (Fig. 6.1A), the distribution ratio of Am(III) in 0.1 M T2EHDGA/[N_{1888}][NO_3] remains nearly constant irrespective of the γ- absorbed dose. There are few reasons responsible for this observation. They are (i) T2EHDGA might not be undergoing significant degradation in the presence of the bulk ionic liquid, which is quite unlikely; (ii) the degradation products of T2EHDGA aiding the extraction of americium and (iii) unlike *n*-DD, the bulk of the medium, $[N_{1888}][NO_3]$, might be extracting Am(III) from nitric acid medium.

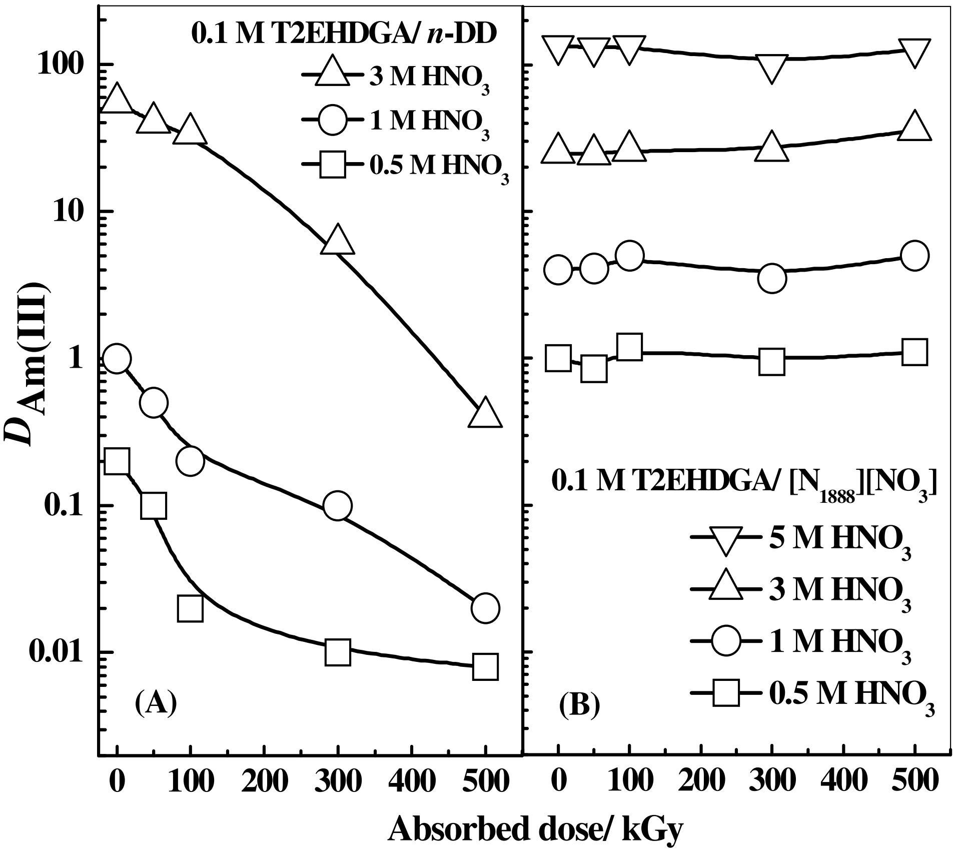

Fig. 6.1. Variation of distribution ratio of Am(III) as a function of the absorbed dose. Ionic liquid phase: (A) 0.1 M T2EHDGA/*n*-DD and (B) 0.1 M T2EHDGA/$[N_{1888}][NO_3]$; Aqueous phase: 0.5–5.0 M HNO_3; Temperature = 298 K; Absorbed dose 0-500 kGy; Equilibration time = 1 h; Phase volume ratio = 1.

To understand these features, T2EHDGA and $[N_{1888}][NO_3]$ was individually γ-irradiated to different absorbed dose levels and the irradiated T2EHDGA was mixed with unirradiated $[N_{1888}][NO_3]$ for the measurement of distribution ratio of Am(III) in 0.1 M T2EHDGA/ $[N_{1888}][NO_3]$ at different concentrations of nitric acid and vice-versa. The results are shown in Fig. 6.2. Previously, we also determined the distribution ratio of Am(III) in a solution of irradiated diglycolamide present in unirradiated *n*-dodecane [38]. It was reported that the distribution ratio of Am(III) in the organic phase decreased with increase of absorbed dose. This was attributed to be radiolytic degradation of diglycolamide that leads to the decrease in the concentration of diglycolamide in organic phase. Since, the distribution ratio of Am(III) was dependent on the concentration of diglycolamide present in the organic phase, the decrease in the distribution ratio of Am(III) observed with the increase of absorbed dose in the unirradiated *n*-dodecane medium was attributed to the radiolytic degradation of diglycolamide. In contrast to this observation, the distribution ratio of Am(III) measured in the solution of irradiated T2EHDGA present in unirradiated $[N_{1888}][NO_3]$, shown in Fig. 6.2 A, indicates that there is no significant change in the distribution ratio of Am(III). Since T2EHDGA is expected to undergo radiolytic degradation upon γ-irradiation, the invariant nature of the distribution ratio of Am(III) observed in the irradiated T2EHDGA present in unirradiated $[N_{1888}][NO_3]$ indicates that the bulk of the medium, namely $[N_{1888}][NO_3]$, might be extracting Am(III) to a large extent, and thus nullifying the decrease in the distribution ratio of Am(III) expected for irradiated T2EHDGA. In this particular feature, the ionic liquid diluent, $[N_{1888}][NO_3]$, cannot be regarded as an ‘‘inert’’, diluent as compared to *n*-dodecane, which is regarded as ‘‘inert’’, generally used for solvent extraction applications.

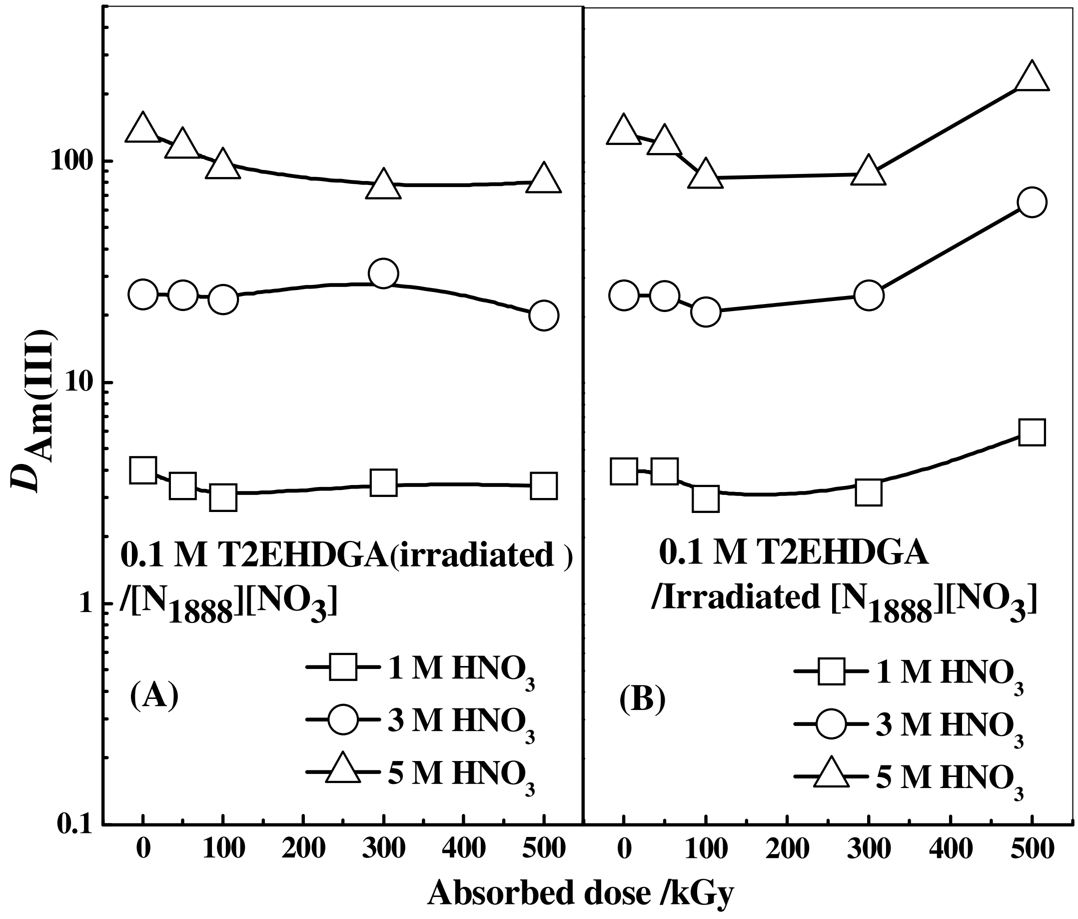

Fig. 6.2. Variation of distribution ratio Am (III) as a function of the absorbed dose. Ionic liquid phase: (A) 0.1 M T2EHDGA (irradiated)/[N_{1888}][NO_3] and (B) 0.1 M T2EHDGA/[N_{1888}][NO_3] (irradiated); Aqueous phase: 1.0-5.0 M HNO_3; Temperature = 298 K; Absorbed dose 0-500 kGy; Equilibration time = 1 h; Phase volume ratio = 1.

6.2.2. Extraction Stoichiometry

The extraction of americium in T2EHDGA can be represented by equation 3.1. The subscripts "aq" and "IL" denote the aqueous and ionic liquid phases respectively. And "x" is the number of T2EHDGA molecules involved in the extraction of americium.

$$Am^{3+}{}_{aq} + 3NO_3^-{}_{aq} + xT2EHDGA_{IL} \Leftrightarrow Am\ (NO_3)_3\,(T2EHDGA)_{x\ \ IL} \qquad (6.1)$$

The equilibrium constant for the above reaction can be represented in equation 6.1.

$$\mathrm{K_{ex}} = \frac{[\mathrm{Am(NO_3)_3(T2EHDGA)x}]_{\mathrm{IL}}}{[\mathrm{Am^{3+}}]_{\mathrm{aq}}[\mathrm{NO_3}]^3_{\mathrm{aq}}\,[\mathrm{T2EHDGA}]^{\mathrm{x}}_{\mathrm{IL}}} \qquad (6.2)$$

Upon rearranging equation 6.1 results in equation 6.2

$$\log D_{Am(III)} \ = \log K_{ex} + 3\log[NO_3^{\ -}]_{aq} + x\ \log[T2EHDGA]_{IL} \qquad (6.3)$$

In order to understand the number of molecules of T2EHDGA coordinated to Am(III) in the ionic liquid medium, the effect of T2EHDGA concentration on the extraction of americium (III) in the ionic liquid medium was studied. The slope obtained from the plot of log $D_{Am(III)}$ against log [T2EHDGA] gives the number of molecules of ligand coordinated to americium in the ionic liquid phase. The organic phase T2EHDGA/ $[N_{1888}][NO_3]$ was irradiated to various dose levels and subjected to distribution ratio measurements. The plot of Fig. 6.3. displays the variation in the distribution ratio of Am(III) as a function of T2EHDGA concentration in the ionic liquid phase at 3 M nitric acid concentration in the aqueous phase. It can be seen that the distribution ratio of Am(III) increases with increase in the concentration of T2EHDGA in the ionic liquid phase. Linear regression analysis of the extraction data results slope value varying from 1.8 to 1.9 at different γ-absorbed doses. A similar result with a slope of 2.3 was also reported for the extraction of Am(III) in unirradiated T2EHDGA/$[N_{1888}][NO_3]$ [25], showing that irradiation of T2EHDGA/[N_{1888}][NO_3] does not have much effect on the mechanism of Am(III) extraction in T2EHDGA/[N_{1888}][NO_3] phase. Slope value ~ 2 at different γ–absorbed doses indicating that about two molecules of T2EHDGA was involved in the extraction of Am(III) in the ionic liquid medium.

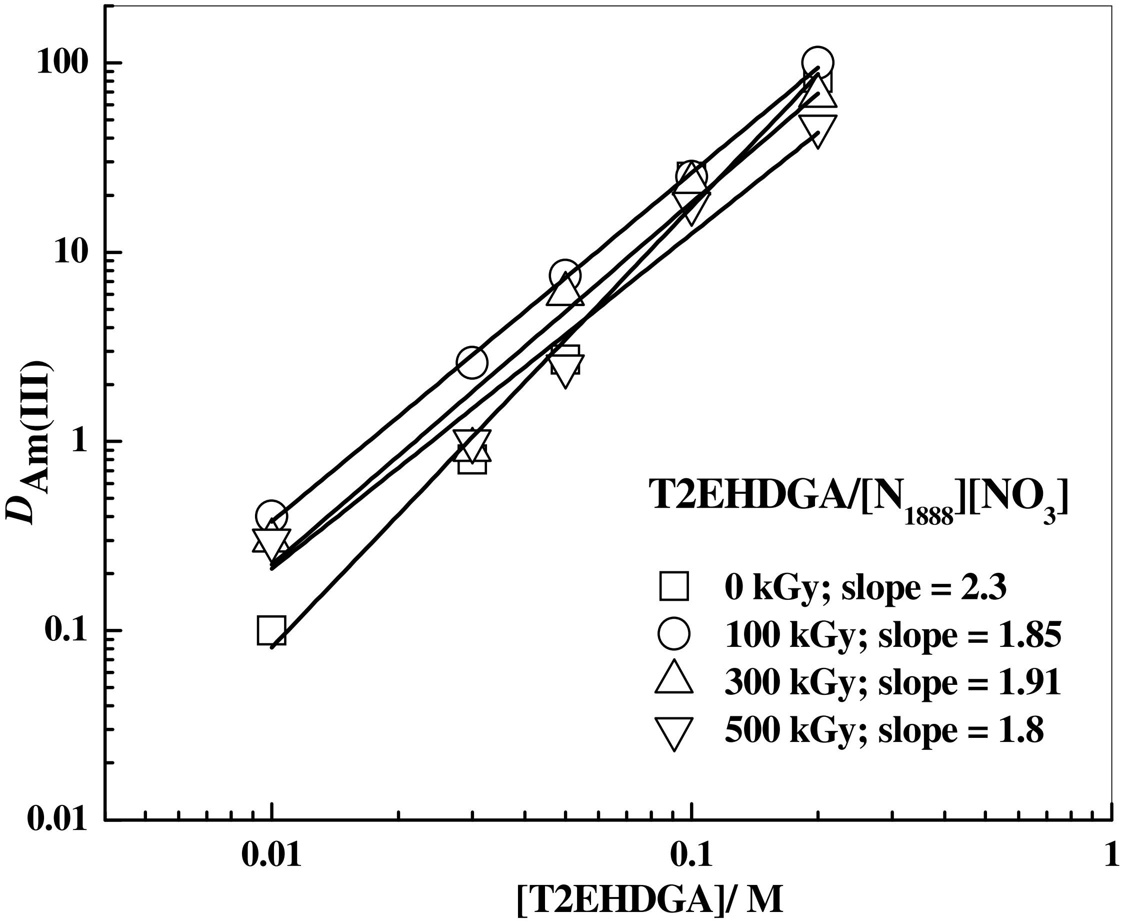

Fig. 6.3. Variation in the distribution ratio of Am (III) as a function of T2EHDGA concentration in ionic liquid phase. Ionic liquid phase: 0.01–0.3 M T2EHDGA/ [N_{1888}][NO_3]; Aqueous phase: 3 M HNO_3 spiked with ^{241}Am tracer; Absorbed dose 0-500 kGy; Temperature = 298 K; Equilibration time = 1 h; Phase volume ratio = 1.

6.2.3. Loading studies

In order to confirm the extraction behavior of Am(III) in $[N_{1888}][NO_3]$ and the possible effect of radiolytic degradation of $[N_{1888}][NO_3]$, the loading behavior of a trivalent lanthanide representative ion Nd(III) was studied in the unirradiated $[N_{1888}][NO_3]$ and the results are compared with the irradiated $[N_{1888}][NO_3]$. Since the distribution ratio measurements, usually carried out at trace levels, would not provide any clarity on the degree of radiolytic degradation of the bulk property of $[N_{1888}][NO_3]$, the bulk loading behavior of Nd(III) in $[N_{1888}][NO_3]$ was performed instead of distribution ratio measurements of Am(III) and the results are displayed in Fig. 6.4A. In this case, the $[N_{1888}][NO_3]$ alone was irradiated to 500 kGy and the extraction behavior of Nd(III) was performed from 3 M nitric acid medium. It can be seen that the loading of Nd(III) in unirradiated $[N_{1888}][NO_3]$ increases with increase in the amount of Nd(III) in 3 M nitric acid medium. This shows that $[N_{1888}][NO_3]$ alone can extract trivalent metal ion from nitric acid medium. The saturation in the loading of Nd(III) in organic phase occurs at 17 g/L. For the irradiated $[N_{1888}][NO_3]$ (500 kGy) also, the loading of Nd(III) increases with increase in the amount of Nd(III) present in aqueous phase followed by saturation in loading of Nd(III). However, it should be noted that the saturation in loading occurs at 10 g/L in the irradiated $[N_{1888}][NO_3]$ as compared to the 17 g/L in the unirradiated $[N_{1888}][NO_3]$. Moreover, the loading of Nd(III) in the irradiated $[N_{1888}][NO_3]$ is always lower than the loading of Nd(III) observed for the unirradiated $[N_{1888}][NO_3]$ at a particular amount of Nd(III) in aqueous phase.

The decrease in the saturation loading of Nd(III) observed in case of irradiated $[N_{1888}][NO_3]$ can be attributed to the radiolytic degradation of $[N_{1888}][NO_3]$. Therefore, it can be expected that the significant radiolytic degradation of the bulk, $[N_{1888}][NO_3]$, can affect the distribution ratio of Am(III) in 0.1 M T2EHDGA/ $[N_{1888}][NO_3]$ irradiated to various absorbed dose levels. However, the Fig. 6.1B showed that there was no change in the distribution ratio of Am(III) in the irradiated solution of 0.1 M T2EHDGA/[N_{1888}][NO_3] when they are irradiated together. To understand the discrepancy, [N_{1888}][NO_3] was irradiated alone and mixed with unirradiated T2EHDGA to obtain the 0.1 M T2EHDGA solution in [N_{1888}][NO_3], and the distribution ratio of Am(III) determined in this solution. Fig. 6.2B shows the variation in the distribution ratio of Am(III) in 0.1 M T2EHDGA/[N_{1888}][NO_3], in which [N_{1888}][NO_3] was irradiated to various dose levels. It can be seen that the distribution ratio of Am(III) is nearly constant at all dose levels, and interestingly a marginal increase in distribution ratio of Am(III) is observed at higher dose levels. The studies thus shows that the distribution ratio of Am(III) is not affected to a significant extent, if T2EHDGA is irradiated alone and mixed with [N_{1888}][NO_3] or [N_{1888}][NO_3] is irradiated alone and mixed with T2EHDGA. These results are significantly different from those observed in conventional solvent system composed of solution of T2EHDGA in *n*-DD, where *n*-DD is regarded as an “inert” diluent and does not participate in extraction. Since [N_{1888}][NO_3] in this case extract trivalent metal ion and it is present in “bulk” quantity in the solution, the distribution ratio of Am(III), shown in Fig. 6.2A and 6.2B, are not apparently affected to any significant extent.

Fig. 6.4B shows the comparison in the loading behavior of Nd(III) in T2EHDGA/[N_{1888}][NO_3]. In one case T2EHDGA was irradiated to 500 kGy and mixed with [N_{1888}][NO_3] and in the other case [N_{1888}][NO_3] was irradiated to 500 kGy and mixed with T2EHDGA. The extraction of Nd(III) in organic phase was carried out from 3 M nitric acid medium. It can be seen that that the loading of Nd(III) increases with increase in the amount of Nd(III) in aqueous phase in both cases leading to the saturation value of 17 g/L, irrespective of [N_{1888}][NO_3] or T2EHDGA are irradiated to 500 kGy. Even though, the irradiated [N_{1888}][NO_3]

(500 kGy) showed the reduction in the loading of Nd(III), as shown in Fig. 6.4A, the irradiated $[N_{1888}][NO_3]$ when mixed with T2EHDGA shows no change in the saturation loading value (Fig. 6.4B). This can be attributed to the participation of T2EHDGA in the extraction of Nd(III), which ultimately leads to the saturation limit of 17 g/L, equivalent to the value obtained for the unirradiated $[N_{1888}][NO_3]$. Similarly, the irradiated T2EHDGA when mixed with unirradiated $[N_{1888}][NO_3]$ also produced a saturation limit of 17 g/L Nd(III) loading in ionic liquid phase.

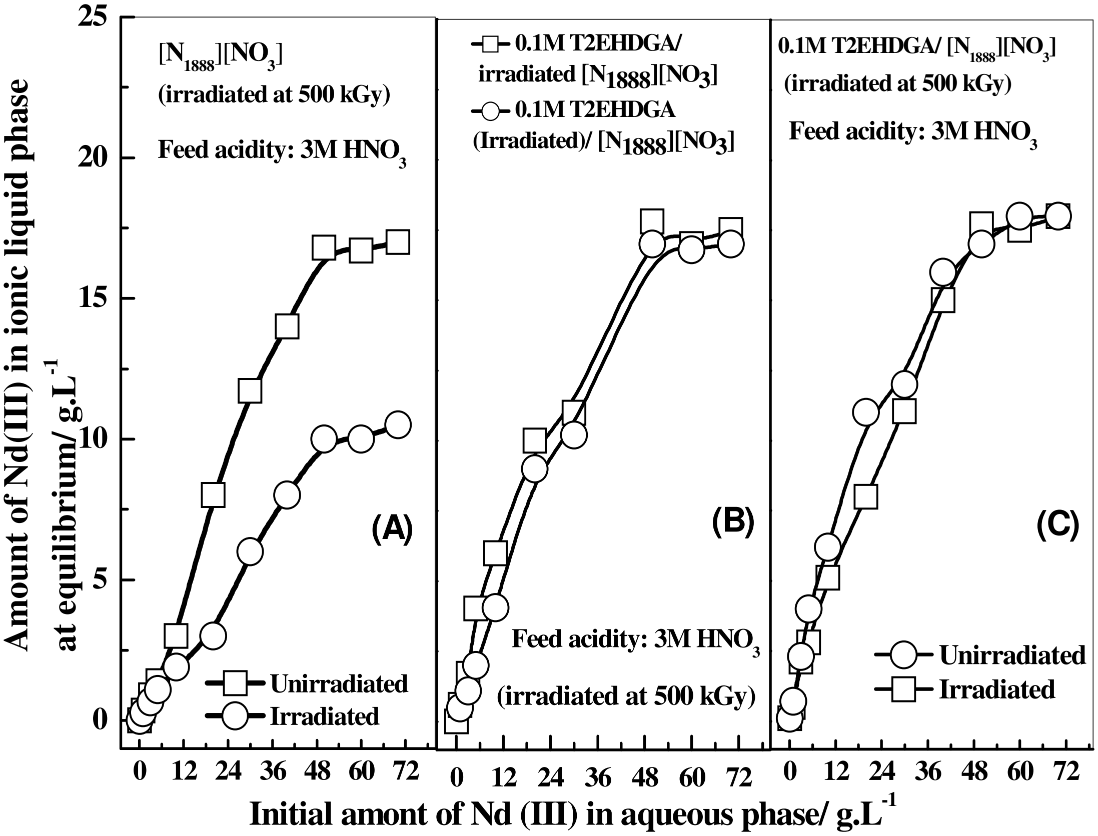

Fig. 6.4. The extraction of Nd (III) in ionic liquid phase as a function of initial concentration of Nd (III) in aqueous phase. Ionic liquid phase: (A) $[N_{1888}][NO_3]$ alone; (B) 0.1 M T2EHDGA /$[N_{1888}][NO_3]$ (irradiated) or 0.1 M T2EHDGA (irradiated)/ $[N_{1888}][NO_3]$; (C) 0.1 M T2EHDGA /$[N_{1888}][NO_3]$ (unirradiated and irradiated); Aqueous phase: 3 M HNO_3 with varied Nd(III) concentrations; Absorbed dose 500kGy; Temperature = 298 K; Equilibration time = 1 h; Phase volume ratio = 1.

6.2.4. Irradiation in binary solution

When T2EHDGA was irradiated together with *n*-dodecane, the distribution ratio of Am(III) measured in irradiated T2EHDGA/*n*-DD was always lower than the distribution ratio of Am(III) measured in a solution of irradiated T2EHDGA containing unirradiated *n*-dodecane [40]. This was attributed to the sensitization effect. Fig. 6.4C shows the loading behavior of Nd(III) in the irradiated solution of 0.1 M T2EHDGA/ $[N_{1888}][NO_3]$. The absorbed γ-dose was 500 kGy and the irradiated solution was subjected to the extraction of Nd(III) from 3 M nitric acid medium. The data compared with unirradiated 0.1 M T2EHDGA/$[N_{1888}][NO_3]$. It can be seen that the loading of Nd(III) in organic phase increases with increase in the amount of Nd(III) aqueous phase in both cases, leading to the saturation loading of 17 g/L in organic phase, indicating that there is no change in the loading behavior of irradiated and unirradiated systems. These results confirm that the extraction of Nd(III) in organic phase is predominantly governed by $[N_{1888}][NO_3]$, even if the degradation occurs either in T2EHDGA or $[N_{1888}][NO_3]$. The degradation of T2EHDGA or $[N_{1888}][NO_3]$ is nullified, when these two are mixed together for the measurement of distribution ratio of Am(III) or loading of Nd(III). This is essentially due to the participation of the bulk ionic liquid, namely $[N_{1888}][NO_3]$ along with T2EHDGA in the extraction of Nd(III) or Am(III), which eventually leads to no change in the distribution ratio of Am(III) or loading of Nd(III) in organic phase.

6.2.5. FT-IR spectroscopy

The radiolytic degradation of $[N_{1888}][NO_3]$ and its solution with T2EHDGA was characterized by FTIR spectroscopy. The FTIR spectrum of $[N_{1888}][NO_3]$ is shown in the spectrum A of Fig. 6.5 The spectrum shows the nitrate stretching bands at different places. The nitrate ion exhibits a weak transmittance band at 830 cm^{-1}, a strong band in the range 1340 cm^{-1} with a shoulder at 1370 cm^{-1}, and very weak bands at 1640 cm^{-1} and 1726 cm^{-1}. The position of nitrate bands at 830 cm^{-1} and the intense band at 1340 cm^{-1} and 1370 cm^{-1} are strongly affected by the nature of cation with which the nitrate is associated. Since $[N_{1888}][NO_3]$ is assumed to contain major component of methyltrioctylammonium nitrate, but it also contains other tetra alkyl cations as reported elsewhere [40], the transmittance band at 1300 cm^{-1} to 1400 cm^{-1} is usually broad. Similarly the weak band at 830 cm^{-1} is also accompanied by some more weak shoulders and transmittance bands from 830 to 900 cm^{-1}. These two transmittance bands positioned at 1300 to 1400 cm^{-1} and 830 to 900 cm^{-1} undergo a number of changes, depending upon the interaction between the cation and nitrate. The FTIR spectrum of $[N_{1888}][NO_3]$ also contained strong transmittance bands in the range at 2800 to 2900 cm^{-1}, due to the C-H stretching frequencies. These bands are not affected upon irradiation or extraction. Therefore, they are not shown in the FTIR spectrum.

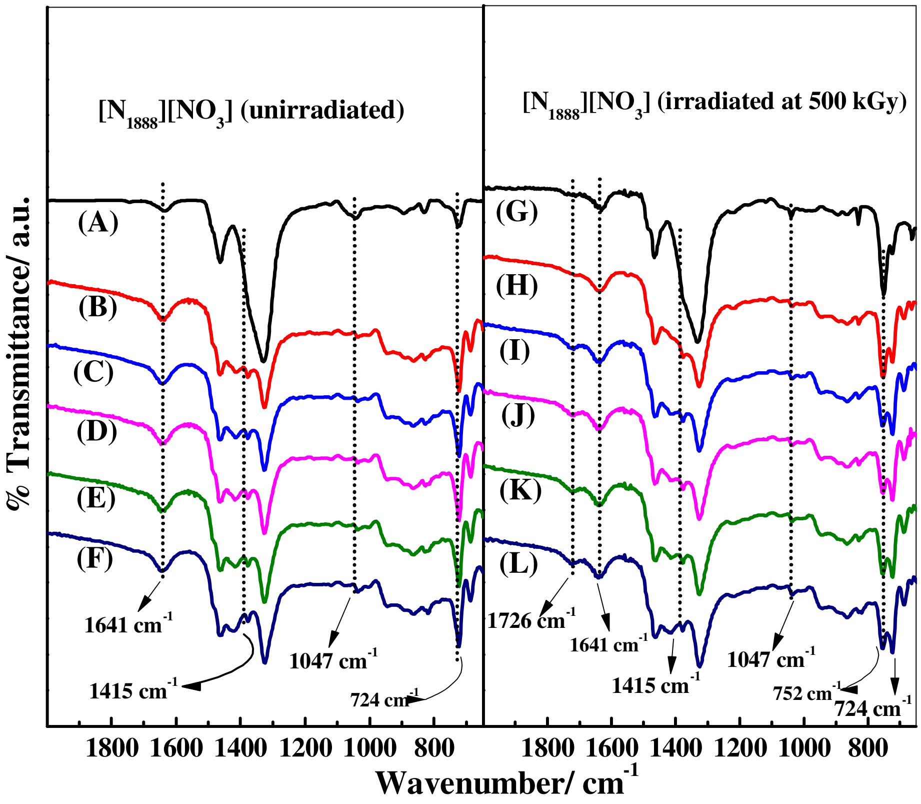

Fig. 6.5. FTIR spectra of unirradiated and irradiated ionic liquid phase as a function of Nd(III) loading in 3 M nitric acid. Ionic liquid phase: Unirradiated (or irradiated at 500 kGy) $[N_{1888}][NO_3]$. A&G) Dry ionic liquid phase; B&H) 3 M HNO3 equilibrated; C&I) 3 M HNO_3 equilibrated with 5 g.L^{-1} Nd(III) loaded; D&J) 3 M HNO_3 equilibrated with 10 g.L^{-1} Nd(III) loaded; E&K) 3 M HNO_3 equilibrated with 20 g.L^{-1} Nd(III) loaded; F&L) 3 M HNO_3 equilibrated with 50 g.L^{-1} Nd(III) loaded.

The spectrum B of Fig. 6.5 corresponds to the $[N_{1888}][NO_3]$ phase recorded after contacting the ionic liquid phase with 3 M nitric acid. A number of changes in the FTIR spectrum is observed in spectrum B upon contacting the $[N_{1888}][NO_3]$ phase with nitric acid. This can be due to the extraction of nitric acid by $[N_{1888}][NO_3]$ phase. The extraction behavior of nitric acid in $[N_{1888}][NO_3]$ and 0.1 M T2EHDGA/$[N_{1888}][NO_3]$ as a function of absorbed dose at different concentrations of nitric acid is shown in Fig. 6.6. It can be seen that significant quantity of nitric acid is extracted into organic phase. The extraction of nitric acid is also accompanied by the co-extraction of water molecules to the $[N_{1888}][NO_3]$ phase [26,28]. The presence of both nitric acid and water molecules in $[N_{1888}][NO_3]$ phase changes the interaction environment between the nitrate ion, H^+ and $[N_{1888}]^+$ ions present in organic phase. As a result, a couple of new nitrate bands at 1375 cm^{-1} and 1415 cm^{-1} appear in the FTIR spectrum of $[N_{1888}][NO_3]$ recorded after equilibrating with nitric acid (spectrum B, Fig 6.5). These bands could be due to the nitrate ions present different environment in the pool of $[N_{1888}]^+$ and H^+ cations. It is also observed that the intensity of 1415 cm^{-1} band increases upon loading of Nd(III) ion in organic phase (spectrum C to F, Fig. 6.5). This can be considered as an evidence for the extraction of Nd^{+3} by $[N_{1888}][NO_3]$, perhaps leading to formation of $[Nd(NO_3)_4]^-$ in organic phase. The nitrate ion bonded to Nd^{+3} as in $[Nd(NO_3)_4]^-$ could be is responsible for the increase in the intensity of the transmittance band at 1415 cm^{-1}. In addition to the above observations which are obviously seen in the FTIR spectrum, a scant changes in the FTIR spectrum of nitric acid and Nd^{+3} extracted $[N_{1888}][NO_3]$ phase did occur in the region 830 to 900 cm^{-1}. In contrast to this, a new transmittance band appears at 1687 cm^{-1} (spectrum B to F, Fig. 6.5) upon contacting the $[N_{1888}][NO_3]$ with 3 M nitric acid, as well as the nitric acid solution containing Nd^{+3} ion. Fig. 6.5 also shows the spectrum of irradiated $[N_{1888}][NO_3]$. The FTIR pattern of irradiated $[N_{1888}][NO_3]$ recorded after contacting the organic phase with 3 M nitric acid and Nd(III) solution in 3 M nitric acid are displayed in Fig. 6.5. Comparing the irradiated $[N_{1888}][NO_3]$ (500 kGy) (spectrum G) with unirradiated $[N_{1888}][NO_3]$ (spectrum A) in Fig. 6.5., the irradiated spectrum shows the appearance of a new band at 752 cm^{-1}. A shoulder at 864 cm^{-1} in the unirradiated $[N_{1888}][NO_3]$ is appearing as a peak at the same position after irradiation. Similarly a broad shoulder at 1041 cm^{-1} in the unirradiated $[N_{1888}][NO_3]$ is split into a couple of weak bands at 1001 cm^{-1} and 1035 cm^{-1}.

The intensity of the transmittance band at 1726 cm^{-1} also increases upon irradiation. The changes seen in the FTIR pattern of unirradiated system (spectrum B to F) also occur in the irradiated [N$_{1888}$][NO$_3$] (spectrum H to L) upon equilibration of irradiated [N$_{1888}$][NO$_3$] with nitric acid or Nd(III) in nitric acid. This involves the appearance of Viscosity and Density of acid equilibrated solvents w bands at 1375 and 1415 cm^{-1} and increase in the intensity of 1415 cm^{-1} band upon Nd(III) loading in [N$_{1888}$][NO$_3$]. Similarly the intensity of 724 cm^{-1} also increased upon HNO$_3$ and Nd(NO$_3$)$_3$ loading in organic phase.

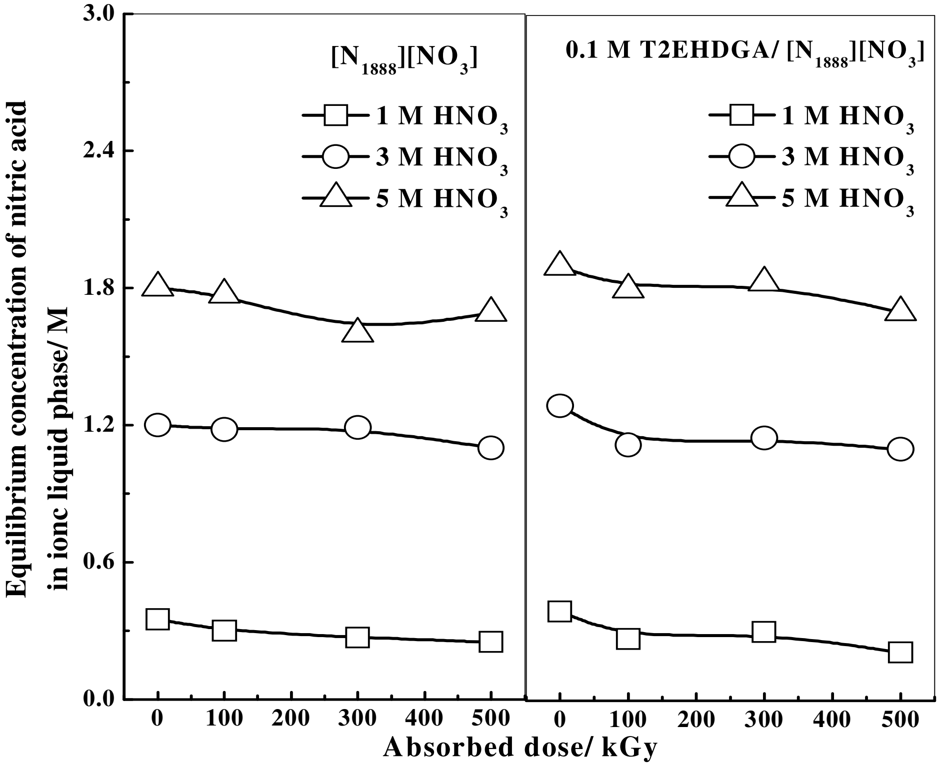

Fig. 6.6. The extraction of nitric acid in the ionic liquid phase as a function of the absorbed dose. Ionic liquid phase: [N$_{1888}$][NO$_3$] alone or 0.1 M T2EHDGA/[N$_{1888}$][NO$_3$]; Aqueous phase: 1–5.0 M HNO$_3$; Temperature = 298 K; Absorbed dose 0-500 kGy; Equilibration time = 1 h; Phase volume ratio = 1.

The FTIR pattern of the irradiated solution of 0.1 M T2EHDGA in $[N_{1888}][NO_3]$ is shown in Fig. 6.7 (spectrum A). The solution was subjected to the extraction of nitric acid (3 M) (spectrum B) and Nd(III) from 3 M nitric acid (spectrum C to F) and the FTIR pattern of organic phase after extraction are also depicted in Fig. 6.7. It can be seen that the changes in the FTIR pattern encountered during the extraction of nitric acid and Nd(III) (spectrum A to F Fig. 6.7.) are similar to those observed in unirradiated $[N_{1888}][NO_3]$, shown in the spectrum A to F of Fig. 6.5 In addition to this, the spectrum of 0.1 M T2EHDGA in $[N_{1888}][NO_3]$ also shows the transmittance bands at 1650 cm^{-1} due to amidic >C=O stretching frequencies, which overlaps with the nitrate transmittance band of $[N_{1888}][NO_3]$. Upon nitric acid extraction in organic phase, the amidic stretching bands are marginally broadened due to the protonation of HNO_3 on amidic >C=O of T2EHDGA (spectrum B, Fig 6.7). Extraction of Nd(III) from nitric acid medium (spectrum C to F, Fig. 6.7) results in the shift of amidic transmittance bands of T2EHDGA from 1650 cm^{-1} to 1610 cm^{-1} due to co-ordination of T2EHDGA with $Nd(NO_3)_3$. This observation shows that T2EHDGA is participating in the extraction of Nd(III) from nitric acid medium. Co-ordination of $Nd(NO_3)_3$ with T2EHDGA results in weakening of amidic >C=O of T2EHDGA and therefore the >C=O stretching frequencies are shifted from 1650 to 1610 cm^{-1}. The shift in the transmittance band from 1642 cm^{-1} to 1610 cm^{-1} is expected to decrease the intensity of the transmittance band at 1642 cm^{-1}. However, the FTIR pattern shown in figure 8 (spectrum C to F) at 1642 cm^{-1} remains unaffected even after Nd(III) loading in 0.1 M T2EHDGA/$[N_{1888}][NO_3]$ phase. This can be due to the overlap of nitrate stretching bands, which also occur at same position (1642 cm^{-1}).

The Fig. 6.7. shows the FTIR spectrum of irradiated 0.1 M solution of T2EHDGA in $[N_{1888}][NO_3]$ (spectrum G). The figure also shows the FTIR spectrum of other samples recorded after contacting the irradiated organic phase with 3 M nitric acid (spectrum H) and Nd(III) in 3 M nitric acid (spectrum I to L). The changes observed in the spectra of all samples of irradiated 0.1 M T2EHDGA/$[N_{1888}][NO_3]$ is similar to those observed in the irradiated $[N_{1888}][NO_3]$ shown in Fig. 6.5 (spectrum G to L). The changes in the FTIR pattern of T2EHDGA observed in spectrum G to L of Fig. 6.7. is similar to that spectrum of B to F of Fig. 6.7. However, the FTIR pattern of unirradiated and irradiated system provides an important confirmation that both T2EHDGA and $[N_{1888}][NO_3]$ are involved in the extraction of Nd(III) from nitric acid medium. The extraction and FTIR investigations of the irradiated ionic liquid phase revealed the following. Since $[N_{1888}][NO_3]$ is present in bulk quantity in the solution of 0.1 M T2EHDGA/ $[N_{1888}][NO_3]$, the extraction of Nd(III) in organic phase is not apparently affected upon irradiation. Since both T2EHDGA and $[N_{1888}][NO_3]$ extract Nd(III), and these extractants aid each other in extraction of Nd(III), even though there is a reduction in the concentration of T2EHDGA and $[N_{1888}][NO_3]$ is expected upon irradiation. In view of this, the distribution ratio of Am(III) as well as the saturation capacity of Nd(III) are not affected upon irradiation of individuals or binary solution.

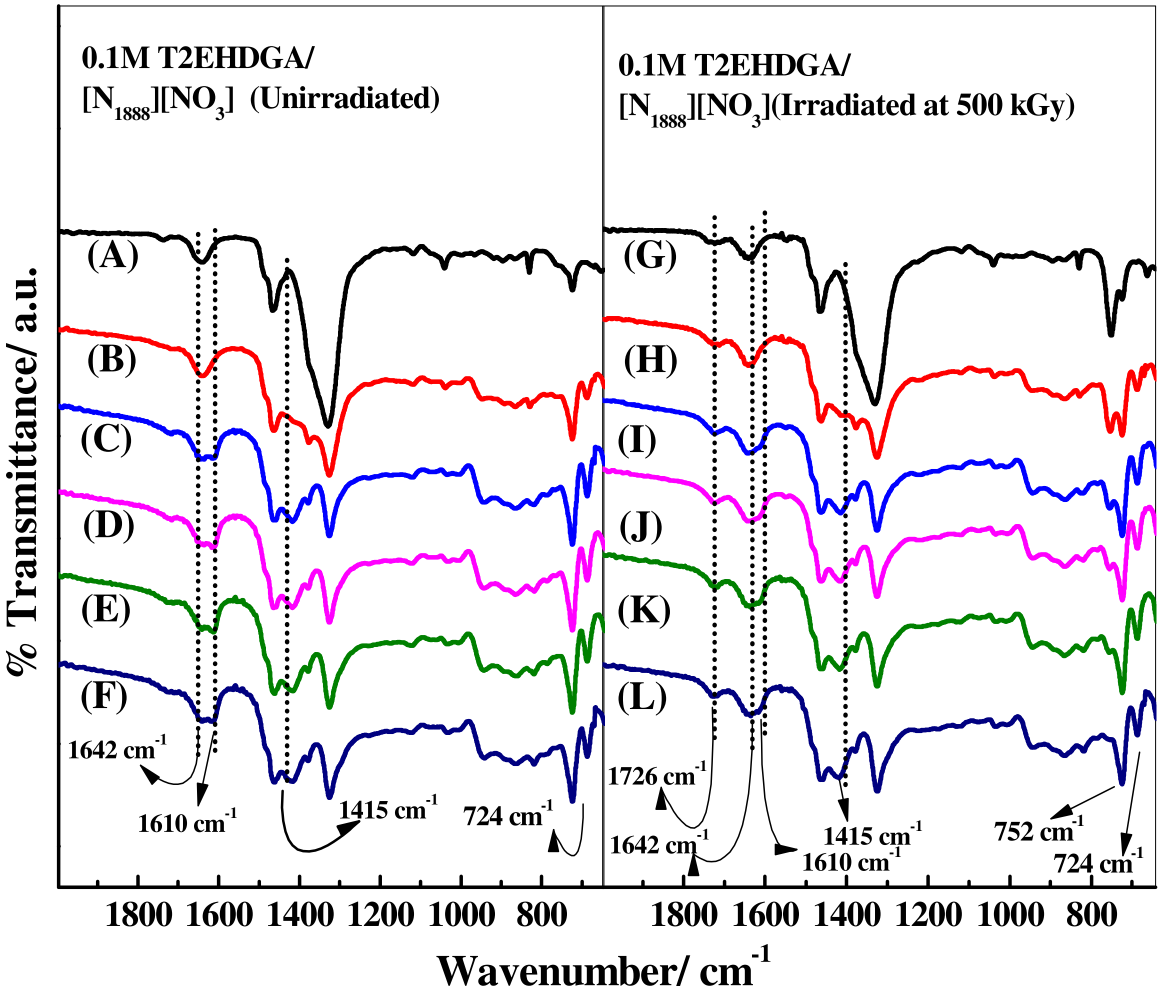

Fig. 6.7. ATR-FTIR spectra of unirradiated and irradiated ionic liquid phase as a function of Nd(III) loading in 3M nitric acid. Ionic liquid phase: Unirradiated (or irradiated at 500 kGy) 0.1M T2EHDGA/ [N_{1888}][NO_3]. A&G) Dry ionic liquid phase; B&H) 3 M HNO3 equilibrated; C&I) 3 M HNO3 equilibrated with 5 g.L^{-1} Nd(III) loaded; D&J) 3 M HNO3 equilibrated with 10 g.L^{-1} Nd(III) loaded; E&K) 3 M HNO3 equilibrated with 20 g.L^{-1} Nd(III) loaded; F&L) 3 M HNO3 equilibrated with 50 g.L^{-1} Nd(III) loaded.

6.2.6. Stripping study

The stripping behavior of Am(III) from the loaded organic phase composed of irradiated and unirradiated solution of 0.1 M T2EHDGA in [N_{1888}][NO_3], was studied and the results are shown in Fig. 6.8. It can be seen that the loaded Am(III) can be quantitatively recovered using dilute nitric acid (0.01 M) in four contacts for the irradiated system. However, five contacts are required for the mixture of irradiated and unirradiated solvent system. Four contacts of the organic phase with 0.01 M nitric acid are required for quantitative recovery of Am(III) from the irradiated 0.1 M T2EHDGA/ [N_{1888}][NO_3] (irradiated together). However, five contacts are required for Am(III) recovery, when either T2EHDGA or [N_{1888}][NO_3] are irradiated above and mixed with the other ligand to form a solution or 0.1 M T2EHDGA/ [N_{1888}][NO_3]. The study shows that the degradation products of T2EHDGA and [N_{1888}][NO_3] are not interfering in the stripping of Am(III) from the loaded organic phase, which is advantageous for using T2EHDGA and [N_{1888}][NO_3] for solvent extraction applications.

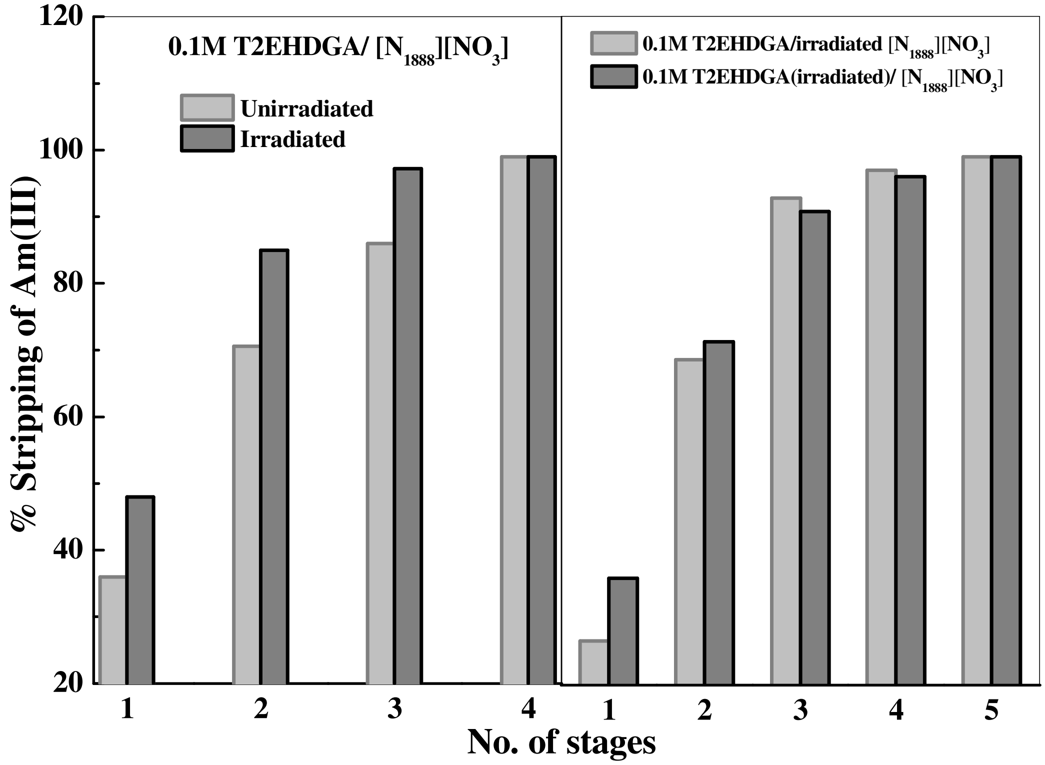

Fig. 6.8. The percentage of stripping of Am(III) as a function of number of contacts of ionic liquid phase with aqueous phase. Ionic liquid phase: 0.1 M T2EHDGA/ [N_{1888}][NO_3]; Absorbed dose 500 kGy; Temperature = 298 K; Stripping solution: 0.01 M HNO_3; Equilibration time = 1 hr; Phase volume ratio = 1.

6.3. Summary

The radiolytic degradation of the CHON system composed of T2EHDGA in [N_{1888}][NO_3] ionic liquid was studied and the results were compared with those obtained in the conventional molecular diluents (*n*-DD) system. The distribution ratio of Am(III) in 0.1 M T2EHDGA/ [N_{1888}][NO_3] remained nearly constant irrespective of the γ-absorbed dose, while the $D_{Am(III)}$ decreased with increase of absorbed dose in T2EHDGA/*n*-DD. To understand this difference, the T2EHDGA alone was irradiated and mixed with [N_{1888}][NO_3] and $D_{Am(III)}$ was determined.

Under this condition T2EHDGA was expected to undergo degradation and lower the distribution ratio of Am(III) in irradiated T2EHDGA present in $[N_{1888}][NO_3]$, but the $D_{Am(III)}$ was invariant in this case also, indicating the participation of the bulk $[N_{1888}][NO_3]$ for the extraction of Am(III). The extraction mechanism suggested that two molecules of T2EHDGA was participated during the extraction of Am(III) in $[N_{1888}][NO_3]$ medium at different γ-absorbed dose.

The possibility of extraction of Am(III) by $[N_{1888}][NO_3]$ was confirmed by loading of Nd(III) to the extent of 17 g/L into the $[N_{1888}][NO_3]$ phase. The FTIR spectroscopic investigations also confirmed the co-ordination of $Nd(NO_3)_3$ by T2EHDGA in $[N_{1888}][NO_3]$. Overall the extraction of trivalent metal ion in organic phase in this system was essentially controlled by $[N_{1888}][NO_3]$ organic phase, even though there was a radiolytic degradation occurred in T2EHDGA as well as $[N_{1888}][NO_3]$. The degradation effect of γ-radiation on the distribution ratio of trivalents was not observed apparently during extraction, since both T2EHDGA and $[N_{1888}][NO_3]$ extract trivalent metal ion, and among these two, the $[N_{1888}][NO_3]$ was present in bulk quantity. The loaded Am(III) recovered using dilute nitric acid (0.01 M) in four contacts for irradiated and unirradiated systems. However five contacts are required for the mixture of irradiated and unirradiated solvent systems. The degradation products seems to be innocuous, since they did not retain Am(III) during stripping. In view of this, the ionic liquid, $[N_{1888}][NO_3]$, can be regarded as a promising substitute to $[C_nmim][NTf_2]$ based ionic liquids studied for possible applications in nuclear fuel cycle over the last two decades.

PART II: Thermophysical properties properties of ionic liquid solvent system

6.4. Introduction

The room temperature ionic liquids (RTILs) are organic salts useful for various applications. RTILs witnessed an extraordinary growth of research and development activity in different areas of science and engineering over the last two decades [41-46]. One of the most difficult tasks at the back end of the nuclear fuel cycle is the mutual separation of lanthanides and actinides. This is obviously due to the very close similarities in the physical and chemical properties of the trivalent lanthanides and actinides present in high-level liquid waste (HLLW) [53, 54]. Nevertheless, these trivalent metal ions exhibit a marginal difference in the chemical reactivity towards ligands [53,54]. In view of this, a number of acidic complexing reagents have been developed and reported for the mutual separation of lanthanides and actinides [55-60]. For instance, the acidic extractants such as, di(2-ethylhexyl)phosphoric acid (D2EHPA) and diglycolamic acid (HDEHDGA) are well studied ligands for the mutual separation of trivalent lanthanides and actinides [59]. These reagents strongly coordinate with lanthanides and trivalent actinides from nirtric acid concentration ranging from 0.001 to 0.1 M [57-60]. It should be noted that D2EHPA is a strong acidic ligand, complexes with trivalent metal ions through –POO- moiety [55, 57], where as HDEHDGA is a chelating type of ligand, coordinates through carboxyl group (-COO-) and etheric moiety [59, 60]. Alok et al. studied the extraction behavior of Eu(III) and Am(III) from dilute nitric acid medium in 0.05 M D2EHPA (or HDEHDGA) dissolved in $[C_8mim][NTf_2]$ medium [61] and compared the results with those obtained in a conventional diluent (*n*-dodecane). Extraordinary separation factor for Eu(III) over Am(III) was achieved in ionic liquid medium as compared to that of *n*-dodecane (*n*-DD). Since these reagents in ionic liquid medium exhibit high potential for the mutual separation of lanthanides and actinides over the existing methods, it is necessary to understand the thermophysical properties of these extractants (D2EHPA and HDEHDGA) in ionic liquid medium for evaluating their suitability of these reagents for actual applications.

Therefore, the objective of the part II in chapter 6 is to report the results on the thermophysical and hydrodynamic properties of the solvent system composed of a solution of D2EHPA and HDEHDGA in 1-butyl-3-methylimidazolium bis(trifluoromethylsulfonyl) imide ([C_4mim][NTf_2]) ionic liquid. The properties such as viscosity, density, phase separation time refractive index etc., were measured for the neat, irradiated and unirradiated solutions. The results were compared with those obtained for the nitric acid equilibrated organic phases. Thermogravimetry analysis was also carried out to understand the thermal stability of the solvent system.

Experimental details for the present chapter are presented in section 2.5.8 of chapter 2. The synthesis of the ionic liquid and extractant was discussed in section 2.6.1 and 2.6.10 of chapter 2 respectively.

Table. 6.2. Structure of molecular extractant and RTIL used in in part II of chapter 6.

Name	Structure
Extractant	
Bis(2-ethylhexyl)phosphoric acid (D2EHPA)	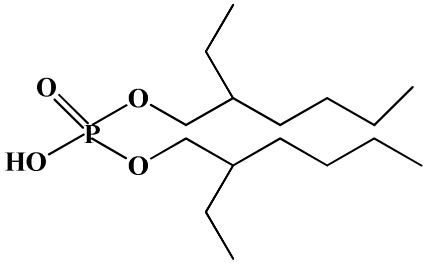
Bis(2-ethylhexyl)diglycolamic acid (HDEHDGA)	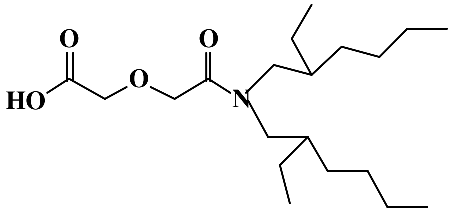
Ionic liquid	
1-butyl-3-methylimidazolim bis(trifluoromethylsulfonyl)imide [C_4mim][NTf_2]	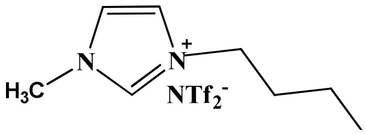

6.5. Results and discussions

6.5.1. *Viscosity and density of dry solvents*

Prior to the measurement of the viscosity and density of HDEHDGA or D2EHPA dissolved in ionic liquid medium, the viscosity and density of pure HDEHDGA and D2EHPA were measured, and the results are tabulated in Table. 6.3. It can be seen that the density value decreases from 0.971 to 0.944 g.cm^{-3} for D2EHPA and 0.965 to 0.941 g.cm^{-3} for HDEHDGA, respectively, with increase of temperature from 298 to 333 K. The viscosity of D2EHPA decreases from 37.8 mPa.s to 11 mPa.s with increase in temperature from 298 K to 333 K. However, the viscosity of HDEHDGA was significantly high at 298 K and therefore the viscosity values are provided only from 313 to 333 K in Table. 6.3. Alok et al. reported the viscosity and density of the present ionic liquid, [C_4mim][NTf_2] [62]. It can be seen from Table. 6.3. that the viscosity and density of the extractants, D2EHPA and HDEHDGA, are quite different from those of [C_4mim][NTf_2]. Therefore, it would be interesting to understand the variation in the physical parameters when these extractants are mixed with [C_4mim][NTf_2] to form a solution. In this context, the concentration of two extractants in [C_4mim][NTf_2] was varied from 0.02 to 0.1 M, and the viscosity and density of the solution at different temperatures were measured. Figure 6.9a& b. depicts the variation in viscosity of HDEHDGA (and D2EHPA)/[C_4mim][NTf_2] as a function of the extractant concentration in the ionic liquid phase. As expected, the viscosity of the ionic liquid phase increases from 40 to 46 mPa.s at 298 K with an increase in the concentration of HDEHDGA from 0.02 to 0.1 M in the ionic liquid phase, which is obviously due to the higher viscosity of HDEHDGA (Table. 6.3). On the contrary, under similar experimental conditions, the viscosity of D2EHPA/[C_4mim][NTf_2] increases initially with an increase in D2EHPA concentration, reaching a maximum value of viscosity at the concentration of 0.06 M, followed by a gradual decrease in viscosity with a further increase in the concentration of D2EHPA in the ionic liquid phase. This finding is different from that of HDEHDGA, and the decreasing viscosity trend could be attributed to the fact that the viscosity of D2EHPA is less (36 mPa.s) than that of [C_4mim][NTf_2] (40 mPa.s).

Table. 6.3. Viscosity and density of neat D2EHPA and HDEHDGA at various temperatures.

T/K	D2EHPA		HDEHDGA	
	Density/ g.cm^{-3}	Viscosity/ mPa.s	Density/ g.cm^{-3}	Viscosity/ mPa.s
298	0.97071	36.81	0.96571	---
303	0.96696	30.70	0.96233	---
313	0.95939	21.11	0.95549	1070
323	0.95181	15.19	0.94855	499
333	0.94424	11.34	0.94178	256

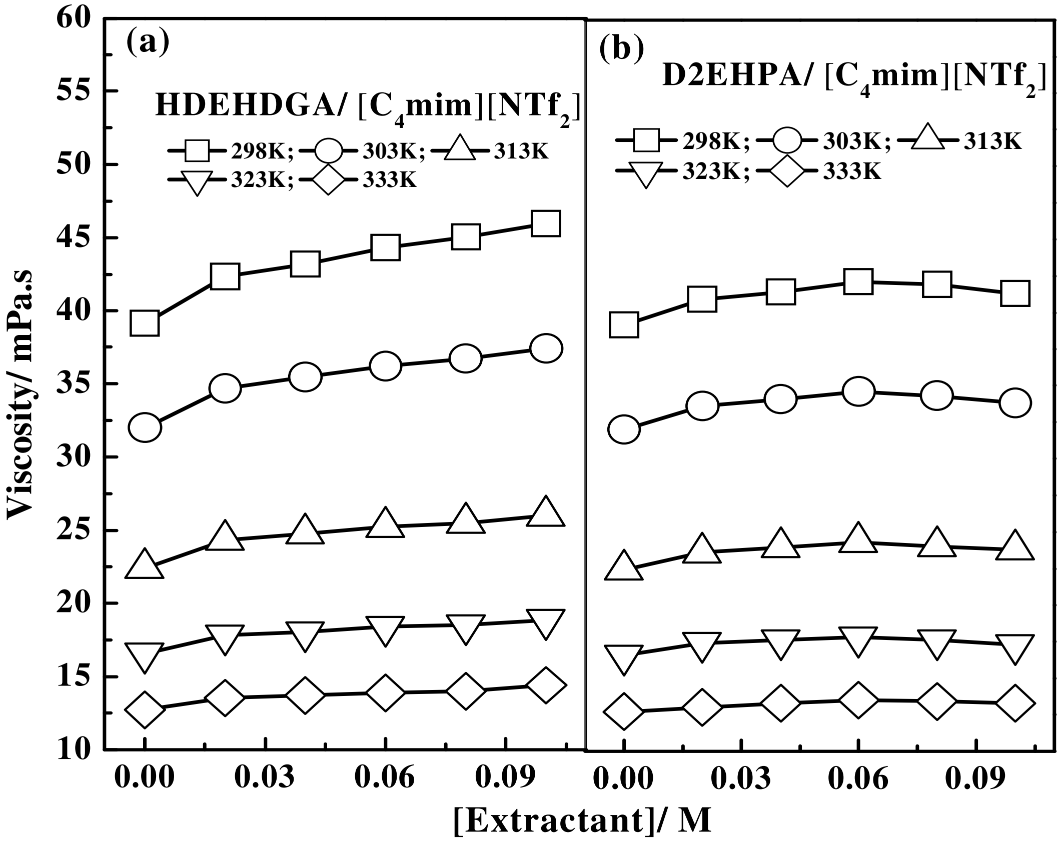

Fig. 6.9. Variation in the viscosity of ionic liquid phase as a function of extractrant concentration. Ionic liquid phase: (a) 0.02-0.1 M HDEHDGA/[C$_4$mim][NTf$_2$], (b) 0.02-0.1 M D2EHPA/[C$_4$mim][NTf$_2$]; Temperature = 298 -333 K.

Similarly, the density of the ionic liquid phase as a function of extractant concentrations in the $[C_4mim][NTf_2]$ phase was determined at different temperatures, and the results are shown in Fig. 6.10. Fig. 6.10a. displays the variation of density of the ionic liquid phase as a function HDEHDGA concentration in ionic liquid at various temperatures. It can be seen that the density decreases linearly with increasing of HDEHDGA concentration in the ionic liquid phase. It is understood that the density of HDEHDGA is 0.965 $g.cm^{-3}$ and that of $[C_4mim][NTf_2]$ is 1.431 $g.cm^{-3}$ at 298 K, and the gradual addition of HDEHDGA (from 0.02 to 0.1 M) to $[C_4mim][NTf_2]$ decreases the density of the ionic liquid phase from 1.431 to 1.415 $g.cm^{-3}$ at 298 K. In contrast to this, the density of the ionic liquid phase upon adding D2EHPA does not show any appreciable change (Fig. 6.10b). Although the density of D2EHPA is also less (0.971 $g.cm^{-3}$) than that of $[C_4mim][NTf_2]$, there is no significant change in the density value upon adding D2EHPA to $[C_4mim][NTf_2]$. However, the density of both the ionic liquid phases showed a decreasing trend with an increase of temperature.

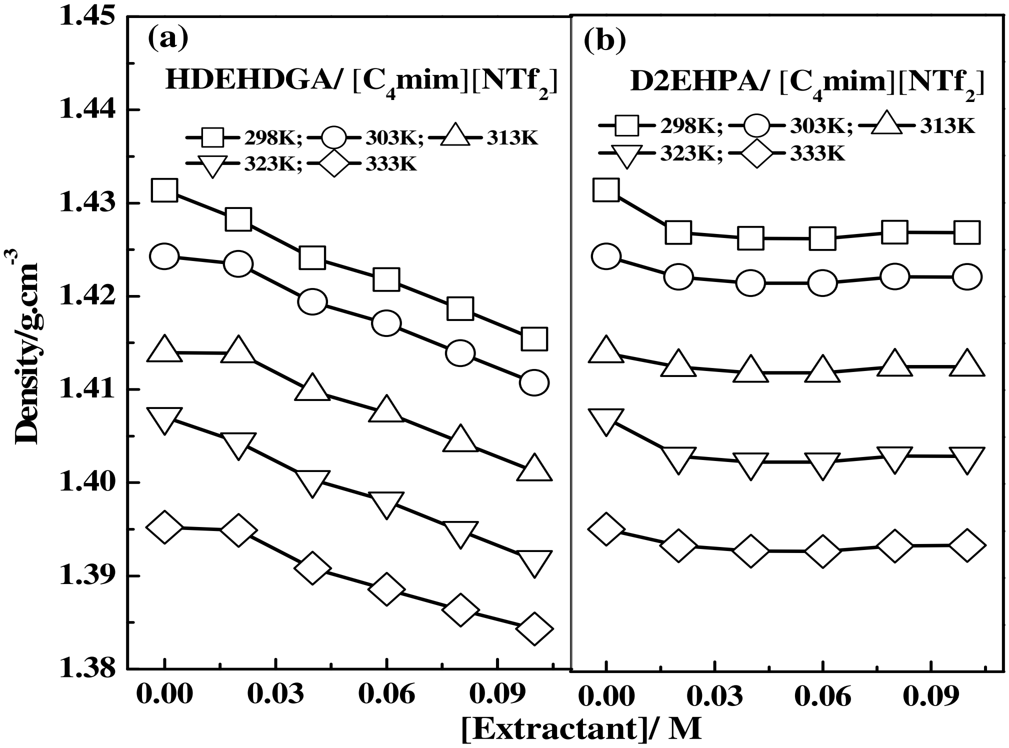

Fig. 6.10. Variation in the density of ionic liquid phase as a function of extractrant concentration. Ionic liquid phase: (a) 0.02-01 M HDEHDGA/[C_4mim][NTf_2], (b) 0.02-0.1 M D2EHPA/[C_4mim][NTf_2]; Temperature = 298 -333 K.

The viscosities of 0.06 M HDEHDGA (or D2EHPA)/[C_4mim][NTf_2] at different temperatures are displayed in Fig. 6.11. As expected, the viscosity values decrease exponentially from 45 to 14 mPa.s and 42 to 13 mPa.s with the increase of temperature for 0.06 M HDEHDGA/[C_4mim][NTf_2] and 0.06 M D2EHPA/[C_4mim][NTf_2], respectively. It should be noted that the viscosity of the solution is higher than that of the ionic liquid (40 mPa.s at 298 K) phase alone, irrespective of the temperature. The inset in Fig. 6.11. shows the logarithmic value of viscosity (logη) as a function of 1/T. It can be seen that log η increases linearly with 1/T. From the slope of the straight line and using equation 1, the energy of activation (E_a) was determined to be 27.4 kJ/mol and 26.85 kJ/mol for the 0.06 M HDEHDGA/[C_4mim][NTf_2] and 0.06 M D2EHPA/[C_4mim][NTf_2] phases, respectively.

$$\log \eta = \log\eta_0 + \frac{E_a}{2.303RT} \tag{6.4}$$

where η is the viscosity at the studied temperature and η_0 is the pre-exponential factor. E_a is the energy of activation and T is the experimental temperature.

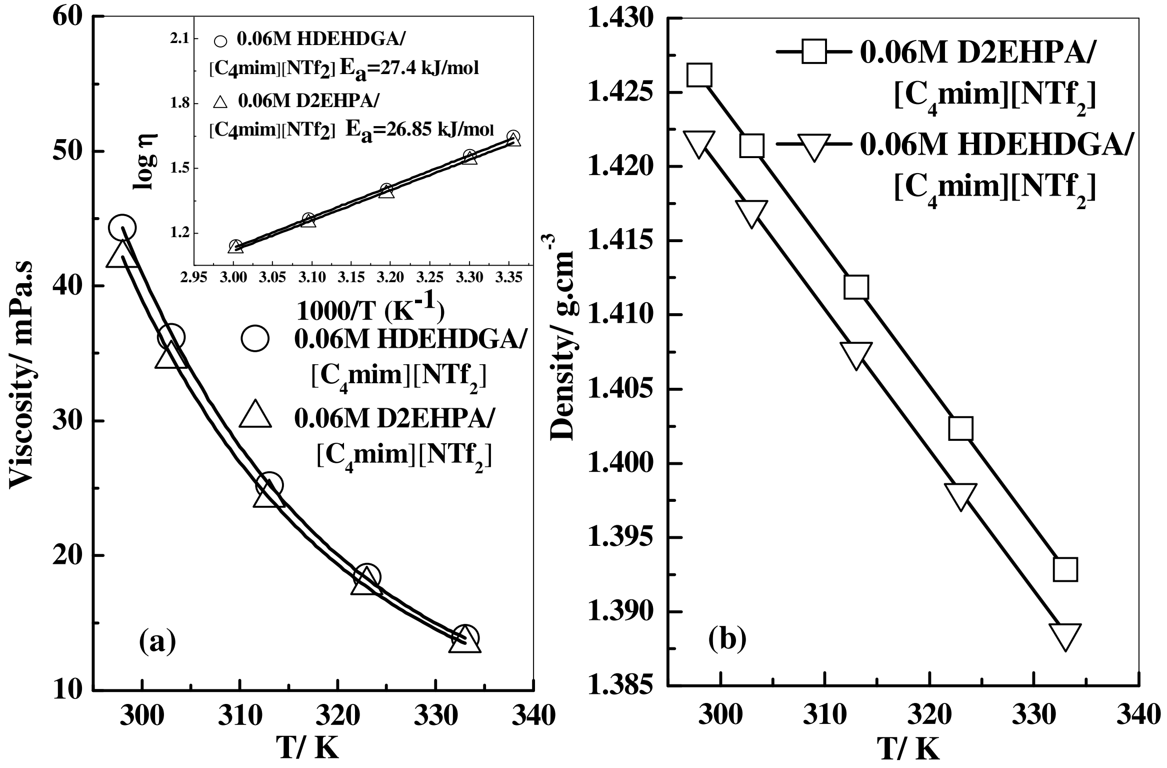

Fig. 6.11. Variation in the viscosity (a) and density (b) of the dry ionic liquid phase composition comprising of 0.06 M HDEHDGA (or D2EHPA) in [C_4mim][NTf_2] as a function of Temperature = 298 – 333 K. (a) Inset: Arrhenius plot

6.5.2. Viscosity and density of acid equilibrated solvents

During the mutual separation of Ln(III)/An(III) by a solvent extraction procedure, the ionic liquid phase is contacted with nitric acid feed solution containing Ln(III) and An(III) [61]. In this context, it is necessary to determine the viscosity and density of the solvent phase, namely 0.06 M HDEHDGA (or D2EHPA)/[C_4mim][NTf_2], which is likely to change upon contact with nitric acid. The viscosity and density of 0.06 M HDEHDGA(or D2EHPA)/[C_4mim][NTf_2] was measured after contacting the ionic liquid phase with different concentrations of nitric acid at various temperatures. The results are shown in Fig. 6.12. and 6.13. It can be seen that there is a sudden drop in both viscosity and density values of both ionic liquid phases after equilibrating with nitric acid solution. For instance, after equilibrating the ionic liquid phase with 0.01 M nitric acid, the viscosity decreases from 44.32 mPa.s to 32.91 mPa.s and 42.14 mPa.s to 30.79 mPa.s for the ionic liquid phases 0.06 M HDEHDGA/[C_4mim][NTf_2] and 0.06 M D2EHPA/[C_4mim][NTf_2] respectively (Fig. 6.12), followed by remaining almost constant with further increase in nitric acid concentrations. The decrease in viscosity can be attributed to the extraction of water and nitric acid into ionic liquid phase during contact with the aqueous phase which lowers the attractive forces (responsible for viscosity) between the cation and anion of the ionic liquid phase. Similarly, the density value of HDEHDGA/[C_4mim][NTf_2] drops from 1.426 to 1.418 $g.cm^{-3}$, and that of D2EHPA/[C_4mim][NTf_2] drops from 1.428 to 1.415 $g.cm^{-3}$ after contact with the ionic liquid phase with 0.01 M nitric acid. This could be due to the extraction of nitric acid and water in the ionic liquid phase upon contact with nitric acid.

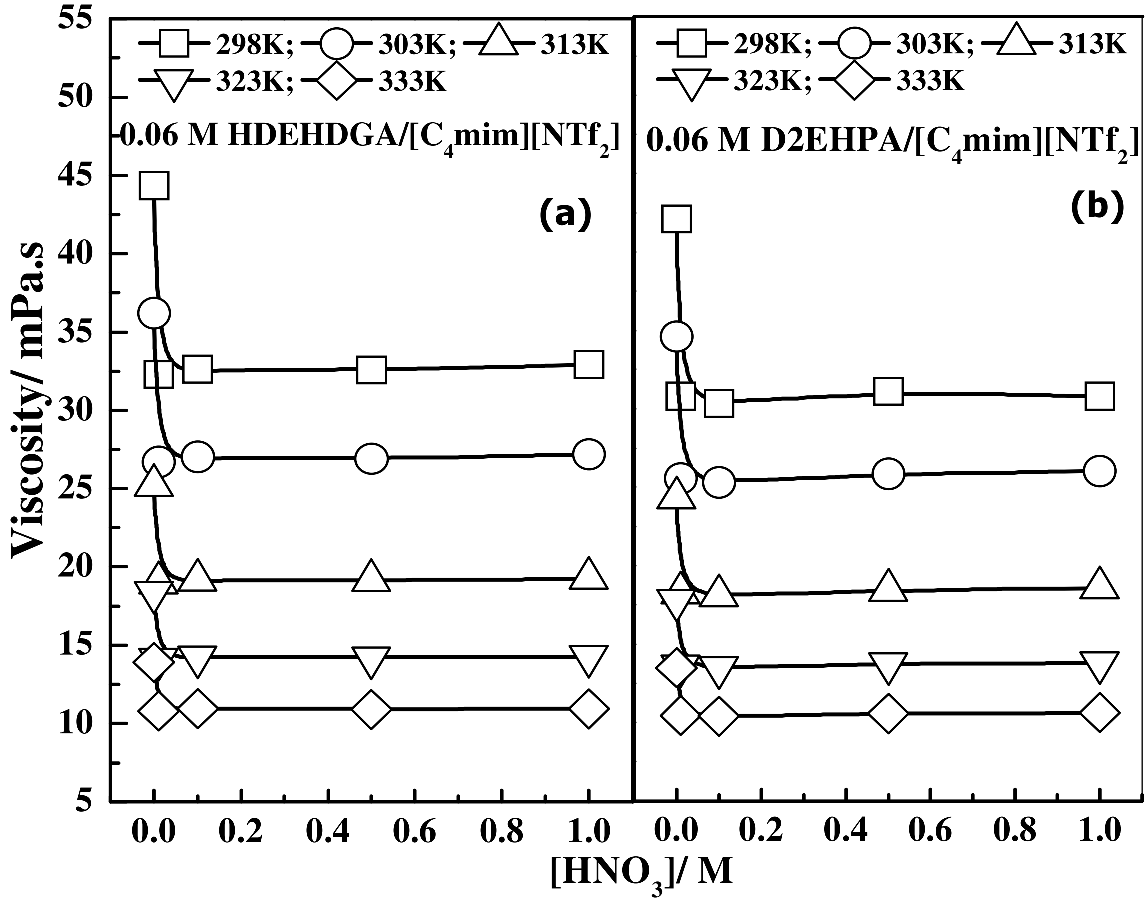

Fig. 6.12. Variation in the viscosity of the ionic liquid phase as a function of nitric acid concentration. Ionic liquid phase: 0.06 M HDEHDGA/[C_4mim][NTf_2] (a) or 0.06 M D2EHPA/[C_4mim][NTf_2] (b); Aqueous phase: 0-1.0 M HNO_3; Temperature = 298-333 K; Phase volume ratio = 1.

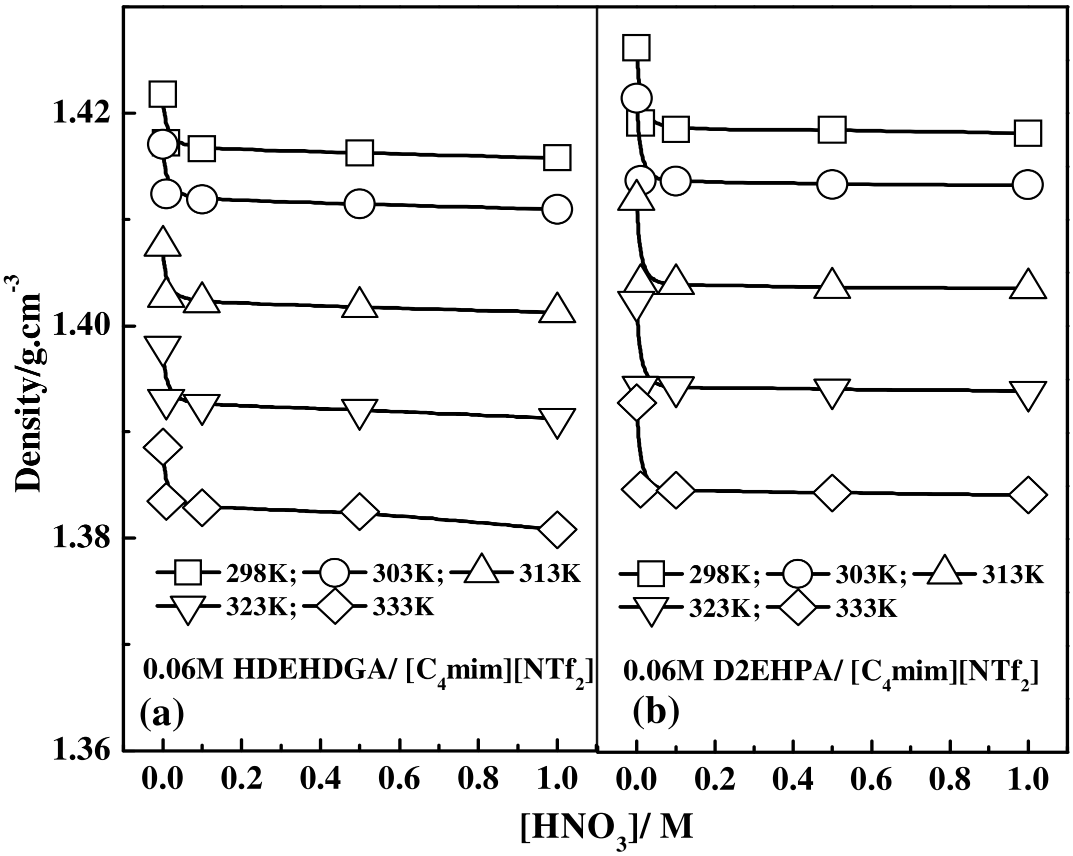

Fig. 6.13. Variation in the density of the ionic liquid phase as a function of nitric acid concentration. Ionic liquid phase: 0.06 M HDEHDGA (a) or 0.06 M D2EHPA (b) /[C_4mim][NTf_2]; Aqueous phase: 0-1.0 M nitric acid; Temperature = 298-333 K; Phase volume ratio = 1.

To understand the extraction of nitric acid into the ionic liquid phase, the extraction behavior of nitric acid in HDEHDGA (or D2EHPA)/[C_4mim][NTf_2] was studied, and the results are shown in Fig. 6.14. It can be seen that the extraction of nitric acid increases with an increase in the concentration of nitric acid, and the degree of extraction is more or less the same for both the extractant phases. Because the density of nitric acid extracted into the organic phase is low (~1 g.cm^{-3}) compared to that of the [C_4mim][NTf_2] phase, the density of the resultant ionic liquid phase obtained after contact with nitric acid is lower than that obtained before contact with nitric acid.

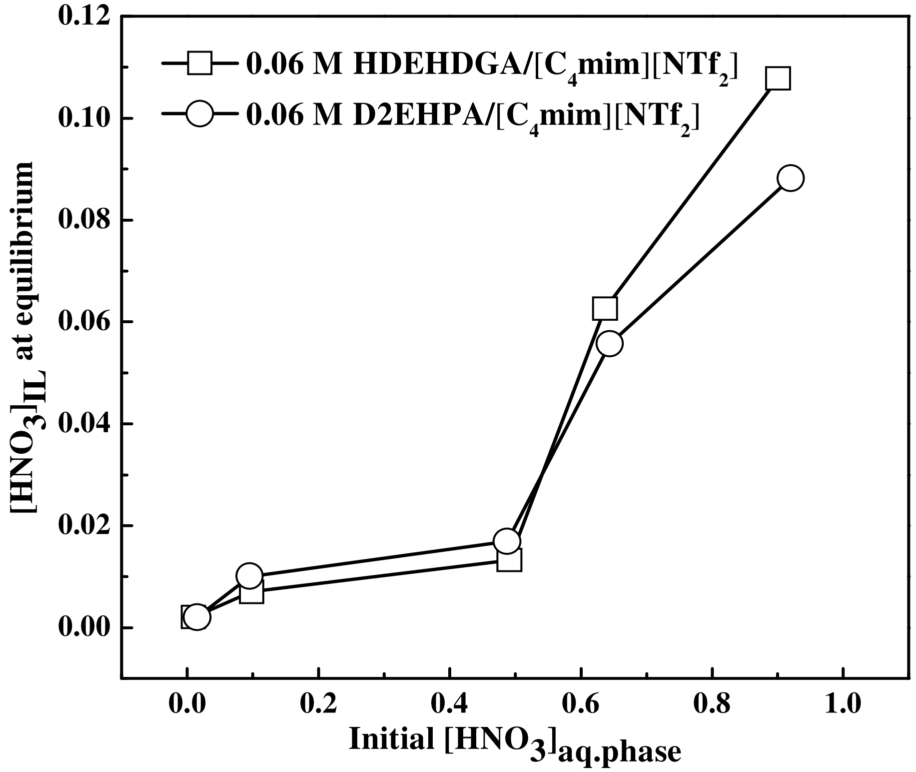

Fig. 6.14. Acid extraction by 0.06 M HDEHDGA (or D2EHPA)/[C$_4$mim][NTf$_2$]. Aqueous phase: 0.01 – 1.0 M HNO$_3$; Temperature = 298 K; Phase volume ratio = 1.

6.5.3 Viscosity of Nd(III) loaded phase

During the extraction of Ln(III)/An(III) from nitric acid medium, the trivalent metal ions are loaded into the organic phase. Under such conditions, it is necessary to understand the thermophysical properties of the loaded organic phase. In this context, the viscosity of the extracted phase after loading of the lanthanide ion representative, namely Nd(III) in 0.06 M HDEHDGA (or 0.06 M D2EHPA)/[C$_4$mim][NTf$_2$], was measured as a function of Nd(III) concentration in the aqueous phase at different temperatures, and the results are shown in Fig.

6.15. It can be seen that the viscosity of the ionic liquid phase shows a gradual increase with an increase in Nd(III) concentration in the aqueous phase at all temperatures in both extractant systems. The increase in viscosity could be attributed to the increase in Nd(III) loading in the organic phase with an increase in Nd(III) concentration in the aqueous phase [28].

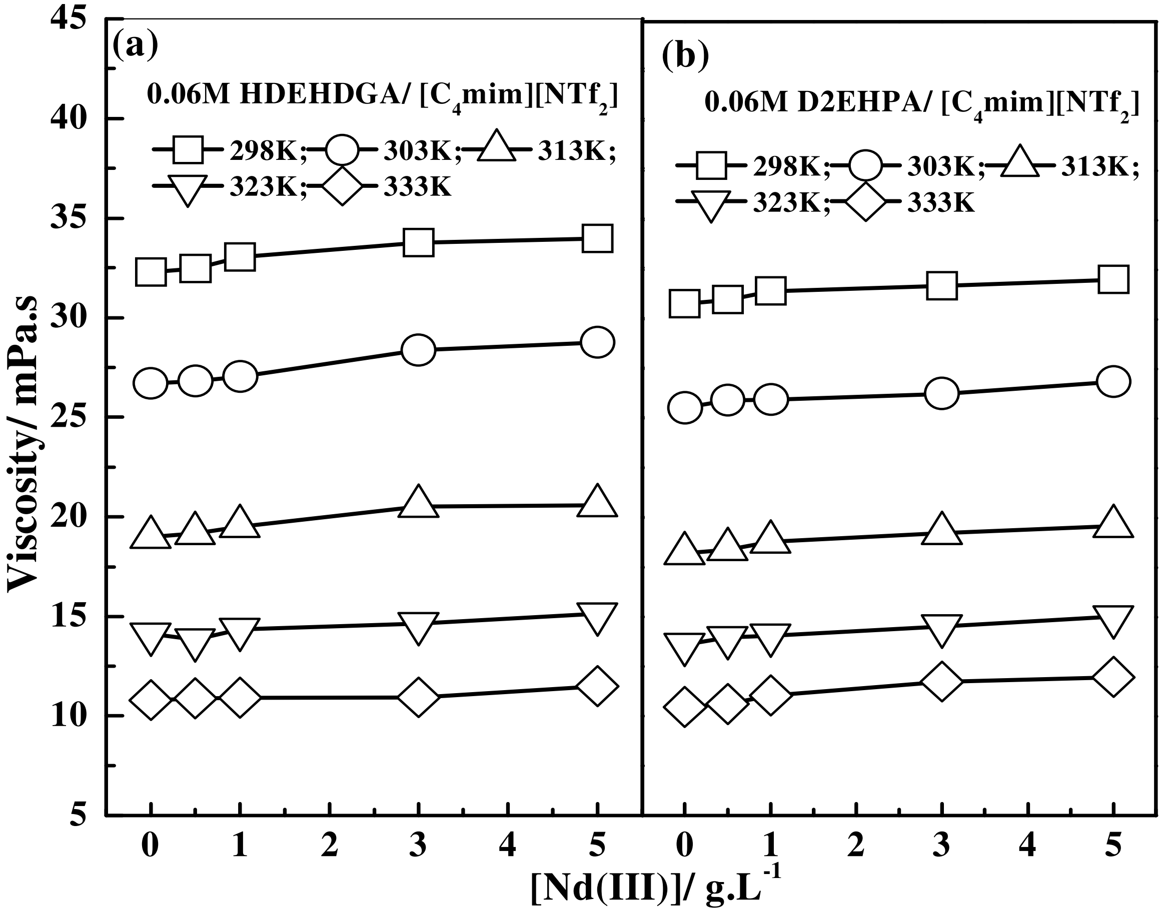

Fig. 6.15. Variation in the viscosity of the ionic liquid phase as a function of Nd(III) concentration in the aqueous phase. Ionic liquid phase: 0.06 M HDEHDGA/[C_4mim][NTf_2] (a) and 0.06 M D2EHPA/[C_4mim][NTf_2] (b); Aqueous phase: 0.01 M HNO_3 + (0 - 5) g/L Nd(III); Temperature = 298 – 333 K; Phase volume ratio = 1.

6.5.4. Thermogravimetry analysis

To understand the thermal stability of the ionic liquid phase, thermogravimetry (TG) analysis of the organic phase, namely [C_4mim][NTf_2], HDEHDGA, D2EHPA, 0.06 M HDEHDGA (or D2EHPA)/[C_4mim][NTf_2] was carried out, and the results are shown in Fig. 6.16. The derivative of the results of Fig. 6.16a is displayed in Fig. 6.16b. It is observed that the ionic liquid phase alone ([C_4mim][NTf_2]) undergoes direct decomposition at 753 K, with the onset of decomposition at 675 K [46]. Similarly, extractants such as HDEHDGA and D2EHPA are stable up to 500 K and 510 K. In contrast, the ionic liquid phase 0.06 M HDEHDGA/[C_4mim][NTf_2] and 0.06 M D2EHPA/[C_4mim][NTf_2] shows the onset of decomposition at 675 K, which is equivalent to the decomposition temperature of the [C_4mim][NTf_2] phase alone. It is also seen from Fig. 6.16a&b that all the organic compositions (except HDEHDGA) undergo single-step decomposition at their decomposition temperatures, while HDEHDGA undergoes two-step decomposition, perhaps due to the presence of the –COOH group and an etheric linkage.

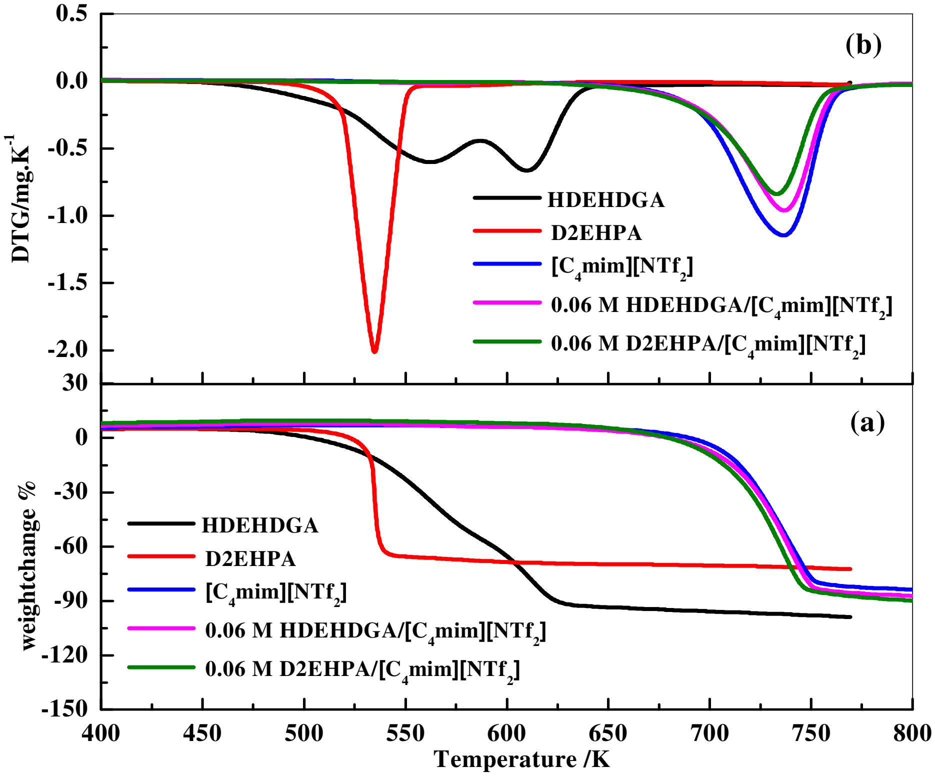

Fig. 6.16. Comparision of TG (a) and DTG (b) plot of different organic phase compositions. Organic phase: HDEHDGA, D2EHPA, 0.06 M HDEHDGA/[C_4mim][NTf_2] and 0.06 M D2EHPA/[C_4mim][NTf_2].

6.5.5. Refractive Index

The refractive index of a molecular or ionic species is a measure of the electronic polarizability of the species and gives the important information while studying the forces between molecules or their behavior in the liquid phase [65, 66]. In this context, the refractive index of the solvent phase compositions such as HDEHDGA, D2EHPA, [C_4mim][NTf_2], 0.06 M HDEHDGA/[C_4mim][NTf_2], and 0.06M D2EHPA/[C_4mim][NTf_2] was measured as a function of temperature, and the results are displayed in Table. 6.4. It can be seen that the refractive index value for HDEHDGA is higher than that of all other solvent systems at all temperatures and the decreasing trend follow the order HDEHDGA (1.4701) > D2EHPA (1.4418) > $[C_4mim][NTf_2]$ (1.4265) > 0.06M HDEHDGA/$[C_4mim][NTf_2]$ (1.4263) > 0.06M D2EHPA/$[C_4mim][NTf_2]$ (1.4260) (the values in brackets are at 298K). The value of the refractive index for the $[C_4mim][NTf_2]$ phase alone is reported elsewhere [27]. The higher value for HDEHDGA could be due to the presence of –COOH and extra etheric linkage, along with the > C = O group, which essentially enables more polarizability compared to the ionic liquid phase alone. Similarly, in the case of D2EHPA, the presence of the –POOH group along with the > P = O group enhances the electronic polarizability like that of HDEHDGA. However, with an increase in temperature, the refractive index shows a linear decrease, irrespective of the solvent composition. Table 6.4 also reports the refractive index of acid (0.01 M nitric acid)-equilibrated ionic liquid phase compositions. It can be seen that the refractive index value decreases after acid equilibration compared to that of the dry state (without acid equilibration). This could possibly be due to the extraction of water molecules (refractive index: 1.33) by the ionic liquid phase, which mainly reduces the refractive index value.

Table. 6.4. Variation in the refractive index of the organic phase compositions at varied temperature and aqueous phase acidity (298K).

T/ K	HDEH DGA	D2EHPA	0.06M HDEHDGA/ $[C_4mim][NTf_2]$	0.06M D2EHPA/ $[C_4mim][NTf_2]$	0.06M HDEHDGA/ $[C_4mim][NTf_2]$ (Equil. with 0.01M HNO_3)	0.06M D2EHPA/ $[C_4mim][NTf_2]$ (Equil. with 0.01M HNO_3)
298	1.4701	1.4418	1.4263	1.4260	1.4251	1.4248
303	1.4688	1.4396	1.4233	1.4242	1.4228	1.4222
313	1.4649	1.4364	1.4221	1.4217	1.4207	1.4203
323	1.4613	1.4328	1.4194	1.4189	1.4183	1.4177
333	1.4577	1.4292	1.4167	1.4162	1.4153	1.4150

6.5.6 Effect of irradiation

Investigation of the radiation stability of D2EHPA (or HDEHDGA)/[C_4mim][NTf_2] is essential when the solvent is proposed for Ln(III) and An(III) separation from nuclear waste [64]. The degradation products formed in the ionic liquid phase are likely to alter the physicochemical and hydrodynamic properties of the organic phase. Therefore, the thermophysical properties such as viscosity, density, and phase separation time were measured for the irradiated 0.06 M HDEHDGA (or D2EHPA)/[C_4mim][NTf_2] solutions, and the results were compared with the unirradiated sample. The absorbed dose in the sample was varied from 0 kGy to 500 kGy. Table. 6.5. shows the variation in the viscosity of 0.06 M HDEHDGA and 0.06 M D2EHPA/[C_4mim][NTf_2] as a function of absorbed dose. It can be seen that the viscosity of 0.06M HDEHGA/[C_4mim][NTf_2] increases from 44.3 mPa.s for the unirradiated sample to 68 mPa.s for the 500 kGy absorbed dose at 298 K. Similarly, the viscosity of 0.06M D2EHPA/[C_4mim][NTf_2] increases from 42 mPa.s to 66 mPa.s with an increase in the absorbed dose from 0 kGy to 500 kGy at 298 K. This could be due to the gradual increase in the generation of degraded products in the organic phase that interact~~s~~ with the ions and molecules present in the ionic liquid phase, leading to an increase in the viscosity of the ionic liquid phase. The increase in temperature obviously results in a decrease in the viscosity values, irrespective of the absorbed dose. It can be noticed from Table. 6.5. that the increase in viscosity of the ionic liquid phase is marginal up to the absorbed dose of 200 kGy, which indicates that degradation products formed up to 200 kGy in the ionic liquid phase are minimal.

Table. 6.5. Variation in the viscosity of ionic liquid phase as a function of absorbed dose. Ionic liquid phase: 0.06 M HDEHDGA/[C_4mim][NTf_2] (a) and 0.06 M D2EHPA/[C_4mim][NTf_2]; Absorbed γ – dose: 0 – 500 kGy; Temperature = 298 – 333K; P = 1 bar.

Dose/ kGy	Viscosity (mPa.s) of the ionic liquid phases at varied temperature 0.06 M HDEHDGA/[C_4mim][NTf_2]				
	298K	303K	313K	323K	333K
0	44.32	36.2	25.22	18.4	13.89
50	44.9	37.2	25.98	18.9	14.07
100	47.2	38.52	26.7	19.4	14.63
200	57.8	46.84	32.84	26.75	19.98
500	68	58	42	32	28
Dose/ kGy	**0.06 M D2EHPA/[C_4mim][NTf_2]**				
0	42.1	34.6	24.3	17.8	13.5
50	42.4	35.1	24.49	17.94	13.62
100	44.97	36.74	25.6	18.7	14.18
200	55.7	48.9	37.87	27.5	22
500	66.32	60.76	49.6	37	29.5

6.5.7. Phase separation time measurement

Fig. 6.17a shows the variation in PST between the two phases after equilibrating the ionic liquid phase and aqueous nitric acid. The data were compared for irradiated (Fig. 6.17b) and unirradiated systems. In case of an unirradiated system (Fig. 6.17a), the PST decreases for HDEHDGA/[C_4mim][NTf_2] from 140 seconds to 40 seconds with an increase in the concentration of nitric acid from 0.01 to 1.0 M in the aqueous phase. Similarly, the PST decreases from 120 seconds to 30 seconds under the same nitric acid concentration range for the D2EHPA/[C_4mim][NTf_2] phase. The reason for such behavior is due to the acidic nature of HDEHDGA and D2EHPA extractants. At low nitric acid concentration, these acidic extractants undergo dissociation and interact with the aqueous phase, leading to higher PST values. Fig. 6.17b shows the PST for the irradiated 0.06 M HDEHDGA (or D2EHPA)/[C_4mim][NTf_2]

measured after contacting the ionic liquid phase with 0.1M nitric acid. The absorbed dose was varied up to 500 kGy. It can be seen that the PST increases from 80 seconds (for unirradiated) to 100 seconds and from 60 seconds (for unirradiated) to 85 seconds for the irradiated 0.06 M HDEHDGA/[C_4mim][NTf_2] and 0.06 M D2EHPA/[C_4mim][NTf_2] with an increase of absorbed dose from 0 kGy to 500 kGy. The increase in the PST could be due to the presence of degradation products in the ionic liquid phase. However, the increase in PST is only marginal, and hence, it can be concluded that the present extractant–ionic liquid mixtures are suitable for mutual separation of lanthanides and actinides from nuclear waste solution.

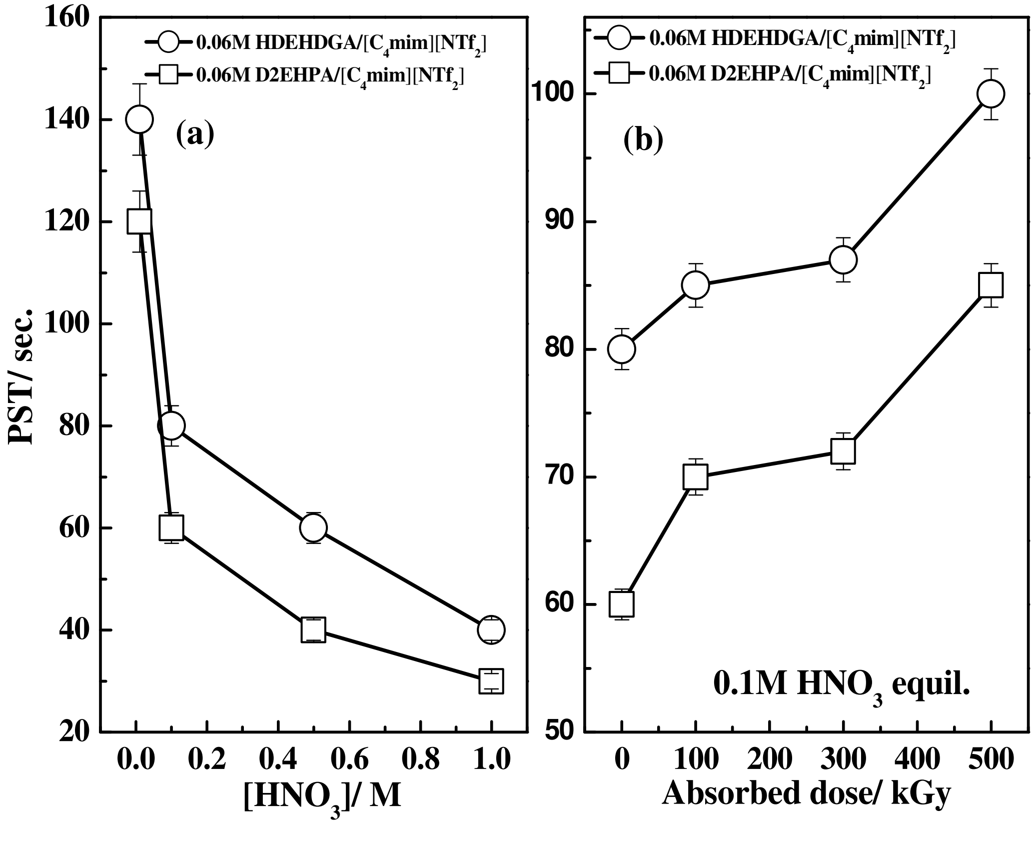

Fig. 6.17. Variation in the phase separation time (PST) as a function of aqueous phase acidity (a) and absorbed dose (b) Ionic liquid phase: 0.06 M HDEHDGA (or 0.06 M D2EHPA)/[C_4mim][NTf_2]; Aqueous phase: 0.01-1.0 M HNO_3; Absorbed dose: 0-500 kGy; Temperature = 298 K; Phase volume ratio =1.

6.6. Summary

The physicochemical properties of HDEHDGA and D2EHPA dissolved [C_4mim][NTf_2] ionic liquid were studied. The viscosity of HDEHDGA and D2EHPA dissolved in [C_4mim][NTf_2] medium decreased with an increase in temperature. The viscosity of the ionic liquid phase initially increased with an increase in concentration of HDEHDGA, followed by a decrease in viscosity values; however, the viscosity of the D2EHPA phase increased with an increase in the concentration of D2EHPA in the ionic liquid phase. The density of D2EHPA and HDEHDGA and their solution with [C_4mim][NTf_2] decreased with an increase in temperature. The viscosity of the loaded ionic liquid phase showed a gradual increase with an increase in loading of Nd(III) in the ionic liquid phase, and the viscosity of the irradiated solvent increased with an increase of absorbed dose. The Viscosity and density values decreased upon acid equilibration for both the extractant-ionic liquid solutions. The PST decreased with an increase in the concentration of nitric acid in the case of unirradiated systems, and PST increased with an increase of absorbed dose. Refractive index values of the ionic liquid compositions decreased with an increase in temperature, as well as upon acid equilibration. The ionic liquid phase was thermally stable up to 675 K, and the presence of the extractants did not alter the thermal stability of the [C_4mim][NTf_2] phase to any significant extent.

References

1. X.Q. Sun, H.M. Luo, S. Dai, Ionic Liquids-Based Extraction: A Promising Strategy for the Advanced Nuclear Fuel Cycle, Chem. Rev. 112 (2012) 2100-2128.
2. N.K. Gupta, Ionic liquids for TRansUranic Extraction (TRUEX)—Recent developments in nuclear waste management: A review, J. Mol. Liq. 269 (2018) 72-91.
3. P.K. Mohapatra, Actinide ion extraction using room temperature ionic liquids: opportunities and challenges for nuclear fuel cycle applications, Dalton Trans. 46 (2017) 46, 1730-1747.
4. P.R. Vasudeva Rao, K.A. Venkatesan, Alok Rout, T.G. Srinivasan, K. Nagarajan, Potential Applications of Room Temperature Ionic Liquids for Fission Products and Actinide Separation, Sep. Sci. Technol. 47 (2012) 204-222.
5. Z. Kolarik, Ionic Liquids: How Far Do they Extend the Potential of Solvent Extraction of f-Elements ? Solvent Extr. Ion Exch. 31 (2012) 24-60.
6. I.A. Shkrob, T.W. Marin, M.P. Jensen, Ionic Liquid Based Separations of Trivalent Lanthanide and Actinide Ions, Ind. Eng. Chem. Res. 53 (2014) 3641–3653.
7. Y. Shen, S. Wang, L. Zhu, J. Wang, W. Wu, Extraction of Th(IV) from an HNO3 Solution by Diglycolamide in Ionic Liquids, Ind. Eng. Chem. Res. 50 (2011) 13990-13996.
8. M.L. Dietz, Ionic liquids as extraction solvents: where do we stand?, Sep. Sci. Technol. 41 (2006) 2047 -2063.
9. Alok Rout, K.A. Venkatesan, T.G. Srinivasan, P.R. Vasudeva Rao, Room temperature ionic liquid diluent for the mutual separation of europium (III) from americium (III), Sep. Purif. Technol. 81 (2011) 109 – 115.

10. Alok Rout, K.A. Venkatesan, T.G. Srinivasan, P.R. Vasudeva Rao, Extraction behavior of actinides and fission products in amide functionalized ionic liquid, Sep. Purif. Technol. 97 (2012) 164-171.

11. J. Wang, J. Zhao, D. Feng, X. Kang, Y. Sun, L. Zhao, H. Liang, Enhancing extraction ability by rational design of phosphoryl functionalized ionic liquids and mechanistic investigation on neodymium (III) extraction, J. Rare Ear. 34 (2016) 83-90.

12. Alok Rout, K. Binnemans, Efficient separation of transition metals from rare earths by an undiluted phosphonium thiocyanate ionic liquid, Phys. Chem. Chem. Phys. 18 (2016) 16039-16045.

13. Alok Rout, K.A. Venkatesan, T. G. Srinivasan, P.R. Vasudeva Rao, Tuning the extractive properties of Purex solvent using room temperature ionic liquid, Sep. Sci. Technol. 48 (2013) 2576-2581.

14. P.K. Mohapatra, P. Kandwal, M. Iqbal, J. Huskens, M.S. Murali, W. Verboom, A novel CMPO-functionalized task specific ionic liquid: synthesis, extraction and spectroscopic investigations of actinide and lanthanide complexes, Dalton Trans. 42 (2013) 4343-4347.

15. P. Giridhar, K.A. Venkatesan, T.G. Srinivasan, P.R. Vasudeva Rao, Extraction of uranium(VI) from nitric acid medium by 1.1 M tri-n-butylphosphate in ionic liquid diluent, J. Radioanal. Nucl. Chem. 265 (2005) 31-38.

16. K.V. Lohithakshan, S.K. Aggarwal, Solvent extraction studies of Pu (IV) with CMPO in 1-octyl 3-methyl imidazolium hexa fluorophosphate (C_8mimPF_6) room temperature ionic liquid (RTIL), Radiochim. Acta 96 (2008) 93-97.

17. S. Carda-Broch, A. Berthod, D.W. Armstrong, Solvent properties of the 1-butyl-3-methylimidazolium hexafluorophosphate ionic liquid, Anal. Bioanal. Chem. 375 (2003) 191-199.

18. Z.B. Alfassi, R.E. Huie, B.L. Milman, P. Neta, Electrospray ionization mass spectrometry of ionic liquids and determination of their solubility in water, Anal. Bioanal. Chem. 377 (2003) 159-164.

19. J.L. Antony, E.J. Maginn, J.F. Brennecke, Solution thermodynamics of imidazolium-based ionic liquids and water, J. Phys. Chem. B 105 (2001) 10942-10949.

20. B.J. Mincher, J.F. Wishart, The radiation chemistry of ionic liquids: a review, Solvent Extr. Ion Exch. 32 (2014) 563-583.

21. L.Yuan, J. Peng, L. Xu, M. Zhai, J. Li, G. Wei, Radiation-induced darkening of ionic liquid [C_4mim][NTf_2] and its decoloration, Rad. Phys. Chem. 78 (2009) 1133-1136.

22. P.K. Verma, R.B. Gujar, A.S. Kanekar, Y.K. Bhardwaj, P.K. Mohapatra, Effect of irradiation on the hydrodynamic parameters and extraction efficiency of several frequently used ionic liquids, Rad. Phys. Chem. 158 (2019)180-187.

23. K. Larsson, K. Binnemans, Separation of Rare Earths by Solvent Extraction with an Undiluted Nitrate Ionic Liquid, J. Sustain. Metall. 3 (2017) 73-78.

24. Alok Rout, K. Chatterjee, K.A. Venkatesan, K.K Sahu, M.P. Antony, P.R. Vasudeva Rao, Solvent extraction of plutonium (IV) in monoamide–ammonium ionic liquid mixture, Sep. Purif. Technol. 159 (2016) 43-49.

25. Alok Rout, K.A. Venkatesan, M.P. Antony, P.R. Vasudeva Rao, Liquid–Liquid extraction of americium (III) using a completely incenerable ionic liquid system, Sep. Purif. Technol. 158 (2016) 137-143.

26. P. Zsabka, K. Van Hecke, L. Adriaensen, A. Wilden, G. Modolo, M. Verwerft, K. Binnemans, T. Cardinaels, Solvent Extraction of Am (III), Cm (III), and Ln (III) Ions from Simulated Highly Active Raffinate Solutions by TODGA Diluted in Aliquat-336 Nitrate Ionic Liquid, Solvent Extr. Ion Exch. 36 (2018) 519–541.
27. Alok Rout, K. A. Venkatesan, T. G. Srinivasan, P. R. Vasudeva Rao, Ionic liquid extractants in molecular diluents: Extraction behavior of europium (III) in quarternary ammonium-based ionic liquids, Sep. Purif. Technol. 95 (2012) 26-31.
28. Ch. Venkateswara Rao, Alok Rout, K.A. Venkatesan, Probing the absence of third phase formation during the extraction of trivalent metal ions in an ionic liquid medium, New J. Chem. 43 (2019) 5099-5108.
29. Alok Rout, K.A. Venkatesan, T.G. Srinivasan, P.R. Vasudeva Rao, Extraction and third phase formation behavior of Eu (III) in CMPO–TBP extractants present in room temperature ionic liquid, Sep. Purif. Technol. 76 (2011) 238–243.
30. G.P. Horne, C.R. Gregson, H.E. Sims, R.M. Orr, R.J. Taylor, S.M. Pimblott, Plutonium and americium alpha radiolysis of nitric acid solutions, J. Phys. Chem. B 121 (2017) 883-889.
31. A. Wright, P.P. Hartmann, Review of physical and chemical properties of tributyl phosphate/diluent/nitric acid systems, Sep. Sci. Technol. 45 (2010) 1753–1762.
32. A.V. Bellido, M.N. Rubenich, Influence of the diluent on the radiolytic degradation of TBP in TBP, 30%(v/v)-diluent-HNO_3 systems, Radiochimica Acta 36 (1984) 61-64.
33. S.A. Ansari, P.N. Pathak, P.K. Mohapatra, V.K. Manchanda, Chemistry of diglycolamides: promising extractants for actinide partitioning, Chem. Rev. 112 (2012) 1751-1772.

34. Y. Sasaki, Y. Sugo, S. Suzuki, S. Tachimori, The novel extractants, diglycolamides, for the extraction of lanthanides and actinides in HNO_3–*n*-dodecane system, Solv. Extr. Ion Exch. 19 (2001) 91–103.

35. G. Koch, H.A.C. Mckay, T.V. Healy, I.L. Jenkins, A. Naylor, Eds, MacMillan: London, UK, (1966) 247–266.

36. R.B. Gujar, S.A. Ansari, A. Bhattacharyya, P.K. Mohapatra, A.S. Kanekar, P.N. Pathak, V.K. Manchanda, Studies on the radiolytic stability of N,N,N′,N′-tetra-2-ethylhexyl diglycolamide in n-dodecane solution containing different phase modifiers, J. Radioanal. Nucl. Chem. 288 (2011) 621–627.

37. P. Deepika , K.N. Sabharwal, T.G. Srinivasan, P.R. Vasudeva Rao, Studies on the use of N,N,N′,N′-Tetra(2-Ethylhexyl) Diglycolamide (TEHDGA) for Actinide Partitioning II: Investigation on Radiolytic Stability, Solvent Extr. Ion Exch. 29 (2011) 230–246.

38. Jammu Ravi, B. Robert Selvan, K.A. Venkatesan, M.P. Antony, T.G. Srinivasan, P.R. Vasudeva Rao, Evaluation of radiation stability of N,N-didodecyl N′,N′-di-octyl diglycolamide: a promising reagent for actinide partitioning, J. Radioanal. Nucl. Chem. 299 (2014) 879-885.

39. S.C. Tripathi, S. Sumathi, A. Ramanujam, Effects of Solvent Recycling on Radiolytic Degradation of 30% Tributyl Phosphate–*n*-Dodecane–HNO_3 System, Sep. Sci. Technol. 34 (1999) 2887–2903.

40. Alok Rout, K. Binnemans, Separation of rare earths from transition metals by liquid–liquid extraction from a molten salt hydrate to an ionic liquid phase, Dalton Trans. 43 (2014) 3186-3195.

41. A.A.C. Toledo Hijo, G.J. Maximo, M.C. Costa, E.A.C. Batista, A.J.A. Meirelles, Applications of Ionic Liquids in the Food and Bioproducts Industries, ACS Sustainable Chem. Eng. 4 (2016) 5347–5369.

42. M. Watanabe, M. L. Thomas, S. Zhang, K. Ueno, T. Yasuda, K. Dokko, Application of Ionic Liquids to Energy Storage and Conversion Materials and Devices, Application of Ionic Liquids to Energy Storage and Conversion Materials and Devices, Chem. Rev. 117 (2017) 7190–7239.

43. R.L. Vekariya, A review of ionic liquids: Applications towards catalytic organic transformations, J. Mol. Liquids 227 (2017) 44-60.

44. G. Durga, A Mishra, Ionic Liquids: Industrial Applications, Encyclopedia of Inorganic and Bioinorganic Chemistry, John Wiley & Sons, Ltd. 2016.

45. N.V. Plechkova, K.R. Seddon, Applications of ionic liquids in the chemical industry, Chem. Soc. Rev. 37 (2008) 123-150.

46. J.G. Huddleston, H.D. Willauer, R.P. Swatloski, A.E. Visser, R.D. Rogers, Room temperature ionic liquids as novel media for ‘clean’ liquid-liquid extraction, Chem. Commun. (1998) 1765-1766.

47. Alok Rout, K.A.Venkatesan, M.P. Antony, P.R. Vasudeva Rao, Liquid–Liquid extraction of americium (III) using a completely incenerable ionic liquid system, Sep. Purif. Technol. 158 (2016) 137-143.

48. Alok Rout., K.A. Venkatesan,T.G. Srinivasan, P.R. Vasudeva Rao, Separation of plutonium (IV) from uranium (VI) using phosphonate-based task-specific ionic liquid, Desalin. Water Treat. 38 (2012) 179-183.

49. Alok Rout, E. Rezende Souza, K. Binnemans, Solvent extraction of europium (III) to a fluorine-free ionic liquid phase with a diglycolamic acid extractant, RSC Adv. 4 (2014) 11899–11906.

50. Alok Rout, K.A. Venkatesan, T.G. Srinivasan, P.R. Vasudeva Rao, Tuning the Extractive Properties of Purex Solvent using Room Temperature Ionic Liquid, Sep. Sci. Technol. 48 (2013) 2576-2581.

51. M. Matsumiya, Y. Kikuchi, T. Yamada, S. Kawakami, Extraction of rare earth ions by tri-n-butylphosphate/phosphonium ionic liquids and the feasibility of recovery by direct electrodeposition, Sep. Purif. Technol. 130 (2014) 91-101.

52. K.V. Lohithakshan, P. Patil, S.K. Aggarwal, Solvent extraction studies of plutonium (IV) and americium (III) in room temperature ionic liquid (RTIL) by di-2-ethyl hexyl phosphoric acid (HDEHP) as extractant. J. Radioanal. Nucl. Chem. 301 (2014) 153-157.

53. G.R. Choppin, Comparative solution chemistry of the 4f and 5f elements, J. Alloys Compd. 223 (1995) 174-179.

54. H.C. Aspinall, Chemistry of f-block Elements, Advanced Chemistry Texts. Gordon and Breach Science Publishers. New York (2001).

55. G.J. Lumetta, A.V. Gelis, G.F. Vandegrift, Review: solvent systems combining neutral and acidic extractants for separating trivalent lanthanides from the transuranic elements, Solvent Extr. Ion Exch. 28 (2010) 287-312.

56. T. Matsumura, Y. Inaba, A. Mori, K. Takeshita, Am/Eu Separation with a new ligand, *N, N, N', N'*- tetrakis ((4-butoxypyridin-2-yl)methyl) ethylenediamine (TBPEN) a hydrophobic derivatives of TPEN, J. Nucl. Sci. Technol. 47 (2010) 123-126.

57. M. Nilsson, K.L. Nash, A Review of the development and Operational Characteristics of the TALSPEAK Process, Solvent Extr. Ion Exch. 25 (2007) 665-701.

58. C.J. Leggett, G. Liu, M.P. Jensen, Do aqueous ternary complexes influence the TALSPEAK Process ?, Solvent Extr. Ion Exch. 28 (2010) 313-334.

59. A.S. Suneesh, K.A. Venkatesan, K.V. Syamala, M.P. Antony, P.R. Vasudeva Rao, Mutual separation of americium (III) and europium (III) using glycolamic acid and thioglycolamic acid, Radiochim. Acta. 100 (2012) 425-430.

60. Y. Zhang, S. Yang, X. Yuan, Y. Zhao, G. Tian, Separating lanthanides and actinides from nitric acid solutions by using N,N-di(2-ethylhexyl)-diglycolamic acid (HDEHDGA), Chem. Commun. 53 (2017) 6421-6423.

61. Alok Rout, K.A. Venkatesan, T.G. Srinivasan, P.R. Vasudeva Rao, Room temperature ionic liquid diluent for the mutual separation of europium(III) from americium(III), Sep. Purif. Technol. 81 (2011) 109-115.

62. Alok Rout, S. Mishra, K.A. Venkatesan, M.P. Antony, N.K. Pandey, Thermophysical properties of tri-n-butylphosphate-ionic liquid mixture, AIP Conf. Proc. 1951 (2018) 30014.

63. W. Srirachat, T. Wannachod, U. Pancharoen, S. Kheawhom, Effect of polarity and temperature on the binary interaction between D2EHPA extractant and organic solvents (kerosene, n-heptane, chlorobenzene and 1-octanol): Experimental and thermodynamics, J. Fluid Phase Equil. 434 (2017) 117- 129.

64. Alok Rout, S. Mishra, K.A. Venkatesan, M.P. Antony, N.K. Pandey, S. Subramanian, Physicochemical and radiolytic degradation properties of dihexyloctanmide-imidazolium ionic liquid, J. Mol. Liquids 247 (2017) 93-99.

65. N. Muhammad, Z.B. Man, M.A. Bustam, M.I.A. Mutalib, C.D. Wilfred, S. Rafiq, Synthesis and Thermophysical Properties of Low Viscosity Amino Acid-Based Ionic Liquids. J. Chem. Eng. Data 56 (2011) 3157–3162.

66. D. Tao, Z. Cheng, F Chen, Z. Li, N. Hu, X. Chen, Synthesis and Thermophysical Properties of Biocompatible Cholinium-Based Amino Acid Ionic Liquids. J. Chem. Eng. Data 58 (2013) 1542–1548.

Chapter 7: Conclusions and scope of the future work

This chapter discusses the summary and conclusions obtained in the previous chapters. It also discusses the scope of the future work emerging from these studies.

7.1. Extraction behavior of uranium in CHON based ligand-ionic liquid system

In this chapter, the extraction behavior of U(VI) was studied in a solution containing *N*,*N*-dioctyl-2-hydroxyacetamide (DOHyA) present in methyl-tri-*n*-octylammonium nitrate ($[N_{1888}][NO_3]$) from nitric acid solution. The extraction of U(VI) in organic phases followed the order of DOHyA/*n*-DD << $[N_{1888}][NO_3]$ < DOHyA/$[N_{1888}][NO_3]$. This observation showed that $[N_{1888}][NO_3]$ and DOHyA were involved in the extraction of U(VI) in the ionic liquid medium. The FTIR and Raman spectroscopic studies on the extracted phase revealed that uranyl nitrate was extracted into DOHyA/$[N_{1888}][NO_3]$ phase by two different modes, seems to be independent of each other. They are U(VI) extraction through (a) the co-ordinate complex formation with DOHyA, and (b) through the association reaction of uranyl nitrate with nitrate ion of ionic liquid. The extraction of U(VI) in both $[N_{1888}][NO_3]$ and 0.1 M DOHyA/$[N_{1888}][NO_3]$ was similar for the unirradiated and irradiated solvent phases. The density functional theory (DFT) calculations and natural population analysis showed the participation of d and f-orbital of U atom during complex formation with the DOHyA and ionic liquid. The atoms in molecule (AIM) calculation showed the involvement of partial covalent character was observed between U and donor O atoms. The calculated values of Gibbs energy of complexation of U(VI) with DOHyA and ionic liquid in the solvent phase using DFT were in line with the experimentally determined complexation behavior of UO_2^{2+} ion with the extractant and ionic liquid. Based on the DFT calculations, it was established that the cation exchange mechanism by both the ionic liquids $[N_{1888}][NO_3]$ and $[N_{1888}][NTf_2]$ was not feasible, but anion exchange mechanism was feasible.

7.2. Extraction behavior of Eu(III) and Zr(IV) in ammonium ionic liquids

In this chapter, the room temperature ionic liquids such as $[N_{1444}][NTf_2]$ and $[N_{1888}][NTf_2]$ were explored as diluent for solvent extraction application. The extractants such as tetra-2-ethylhexyldiglycolamide (T2EHDGA) or carbamoylphospinoxide (CMPO) were explored for the extraction of Eu(III) and the alkyl derivatives of benzodioxodiamide such as 2-ethylhexylbenzodioxodiamide (BD) and decylbenzodioxodiamide (BDD) were explored for the extraction of zirconium from nitric acid medium and results obtained from these studies were presented in two sections and the conclusions arising from those studies are described below.

7.2.1. Europium(III) complexation behavior in ammonium ionic liquid medium containing neutral extractants

The solvent extraction of europium(III) in a solution of T2EHDGA or CMPO dissolved in $[N_{1444}][NTf_2]$ was studied. The distribution ratio of Eu(III) decreased with increase in the concentration of nitric acid in both T2EHDGA and CMPO cases. The study established that three molecules of T2EHDGA and two molecules of CMPO were involved in the complex formation with Eu(III) in ionic liquid phase. The FT-IR spectrum of the ionic liquid phase containing T2EHDGA/$[N_{1444}][NTf_2]$ showed the appearance of a transmittance band at 1590 cm^{-1} which was due to the co-ordination of Eu(III) with the amidic carbonyl group of T2EHDGA. A similar behavior was also observed in case of CMPO/$[N_{1444}]]$$[NTf_2]$. The ionic liquid undergoes self-aggregation in organic phase. The average size of acid or Eu(III) extracted aggregates increased with increase in the concentration of nitric acid as well as Eu(III) in the aqueous phase. Luminescence spectroscopic study on the Eu(III) extracted ionic liquid phase (T2EHDGA (or CMPO)/$[N_{1444}][NTf_2]$) confirmed the coordination of T2EHDGA or CMPO in the first coordination sphere of europium (III). The radiolytic degradation studies revealed that that the ionic liquid phase was stable up to 500 kGy absorbed dose.

7.2.2. Selective separation of zirconium(IV) from uranium(VI) using dioxoamide ligand present in ammonium ionic liquid medium

In this study, the alkyl derivaties of benzodioxodiamide ligands were prepared and studied for the extraction of Zr(IV) from nitric acid solution. The extraction of Zr(IV) in [N_{1444}][NTf_2] was negligible, but the addition of small amount of BD to [N_{1444}][NTf_2] increased the distribution ratio of Zr(IV) from the value of 1 at 0.1 M nitric acid to the value of about 100 at 5 M nitric acid concentration. The extraction trend of Zr(IV) observed in ionic liquid and n-dodecane medium were similar, suggesting that the mechanism of Zr(IV) extraction ion both the cases could be similar. However, the $D_{Zr(IV)}$ values were higher in ionic liquid medium as compared to *n*-dodecane. The linear dependence of $D_{Zr((IV))}$ on concentration of BD with a slope of 2.1, suggested that 2 molecules of BD were involved in the extraction of zirconium(IV) in ionic liquid phase. In contrast, the saturation in the loading of Zr(IV) observed in the extraction of Zr(IV) isotherm suggested a molecule of BD was coordinated to Zr(IV) at higher Zr(IV) loading. The results showed that the stoichiometry of Zr(IV) to BD could change from 1: 2 to 1:1 depending upon loading of Zr(IV) in ionic liquid phase. The distribution ratio of U(VI) in 0.05 M BD/[N_{1444}][NTf_2] was significantly small as compared to $D_{Zr(IV)}$ values at all nitric acid concentrations, leading to the separation factor of zirconium over uranium varying from 2 to 100 with increase in the concentration of nitric acid from 0.1-5 M. The magnitude of separation factor shows the possibility of separation zirconium from uranium matrix present in nitric acid medium.

7.3. Studies related to aggregation behavior and empirical polarity index of ionic liquid phase

In this chapter, the extractants such as T2EHDGA or CMPO were dissolved in [N_{1888}][NO_3] and explored for the extraction and aggregation behavior of trivalent actinides from nitric acid medium. The aggregation behavior of ammonium ionic liquid containing strongly coordinating anion, methyl-tri-*n*-octyl ammonium bis(2-ethylhexyl) phosphate [N_{1888}][D2EHP] in *n*-dodecane was investigated in detail. In addition, the empirical polarity index of RTILs such as [C_4mim][NTf_2], [C_4mpyr][NTf_2] and [C_4mpip][NTf_2] was determined using Reichardt's dye as polarity probe. The results obtained from these studies are presented in three sections and the conclusions arising from those studies are described below.

7.3.1. Probing the absence of third phase formation during the extraction of trivalent metal ions in an ionic liquid medium

The extraction behavior of Am(III) and Nd(III) from nitric acid medium was studied in a solution of T2EHDGA or CMPO in [N_{1888}][NO_3] ionic liquid. The extraction behavior of metal ions in [N_{1888}][NO_3] medium was very unique as it did not undergo cation exchange with metal ions from aqueous phase at low nitric acid concentration range. The extraction of Am(III) in [N_{1888}][NO_3] was negligible at all nitric acid concentrations investigated in the present study. The addition of T2EHDGA or CMPO in [N_{1888}][NO_3] increased in the extraction of Am(III). About two molecules of T2EHDGA or CMPO were involved in the extraction of Am(III). Even though the extraction trend of trivalent metal ion in T2EHDGA or CMPO in [N_{1888}][NO_3] was similar to *n*-dodecane, it was realized that the third phase formation behavior in ionic liquid phase was significantly different. The third phase was not observed even at the loading of 1.4 g/L Nd(III) in case of 0.1 M CMPO and 2.8 g/L of Nd(III) in case of 0.1 M T2EHDGA in $[N_{1888}][NO_3]$ medium.

To understand the absence of third phase formation in ionic liquid system, dynamic light scattering studies were performed and the results revealed that ionic liquid itself formed aggregates with the average size of 20 nm. The addition of T2EHDGA or CMPO to $[N_{1888}][NO_3]$ increased the average aggregate size and their distribution in ionic liquid. An important understanding of the present study was that the aggregate size decreased with increasing the extraction of nitric acid in ionic liquid phase. The decrease in the average aggregate size observed in ionic liquid phase was attributed to the reduced interaction of cations and anions of the ionic liquid phase. All these observations point out that the polar metal-ligand aggregates were stabilized by the polar nature of $[N_{1888}][NO_3]$. The question of third phase formation did not arise in the present ionic liquid, perhaps, this fact seems to be applicable to other ionic liquid systems also, as the size of aggregates lowered upon extraction of nitric acid. As a result, the aggregates formed in ionic liquid phase were much smaller than those observed in *n*-dodecane phase under similar conditions. Therefore, it was possible to load significant amount of Nd(III) in ionic liquid phase without the concern of third phase formation.

7.3.2. Aggregation behavior of ionic liquid in molecular liquid medium

The dynamic light scattering studies were performed in an ionic liquid phase containing $[N_{1888}]$[D2EHP] in *n*-dodecane. The average aggregate size of ionic liquid was measured as function of various experimental parameters. The results revealed that $[N_{1888}]$[D2EHP] undergo aggregation in *n*-dodecane medium, due to the interaction between the cation and anion of the ionic liquid. It is observed that the average aggregate size of organic phase is increasing with increasing the concentration of $[N_{1888}]$[D2EHP] in *n*-dodecane. For e.g. A 30 fold increase in the average aggregate size was observed with 10-fold increase in the concentration of $[N_{1888}]$[D2EHP]. Beyond 0.07 M concentration of $[N_{1888}]$[D2EHP] in *n*-dodecane, the aggregate distribution in *n*-dodecane phase was more. Upon contacting the organic phase $[N_{1888}]$[D2EHP] /*n*-DD with nitric acid resulting the formation of its precursor namely, $[N_{1888}][NO_3]$ and D2EHPA. These precursors seem to associate together and forms an adduct. In view of the formation of adduct, the aggregate size determined after contacting with nitric acid was more. Since, the precursors enhanced the formation of adduct, the addition of one component of the precursor increased the adduct formation, and the aggregates of particular type (1:1 adduct) was maximum, when the concentration of precursors were equal. The average aggregate size of organic phase containing Nd(III) was also studied. The results showed that the the average aggregate size of organic phase was increased with increasing the loading of Nd(III) concentration. However, the increase of temperature decreased the average aggregate size due to the dispersion of $[N_{1888}]$[D2EHP] aggregates in *n*-dodecane.

7.3.3. Normalized polarity indices of tri-n-butyl phosphate complexes in ionic liquid using Reichardt's dye as polarity probe

The spectrophotometric measurements were performed in Reichardt's dye in acetonitrile solution containing $[C_4mim][NTf_2]$, $[C_4mpyr][NTf_2]$ and $[C_4mpip][NTf_2]$, nitric acid, TBP and metal ions such as Th^{4+}, Nd^{3+}, UO_2^{2+}. The normalized polarity of the ionic liquid phase was measured using Reichardt's dye as a polarity probe. The results revealed that the normalized polarity of ionic liquid phase increased with the increase in the concentration of ionic liquid, nitric acid and other metal nitrates in acetonitrile. In the the presence of TBP, the normalized polarity of ionic liquid phase decreased with increase in the concentration of TBP. However, the normalized polarity of ionic liquid phase increased with increase in the concentration of metal ion in ionic liquid phase (TBP/ionic liquid).

7.4. Radiolytic stability and thermophysical properties of ionic liquid solvent system

The radiolytic stability and thermophysical properties of the ionic liquid phase containing T2EHDGA/[N_{1888}][NO_3] and D2EHPA or HDEHDGA/[C_4mim][NTf_2] were determined and the results obtained from these studies were presented in two sections. The conclusions arising from those studies are described below.

7.4.1. Investigations on the radiolytic stability of incinerable CHON based ionic liquid containing diglycolamide

The radiolytic degradation of the CHON system composed of T2EHDGA in [N_{1888}][NO_3] ionic liquid was studied and the results were compared with those obtained in the conventional molecular diluent, *n*-DD, system. The distribution ratio of Am(III) in 0.1 M T2EHDGA/ [N_{1888}][NO_3] remained nearly constant irrespective of the γ-absorbed dose, while the $D_{Am(III)}$ decreased with increase of absorbed dose in T2EHDGA/*n*-DD. To understand this difference, the T2EHDGA alone was irradiated and mixed with [N_{1888}][NO_3] and $D_{Am(III)}$ was determined. Under this condition T2EHDGA was expected to undergo degradation and lower the distribution ratio of Am(III) in irradiated T2EHDGA present in [N_{1888}][NO_3], but the $D_{Am(III)}$ was invariant in this case also, indicating the participation of the bulk [N_{1888}][NO_3] for the extraction of Am(III).

The possibility of extraction of Am(III) by [N_{1888}][NO_3] was confirmed by loading of Nd(III) to the extent of 17 g/L into the [N_{1888}][NO_3] phase. The FTIR spectroscopic investigations also confirmed the co-ordination of $Nd(NO_3)_3$ by T2EHDGA in [N_{1888}][NO_3]. Overall the extraction of trivalent metal ion in ionic liquid phase in this system was essentially controlled by [N_{1888}][NO_3], even though there was a radiolytic degradation occurred in

T2EHDGA as well as [N_{1888}][NO_3]. The degradation effect of γ-radiation on the distribution ratio of Am(III) or Nd(III) was not observed apparently during extraction, since both T2EHDGA and [N_{1888}][NO_3] extract trivalent metal ion, and among these two, the [N_{1888}][NO_3] was present in bulk quantity. The loaded Am(III) from ionic liquid phase was recovered using dilute nitric acid (0.01 M) in four contacts for irradiated and unirradiated systems. However five contacts are required for the mixture of irradiated and unirradiated solvent systems. The degradation products seems to be innocuous, since they did not retain Am(III) during stripping. In view of this, the ionic liquid, [N_{1888}][NO_3], can be regarded as a promising substitute to [$C_n$mim][NTf_2] based ionic liquids studied for possible applications in nuclear fuel cycle over the last two decades.

7.4.2. Thermophysical properties of ionic liquid solvent system

The thermophysical properties of D2EHPA, HDEHDGA and their solution in [C_4mim][NTf_2] ionic liquid was studied. The viscosity of D2EHPA or HDEHDGA and their solution in [C_4mim][NTf_2] medium decreased with an increase in temperature. The viscosity of the ionic liquid phase D2EHPA/[C_4mim][NTf_2] initially increased with an increase in the concentration of D2EHPA, followed by a decrease in viscosity values. However, the viscosity of the HDEHDGA/[C_4mim][NTf_2] phase increased with increase in the concentration of HDEHDGA in the ionic liquid phase. The density of D2EHPA or HDEHDGA and their solution in [C_4mim][NTf_2] was decreased with an increase in temperature. The viscosity of the loaded ionic liquid phase showed a gradual increase with an increase in loading of Nd(III) in the ionic liquid phase and the viscosity of the irradiated solvent phase increased with an increase of absorbed dose. The Viscosity and density values decreased upon acid equilibration for both the ligand–ionic liquid solutions. PST decreased with an increase in the concentration of nitric acid in the case of unirradiated systems, and PST increased with an increase of absorbed dose.

Refractive index values of the ionic liquid compositions decreased with an increase in temperature, as well as upon acid equilibration. The ionic liquid phase was thermally stable up to 675 K, and the presence of the extractants did not alter the thermal stability of the [C_4mim][NTf_2] phase to any significant extent.

7.5. Scope of the future study

In the present work, RTILs have been explored as a diluent for solvent extraction applications. The results showed that RTILs are promising candidates for the separation of actinides and fission products in nuclear fuel cycle. Though these results hold great promise, further studies are needed to develop a separation robust separation technology based on RTIL medium. The studies needed are highlighted below.

1. Since the solvent extraction studies in RTIL medium have been carried out only for the limited number of metal ions such as U(VI), Am(III), Eu(III) and Nd(III) in the present work, the other metal ions which are likely to be present in HLLW also need to be studied using RTIL medium.
2. The DFT calculations, ATR-FTIR and Raman spectroscopic studies were conducted for understanding the interaction of metal-ligand complex in ionic liquid phase. These studies provided some insights into the extraction mechanism. To understand further, advanced spectroscopic techniques such as ^{1}H, ^{13}C, ^{31}P NMR, ESI-MS, EXAFS studies can be employed to obtain more clarity on the structure of metal-ligand complex in ionic liquid phase.
3. Though interesting results have been obtained in the present study with the use of quaternary alkylammonium based RTILs, as compared to imidazolium or pyrrolidinium based RTIL, the higher viscosity of ammonium based ionic liquids limits its actual

applications. Therefore, there is a need to develop advanced ionic liquids having low viscosity and study the solvent extraction behavior of actinides and fission products in those ionic liquids.

4. The aggregation behavior of metal-ligand complex in RTIL medium was studied using dynamic light scattering technique. These studies can be further investigated by other advanced complementary techniques such as small angled X-ray scattering (SAXS), small angle neutron scattering (SANS), tensiometry and vapour pressure osmometry (VPO) etc. to understand the parameters that influence the aggregation behavior in ionic liquid phase. In addition, the results obtained from those studies can be validated by computational methods such as density functional theory and molecular dynamics simulations.
5. The radiation stability of RTILs was investigated using gamma irradiator. A similar study can be conducted by irradiating ionic liquid phase to α-radiation, since the ionic liquid phase was proposed for the separation of alpha emitting radionuclides from HLLW. Moreover, the degradation products formed in the ionic liquid phase need to be characterized in detail.

Glossary

Abbrevation	Full name
An(III)	Trivalent Actinides
ADS	Accelerator driven system
ATR	Attenuated Total internal Reflectance
BD	Benzodioxodi(2-ethylhexyl)diamide
BDD	Benzodioxodidecyldiamide
BRIT	Board of Radiation and Isotope Technology
BWR	Boiling Water Reactor
CMPO	*n*-Octyl(phenyl)-*N,N*-diisobutylcarbamoylmethylphosphine oxide
[C_4mim][Cl]	l-butyl-3-methyl imidazolim chloride
[C_4mim][NTf_2]	l-butyl-3-methyl imidazolim bis(trifluoromethylsulfonyl)imide
[C_4mpyr][NTf_2]	1-butyl-1- methyl pyrrolidinium bis(trifluoromethylsulfonyl)imide
[C_4mpip][NTf_2]	1-butyl-1-methyl piperidinium bis(trifluoromethylsulfonyl)imide
D_M	Distribution ratio of metal ion
DLS	Dynamic Light Scattering
D2EHPA	Bis(2-ethylhexyl) phosphoric acid
DOHyA	*N,N*-dioctyl-2-hydroxy acetamide
DFT	Density Functional Theory
EDTA	Ethylene Diammine Tetra Acetic acid
FBRs	Fast Breeder Reactors
FBTR	Fast Breeder Test Reactor
FTIR	Fourier Transform Infra Red
GWe	Giga Watt Electric
HDEHDGA	*N,N*-di-2-ethylhexyl diglycolamic acid
HLLW	High Level Liquid Waste
ILs	Ionic Liquids
KAMINI	KAlpakkam MINI reactor
kGy	kilo Gray
Ln(III)	Trivalent Lanthanides

$LiNTf_2$	Lithium bis(trifluoromethylsulfonyl)imide
MeV	Mega electron Volt
MWd	Mega Watt days
MAs	Minor actinides
NaI(Tl)	Sodium Iodide (Thalium)
NFC	Nuclear Fuel Cycle
n-DD	*n*-dodecane
P & T	Partitioning and Transmutation
$[N_{1444}][NTf_2]$	Tri-*n*-butyl-methylammonium bis(trifluoromethylsulfonyl)imide
$[N_{1888}][NTf_2]$	Methyl-tri-*n*-octylammonium bis(trifluoromethylsulfonyl)imide
$[N_{1888}][NO_3]$	Methyl-tri-*n*-octylammonium nitrate
PUREX	Plutonium Uranium Recovery by Extraction process
PALADIN	Partition of Actinides and Lanthanides with Acidic extractant Diamide and INcinerable complexants
PFBR	Prototype Fast Breeder Reactor
PHWRs	Pressurized Heavy Water Reactors
PWR	Pressurized water Reactor
RTILs	Room Temperature Ionic Liquids
SANEX	Selective ActiNide Extraction
SETFICS	Solvent Extraction for Trivalent f-element Intragroup Separation in CMPO-complexant Solvent
SF	Separation Factor
TALSPEAK	Trivalent Actinides Lanthanide Separation Phosphorous based reagent Extraction from Aqueous Komplexes
TRUEX	TRans Uranium element EXtraction
TRUSPEAK	TRansUranic elements Separation by Phosphours based Extractants from Aqueous Komplexes
TBP	Tri-*n*-butyl phosphate
T2EHDGA	*N,N,N',N'*-tetra-2-ethylhexyldiglycolamide